Screen for proteins that regulate sensitivity to inhibition of the insulin-like growth factor 1 receptor

Shan Gao (B.Sc, M.Sc)

Wolfson College

Submission for the degree of Doctor of Philosophy (D.Phil)

Department of Medical Oncology

University of Oxford



Trinity 2012

Table of Contents

Abstract viii

Acknowledgements ix

List of figures x

List of tables xiv

Abbreviations xv

CHAPTER 1 1

INTRODUCTION 1

1.1 Insulin-like growth factor (IGF) system 2

1.1.1 The relationship of IGF system components 3

1.1.2 IGF-1R 5

1.1.3 The signaling pathways activated by IGF-1R 7

1.1.4 Crosstalk between IGF-1R and other signaling pathways 11

1.1.4.1 IGF-1R and insulin receptor (IR) 11

1.1.4.2 IGF-1R and wingless (Wg)/integration (Int) (WNT) 12

1.1.4.3 IGF-1R and Epidermal Growth Factor Receptor (EGFR) 15

1.1.4.4 IGF-1R and Estrogen Receptor (ER) 17

1.1.4.5 IGF-1R and Androgen Receptor (AR) 18

1.2 The role of IGF-1R in cancer 18

1.2.1 IGF-1R mediates malignant transformation 21

1.2.2 Role of IGF-1R in malignant cell growth 22

1.2.3 IGF-1R mediates protection from apoptosis 24

1.2.3 IGF-1R in metastasis 26

1.2.4 Involvement of IGF-1R in the repair to DNA damage 30

1.3 IGF-1R inhibitors and antibodies in clinical trials 31

1.4 RNA interference (RNAi) and SLL screens 33

1.4.1 RNAi 33

1.4.2 Synthetic sickness/lethality (SLL) and its application 35

1.4.3 siRNA high-throughput screen (HTS) 37

1.5 The aims of this project 40

CHAPTER 2 41

MATERIALS AND METHODS 41

2.1 Cell lines and culture 41

2.2 Chemical compounds and treatments 42

2.3 Protein analysis **43**

2.3.1 Collection and lysis of adherent cells 43

2.3.2 Immunopreciptation 44

2.3.3 Co-immunprecipitation 44

2.3.4 Western blot 45

2.3.5 Quantification of radiographs 46

2.3.6 Glutathione S-transferase (GST) pull-down 46

2.3.6.1 GST or GST fusion protein purification 46

2.3.6.2 RAS activation assays 48

2.3.6.3 GST pull-down assay 49

2.3.7 Lambda protein phosphatase assay 50

2.4 Handling of DNA **50**

2.4.1 Handling of bacteria 50

2.4.2 Preparation of plasmids 50

2.4.3 DNA digest with restriction enzymes 51

2.4.4 Transfection of plasmid DNA 52

2.5 Cell based assays **52**

2.5.1 Growth assays 52

2.5.1.1 Cell proliferation assay/Celltiter-Glo 52

2.5.1.2 Clonogenic survival assay 53

2.5.2 Immunostaining and microscopy 54

2.6 siRNA screens 55

2.6.1 RNAi libraries and siRNAs 55

2.6.2 siRNA screen method 57

2.6.2.1 Z-score for cell growth: 58

2.6.2.2 Z-score for inhibitor effect: 58

2.6.2.3 Z' factor calculation 59

2.6.3 Validation of siRNA screen 59

2.7 Validation of hits 60

2.7.1 siRNA reverse transfection in 6-well plate 60

2.7.2 Primer design 60

2.7.3 Extraction of total RNA and reverse transcription 62

2.7.4 qRT-PCR 63

2.8 Statistical analysis 63

CHAPTER 3 64

IGF-1R INHIBITION IN HUMAN PROSTATE AND BREAST CANCER CELLS 64

3.1 Introduction 64

3.2 Results and discussion 64

3.2.1 Inhibition of IGF-1R activity by AZ12253801 65

3.2.2 AZ12253801 inhibited IGF-1R signaling 66

3.2.3 Testing effects of IGF-1R inhibition on proliferation of DU145 and MCF-7 cells 70

3.2.4 Testing effect of overexpression of IGF-1R on sensitivity to AZ12253801 74

CHAPTER 4 **77**

SIRNA SCREEN TO IDENTIFY GENES WHOSE SILENCING INFLUENCES SENSITIVITY TO IGF-1R INHIBITION **77**

4.1 Introduction **77**

4.2 Results and discussion **77**

4.2.1 Optimization of siRNA screen 77

4.2.2 Primary siRNA Screen 79

4.2.2.1 Screen process 80

4.2.2.2 Analysis of screen data 81

4.2.2.3 Results of primary screen 88

4.2.3 Validation of primary siRNA screen hits 90

4.2.4 Validation of Kinome hits 94

4.2.5 Validation of DNA repair-associated hits 99

CHAPTER 5 **106**

INVESTIGATING DVL3 AS A SCREEN HIT 106

5.1 Introduction 106

5.2 Results and discussion 109

5.2.1 Abundant expression of DVL3 in DU145 prostate cancer cells 110

5.2.2 DVL3 not DVL1 or DVL2 knockdown enhanced sensitivity to IGF-1R inhibiton 110

5.2.2.1 Isoform-specific DVL3 knockdown enhanced sensitivity to AZ12253801 110

5.2.2.2 Knockdown of either DVL1 or DVL2 did not enhance sensitivity to AZ12253801 113

5.2.2.3 Testing effects of DVL3 silencing on sensitivity to alternative forms of IGF-1R 118

5.2.3 Effects of DVL3 knockdown on IGF WNT and IGF signaling 121

5.2.4 Overexpressed DVL3 decreased the sensitivity of IGF-1 on ERK1/2 activation 127

CHAPTER 6 129

TESTING ABILITY OF WNT INHIBITORS TO RECAPITULATE EFFECTS OF DVL3 DEPLETION 129

6.1 Introduction 129

6.2 Results and discussion 129

6.2.1 Testing effects of AXIN stabilization using XAV939 129

6.2.2 Effects of DVL3 knockdown were phenocopied by a small molecule DVL inhibitor 131

6.2.3 DVL inhibition sensitized to IGF-1R inhibition in cells with active ERK1/2 136

6.2.4 DVLi enhanced the sensitivity of MCF-7 cells to IGF-1R inhibition 143

6.2.5 Investigating how DVL3 regulates ERK1/2 activation 144

6.2.5.1 β-arrestin1/2 and IRS-1 knockdown did not abolish DVLi-induced ERK1/2 activation 145

6.2.5.1 GRB2 knockdown abolished ERK1/2 activation induced by DVLi 145

6.2.5.2 Investigating interaction between DVL3, GRB2 and DAB2 150

6.2.5.3 DAB2 knockdown enhanced sensitization to AZ12253801 155

6.2.5.4 Investigating effects of DVLi on complex of GRB2, DVL3 and DAB2 157

6.2.6 Proposed model for DVL3 regulating sensitivity to IGF-1R inhibition 159

CHAPTER 7 **162**

CONCLUSIONS AND FUTURE DIRECTIONS **162**

7.1 Conclusions **162**

7.2 Future Directions **164**

BIBLIOGRAPHY **173**

APPENDIX **206**

Abstract

The type 1 insulin-like growth factor receptor (IGF-1R) plays a significant role in tumor growth and spread, and IGF-1R inhibitors and antibodies are now undergoing clinical testing. However, factors that regulate sensitivity to IGF-1R inhibition remain unclear. The aim of this project is to identify proteins whose depletion regulates sensitivity to IGF-1R inhibition, in order to design effective combination treatments to benefit patients. An IGF-1R kinase inhibitor, AZ12253801 (provided by AstraZeneca) was able to block IGF-induced phosphorylation of IGF-1R in DU145 prostate cancer and MCF-7 breast cancer cells, inhibited downstream signalling in DU145 cells, and also inhibited proliferation and cell survival of both cell lines. AZ12253801 was used in an unbiased siRNA screen in both cell lines, using two siRNA libraries (779 kinase-related Kinome and 230 DNA repair-associated siRNAs). Eight Kinome and five DNA repair-associated hits have been identified after primary and second round screens, and further validated. The strongest hit was dishevelled homolog 3 (DVL3), a member of the WNT signalling pathway, which is highly expressed in both cell lines. DVL3 silencing caused reduction in active β-catenin and inactivated the mTOR pathway, consistent with previous studies, and did not affect IGF-1R and AKT activity. However, DVL3 silencing led to activation of MEK1/2-ERK1/2 in serum-starved cells and sensitized this pathway to IGF-1 stimulation, with translocation of ERK1/2 into the nucleus and increased expression of ERK1/2 target genes. A DVL PDZ domain inhibitor (DVLi) showed similar effects on active β-catenin, mTOR signalling and ERK1/2 signalling activity. The administration of DVLi increased sensitivity to AZ12253801 in cell lines with detectable ERK1/2 activation, but not prostate cancer cells in which ERK signalling was suppressed and AKT was activated in the context of loss of functional PTEN. Furthermore, DVL3 regulated activation of ERKs by influencing signaling downstream of the IGF-1R and upstream of RAS, and DVL3 was found in a complex with the adaptor proteins GRB2 and DAB2. GRB2 knockdown was capable of abolishing ERK1/2 activation induced by DVLi, further implicating involvement of GRB2, and DAB2 silencing sensitized to IGF-1R inhibition, mimicking effects of DVL3 depletion. Taken together, DVL3 silencing or inhibition enhances sensitivity to IGF-1R inhibition by negatively regulating the ERK1/2 signaling pathway. These investigations shed new light on the factors that regulate IGF signaling, and provide a rational basis for design of clinical trials of IGF-1R inhibitors.

Acknowledgements

First of all, I would like to thank my supervisor, Dr. Val Macaulay, for giving me this wonderful opportunity to work in her laboratory. On middle summer of 2008, I just finished my last project and hesitated about my future destination. I got some offers during that time, and after comparison, I decided to change my research field and contribute to the challenge of cancer research. I am truly grateful for her continued support and great guidance over the course of this degree. Many thanks to our collaborators: Prof. Alan Ashworth, Dr. Chris Lord and Ms. Ilirjana Bajrami gave great supervision and help on siRNA screens, and I had a fantastic time in London and amazing experience commuting between Oxford and London every day. Dr. Stephan Feller provided many constructs and soluble proteins, and shared many wonderful ideas on signaling pathways, boosting my research speed. I was also fortunate to be one of a great team. Tamara Aleksic, Meenali Chitins, Philip Earwaker, Mark Goodfellow, Martin Kerr, Kunal Lodhia, and Roger Ramcharan- you guys create the harmony of lab and have so great time laughing in lab.

I have had such a wonderful time in Oxford for seven years, and recognized it as my second home town. I have so great memories in Oxford- I got married and had a lovely daughter here. I have so many friends from different countries, but all have a great time together.

I am also grateful to my funding sponsors, AstraZeneca and UCARE for supporting this work.

List of Figures

Chapter 1

		Page
Figure 1.1	The major signaling pathways activated by IGF-1R	9
Figure 1.2	WNT signaling pathways	15
Figure 1.3	Schematic pathways of apoptosis and IGF-1R role in apoptosis	27

Chapter 3

Figure 3.1	AZ12253801 inhibited IGF-1-induced IGF-1R activation in MCF-7 cells	67
Figure 3.2	AZ12253801 inhibited IGF-1-induced IGF-1R activation in DU145 cells	68
Figure 3.3	AZ12253801 inhibited IGF-1-induced AKT and ERK1/2 activation in DU145 cells	69
Figure 3.4	Effect of AZ12253801 on cell proliferation	71
Figure 3.5	AZ12253801 inhibited clonogenic survival of DU145 prostate cancer cells	72
Figure 3.6	AZ12253801 inhibited clonogenic survival of MCF-7 breast cancer cells	73
Figure 3.7	Overexpression of IGF-1R did not enhance sensitivity to AZ12253801 in PC3 prostate cancer cells	76

Chapter 4

Figure 4.1 AZ12253801 inhibited IGF-1-induced IGF-1R activation in MCF-7 cells 79

Figure 4.2 AZ12253801 inhibited IGF-1-induced IGF-1R activation in DU145 cells 81

Figure 4.3 AZ12253801 inhibited IGF-1-induced AKT and ERK1/2 activation in DU145 cells 83

Figure 4.4 Effect of AZ12253801 on cell proliferation 84

Figure 4.5 AZ12253801 inhibited clonogenic survival of DU145 prostate cancer cells 85

Figure 4.6 AZ12253801 inhibited clonogenic survival of MCF-7 breast cancer cells 86

Figure 4.7 Scatter plots of average Z-scores of inhibitor effect 89

Figure 4.8 Validation of hits from primary screens 93

Figure 4.9 Depletion of Kinome hits by screen siRNAs 95

Figure 4.10 Knockdown of Kinome hits sensitized to AZ12253801 97

Figure 4.11 Depletion of DNA repair hits was confirmed by qRT-PCR or western blot 101

Figure 4.12 Assessment of cell viability after depletion of hits by screen siRNAs 102

Figure 4.13 Knockdown of DNA repair hits sensitized DU145 cells to AZ12253801 103

Chapter 5

Figure 5.1 Schematic DVL structure 107

Figure 5.2 Expression of DVL1-3 in DU145 cells 111

Figure 5.3 DVL3 siRNA 4 specifically silenced its target gene 113

Figure 5.4 DVL3 knockdown enhanced the sensitivity of DU145 cells to AZ12253801 114

Figure 5.5 Isoform specific gene silencing by DVL1 and DVL2 siRNA 116

Figure 5.6 DVL1 or DVL2 knockdown did not enhance sensitivity of DU145 cells to AZ12253801 117

Figure 5.7 DVL3 knockdown enhanced sensitivity to IGF-1R knockdown in DU145 cells 119

Figure 5.8 DVL3 silencing sensitized DU145 cells to IGF-1R inhibition 120

Figure 5.9 Effects of DVL3 knockdown on WNT and IGF signaling in DU145 cells 124

Figure 5.10 ERK1/2 nuclear translocation and functional activation after DVL3 knockdown in DU145 cells 126

Figure 5.11 Overexpression of FLAG-DVL3 reduced IGF-induced ERK1/2 activation 128

Chapter 6

Figure 6.1 XAV939 inhibited the growth of DU145 cells and inactivated the mTOR pathway 131

Figure 6.2 XAV939 did not sensitize to IGF-1R inhibition or activate ERK1/2 132

Figure 6.3 Effects of DVLi in DU145 cells 134

Figure 6.4 Reciprocal sensitization by inhibitors of IGF-1R and DVL 135

Figure 6.5 Characterization of prostate cancer cell lines 138

Figure 6.6 PTEN WT prostate cancer cells are sensitized to AZ12253801 by DVLi 139

Figure 6.7 ERK1/2 activation by DVLi in DU145 and 22Rv1 cells 140

Figure 6.8 HCT166 wild-type or PTEN knockout (KO22) cells sensitized to AZ12253801 by DVLi 142

Figure 6.9 Sensitization to AZ12253801 by DVLi in MCF-7 cells 144

Figure 6.10 Knockdown of β-arrestin1/2 or IRS-1 did not abolish DVLi-induced ERK1/2 activation in DU145 cells 146

Figure 6.11 RAS was activated by DVLi in DU145 cells 148

Figure 6.12 DVLi-induced ERK1/2 activation was abolished by GRB2 knockdown in DU145 cells 149

Figure 6.13 Schematic structure of GRB2 and DAB2 151

Figure 6.14 Physical interaction between DVL3, GRB2 and DAB2 in DU145 cells 153

Figure 6.15 DVL3 and DAB2 bind to GRB2 domains in DU145 cells 154

Figure 6.16 DAB2 knockdown activated ERK1/2 and enhanced sensitivity to AZ12253801 156

Figure 6.17 DVL inhibition did not influence GRB2 binding partners 158

Figure 6.18 Proposed model for interaction between IGF-1R inhibition and DVL3 silencing 161

Chapter 7

Figure 7.1 DVL3 expression in cancers 169

Figure 7.2 HUNK knockdown enhances IGF-1 response of IGF-1R and AKT 172

List of tables

Chapter 2

		Page
Table 2.1	Antibodies used for western blot	47
Table 2.2	siRNAs used for gene silencing	56
Table 2.3	Primers used for qRT-PCR	61

Chapter 4

Table 4.1	The summary of duplicate screens in MCF-7 cells	85
Table 4.2	Results of IGF-1R siRNA primary screens using kinome and DNA repair-assosiated siRNAs	89
Table 4.3	Summary of validation hits from Kinome screen	97
Table 4.4	Summary of validation hits from DNA repair-associated screen	102

Appendix

Table S1	Kinase siRNA library	206
Table S2	DNA repair siRNA Set V1.0	224
Table S3	DNA repair Flexitube siRNAs	228

Abbreviations

4E-BP1	eIF4E-binding protein 1
AKAP1	A kinase anchor protein 1
AKT	Protein kinase B
ANOVA	Analysis of variance
Apaf-1	Apoptotic protease activating factor-1
APC	Adenomatous polyposis coli
APEG1	Aortic preferentially expressed gene 1
AR	Androgen receptor
AS	Allstars negative control
BAD	Bcl-2 antagonist of cell death
BAK	Bcl-2 homologous antagonist killer
BAX	Bcl-2-associated X protein
Bcl-2	B-cell lymphoma 2
Bcl-XL	B-cell lymphoma extra large
BIM	Bcl-2-interacting mediator of cell death
BRCA1	Breast cancer type 1 susceptibility protein
BRCA2	Breast cancer type 2 susceptibility protein
BSA	Bovine serum albumin
Caspase	Cystein-dependent aspartate-specific protease
CDKN2C	Cyclin-dependent kinase inhibitor 2
CDKN3	Cyclin-dependent kinase inhibitor 3
CNKSR1	Connector enhancer of kinase suppressor of Ras1
CREB	cAMP response element binding
CTG	CellTiter-Glo
DAB2	Disabled homolog 2
DNA	Deoxyribonucleic acid
DSB	Double stranded DNA break
DUSP5	Dual specificity phosphatase 5
DVL	Dishevelled (Dsh) homolog
DVLi	DVL PDZ domain inhibitor II
ECM	Extracellular matrix

EGFR/HER1	Epidermal growth factor receptor
eIF4E	eukaryotic translation initiation factor 4E
ELK1	E twenty-six like transcriptional factor 1
ER	The estrogen receptors
ERK1/2	Mitogen-activated protein kinase/extracellular signal-regulated kinase 1/2
FADD	Fas-associated death domain protein
FCS	Fetal calf serum
FKHR1	Forkhead homolog like 1
Fz	Receptor frizzed
GH	Growth hormone
GI_{50}	The concentration required to inhibit growth of cells to 50% of that in solvent-treated cells
GRB2	Growth factor receptor-bound protein 2
GSK3β	glycogen synthase kinase 3β
GST	Glutathione S-transferase
GST-RBD	GST-c-Raf-1 Ras binding domain
HIF	Hypoxia-inducible transcriptional factor
HR	Homologous recombination
HSP	Heat shock protein
HTS	High-through-put screen
HUNK	Hormonally up-regulated Neu-associated kinase
IC_{50}	The half maximal inhibitory concentration
IGF	Insulin-like growth factor
IGF-1R	The type 1 insulin-like growth factor receptor
IGF-2R	the type 2 IGF receptor
IGFBP	IGF-binding proteins
I**NO80C**	INO80 complex subunit C
IP-western	Immunoprecipitation and western blot
IR	Insulin receptor
IRS	Insulin receptor substrate
JAK1/2	Janus kinase 1
LB	Lysogeny broth
LEF	Lymphoid enhancer factor
LMTK3	Lemur tyrosine kinase 3
LRP5/6	Low density lipoprotein receptor-related protein 5/6

MCL-1	Myeloid cell leukemia 1
MDM2	Mouse double minute 2
MEF	Mouse embryo fibroblast
MEK1/2	Mitogen-activated protein kinase kinase 1/2
MMPs	Matrix metalloproteinases
MPP2	Membrane protein palmitoylated 2
MSTR1R	Macrophage-stimulating 1 receptor tyrosine kinase
MT1-MMP	Membrane type 1-MMP
mTORC1	The mammalian target of rapamycin complex 1
NFκB	kappa-light-chain-enhancer of activated B cells
p53	Protein 53
PARP	Poly(ADP-ribose) polymerase
PBS	Phosphate buffered saline
PBST	Triton-X-100 in PBS
PI3K	Phosphoinositide 3-kinase (PI3K)
PID	N-terminal phosphotyrosine-binding/interacting domain
PIP2	Phosphatidylinositol-4,5-bis-phosphate
PIP3	Phosphatidylinositol 3,4,5-triphosphate
PLK1	Polo-like kinase 1
PSA	Prostate-specific antigen
PTEN	Phosphatase and tensin homolog
qRT-PCR	Quantitative real-time reverse transcription PCR
RISC	RNA-induced silencing complex
RNAi	RNA interference
RTK	Receptor tyrosine kinase
SD	Standard deviation
SDS-PAGE	SDS polyacrylamide gel electrophoresis
SEM	Standard error of the mean
SF_{50}	The concentration required to inhibit survival by 50% of that solvent-treated cells
SHC	Src homology and collagen domain protein
shRNA	short hairpin RNAs
siRNA	short interfering RNA
SLL	Synthetic sickness/lethality
SOS	Son of sevenless gene
SSB	Single stranded DNA break

STAT	Signal transducer and activator of transcription
STR	Short tandem repeat
TCF	T-cell factor
TIMPs	Tissue inhibitors of metalloproteinases
TNF	Tumor necrosis factor
TNFR1	TNF receptor 1
TRAIL	TNF-related apoptosis inducing ligand
TSC1	Tuberous sclerosis complex 1
TSC2	Tuberous sclerosis complex 2
VEGF	Vascular endothelial growth factor
VEGFR-2	VEGF receptor 2
VHL	Von Hippel-Lindau
WNT	Wingless (Wg)/integration (Int)

Chapter 1

Introduction

The type 1 insulin-like growth factor (IGF-1R) mediates cell proliferation, protection from apoptosis, transformation and tumor spread (Chitnis et al. 2008; Pollak 2008). Strategies that block IGF-1R signaling have been shown to inhibit tumor growth and metastasis in animal models (Samani et al. 2007). Work from our lab and others indicate that blocking or depleting IGF-1R can enhance chemosensitivity, via effects on apoptosis susceptibility, and possibly also via effects on the response to deoxyribonucleic acid (DNA) damage (Dunn et al. 1997; Macaulay et al. 2001; Rochester et al. 2005; Turney et al. 2012).

Based on these findings, IGF-1R is an attractive target for cancer therapy. Various inhibitors and antibodies targeting IGF-1R have been tested in clinical trials in the past 4-5 years. From the clinical evidence, IGF-1R inhibition has striking effects in a subset of uncommon cancers, but limited effects in common cancers (Yuen and Macaulay 2008; Gualberto and Pollak 2009; Olmos et al.

2010). While many studies have elucidated the crosstalk between the IGF-1R axis and other signaling pathways, there have been few systematic strategies to identify proteins that regulate sensitivity to IGF-1R inhibition.

This project attempts to identify genes whose depletion regulates sensitivity to IGF-1R inhibition, and to use this information to design the most effective combination treatments. The project was set up as collaboration between our laboratory and Professor Alan Ashworth's and Dr. Chris Lord at the Breakthrough Breast Cancer Research Center. Professor Ashworth's team has already performed many short interfering RNA (siRNA) highthrough-put screens (HTSs) to investigate synthetic sickness/lethality (SSL) (Iorns et al. 2008; Lord et al. 2008; Turner et al. 2008). A modified screen strategy has been proposed based on their previous methods.

1.1 Insulin-like growth factor (IGF) system

The insulin-like growth factor (IGF) system is a complex network that contains two cognate ligands which are IGF-1 and IGF-2, two cell surface transmembrane receptors consisting of IGF-1R and the type 2 IGF receptor (IGF-2R), six soluble circulating high-affinity IGF-binding proteins (IGFBPs) and

IGFBP-specific proteases (Denley et al. 2005). The IGF system performs multiple functions in normal tissues and in neoplasia (Samani et al. 2007; Pollak 2008; Pollak 2012).

1.1.1 The relationship of IGF system components

IGF-1 and IGF-2 are evolutionally conserved peptide hormones, similar in both amino acid sequence and molecular structure and closely related to insulin. IGFs are primarily synthesized in liver, and also produced by other tissues and cells by autocrine and paracrine pathways (Underwood et al. 1994). IGF-1 secretion from the liver is tightly regulated by growth hormone (GH), while IGF-2 expression is only weakly GH-regulated. Thus levels of IGF-1 mRNA but not IGF-2 mRNA are decreased 10 fold in GH-deficient mice, and IGF-1 can be restored to normal levels by GH treatment (Mathews et al. 1986). IGFs are important growth mediators and have a key role in development. Due to lower expression of IGF-1 in embryonic development compared to IGF-2, it has been thought that IGF-1 is dispensable in embryonic development. However, mice harboring disrupted IGF-1 gene have approximately 40% reduction in body weight compared to wild type littermates at birth, while the majority of pups die at the perinatal stage, suggesting that IGF-1 is critical for correct prenatal development (Liu et al. 1993; Powell-Braxton et al. 1993). By contrast, mice

harboring liver-specific knockout of IGF-1 that keeps peripheral synthesis intact, develop normally with less than 10% reduction in adult size, despite 80% reduction in serum IGF-1 level, suggesting that IGF-1 produced in the periphery is the main determinant of somatic growth in mice (Stratikopoulos et al. 2008). The IGF-2 gene is subjected to maternal imprinting, and heterozygous mutants carrying a paternally derived disrupted gene (-/m) or IGF-2 null mutants (-/-) are phenotypically indistinguishable, with growth retardation similar to IGF-1 null mice at birth. Also the IGF-2 mutants (-/- or -/m) are fertile with normal postnatal growth (DeChiara et al. 1990). There has been an isolated report of a severely affected patient with a partial IGF-1 gene deletion, with significant pre- and postnatal growth retardation, sensorineural deafness, mental retardation, developmental delay, and severe microcephaly (Woods et al. 1996).

IGFs signal and function mainly through IGF-1R. IGF-1 binds IGF-1R with 6 to 8 fold higher affinity than IGF-2 (Clemmons 2007). IGF-2R is completely different in structure and function from IGF-1R and is mainly bound by IGF-2. Unlike IGF-1R, IGF-2R has no signaling function and mediates internalization and degradation of IGF-2, which is important to regulate the activity of IGF-1R, so that IGF-2R has a tumor suppressor function (Pavelic et al. 2002). Unlike IGF-2, IGF-2R is subjected to paternal imprinting. Mice harboring disrupted IGF-2R genes (-/-) or with null maternal allele (-/p) show overgrowth during

embryonic development and die at the neonatal stage due to somatic overgrowth with abnormal skeleton, cardiac muscle and lung (Wylie et al. 2003).

The family of IGFBPs is the major regulator of IGF bioactivity, by binding and releasing IGFs (Figure 1.1) (Shimasaki and Ling 1991). IGFBPs bind to more than 99% of circulating IGFs and protect IGFs from degradation. At least 75% of circulating IGFs are bound by a ternary complex composed of IGFs, IGFBP-3 and the acid labile subunit, which is capable of prolonging the half-life of the IGF/IGFBP-3 binary complex (Hwa et al. 1999; Yu et al. 1999a). IGFBPs are negatively regulated by IGFBP-specific proteases, which cleave IGFBPs from IGFs/IGFBPs complexes (Figure 1.1), leading to release IGFs, thus activating IGF signaling (Collett-Solberg and Cohen 1996). For example, prostate-specific antigen (PSA) is characterized as an IGFBP-3 protease, which can cause proteolysis of IGFBP-3, reducing its binding affinity to IGF-1 (Moschos and Mantzoros 2002).

1.1.2 IGF-1R

IGF-1R is a cell surface receptor tyrosine kinase (RTK) that is expressed in all types of cells except hepatocytes and T lymphocytes (Sachdev and Yee 2001).

The human IGF-1R is transcribed from a single gene and synthesized as a single chain with a 30-amino acid signal peptide that is cleaved after translation, leading to processing of the remaining polypeptide into alpha and beta subunits (Ullrich et al. 1986). Disulfide bonds link two extracellular alpha subunits and two transmembrane beta subunits, which contain tyrosine kinase activity, to form a heterotetrameric complex that constitutes mature IGF-1R (Lemmon and Schlessinger 2010). The IGF-1R is activated by IGF-1 and IGF-2, and by insulin only at supra-physiological concentration (micromolar). The signaling pathways controlled by IGF-1R play a crucial role in normal cell growth and differentiation, as well as many key aspects of neoplasia including transformation and anti-apoptotic signaling (Baserga et al. 2003; Chitnis et al. 2008; Pollak 2008).

The importance of IGF-1R in development is demonstrated by genetic studies, reporting that IGF-1R null mice have more severe growth deficiencies (45% size of wild-type mice) compared to IGF-1 null mutants. In addition to developmental delay, IGF-1R null mice die after birth resulting from respiratory failure, and have other defects in muscle and central nerve system (Liu et al. 1993). Patients have been reported with a missense IGF-1R mutation, showing mild intrauterine growth failure, progressive postnatal growth retardation, severe failure to thrive, and microcephaly (Abuzzahab et al. 2003; Walenkamp

et al. 2006).

1.1.3 The signaling pathways activated by IGF-1R

IGF-1R activation is triggered by ligand binding, inducing IGF-1R clustering and autophosphorylation at sites 950, 1131, 1135 and 1136 (OConnor et al. 1997). Receptor autophosphorylation leads to the activation of several key signaling pathways (Figure 1.1). Phosphorylated tyrosine 950 serves as a major docking site for several receptor substrates, including insulin receptor substrates 1 to 4 (IRS-1 to IRS-4) and Src homology and collagen domain protein (SHC) (Sehat et al. 2007). Phosphorylated IRS-1 binds the regulatory subunit p85 of phosphoinositide 3-kinase (PI3K) to activate PI3K activity, leading to increased levels of membrane bound phosphatidylinositol 3,4,5-triphosphate (PIP3) resulting from phosphatidylinositol-4,5-bis-phosphate (PIP2) phosphorylation. In turn, this event results in the phosphorylation of protein kinase B (AKT) by two kinases, which are respectively PIP3-dependent protein kinase-1 (PDK1) and the mammalian target of rapamycin complex 2 (mTORC2). AKT enhances the activity of the mammalian target of rapamycin complex 1 (mTORC1) by phosphorylating and inactivating the tumor suppressor tuberous sclerosis complex 2 (TSC2). Tuberous sclerosis complex 1 (TSC1) and TSC2 form a heterodimer that inhibits the activity of RAS homologue enriched in brain

(Rheb), a small GTPase that regulates the activation of mTORC1. There are a number of downstream signaling events mediated by active mTORC1, including induction of protein synthesis via activating or inhibiting phosphorylation of downstream targets. mTORC1 inactivates eukaryotic translation initiation factor 4E (eIF4E)-binding protein 1 (4E-BP1) by phosphorylation to release eIF4E to initiate protein synthesis. Conversely, phosphorylation by mTORC1 activates p70 S6 kinase, which phosphorylates and activates ribosomal protein S6 to induce translation at the ribosome (Chitnis et al. 2008; Laplante and Sabatini 2009; Zha and Lackner 2010) (Figure 1.1).

The activity of PI3K-AKT signaling is regulated at several levels. The continuous activity of mTORC1 negatively regulates IGF-1R signaling by phosphorylating and inactivating IRS-1 to attenuate PI3K-AKT activity (Manning and Cantley 2007). AKT is also negatively regulated by phosphatase and tensin homolog (PTEN), which is a tumor suppressor gene that dephosphorylates PIP_3 to PIP_2, thereby suppressing AKT signaling activity to inhibit cell survival. Mice harboring mutated-PTEN die at day E9.5 of development, and show overgrowth in cephalic and caudal regions (Stambolic et al. 1998).

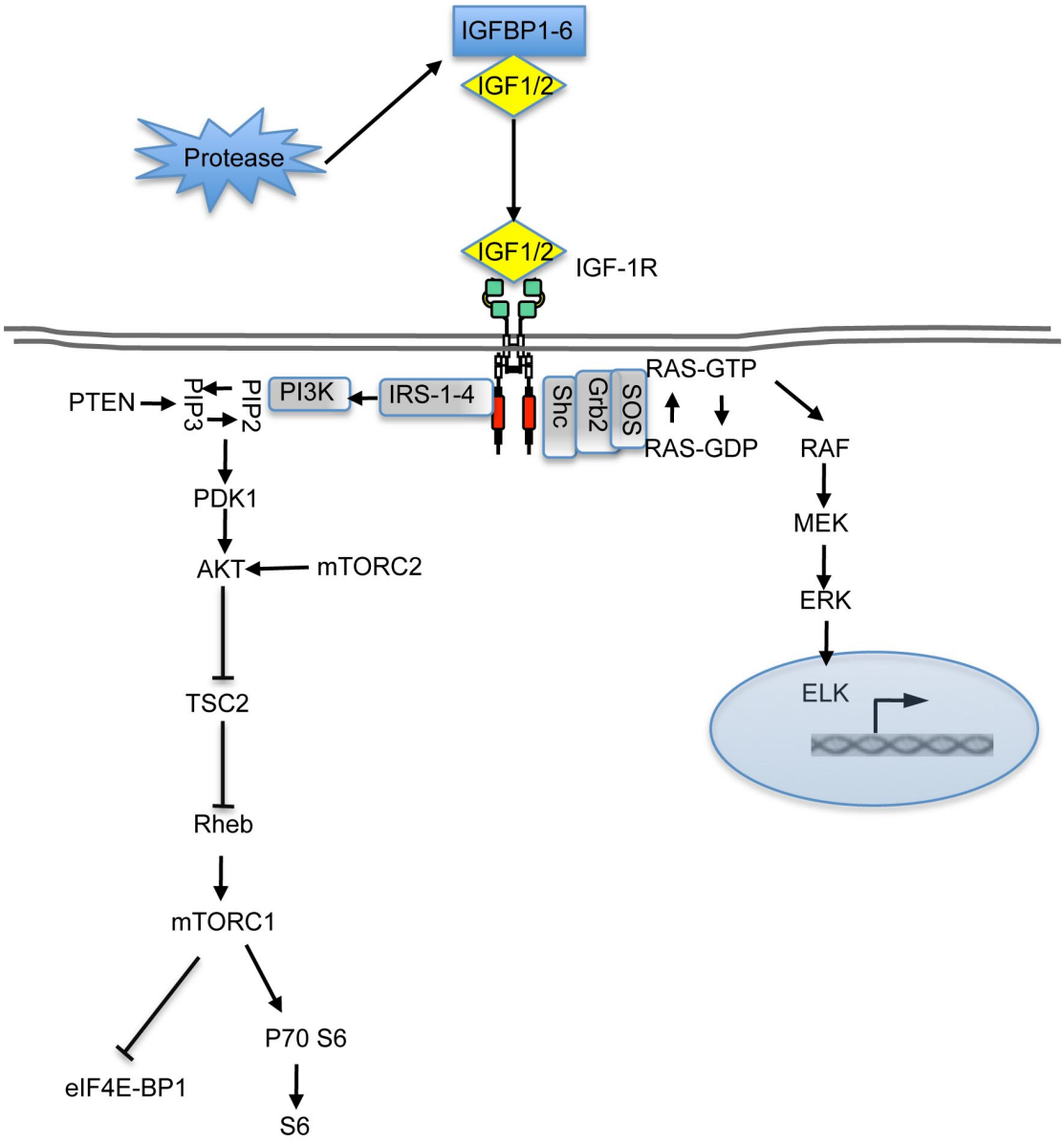

Figure 1.1 The major signaling pathways activated by IGF-1R. Binding of IGF1/2 results in activation of PI3K-AKT and MAPK cascades.

The second main signaling pathway activated by IGF-1R is the mitogen-activated protein kinase/extracellular signal-regulated kinase 1/2 (ERK1/2) pathway (Figure 1.1). Binding of SHC to the IGF-1R leads to recruitment of growth factor receptor-bound protein 2 (GRB2) and the mammalian homolog of son of sevenless (SOS). This event results in the activation of RAS, a small GTPase. Subsequently, the activated RAF serine/threonine-protein kinase, mainly c-RAF, phosphorylates and activates the dual specificity mitogen-activated protein kinase kinase 1/2 (MEK1/2), which, in turn, phosphorylates and activates ERK1/2. There are approximately 160 target genes identified as being regulated by ERK1/2, which play an important role in cell proliferation and differentiation (Skolnik et al. 1993; Yoon and Seger 2006; Chitnis et al. 2008) (Figure1.1).

In addition to the above two major pathways, there are additional signaling pathways activated by IGF-1R. Firstly, IGF-1R directly phosphorylates janus kinase 1/2 (JAK1/2), which then phosphorylates and activates a family of signal transducers and activators of transcription (STATs) that regulates growth, survival and differentiation (Zong et al. 2000). Secondly, PI3K is activated by IGF-1 to promote activation of Rac, a Rho GTPase, which further leads to the activation of the downstream effectors LIM kinase and cofilin, leading to cell motility and migration via the actin reorganization and actin/myosin contractility

(Meyer et al. 2005).

1.1.4 Crosstalk between IGF-1R and other signaling pathways

Biological crosstalk occurs when one or more components of one signaling pathway affect another signaling pathway by direct interaction or regulation of its components, and the combinatorial signal should produce a different signal than that triggered by each pathway alone (Vert and Chory 2011). The IGF system interacts with or regulates many other signaling pathways. Some key interactions are summarized below.

1.1.4.1 IGF-1R and insulin receptor (IR)

The insulin receptor (IR) shares 70% similarity in amino acid sequence with the IGF-1R, and like IGF-1R, is also transcribed from single gene, processed into an alpha and beta subunits and expressed as $\alpha_2\beta_2$ tetramers on the cell surface (Ullrich et al. 1986). The two receptors have similar structure but completely different functions in organisms and cells. Unlike the IGF-1R which regulates cell proliferation and differentiation, IR promotes the uptake of glucose via phosphorylation of IRS leading to high affinity binding of glucose transporters to

the outer membrane of insulin-responsive cells or tissues (Saltiel and Kahn 2001). Mice harboring disrupted IR alleles are born at the normal size and with no obvious deficiencies, suggesting that IR is dispensable for murine intrauterine development. However, they rapidly develop diabetes accompanied by a marked postnatal growth retardation (up to 30-40% of littermate size), skeletal muscle hypotrophy and fatty infiltration of the liver, leading to death within 7 days (Joshi et al. 1996).

Human cells express two IR isoforms resulting from alternative splicing. IR-B is the classical IR that includes sequence encoded by exon 11, and plays a major role in the uptake of glucose. By contrast, IR-A lacks exon 11, and has been shown to be activated not only insulin and proinsulin but also IGF-2, leading to proliferation and protection from apoptosis (Malaguarnera et al. 2012). Thus IR-A functions more like IGF-1R, and is suggested to play a critical role in cancer biology. In addition, IR-A/B can form hybrid receptors with IGF-1R, with different ligand-binding affinity properties (Belfiore et al. 2009; Pollak 2012).

1.1.4.2 IGF-1R and wingless (Wg)/integration (Int) (WNT)

The wingless (Wg)/intergration (Int) (WNT) signaling pathway is involved in cell proliferation, migration, polarity establishment and stem cell self-renewal

(Logan and Nusse 2004; Reya and Clevers 2005). Deregulation of WNT signaling is associated with cancer development, typically in the intestine, but also in the prostate (Reya and Clevers 2005; Yardy and Brewster 2005).

There are two typical WNT signaling pathways, classfied according to the involvement of β-catenin (Figure 1.2). These are the canonical pathway, which regulates the activity of β-catenin, and the non-canonical pathway that does not involve β-catenin (Logan and Nusse 2004; Semenov et al. 2007). The WNT canonical signaling pathway consists of the WNT ligands, receptors Frizzled (Fz) and low density lipoprotein receptor-related protein 5/6 (LRP5/6). Activated receptors recruit Drosophila dishevelled (Dsh) homlogs (DVLs) to Fz and Axin to LRP5/6 respectively. This leads to disassembly of the β-catenin destruction complex consisting of Axin, adenomatous polyposis coli (APC), and glycogen synthase kinase 3β (GSK3β), resulting in the stabilization of β-catenin. Subsequently, stabilized β-catenin translocates into the nucleus, and binds to the transcription factors of the lymphoid enhancer factor/T cell factor (LEF/TCF) family. Binding of β-catenin switches LEF/TCF to the activated state inducing transcription of WNT target genes (Gordon and Nusse 2006). Besides the above canonical pathway, WNTs can also signal via DVL to activate various non-canonical pathways including Rho/JNK planar cell polarity, and the mTOR pathway (Semenov et al. 2007). WNTs were shown to be capable of activating

the mTOR pathway by inactiviting GSK3β, thereby relieving GSK3β-mediated phosphorylation and inactivation of TSC2, leading to activation of mTOR (Inoki et al. 2006).

There are several known interactions between IGF-1R and WNT signaling pathways. Firstly, IGF-1 stimulation increases the transcriptional activity of LEF/TCF via GSK3β inhibition by AKT and RAS activity (Desbois-Mouthon et al. 2001). Sceondly, activation of IGF-1R leads to dissociation of β-catenin/E-cadherin complexes, and binding of β-catenin to the adaptor protein IRS-1. This complex is capable of translocating to the nucleus, to enhance the transcriptional activity of LEF/TCF (Playford et al. 2000; Chen et al. 2005). Thirdly, recent studies from our group and others showed that IGF-1R is able to translocate into the nucleus, via SUMOylation following kinase activation, and nuclear IGF-1R binds to chromatin, suggesting that nuclear IGF-1R functions as a transcriptional regulator or chromatin modifier (Aleksic et al. 2010; Sehat et al. 2010). It has been further shown that nuclear IGF-1R interacts with β-catenin and LEF/TCF to increase the expression of Axin2 and Cyclin D1 (Warsito et al. 2012).

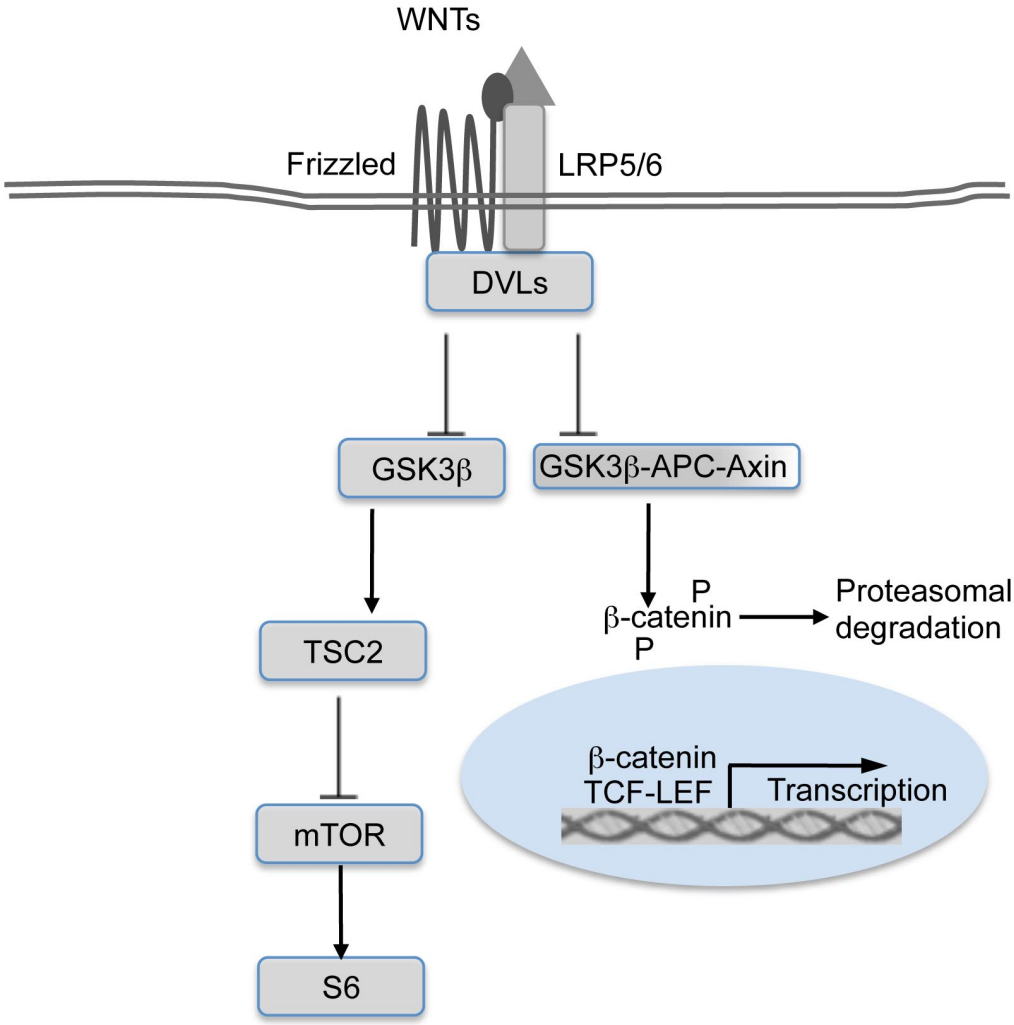

Figure 1.2 WNT signaling pathways. Left side: WNT noncanonical signaling pathway, showing how WNTs positively regulate the mTOR pathway. Right side: WNT canonical signaling pathway.

1.1.4.3 IGF-1R and Epidermal Growth Factor Receptor (EGFR)

The epidermal growth factor receptor (EGFR/HER1) is a member of the EGFR family, which includes four structurally related transmembrane RTKs (HER1-4) consisting of an extracellular ligand binding domain, a single transmembrane region and a cytoplasmic tyrosine kinase domain (Yarden 2001). EGFR is activated by its ligands including epidermal growth factor and transforming growth factor alpha to form EGFR homodimers or heterodimers with other HER receptors. Dimerization results in receptor autophosphorylation and activates downstream signaling pathways including the AKT, ERK1/2 and c-Jun N-terminal kinase pathways (Normanno et al. 2006).

IGF-1R and EGFR have similar roles in cell proliferation, protection from apoptosis, and differentiation, and also share the same downstream signaling pathways (van der Veeken et al. 2009). The interaction between IGF-1R and EGFR is observed by reciprocal coimmunoprecipitation, and EGFR is reported to regulate the stability of IGF-1R protein (Riedemann et al. 2007). Blocking EGFR results in increased activity of IGF-1R, and in turn, depletion of IGF-1R leads to enhanced activation of EGFR. Consequently, activation of IGF-1R or EGFR is reported as a mechanism to enhance resistance to inhibitions of either receptor (Burgaud and Baserga 1996; Riedemann et al. 2007).

It has been shown that IGF-1R and HER2 are able to form a complex in cells that are resistant to anti-HER2 antibody Trastuzumab, but not in Trastuzumab-sensitive parental cells. IGF-1 stimulation increases the phosphorylation of HER2 in resistant cells, and treatment with IGF-1R antibody disrupts IGF-1R/HER2 complexes and increases sensitivity to Trastuzumab (Nahta et al. 2005).

1.1.4.4 IGF-1R and Estrogen Receptor (ER)

The estrogen receptors (ERs) are a group of estrogen-activated receptors consisting of ERα and ERβ. The main function of ERs is as transcriptional factors that regulate gene expression (McDonnell and Norris 2002). There are several different regulatory connections between ER and IGF signaling. Upon binding by estrogen, ERα is released from a complex with heat shock protein (HSP) and forms a dimer which can directly bind to the IGF-1R promoter to increase its transcription (Fagan and Yee 2008). IGFs have been shown to activate ERα to increase its transcriptional activity, independent of estrogen (Lee et al. 1997). The two major signaling pathways activated by IGF-1R have been demonstrated to activate ER via phosphorylation, by AKT on ER at the site of serine 167, and by active ERK1/2 via phosphorylation of ER at serine

118 (Kato et al. 1995; Campbell et al. 2001). Conversely, estrogen has been shown to induce rapid phosphorylation of IGF-1R and ERK1/2, and interaction between IGF-1R and overexpressed ERα are detected in COS7 and L6 cells (Kahlert et al. 2000).

1.1.4.5 IGF-1R and Androgen Receptor (AR)

The androgen receptor (AR) is a type of nuclear receptor that is activated by binding of androgen. Activated AR disassociates from HSPs, and undergoes dimerization, leading to translocation from the cytoplasm to the nucleus where it acts as a transcription factor (Gao 2010). As with ER signaling, there is crosstalk between AR and the IGF axis. AR can bind to the promoter of IGF-1 to increase the expression level of IGF-1 (Cardozo et al. 2007). It has been shown that inhibition of PI3K/AKT promotes AR transcriptional activity. In turn, blockade of AR results in activation of PI3K/AKT in PTEN-deficient mouse prostate cancer and human prostate cancer cells (Sawyers et al. 2011).

1.2 The role of IGF-1R in cancer

Cancer is a clinical entity that includes more than 100 diseases in which uncontrolled cell growth is accompanied by the ability to invade and

metastasize to distant sites. During cancer development, normal cells acquire a set of genetic mutations, resulting in the malignant state. For example, activated oncogenes can acquire function, or conversely tumor suppressor gene can lose function via mutations, enabling normal cells to gain a series of characteristics termed “hallmarks of cancer“ that facilitate malignant progression, including: 1) the ability to sustain cell proliferation, 2) escape from growth suppressor signals, 3) resisting cell death signals, 4) limitless replicative potential, 5) induction of angiogenesis, 6) acquired ability to invade and metastasize, 7) new program for energy metabolism, 8) ability to evade immune destruction (Hanahan and Weinberg 2000; Hanahan and Weinberg 2011). These characteristics are not independent but are highly inter-related.

The importance of IGF-1R signaling in tumor biology is supported by many pieces of evidence. Firstly, it has been established that high circulating levels of IGF-1 are associated with increase in the relative risk for developing colon (Rinaldi et al. 2010), breast (Hankinson et al. 1998; Key et al. 2010), prostate (Chan et al. 1998; Roddam et al. 2008) and lung cancer (Yu et al. 1999b). It is also found that IGF-1, IGF-2 and/or IGF-1R are overexpressed in many human tumors, including colon (Tricoli et al. 1986), lung (Minuto et al. 1986), melanoma (Kanter-Lewensohn et al. 1998), and in work from our lab, bladder (Rochester et al. 2007), kidney (Yuen et al. 2007), and prostate cancers

(Hellawell et al. 2002). It has been shown that IGF-1R promoter is targeted by several oncogenes including c-myb and hepatitis B virus X protein to increase IGF-1R expression at the transcriptional level (Reiss et al. 1991; Kim et al. 1996). The tumor suppressor protein 53 (p53) is a core guardian protein that regulates many processes including cell cycle progression, genome stability and apoptosis. Mouse double minute 2 (MDM2) is a negative regulator of p53 which functions as an E3 ubiquitin ligase to degrade p53 (Michael and Oren 2003). It has been shown that wild-type p53 negatively regulates IGF-1R and IGF-2 expression via suppressing the IGF-1R and IGF-2 promoters. In contrast, tumor-derived, mutated p53 significantly increases IGF-1R promoter activity, suggesting increased IGF-1R expression resulting from p53 loss-of function may facilitate malignant cell progression (Ohlsson et al. 1998; Larsson et al. 2005). IGF-1R expression is also negatively regulated by Von Hippel Lindau (VHL) tumor suppressor gene as shown by our group work (Yuen et al. 2007). Also tumor suppressor genes and oncogenes can also regulate IGF-1R at the protein levels and activity. IGF-1R can be activated by the src oncogene of Rous sarcoma virus via increased phosphorylation (Larsson et al. 2005). By contrast, MDM2 can bind to and ubiquitinate IGF-1R, leading to IGF-1R degradation (Girnita et al. 2003).

Secondly, the IGF-1R has an important role in the establishment and

maintenance of transformation (Sell et al. 1994) and in properties required for tumor growth including cell proliferation and protection from apoptosis (Baserga et al. 2003; Pollak 2012). Finally, IGF-1R has an important role in cancer metastasis (Samani et al. 2007).

1.2.1 IGF-1R mediates malignant transformation

Baserga's group established a fibroblast cell line, the R- cell line, from IGF-1R null mouse embryo fibroblasts (MEFs) (Sell et al. 1994). It was found that R- cells are unable to be transformed by many cellular and viral oncogenes including SV40 T antigen, activated H-RAS, c-RAF and bovine papilloma virus, which are capable of transforming many cell lines. The resistance of R- cells to transformation can be abolished by expression of wild-type human IGF-1R. In contrast, wild-type MEFs are easily transformed by these oncogenes, suggesting that IGF-1R is important for transformation (Sell et al. 1993; Sell et al. 1994; Baserga 1995; Morrione et al. 1995). However, subsequent study showed that R- cells can be transformed by v-src, which is a oncogenic tyrosine kinase, and GTPase-deficient mutant human Galpha13, which is highly oncogenic when overexpressed *in vitro*, suggesting that IGF-1R is necessary for cells to be transformed by certain oncogenes but not all (Liu et al. 1997; Valentinis et al. 1997).

Additional IGF axis components are also required for transformation. Cells fail to transform if IRS-1 is not expressed, disrupted by siRNA knockdown, or unable to be phosphorylated on tyrosine residues due to mutation. In these situations, ectopic expression of IRS-1 can reverse the failure of transformation (Dambrosio et al. 1995; DeAngelis et al. 2006; Baserga 2009). It has been shown that constitutive PI3K and AKT activity resulting from mutated PI3K is also involved in transformation (Kang et al. 2005).

1.2.2 Role of IGF-1R in malignant cell growth

IGF-1R has an important role in regulation of the cell cycle and proliferation, mainly via its two major signaling pathways described in the previous section. IGF-1R is particularly required for anchorage-independent growth, which is an important property for malignant cell growth (Baserga 1995; Baserga et al. 2003).

IGF-1R regulates cell cycle progression mainly by facilitating the G1-S transition, through increasing expression of cyclin D1 and cyclin-dependent kinase 4, leading to phosphorylation of retinoblastoma protein to release the

transcription factor E2F (Rosenthal and Cheng 1995). The ability of IGF-1R to regulate cyclin D1 expression is mediated by ERK1/2 or PI3K/AKT (Lavoie et al. 1996; Muise-Helmericks et al. 1998).

In the majority of metazoan cells, a solid substratum is required to grow and divide, and cells will undergo apoptosis if they lose contact with other cells or the substratum. This is anchorage dependence of growth. In contrast, transformed or tumor-derived cells show anchorage-independent growth *in vitro*, and this strongly correlates with their invasion capacity *in vivo* (Shin et al. 1975; Carney et al. 1980). It has been shown that anchorage-independent growth can be acquired by the ectopic expression of IGF-1R and IRS-1 (Baserga 1999). The depletion of IGF-1R can significantly reduce cell growth under anchorage-independent conditions and inhibit formation of tumors in immunodeficient mice. By contrast, the antisense-mediated depletion of IGF-1R has no major effect on cell growth in monolayer growth conditions (Resnicoff et al. 1994). However, more recent data have challenged this finding, showing that IGF-1R inhibition can inhibit growth of monolayer conditions (Stromberg et al. 2006; Moser et al. 2008; Potratz et al. 2010).

1.2.3 IGF-1R mediates protection from apoptosis

IGF signaling has been demonstrated to protect against apoptosis, and inhibition or knockdown of IGF-1R induces apoptosis in many cancer cells (D'Ambrosio et al. 1996; O'Connor et al. 1997; Jernberg-Wiklund and Nilsson 2007). Apoptosis is a major form of cell death that is mediated by an intracellular program (Lawen 2003). There are four major cell death pathways, distinguished according to their morphological appearances: apoptosis, necrosis, autophagy and association with mitosis such as mitotic spindle catastrophe (Kroemer et al. 2009).

Apoptosis can be activated by intrinsic and extrinsic pathways as illustrated in Figure 1.3. The intrinsic signaling pathway is initiated by the perturbation of intracellular homeostasis, such as by DNA damage, oxidative stress, hypoxia or the deprivation of growth factors (Elmore 2007). A healthy cell is protected by anti-apoptotic proteins including B-cell lymphoma 2 (Bcl-2), B-cell lymphoma extra large (Bcl-XL), and myeloid cell leukemia 1 (MCL-1), expressed on the outer membrane of mitochondria to inhibit apoptosis by governing the permeability of the mitochondria membrane. Internal damage signals inhibit anti-apoptotic proteins and activate pro-apoptotic proteins including BCL-2 antagonist of cell death (BAD), Bcl-2 homologous antagonist killer (BAK),

Bcl-2-associated X protein (BAX), BCL-2-interacting domain death agonist (BID) and BCL-2-interacting mediator of cell death (BIM) to open pores in the mitochondrial membrane. This event leads to release of cytochrome c to bind and activate apoptotic protease activating factor-1 (Apaf-1) and pro cysteine-dependent aspartate-specific protease 9 (caspase-9), known as apoptosome bodies (Yang et al. 1997; Marsden et al. 2002). This further leads to cleavage of pro-caspase-9 to activate the executor caspases 3 and/or 7 by a further series of proteolytic steps (Li and Yuan 2008). The extrinsic signaling pathway is initiated by the tumor necrosis factor (TNF) receptor gene superfamily including TNF receptor 1 and Fas receptor. The activated receptors recruit Fas-associated death domain protein (FADD), caspase 8 and 10 to form a complex termed the death inducing signaling complex (DISC), which leads to activation of executor caspase-3 and 7 (Igney and Krammer 2002).

IGF-1R protects cells from apoptosis, principally by the PI3K-AKT pathway, which regulates the expression and activity of Bcl-2 family proteins at different levels (Kooijman 2006). IGF-1R activation phosphorylates and inactivates BAD to prevent apoptosis via AKT signaling (Peruzzi et al. 1999). Again, via PI3K-AKT, IGF-1R mediates the phosphorylation of cAMP-responsive element binding (CREB) protein to enhance CREB protein transcriptional activity, leading to increased expression levels of Bcl-2, Bcl-XL and MLC-1 (Du and

Montminy 1998; Pugazhenthi et al. 1999; Pugazhenthi et al. 2000).

IGF-1R is also reported to affect the extrinsic apoptotic pathway by regulating TNF receptors and their ligands. Blockade of IGF-1R signaling pathway has been show to lead to the overexpression of TNF-related apoptosis inducing ligand (TRAIL) in melanoma and colon cancer cells (Wang et al. 2002; Karasic et al. 2010). IGF-induced AKT activation leads to phosphorylation and inactivation of forkhead box O3 (FOXO3), resulting in decreased expression of Fas ligand to prevent apoptosis (Brunet et al. 1999). It has also been shown that IGF-1R can downregulate Fas receptor in ovarian mesothelial cells (Coppola et al. 1999). Taken together, IGF-1R signaling protects cell from apoptosis via affecting both the intrinsic and extrinsic pathways of apoptosis.

1.2.3 IGF-1R in metastasis

Metastasis occurs when cancer cells spread to distant sites and colonize there to form new tumors. The expression of IGF-1R is highly associated with development of lung metastasis in synovial sarcoma (Xie et al. 1999), and with incidence of liver metastasis and mortality in uveal melanoma patients (All-Ericsson et al. 2002). Overexpression of IGF-1R in lung carcinoma cells enhances cell proliferation, clonogenic survival and invasion, and gives rise to

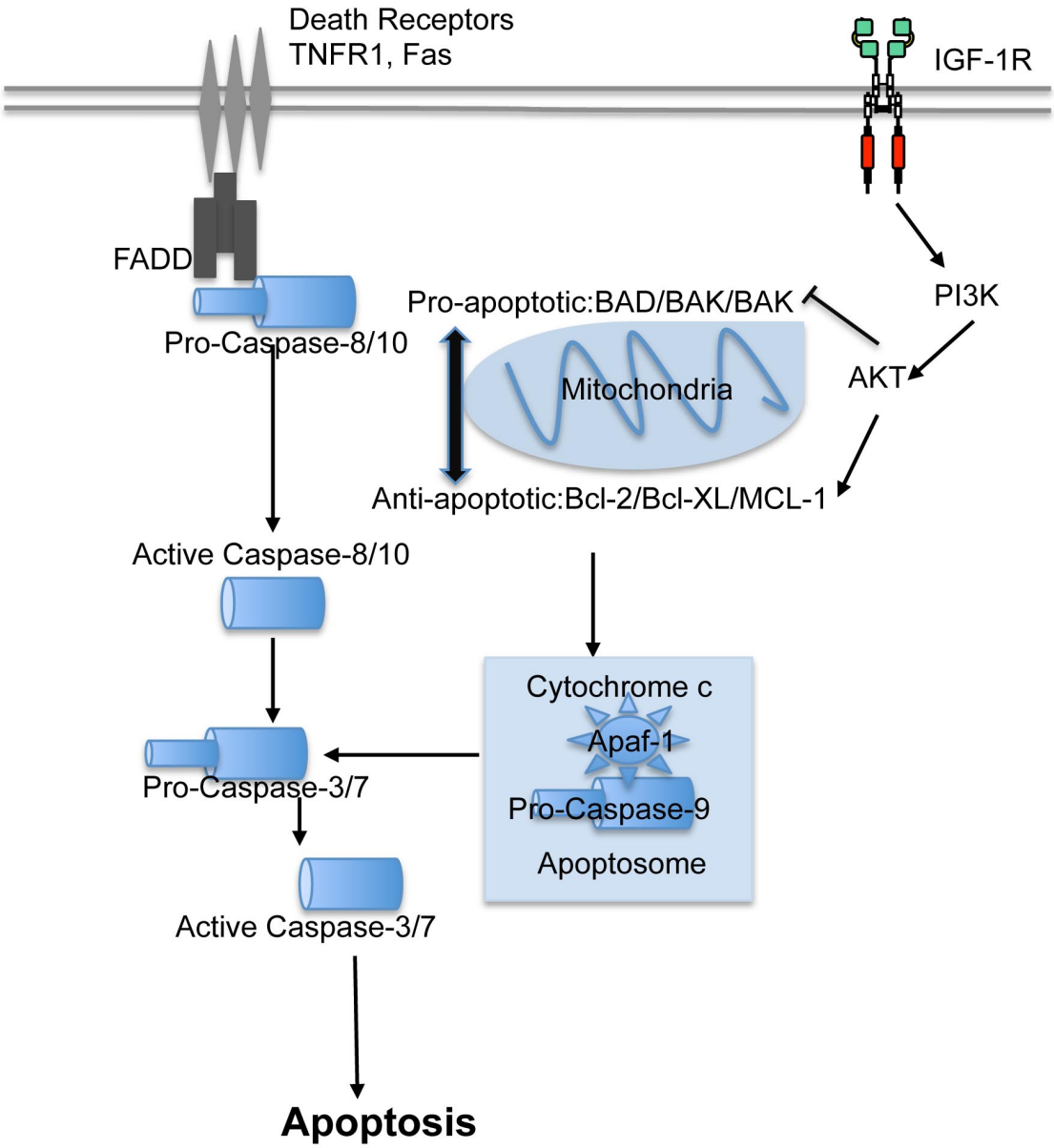

Figure 1.3 Schematic pathways of apoptosis and IGF-1R role in apoptosis. The left side shows the extrinsic apoptotic signaling pathway, the central panel represents the intrinsic apoptotic signaling pathway, and the right side shows regulation of apoptosis by IGF-1R.

multiple tumor nodules and an increased incidence of liver metastasis in immunodeficient mice (Long et al. 1998). In mice expressing the SV40 T antigen in the pancreas under the control of the rat insulin promoter, overexpression of IGF-1R accelerates the development of invasive cancers that metastasize to lymph nodes (Lopez and Hanahan 2002).

The classical process of metastasis is an orderly sequence, involving tumor-induced new vascularization (angiogenesis and lymphangiogenesis), extracellular matrix (ECM) degradation, cell movement through blood vessels, cell survival and proliferation in the circulation, and colonization at the new sites (Pantel and Brakenhoff 2004; Nguyen et al. 2009). IGF-1R has an important role at each of these steps (Samani et al. 2007). As tumors grow, it is essential to develop new blood vessels, a process called angiogenesis, which provides nutrition and oxygen, and disposes of metabolic waste. This process is mainly mediated by vascular endothelial growth factor (VEGF)-A that binds to VEGF receptor 2 (Ferrara 2002). Hypoxia is a strong stimulus for angiogenesis in solid tumors, leading to the activation of hypoxia-inducible factor 1α (HIF-1α) and 2α (HIF-2α), which are transcription factors that induce expression of VEGF (Carmeliet and Jain 2000). It has been shown that IGF-1 and IGF-2, by activating PI3K and ERK1/2, increase synthesis of HIF-1α protein and enhance the expression of VEGF under normoxia in the colon cancer cells (Fukuda et al.

2002). In turn, HIF-1α can regulate expression of IGF-2, IGF-2R and IGFBP-3 (Feldser et al. 1999). IGF-1 and IGF-2 also affect the migration and morphological differentiation of endothelial cells to induce angiogenesis (Shigematsu et al. 1999; Lee et al. 2000). Mice harboring vascular endothelial cells with specific knockout of IR or IGF-1R show significant reduction in retinal neovascularization under hypoxia compared with normoxia, also suggesting that IR or IGF-1R play an important role in angiogenesis (Kondo et al. 2003). Tumor cells can also induce the formation of new lymphatic vessels, termed lymphangiogenesis, which is mediated by VEGF-C and VEGF-D. The regional lymph nodes are a common site for initial spread of some malignancies including carcinomas of breast, colon and prostate (Oliver and Detmar 2002). It has been shown that IGF-1R via PI3K/AKT and ERK1/2, positively regulates the expression of VEGF-C and lymphatic metastasis, and the induced expression of VEGF-C can be abolished by ectopic expression of kinase-domain-mutated IGF-1R (Tang et al. 2003). IGFs can also promote the increased motility and proliferation of lymphatic endothelial cells (Bjorndahl et al. 2005).

In order for tumor cells to spread, it is essential that ECM is broken down by a family of proteinases known as the matrix metalloproteinases (MMPs) (Zhang et al. 2003). This is a family of zinc-dependent endoproteinases that are

synthesized and secreted as inactive pro-MMPs in most cases, and are regulated by the tissue inhibitors of MMPs (TIMPs) (Kleiner and Stetler-Stevenson 1999). Membrane type 1-MMP (MT1-MMP) is expressed in the majority of invasive tumors. MT1-MMP binds to proMMP-2 and TIMP-2, leading to the proteolytic cleavage and activation of MMP-2, and ECM proteolysis (Nishida et al. 2008). It has been shown that IGF-1R regulates the expression of MT1-MMP and MPP-2 via the PI3K-AKT pathway, to affect the invasion of cancer cells (Zhang and Brodt 2003; Zhang et al. 2003).

1.2.4 Involvement of IGF-1R in the repair to DNA damage

Cancer development is associated with defects of DNA repair signaling pathways (Lord and Ashworth 2012). It has been shown that overexpression of IGF-1R leads cells to resist killing by ionizing radiation, and is associated with cancer recurrence in irradiated sites in breast cancer patients, suggesting that IGF-1R mediates radioresistance (Turner et al. 1997). Subsequently, it has been found by our group and others that IGF-1R inhibition or gene silencing enhances sensitivity to ionizing radiation and DNA-damaging cytotoxic drugs. This is associated with reduction in DNA stranded breaks (DSBs) repair by homologous recombination (HR) (Rochester et al. 2005; Allen et al. 2007; Iwasa et al. 2009; Riesterer et al. 2011; Turney et al. 2012). IGF-1 is reported to

promote the interaction of IRS-1 with Rad51, facilitating Rad51 import into the nucleus, and its participation in the strand invasion step of HR repair (Trojanek et al. 2003), although this interaction is not detected by our group in human prostate cancer cells (Turney et al. 2012).

1.3 IGF-1R inhibitors and antibodies in clinical trials

Given these roles of IGF-1R in cancer biology, IGF-1R becomes an attractive target for cancer treatment. There are several approaches targeting the IGF-1R axis that have been developed and tested, including reduction of IGF-1R expression, blockade of interaction between ligand and receptor, and inhibition of receptor kinase activation (Yuen and Macaulay 2008; Zha and Lackner 2010). In the clinic, two major approaches are used to inhibit IGF-1R. Antibodies block the interaction between ligands and receptor, and small molecule inhibitors block the activity of the IGF-1R kinase. More than 30 agents targeting IGF-1R have been in pre-clinical or clinical development, with at least 70 clinical trials evaluating anti-IGF-1R agents alone or in various combinations (Gualberto and Pollak 2009)(www.clinicaltrials.gov).

IGF-1R antibodies have shown little single agent activity in common cancers,

but in combination with chemotherapy have shown activity in non-small cell lung cancer (NSCLC), and pancreatic cancer, and there are no major side effects (Karp et al. 2009; Tolcher et al. 2009; Javle 2011). Figitumumab, a fully human IgG2 monoclonal IGF-1R antibody, (CP-751,871, Pfizer) has single agent anti-tumor activity in Ewing Sarcoma (Olmos et al. 2010), and in NSCLC almost doubled the response rate to carboplatin/taxol chemotherapy (Karp et al. 2009). However, phase III figitumumab clinical trials have been suspended because no benefit was observed in unselected NSCLC patients after interim analysis (Jassem 2010). So far, there are limited data on small molecule inhibitors. One inhibitor, INSM18, which also inhibits HER2, has shown limited activity in prostate cancer (Harzatark 2007). More clinical results from inhibitor trials including kinase domain inhibitors are expected. It is essential to know why some patients get a lot of benefit, but others do not. One example where targeted treatments are shown to benefit specific molecularly defined cancers is gefitinib (Iressa), an EGFR tyrosine kinase inhibitor. This agent initially failed to show benefit in unselected NSCLC patients. However, gefitinib has become an important therapeutic, after it was shown that EGFR kinase domain mutations increase sensitivity to gefitinib (Paez et al. 2004), and this mutation is enriched in Asian, non-smoking female patients with adenocarcinoma, where there was clear and significant benefit after treatment with gefitinib (Mok et al. 2009). Such kinase domain mutations have not been found in the IGF-1R, and

aside from reports of a link of circulating IGF levels or expression levels of IGF-1R to sensitivity to IGF-1R inhibition (Gong et al. 2009; Gualberto et al. 2011), there has been no clear identification of tumor factors that regulate sensitivity to IGF-1R inhibition. It is important to be able to identify factors that regulate sensitivity to IGF-1R inhibition, to develop predictive biomarkers for IGF-1R treatment, to increase the efficacy of IGF-1R inhibition, and to design rational combination treatments in the clinic.

1.4 RNA interference (RNAi) and SLL screens

1.4.1 RNAi

RNA interference (RNAi), or post-transcriptional gene silencing, is a highly evolutionarily conserved pathway, and a common mechanism of regulating gene expression in eukaryotic organisms. It has been shown that small double-stranded RNA (dsRNA) suppresses target gene expression by the complementary binding and degradation of its target mRNA in a homology-dependent way (Hannon 2002; Almeida and Allshire 2005). The RNAi phenomenon was originally identified in plants when studies aimed at overexpressing genes led unexpectedly to co-suppression of the endogenous gene (Napoli et al. 1990). Then a similar phenomenon was observed in Caenorhabditis elegans, but how gene silencing was triggered by introduction

of RNA remained unclear, because anti-sense and sense RNA were both able to silence the target (Guo and Kemphues 1995). Pioneering work by Mello and Fire in 1998 involved injection of long dsRNA into Caenorhabditis elegans, leading to 10-100 fold more effective gene silencing than could be induced by single-stranded RNA (Fire et al. 1998).

Subsequently, it was shown that after delivery into cells or organisms, dsRNA was cut by an enzyme called Dicer into small fragments known as short interfering RNA (siRNA). These are 21- to 27-nucleotide double-stranded oligonucleotides with a characteristic 2-nucleotide 3′ overhang (Bernstein et al. 2001). These duplexes are incorporated into the RNA-induced silencing complex (RISC) containing the core Argonaute protein, where siRNAs are unwound and the antisense strand hybridizes to the complementary mRNA. This allows the nuclease activity of RISC to induce the destruction of the target transcript (Martinez et al. 2002).

In mammalian cells, however, long dsRNAs are able to induce an interferon response, which is the first line of defense against viral infection, and subsequently leads to a global shutdown of protein synthesis (Reynolds et al. 2006). However, synthetic siRNAs, designed to mimic endogenous 21

nucleotide siRNAs, or plasmids expressing short hairpin RNAs (shRNA), can be introduced into mammalian cells to avoid the interferon response, mediating gene silencing without significant adverse effects (Elbashir et al. 2001; Kim and Rossi 2007). With the availability of whole genome sequence, siRNA libraries have been assembled, and are designed to maximize the probability of potent target gene silencing while minimizing the risk of off-target effects (Huesken et al. 2005; Turner et al. 2008).

1.4.2 Synthetic sickness/lethality (SLL) and its application

Synthetic lethality is defined as a situation when a combination of mutations in two or more genes leads to cell death, while a mutation in only one of these genes does not. It was first described in Drosophila *melanogaster,* where crossing between organisms harboring mutations in certain non-allelic genes was lethal even though the homozygous parents were perfectly viable (Dobzhansky 1946; Lucchesi 1968). Subsequently, this concept was extended to describe the situation in which the combination of two defects impairs the fitness of organism or cell, rather inducing lethality, and this has been called synthetic sickness (Rehman et al. 2010). SLL can occur between genes sharing the same biochemical pathway (Hartman et al. 2001), or in distinct but compensatory pathways, and the members of the same biochemical pathway

often have the same partners (Brough et al. 2011). SSL has been applied in range of experimental conditions, including combinations of perturbations such as gene overexpression, gene silencing, inhibition of protein function using chemical inhibitors, or environmental change (Luo et al. 2009b; Ferrari et al. 2010; Yang et al. 2010).

SSL provides a way to develop cancer specific agents by targeting the defects of cancer. This can increase therapeutic efficacy and decrease toxicity to patients. The importance of SSL in cancer therapy has been demonstrated by effects of poly(ADP-ribose) polymerase (PARP) inhibition in cells harboring mutation in breast cancer type 1 susceptibility protein (BRCA1) or breast cancer type 2 susceptibility protein (BRCA2). Cells defective in BRCA1/2 are unable to repair DSBs by HR, and are therefore highly sensitive to inhibition of PARP, required for the base excision repair pathway, and for the repair of single stranded breaks (SSBs). After PARP is inhibited, persistent SSBs accumulate and cause stalling and collapse of the replication fork, generating more DSBs. In normal cells, these can be repaired by HR. However, BRCA1/2 mutant cells are unable to repair these DSBs, resulting in lethality (Bryant et al. 2005; Farmer et al. 2005). *In vitro*, cells with mutated BRCA1 and/or BRCA2 are over 1000 times more sensitive to PARP inhibitors than wild-type cells. This effect has been observed in breast, ovarian, pancreatic and cervical cancer

cells either with endogenous or experimentally imposed BRCA defects, indicating that synthetic lethality between PARP and BRCA1/2 is a highly dominant effect (Farmer et al. 2005; McCabe et al. 2005; Edwards et al. 2008). These observations paved the way for clinical studies of PARP inhibitors. An orally active PARP inhibitor Olaparib (AZD2281, AstraZeneca) has been tested in the clinic. Phase 1 and 2 trial results suggest that this inhibitor has anti-tumor activity in patients harboring BRCA1 and/or BRCA2 mutations, without causing many serious side effects compared to conventional chemotherapy (Fong et al. 2009; Audeh et al. 2010; Tutt et al. 2010).

1.4.3 siRNA high-throughput screen (HTS)

Traditionally genetic studies to investigate gene function are carried out by inducing gene mutations at random, and then identifying and mapping the mutated gene that caused the abnormal phenotype, so called forward genetics. The process is quite time-consuming and not easily applicable to mammalian cell systems. Conversely, reverse genetic strategies are able to direct the mutated gene of interest, so as to determine its function based on the observed phenotype. The traditional gene knockout, either in cell systems or organisms, is expensive and time-consuming and not suitable for genome-scale screens. RNAi provides a way of investigating effects of loss of function, and represents

a tool to carry out large-scale screens in cell culture systems (Echeverri and Perrimon 2006; Boutros and Ahringer 2008). One of its applications is the HTS for SSL.

There are now examples of successful siRNA screens to identify SSL circuits, shedding light on tumor biology and with relevance to treatment. K-RAS is a small GTPase that is often activated by mutation in colorectal, pancreatic and lung cancers. A genome-wide siRNA screen has been employed to identify a set of genes, including polo-like kinase 1 (PLK1) and anaphase promoting complex/cyclosome, whose depletion significantly impaired the viability of K-RAS mutated NSCLC cell lines (Luo et al. 2009a). The Ashworth group has successfully applied siRNA screens to identify determinants of sensitivity to different therapeutic targets. For example, patients often develop resistance to drugs that target estrogen signaling in breast cancer. Cyclin-dependent kinase 10 (CDK10) has been shown to be an important biomarker for resistance to tamoxifen, since CDK10 silencing results in increased expression of c-RAF and activation of ERK1/2, which leads to loss of tumor cell reliance upon estrogen signaling (Iorns et al. 2008). Also, they identify a new set of transcription-coupled DNA repair genes, including proliferating cell nuclear antigen (PCNA) and XPA binding protein 2, whose silencing increases sensitivity to PARP inhibitor. This suggests that DNA repair pathways other

than HR regulate sensitivity to PARP inhibition (Lord et al. 2008; Turner et al. 2008).

1.5 The aims of this project

IGF-1R inhibitory drugs have been in clinical use for only 4-5 years and a major challenge is to identify factors mediating sensitivity to these agents. A small molecule inhibitor (AZ12253801) targeting the IGF-1R kinase has been provided by AstraZeneca for use in a siRNA screen. The goals of my work were outlined as following:

1) To evaluate effects of IGF-1R inhibition by AZ12253801 in human DU145 prostate cancer and MCF-7 breast cancer cells
2) To screen siRNA libraries targeting DNA repair-associated and kinase-related genes, to identify proteins that regulate sensitivity to IGF-1R inhibition
3) To validate screen hits
4) To address the molecular mechanisms behind any observed synthetic sickness/lethal interaction

Chapter 2

Materials and methods

2.1 Cell lines and culture

Human DU145 prostate cancer and MCF-7 breast cancer cells were obtained as low passage stocks from Cancer Research UK Cell Services. Human PC3, LNCaP, LNCaP-LN3 and 22Rv1 prostate cancer cells were gifts from Sir. Walter Bodmer, University of Oxford. Human HCT116 and HCT116 KO22 colon cancer cells were gifts from Prof. Todd Waldman in Georgetown University School of Medicine. All cell lines were grown in sterile, mycoplasma-tested media in tissue culture grade flasks, dishes and plates, and were cultured in RPMI-1640 (DU145, LNCaP, LNCaP-LN3), Ham's F12 (PC3), DMEM (MCF7) or McCoy's 5A (HCT116, HCT116 KO22) medium supplemented with 10% fetal calf serum (FCS). Cultures were maintained in a humidified atmosphere of 5% CO_2 and 95% air (DU145, PC3, LNCaP, LNCaP-LN3, HCT116 and HCT116 KO22) or 10% CO_2 and 90% air (MCF-7).

The identity of the prostate cancer cell lines was validated by short tandem repeat (STR) assay performed at Cancer Research UK laboratory, Clare Hall, Hertfordshire UK.

For routine passage, cells were disaggregated using 3mM EDTA in phosphate buffered saline (PBS) or Trypsin. Cells were washed in complete medium and reseeded into new flasks or plates. At the start of this project, early passage cells were expanded for cryopreservation: cells were resuspended in 10% dimethyl sulphoxide (DMSO), 50% FCS in the appropriate medium, aliquoted into sterile Nunc vials, frozen overnight to -80°C and then transferred to liquid nitrogen. To recover frozen stocks, the frozen cell suspension was thawed rapidly to 37°C and transferred to flasks with complete medium to culture. All primary screens were performed using cells of passage 3-4, and all experiments in this thesis were performed using cells at passage 3-10.

2.2 Chemical compounds and treatments

The IGF-1R inhibitor AZ12253801 was provided by AstraZeneca. XAV939 was obtained from Selleck Chemical, DVL PDZ domain inhibitor II (DVLi) from Calbiochem. All compounds were dissolved in DMSO to a final concentration of

10mM (AZ12253801, XAV939 and PPP) or 100mM (DVLi), aliquoted and stored at -80°C. Compounds were further diluted in the appropriate culture medium to achieve the correct working concentration.

2.3 Protein analysis

2.3.1 Collection and lysis of adherent cells

Adherent cells were washed twice with ice-cold PBS and lysed in the dish by scraping into IGF-1R lysis buffer (50mM Hepes, 100mM sodium chloride, 10mM EDTA, 4mM sodium pyrophosphate, 2mM sodium orthovanadate, 10mM sodium fluoride and 1% Triton-X-100, EDTA-free protease inhibitor cocktail, and 1.5mM Pefabloc SC Plus® (Roche)). Alternatively cells were scraped into cold PBS, centrifuged at 13,000rpm for 5 minutes at 4°C and cell pellets were frozen in liquid nitrogen and stored at -80°C. Cell pellets were thawed on ice and lysed in lysis buffer as above. Lysates were incubated on ice for 30 minutes and insoluble debris was pelleted by centrifugation at 13,000rpm for 10 minutes at 4°C. Supernatants were collected and the protein concentrations were determined by BCA™ Protein Assay (Thermo Scientific).

2.3.2 Immunopreciptation

Approximately 1-2mg of total protein was used in immunoprecipitation, using IGF-1R lysis buffer to equalize the concentrations of all samples in a small volume (0.1-1ml). Samples were pre-cleared with 1μg of random IgG (rabbit IgG, Sigma) and 50μl protein A or G beads at 4°C for one hour. After centrifugation at 13,000rpm for 2 minutes, pre-cleared supernatants were incubated with 1-5μg of primary antibodies or random IgG at 4°C from 4 hours to overnight. Immunoprecipitates were collected using swelled protein A or G beads for one hour. Beads were washed 3-6 times with IGF-1R lysis buffer containing protease inhibitors. After the final removal of all wash buffer, 3X Laemmli loading buffer was added to each sample and samples were vortexed, and denatured for 5 minutes at 95°C. After centrifugation at 13000rpm for three minutes, samples were loaded onto SDS-PAGE gels for electrophoresis and western blot.

2.3.3 Co-immunprecipitation

Cells were lysed in Co-IP buffer (150mM NaCl, 50mM Tris-HCl PH 7.5, 0.5% NP-40, with protease inhibitors as section 2.3.1 and Sigma phosphatase inhibitor cocktails II and III). A total 1-5mg of cell extract was pre-cleared as above and incubated with 1-5μg specific antibodies or random IgG overnight at

4°C on a rotating wheel. Antibodies were collected using swelled protein A or G beads at 4°C for one hour. Beads were washed 3 times with Co-IP lysis buffer, and analyzed by SDS-PAGE and western blot. Membranes were probed for co-precipitated proteins and then reprobed for the precipitated protein.

2.3.4 Western blot

Proteins were separated by SDS polyacrylamide gel electrophoresis (SDS-PAGE) according to molecular weight, and transferred onto Hybond-C extra nitrocellulose membrane (Amersham Pharmacia Biotech) in semi-dry transfer buffer (48mM Tris-Cl, 39mM glycine, 20% methanol, 1.3mM SDS (final pH 9.2) using a semi-dry transfer apparatus (Hoefer Semiphor Transfer Unit, Amersham Biosciences) at a constant current of 150mA per 8X10cm gel for 1 hour. The membranes were blocked in blocking buffer (5% non-fat milk or 5% Bovine serum albumin (BSA) (Sigma) in 0.1% Triton-X-100 in PBS (PBST) for thirty minutes at room temperature on a shaking platform. Antibodies used are listed in the Table 2.1. Membranes were incubated with the primary antibody diluted in blocking buffer overnight at 4°C or two hours at room temperature. After washing three times for 10 minutes with 0.1% PBST, membranes were incubated with goat anti-rabbit or goat anti-mouse secondary antibody conjugated to horse-radish peroxidase (DAKO, Ely, UK) for one hour at room

temperature. Membranes were washed as above and proteins were detected using an Enhanced Chemiluminescence kit (ECLplus®, Amersham Pharmacia Biotech). Antibodies used for western blot were listed in table 2.1

2.3.5 Quantification of radiographs

The radiographs were scanned and imported into Adobe Photoshop. Generally, faint exposures were used for quantification to minimize errors resulting from signal saturation. Band intensity was quantified using ImageJ software, and measured protein levels were corrected by normalizing to the loading control.

2.3.6 Glutathione S-transferase (GST) pull-down

2.3.6.1 GST or GST fusion protein purification

GST, and GST-c-RAF RAS binding domain (aa1-149) (GST-RBD) fusion constructs were gifts from Dr. Stephan Feller, Department of Oncology, University of Oxford. The plasmids were transformed into BL21 Escherichia coli cells and a single colony was picked into 10ml of lysogeny broth (LB) medium with 100μg/ml ampicillin. After growth overnight at 37°C with shaking (230rpm), 2ml of the overnight culture was diluted into 100ml fresh medium and cultured until the OD_{600} reached 0.8-1. At this point, protein expression was induced by

Table 2.1 Antibodies used for western blot

Antibody	Source	Primary Dilution	Molecular Weight
IGF-1Rβ	Cell Signaling (3027)	1:3000	95kDa
P-IGF-1Rβ	Cell Signaling (3024)	1:1000	95kDa
DVL3	Cell Signaling (3218)	1:1000	88-93kDa
DVL2	Cell Signaling (3216)	1:1000	90-95kDa
P-ERK/2	Cell Signaling (4377)	1:1000	42 & 44kDa
Total ERK1/2	Cell Signaling (4695)	1:1000	42 & 44kDa
P-mTOR	Cell Signaling (2971)	1:1000	289kDa
Total mTOR	Cell Signaling (2972)	1:1000	289kDa
P-S6	Cell Signaling (2215)	1:3000	32kDa
Total S6	Cell Signaling (2217)	1:1000	32kDa
PTEN	Cell Signaling (9559)	1:1000	54kDa
P-MEK1/2	Cell Signaling (2338)	1:1000	45kDa
MEK1/2	Cell Signaling (4694)	1:1000	45kDa
AR	Cell Signaling (3202)	1:1000	110kDa
IRS-1	Cell Signaling (2382)	1:1000	180kDa
β-arrestin1/2	Cell Signaling (4674)	1:1000	50kDa
Pan-Ras	Calbiochem(OP40)	1:5000	21kDa
Rad51	Abcam (ab1837)	1:1000	37kDa
DAB2	Abcam (ab76253)	1:1000	96kDa
Active β-catenin	Millipore (05-665)	1:5000	92kDa
SHC	BD Transduction Lab (610878)	1:1000	66, 52 & 46kDa
Rad23B	BD transduction Lab (611018)	1:1000	60kDa
GRB2	BD Transduction Lab (610111)	1:5000	24kDa
SOS1	BD Transduction Lab (610096)	1:1000	170kDa
β-tubulin	Sigma (T2046)	1:10000	50 kDa

adding 2mM Isopropyl β-D-1-thiogalactopyranoside. After 3 hours, bacteria were collected by centrifugation at 8,000rpm for 5 minutes at 4°C and crude bacterial lysates were prepared by sonication in lysis buffer (50 mM Tris-HCl, pH 7.4, 1.5 mM EDTA, 1mM dithiothreitol, 10% (v/v) glycerol, 150mM NaCl and protease inhibitor as section 2.3.1) and centrifuged at 13,000rpm for 30 minutes at 4°C to remove insoluble debris. Lysates were incubated with glutathione sepharose beads for 30 minutes at room temperature or 2 hours at 4 °C on a rotating wheel. The beads were washed in lysis buffer 3-6 times, incubated with elution buffer (10mM reduced glutathione/ 50mM Tris-HCL pH 8.0/ 5% glycerol) for 15 minutes at room temperature and pelleted by centrifugation at 6,000 rpm for 5 minutes. The yield and purity of expressed protein was checked by SDS-PAGE, and concentration was determined by BCA™ Protein Assay (Thermo Scientific).

2.3.6.2 RAS activation assays

This assay exploits the ability of activated (GTP-bound) RAS, but not inactive (GDP-bound) RAS to bind to RAF (Vojtek et al. 1993). Prostate cancer cells were collected in RAS assay lysis buffer (25mM Hepes pH7.5, 150mM NaCl, 10mM $MgCl_2$, 1mM EDTA, 10% glycerol, 1% NP-40, 0.25% deoxycholate with EDTA-free protease inhibitors (Roche)). Lysates were cleared by centrifugation

at 13,000 rpm for 30 minutes at 4°C. A total of 500µg of cell lysate was incubated with 50µg of the appropriate purified GST or GST-RBD beads at 4°C for one hour with rotation. After washing 3-6 times with RAS assay lysis buffer, samples were analyzed by western blot for RAS.

2.3.6.3 GST pull-down assay

Recombinant GST, and GST fusion proteins representing full length GRB2 (GST-GRB2), GRB2 amino- or carboxy terminal SH3 domain (GST-N-SH3, GST-C-SH3) or GRB2 SH2 domain (GST-SH2) were gifts from Dr. Stephan Feller. Collected prostate cancer cells were lysed in Co-IP lysis buffer, and lysates were cleared by centrifugation at 13,000 rpm for 30 minutes at 4°C. A total 1-3mg of cell lysate was incubated with 50µg of the appropriate purified GST or GST fusion protein for overnight with rotation at 4°C. The binding reaction was then added to 30µl of glutathione sepharose beads and mixed at 4 °C for 2 hours. After 3 washes with Co-IP lysis buffer, samples were analyzed by western blot.

2.3.7 Lambda protein phosphatase assay

Cells were lysed in phosphatase assay lysis buffer (150mM NaCl, 50mM Tris.Cl pH7.5, 0.5% NP-40) for 30 minutes on ice, and cleared by centrifugation at 13,000rpm for 30 minutes at 4°C. A total of 100μg protein was incubated with solvent control or 800 units of lambda protein phosphatase (Sigma # P9614) with or without phosphatase inhibitor cocktail II and III (Sigma) at 30°C for 20 minutes. Samples were analyzed by SDS-PAGE and western blot.

2.4 Handling of DNA

2.4.1 Handling of bacteria

A plasmid encoding human DVL3 (pCDNA3.1(+zeo)-Flag-DVL3) was obtained from Addgene (www.addgene.org/16758) as a bacterial stab, which was streaked onto LB-agar with ampicillin and incubated at 37°C overnight. The individual single colony was visible in the second day.

2.4.2 Preparation of plasmids

A single colony was picked into LB medium with ampicillin and grown overnight in a 230rpm shaker at 37°C. Preparation of plasmids used the QIAGEN plasmid

mini kit or midi kit. To prepare miniprep DNA, briefly, 3ml overnight growing bacterial culture was collected by centrifugation at 8000rpm for 1 minute. Cells were resuspended in 250μl of P1 buffer with RNase. Then 250μl of P2 buffer was added to lyze cells and denature DNA. Within 5 minutes, 350μl N3 buffer was added for neutralization. After centrifugation at 13,000rpm for 15 minutes, the supernatant was applied to a column containing silica-gel that is the DNA binding reagent. After a wash using PE buffer, 50μl of water was added to elute plasmid DNA. For midi-scale preparation of DNA, 50ml overnight growing bacterial culture was collected by centrifugation and resuspended in 4ml P1 buffer. Then 4ml P2 lysis buffer and 4ml neutralizing P3 buffer were added sequentially. The supernatant was applied to a QIAGEN-tip 100 equilibrated with 10ml QBT buffer. After washing the tip using QC buffer, DNA was eluted using 5ml QF buffer. DNA was pelleted by adding 0.7 volume of isopropanol and centrifuging for 30 minutes at 13,000rpm. The Flag-DVL3 construct was verified by restriction enzyme digest and sequencing in the WIMM sequencing facility.

2.4.3 DNA digest with restriction enzymes

Plasmid DNA was digested with restriction enzymes using manufacturer's recommended 10X restriction buffer. Routinely, 1μg of plasimid DNA was

digested with 3-6 units of restriction enzyme for 1 hour at 37°C in a total volume of 20µl, and then analyzed by agarose gel electrophoresis.

2.4.4 Transfection of plasmid DNA

The day before transfection, $2X10^6$ DU145 cells were seeded in 10cm dishes. The following day, 10µg of plasmid DNA was diluted in 1.5ml Opti-MEM and incubated at room temperature or 10 minutes, and 30µl of Fugene HD transfection reagent (Promega) was added in 1.5ml Opti-MEM and incubated at room temperature for 10 minutes. The plasmid and Fugene HD mixes were combined and incubated at room temperature for 30 minutes, and then added dropwise to the plated cells. After 4 hours, 7ml of fresh culture medium with 10% FCS was added. Samples were collected after 48-72 hours for further analysis.

2.5 Cell based assays

2.5.1 Growth assays

2.5.1.1 Cell proliferation assay/Celltiter-Glo

Cells were seeded or reverse transfected with siRNAs into u-clear 96-well plates (Grenier Bio-one) using 1000 DU145 cells or MCF-7 cells per well, and

after two days, triplicate wells were treated with inhibitor or solvent. The CellTiter-Glo (CTG) Luminescent cell viability assay (Promega) measures ATP-induced luminescence, a measure of the number of metabolically active viable cells. The assay reagent, containing cell lysis buffer and a thermostable luciferase, was added directly to wells containing cells and an equal volume of medium. Plates were shaken for 2 minutes at room temperature, and after 10 minutes at room temperature to allow the signal to stabilize, the plates were read in a luminometer (Fluorstar Optima, BMG Labtech). All scores were normalized to solvent (DMSO)-treated cells (designated 100% growth). Using data from at least 3 independent experiments, curves were fitted to the data points using GraphPad Prism v5, and the GI_{50} values (concentration required to inhibit 50% of growth) were extrapolated from these curves.

2.5.1.2 Clonogenic survival assay

Clonogenic survival assay determines the ability of a cell to proliferate indefinitely, thereby retaining its reproductive ability to form a large colony or a clone (Munshi et al. 2005). In order to assay clonogenic survival, 1000 cells were seeded per well of 6-well plates. The following day, cells were treated with solvent or compound, and allowed to proliferate for 10-14 days at 37°C in 5% or 10% CO_2 until visible colonies were observed. Cell colonies were fixed in

Methanol:Acetic Acid (3:1) for one hour, and stained using 0.1% crystal violet (Sigma) overnight. After washing, cell colonies were counted using either a manual Colony Counter (Stuart Scientific, Stone, UK) or an automated Colcount (Optronix, Oxford, UK). All colony numbers were normalized to the solvent-treated cells (designated 100% survival). Curves were fitted to the data points using GraphPad Prism v5, and the SF_{50} values were calculated from these curves.

2.5.2 Immunostaining and microscopy

Cells were seeded onto coverslips, and transfected with siRNA or treated using chemical inhibitors. Cells then were washed twice with ice-cold PBS, fixed with 4% paraformaldehyde or formaldehyde in PBS for 15 minutes, and blocked with 5% BSA (Sigma) in PBST for 30 minutes at room temperature. Cells were stained with primary antibodies diluted in PBST overnight at 4°C. After three washes with PBST, cells were incubated with secondary antibody conjugated to Alexa Fluor 488 (1:2000, Molecular Probes AF21206) for one hour in the dark. After washing three times in 0.1% PBST, coverslips were mounted with ProLong Gold antifade reagent with DAPI (Molecular Probes). Preparations were analyzed using either a Zeiss Axioskop 2 plus or a Nikon Eclipse 80i

fluorescence microscope equipped with a Plan Apo 63 or 63/1.4 objective. Images were acquired using either AxioVision or Lucia G/F software.

2.6 siRNA screens

2.6.1 RNAi libraries and siRNAs

The protein kinase siRNA library (siARRAY, targeting 779 known and putative human protein kinase genes, Appendix Table S1) was obtained in ten 96-well plates from Dharmacon (USA). Each well in this library contained a SMARTPool of four distinct siRNAs targeting different sequences of individual target transcripts. The human DNA Repair siRNA Set V1.0 siRNA library (Qiagen, UK, Appendix, Table S2) was arrayed in six 96-well plates. To the libraries were added Allstars (AS) and PLK1 siRNAs, diluted to a final concentration of 2μM and aliquoted into plates at 7.5μl in each well. Prepared plates were stored at -20°C.

In second round screens of 53 potential hits, the kinome pooled siRNAs were deconvoluted into four individual siRNAs, information on siRNA sequence in Appendix Table S1. The siRNAs to DNA repair-associated genes were ordered from QIAgen as Flexitube siRNA, containing 4 distinct siRNAs targeting one

Table 2.2 siRNAs used for gene silencing

siRNA	Source
AllStars negative control siRNA	QIAgen (1027281)
Hs_PLK1_6	QIAgen (SI02223837)
Hs_DVL3_6	QIAgen (S102781387)
Hs_DVL3_7	QIAgen (S1030954630)
Hs_DVL1_7	QIAgen (S102757384)
Hs_DVL2_1	QIAgen (S100063434)
Hs_IGF1R_1	QIAgen (S100017521)
Hs_GRB2_5	QIAgen (S100300328)
Hs_DAB2_6	QIAgen (S102780386)
Hs_IRS1_1	QIAgen(S100078631)
Hs_β-arrestin-1_11	QIAgen (S102776921)
Hs_β-arrestin-2_10	QIAgen (S102776928)

gene (Appendix Table S3). Other specific siRNAs used in this study are listed in Table 2.2

2.6.2 siRNA screen method

Prepared plates containing siRNAs were thawed at room temperature. For reverse transfection, Dharmafect transfection reagent was added to wells containing siRNAs, using 0.225µl Dharmafect transfect reagent 1 per well for DU145 and 0.3µl/well Dharmafect 3 for MCF-7 cells, in 52.5µl of the appropriate medium (without antibiotics and FCS). Then 20µl of the transfection mix was aliquoted into two new plates. After 30 minutes, 1000 cells per well in 80µl appropriate medium (RPMI-1640 for DU145 and DMEM for MCF-7, without antibiotics) were added into every well. The plates were incubated at 37°C for 6.5 hours and then the transfection medium was removed and replaced with 100µl complete medium including 10% FCS and antibiotics. At 48 hours after transfection, half of the plates were treated with 100µl of the appropriate medium containing 0.01% DMSO vehicle and the other half with AZ1223580 at the GI_{50} concentration, previously established in CTG assays for DU145 and MCF-7 cells. Cell viability was assessed after 5 days using CTG assay. The full primary screen was completed in duplicate, and the data were analyzed as described (Boutros et al. 2006; Martin et al. 2011), to derive a

Z-score that represented the effect of siRNA on cell growth or effect of inhibitor, corrected for within plate and between plate variations:

2.6.2.1 Z-score for cell growth:

1) The raw CTG reading (Y) for each individual siRNA on cell growth was transformed using Log2 (Log2(Y)).

2) The transformed log2(Y) score was firstly corrected to the median of each plate (M), i.e., $\mathrm{Y_{corrected}} = \mathrm{Log2(Y)} - \mathrm{M}$.

3) $M_{absolute}$ is a median which was $Y_{corrected}$ absolutely corrected to the median of $Y_{corrected}$.

4) Median absolute deviation (MAD) was derived from $M_{absolute}$ with an adjusted factor of 1.4826, i.e., $\mathrm{MAD} = 1.4826 \times \mathrm{M_{absolute}}$.

5) $Y_{corrected}$ was normalized based on $M_{corrected}$ and MAD. $M_{corrected}$ is the median of all corrected scores, i.e., $\mathrm{Z_{cell\ growth}} = \frac{\mathrm{Y_{corrected}} - \mathrm{M_{corrected}}}{\mathrm{MAD}}$.

2.6.2.2 Z-score for inhibitor effect:

1) The corrected growth score in inhibitor-treated group ($Y_{inhibitor\text{-}corrected}$) was subtracted by the corrected growth score of DMSO-treated group ($Y_{DMSO\text{-}corrected}$) ($Y_{effect}=Y_{inhibitor\text{-}corrected}-Y_{DMSO\text{-}corrected}$).

2) $Z_{\text{inhibitor}} = \frac{Y_{\text{effect}} - M_{\text{effect}}}{MAD_{\text{effect}}}$

2.6.2.3 Z' factor calculation

The Z' factor that represents the screen windows, was calculated using the AS and PLK1 control wells. AS and PLK1 values were calculated relative to the surviving fraction in the mock-transfected wells (transfection reagent only).

$Z' = 1 - \frac{(3\times(A+B))}{C+D}$, where A equals the mean of the relative surviving fraction from the negative control wells (AS), B the mean of relative surviving fraction from the positive controls (PLK1) and C and D, standard deviations of relative surviving fraction from positive and negative controls, respectively.

2.6.3 Validation of siRNA screen

Four individual siRNAs and a pool of the four siRNAs targeting each gene were used to revalidate hits from the primary screen. Three independent replicates were performed in both cell lines. The average effect of each individual or pooled siRNA on cell growth ($Y_{averaged}$) was centered on the median of every plate (M_{plate}) ($Y_{corrected}$= $Y_{averaged}$- M_{plate}). The cell surviving fraction for each individual or pooled siRNA was calculated as the centered average effect of each siRNA in inhibitor-treated wells divided by the average effect of each siRNA in DMSO-treated wells (SF= $Y_{corrected\text{-}inhibitor}$/ $Y_{corrected\text{-}DMSO}$). Then this

surviving fraction was transformed to log2 as the final score of the effect of IGF-1R inhibition on each siRNA. Any score < -0.2 was regarded as significant (Lord et al. 2008).

2.7 Validation of hits

2.7.1 siRNA reverse transfection in 6-well plate

For validation of knockdown, 5µl of 20µM siRNA was diluted in 500µl of serum-free culture medium, Dharmafect 1 or 3 (5µl) was diluted in 500µl of serum-free culture medium, and after 5 minutes the two were mixed and incubated for 30 minutes at room temperature. Then $2X10^5$ DU145 or $4X10^5$ MCF-7 cells were added in antibiotic-free, 10% FCS medium and incubated for 6.5 hours at 37°C. The mix was removed and replaced with 3 ml of culture medium with 10% FCS and antibiotics. After 48 or 72 hours, cells were collected and lysed in IGF-1R lysis buffer for by western blot, or used for RNA extraction and quantitative real-time reverse transcription PCR (qRT-PCR).

2.7.2 Primer design

Primers for qRT-PCR were designed using a web-based tool (Primer-BLAST) (http://www.ncbi.nlm.nih.gov/tools/primer-blast/) to generate product size <

Table 2.3 Primers used for qRT-PCR

Target	Primer	Sequences (5' – 3')	Annealing temp	Product size
DVL1	Forward	TGAAGCACGGCTTCCTGCGG	60	242bp
	Reverse	GTCCTGGTAGGCAGGCGGGA		
DVL2	Forward	AGCAGTGAGCATGGCGCTGG	60	249bp
	Reverse	TGACGTCCTCTCCAGGCGGG		
DVL3	Forward	GGCGGCGGAAGCAGAAGGTT	63	163bp
	Reverse	CCGTCACCACGCTCGTTGCT		
GAPDH	Forward	AGCCACATCGCTCAGACAC	60	65bp
	Reverse	GCCCAATACGACCAAATCC		
AKAP1	Forward	ATGCCGGGCACCTGTTCGTG	60	183bp
	Reverse	CCACTTGGGCTCGCCACCAG		
APEG1	Forward	GAGTGCCCCCGAAAAGGGCC	60	102bp
	Reverse	ACACCGCCGCGTTCTTCAGG		
CNSR1	Forward	CCAGCTCTGCCCCCAAAGCC	60	78bp
	Reverse	TCCACCCCGCCCAGGATGAG		
LMTK3	Forward	GCGCATCGGAGACTACGGGC	60	248bp
	Reverse	CACATGCTGCTGGCGGACCA		
HUNK	Forward	AGGAGGGCCTGTGTTGCCCA	60	153bp
	Reverse	GCTGGCCTCCAGGGGCCTAT		
DUSP5	Forward	TGCCGGCCCTATCTGGCCTT	60	219bp
	Reverse	TCGCAGCTTCTGCCAGTGGC		
MPP2	Forward	GCACCACGGTGCCCTACACC	60	229bp
	Reverse	ACCTTCACCGCCTGGGGGTT		
FOS	Forward	GCCTGTCAACGCGCAGGACT	60	106bp
	Reverse	CACCAGCCACTGCAGGTCCG		
TAF1	Forward	GGACCCGGCTGCGATTTGCT	60	166bp
	Reverse	CGCTTTCCCCCTCCAGCTGC		
TBP	Forward	CAGGCCAGGCACCACAGCTC	60	230bp
	Reverse	TTCGGCGTTTCGGGCACGAA		
Cyclin D1	Forward	GAAGATCGTCGCCACCTG	60	60bp
	Reverse	GACCTCCTCCTCGCACTTCT		
CDKN3	Forward	CGCAGATGGAGGGACTCCTGACA	60	193bp
	Reverse	TCGCAGGCTGTCTATGGCTTGC		
INO80C	Forward	GGTGGCGCAGTAGCTGGCAA	65	275bp
	Reverse	CTCAGGGCCAGGTAGCCGGT		
Rad23B	Forward	GCAGTGAGCTCCTGCCAGCA	60	105bp
	Reverse	GCAGGTGTGGAAGTGGGGGC		

300bp and were purchased from Invitrogen. The primers for qRT-PCR are listed in the table 2.3.

2.7.3 Extraction of total RNA and reverse transcription

Total RNA was extracted using the RNeasy micro kit (QIAgen) according to the manufacturer's instruction and treated to remove DNA using the DNA-free™ Kit (AB Applied Biosystems). RNA concentrations were measured by Nanodrop spectrophotometer (Nanodrop technologies, Wilmington, DE, USA). cDNA was synthesized by reverse transcribing total RNA using the High Capacity cDNA Archive® Kit (AB Applied Biosystems) according to the manufacturer's instructions. Briefly, up to 1µg of total RNA was added to PCR reaction tubes and DEPC-treated water was added to a final volume of 50µl. A reaction mastermix was prepared, comprised of 10µl of 10x RT buffer, 10µl of 10x Random primers, 4µl of 25x dNTPs, 21µl of DEPC water and 5µl of reverse-transcriptase per reaction. Then 50µl of this mix was added to each sample, and reactions were incubated at 25°C for 10 minutes and 37°C for two hours in a PCR machine. Then cDNAs were stored at -20°C until further analysis.

2.7.4 qRT-PCR

The qRT-PCR reactions were performed in triplicate, prepared by robot, in the Rotor Gene 3000® qPCR system (Corbett Research, Sydney, Australian) using the SensiMixTM SYBR Kit (www.quantace.com) according to the manufacturer's instructions. Briefly, 20µl of one reaction contained 20ng of total cDNA, 10pmol of each primer, 10µl of 2x SYBR mixture consisting of Heat-activated DNA polymerase, ultra-pure dNTPs, $MgCl_2$ (6mM), and SYBR® Green I. The reactions were first incubated at 95°C for 15 minutes to activate the DNA polymerase, followed by 40 cycles of 95°C for 10 seconds and 60°C for 40 seconds, and melted from 50°C to 99°C to check the peak of the melting curve.

2.8 Statistical analysis

The graphing and statistical analysis software Prism v.5.0 (GraphPad) and Excel (Microsoft) were used to plot and analyze data. Graphs were plotted to show mean values, and error bars. Error bars were standard deviation (SD) or the standard error of the mean (SEM). The student's t-test and analysis of variance (ANOVA) were used for the comparison of mean values between two and multiple (>2) data sets, respectively. A minimum of 95% level of significance ($p<0.05$) was used to define statistical significance.

Chapter 3

IGF-1R inhibition in human prostate and breast cancer cells

3.1 Introduction

The aim of this project is to identify genes whose silencing regulates sensitivity to IGF-1R inhibition. The initial starting point was to test whether IGF-1R was inhibited by a small molecule inhibitor in DU145 prostate cancer and MCF-7 breast cancer cells, testing its effects on IGF-1R signaling and cell viability.

3.2 Results and discussion

An IGF-1R inhibitor was obtained from AstraZeneca and was tested for its effect in DU145 prostate cancer and MCF-7 breast cancer cells, in which the IGF-1R signaling pathway is known to be functional (Kimura et al. 1996; Dupont and Le Roith 2001; Saikali et al. 2008). In particular, DU145 cells have been

characterized as IGF-responsive in previous work from our group (Rochester et al. 2005; Turney et al. 2012). Breast and prostate cancers are amongst the commonest cancers, and it was hoped that factors that regulate sensitivity to IGF-1R inhibition in these common tumor types may be robust and potentially of wide significance.

3.2.1 Inhibition of IGF-1R activity by AZ12253801

The compound AZ12253801 was specifically designed to compete with ATP for binding to the IGF-1R, to block the activity of this receptor. Information provided by AstraZeneca indicated that AZ12253801 showed approximately ten-fold higher binding to the IGF-1R than the closely related IR. The half maximal inhibitory concentration (IC_{50}) values for inhibition of phosphorylation of IGF-1R and IR *in vitro* were said to be respectively 2.1 and 19 nM. Additionally, a wide range of relevant kinases had been tested, revealing that the IC_{50} values were greater than 1 μM, with no significant inhibitory activity at 10 μM. Recent work in our laboratory had shown that AZ12253801 inhibited IGF-1-induced phosphorylation with IC_{50} of approximately 2 nM in DU145 cells, by IGF-1R immunoprecipitation and western blot (IP-western) for activated IGF-1R (Aleksic et al. 2010). For this project, a similar assessment was performed in MCF-7 cells, which were serum-starved overnight and treated with

AZ12253801 or solvent (0.001% DMSO) for one hour, and in the final 15 minutes with 50nM IGF-1. Cells were lyzed, immunoprecipitated with IGF-1R beta subunit antibody, and phosphorylated and total IGF-1R levels were detected by western blot (Figure 3.1, A). From the curve fit of data generated by three independent experiments, the IC_{50} value for IGF-1R phosphorylation inhibition in MCF-7 cells was determined to be 2 nM (Figure 3.1, B), equivalent to results in DU145 cells.

The inhibition of IGF-1R activity by AZ12253801 was tested in DU145 cells by western blot from samples prepared by direct lysis. DU145 cells were serum-starved overnight and treated either with AZ12253801 or solvent (0.01% DMSO) for one hour, and in the final 10 minutes with 10nM IGF-1. Phosphorylated and total IGF-1R levels were evaluated by western blot (Figure 3.2, A). The IC_{50} value for IGF-1R phosphorylation inhibition in DU145 cells was approximately 2nM (Figure 3.2, B), which was the same value that had previously been determined by IP-western (Aleksic et al. 2010).

3.2.2 AZ12253801 inhibited IGF-1R signaling

Effects of AZ12253801 on signaling downstream of IGF-1R were evaluated using western blot. DU145 cells were serum-starved overnight and treated with

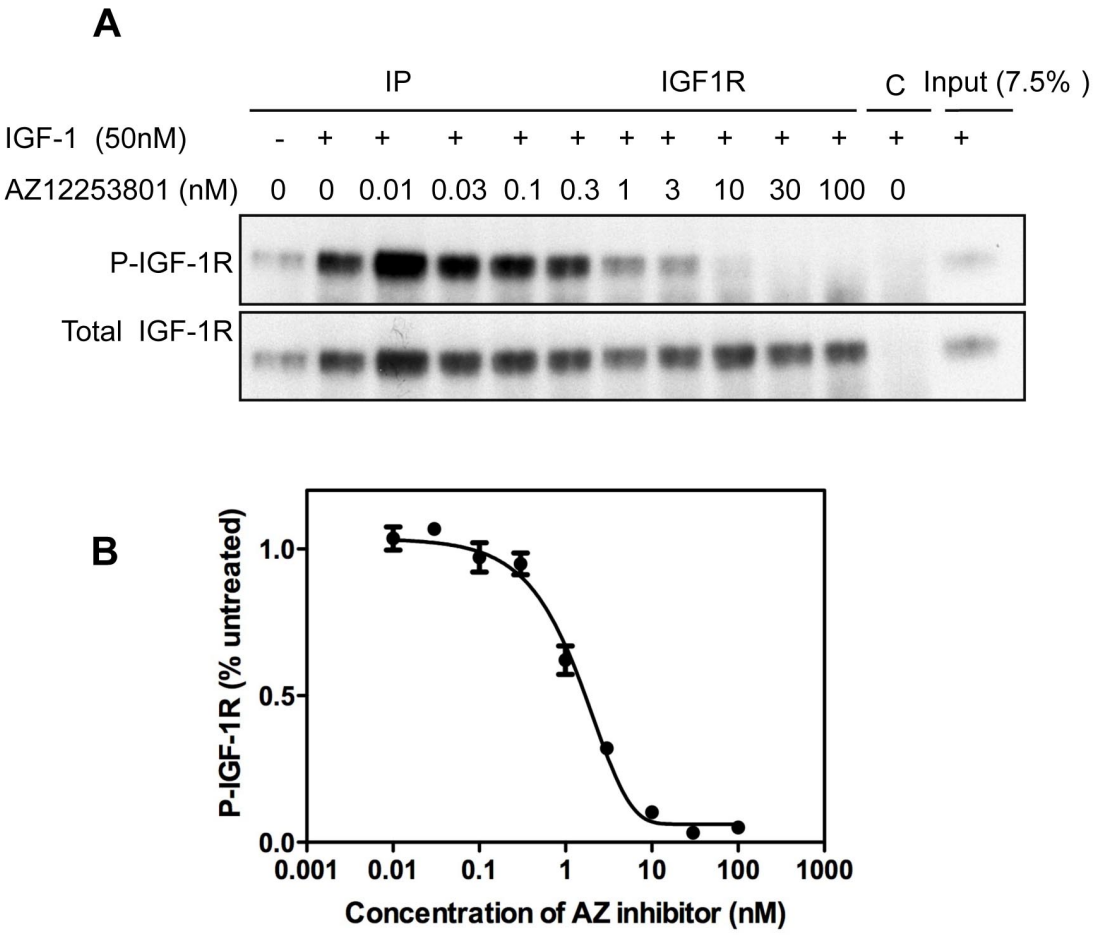

Figure 3.1 AZ12253801 inhibited IGF-1-induced IGF-1R activation in MCF-7 cells. (A) Cells were serum-starved overnight, treated with AZ12253801 for one hour and in the final 15 minutes were stimulated with 50 nM IGF-1. IGF-1Rβ or control (C) immunoprecipitates were probed for phospho-IGF-1R (Tyr1135/1136) and total IGF-1R. Similar results were obtained in two more independent experiments. (B) The phospho-signal was quantified by ImageJ software, corrected for total IGF-1R and expressed as percentage signal of IGF-1-induced, AZ12253801-untreated cells. Graph shows mean values (n=3) and error bars (SD). The data points were curve fitted using GraphPad Prism 5, and the IC_{50} value for inhibition of phosphorylation was extrapolated from this curve.

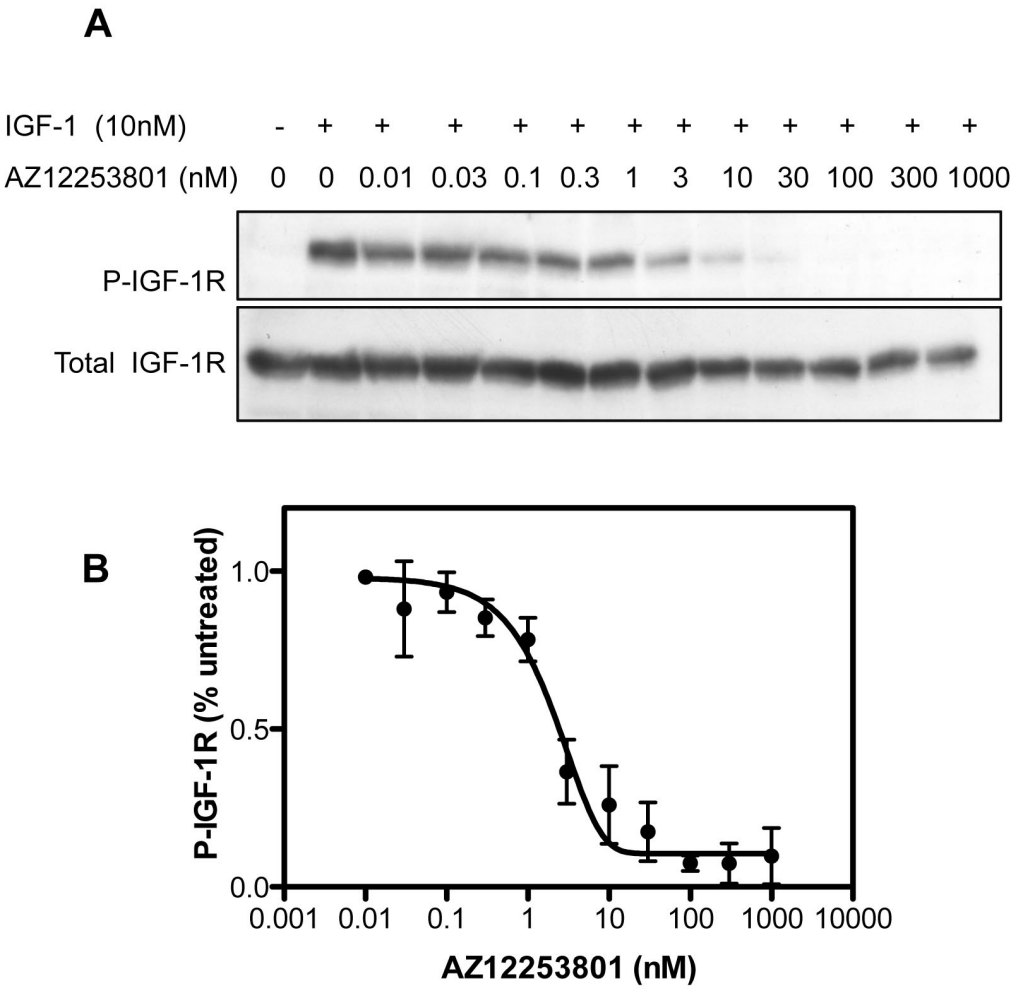

Figure 3.2 AZ12253801 inhibited IGF-1-induced IGF-1R activation in DU145 cells. (A) Cells were serum-starved overnight, treated with AZ12253801 for one hour and stimulated with 10nM IGF-1 for 10 minutes. Cell lysates were analyzed by western blot for phospho-IGF-1R (Tyr1135/1136) and total IGF-1R. The similar result was obtained in one more independent experiment. (B) The phospho-signal was quantified by ImageJ software, corrected for total IGF-1R and expressed as percentage signal of IGF-1-induced, AZ12253801-untreated cells. Graph shows mean values (n=2) and range. The data points were curve fitted using GraphPad Prism 5, and the IC_{50} value for inhibition of phosphorylation was extrapolated from this curve.

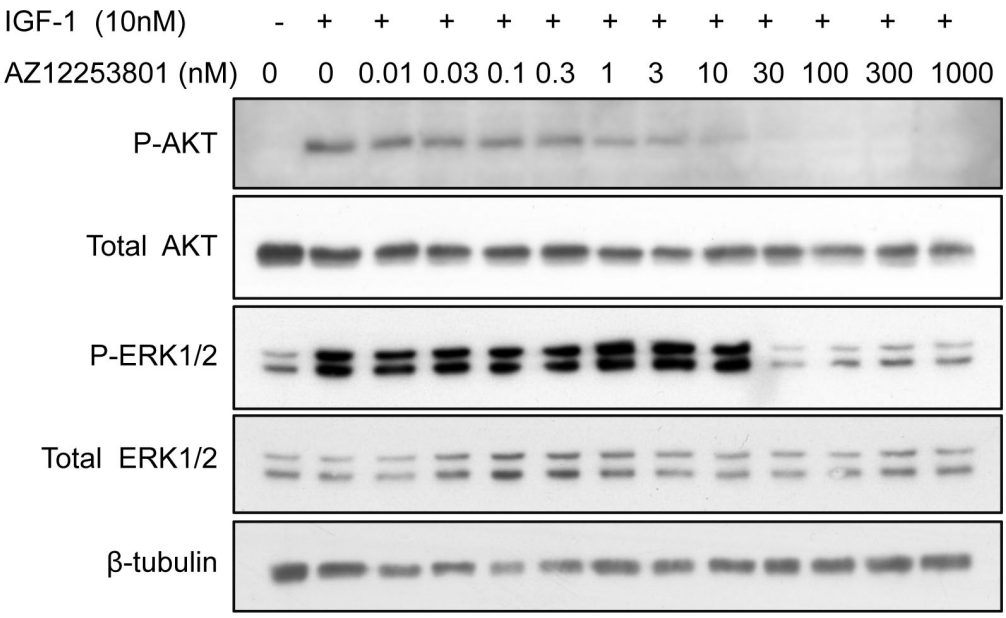

Figure 3.3 AZ12253801 inhibited IGF-1-induced AKT and ERK1/2 activation in DU145 cells. Cells were serum-starved overnight, treated with AZ12253801 for one hour and stimulated with 10nM IGF-1 for 10 minutes. Cell lysates were probed for phospho-AKT (Ser473), total AKT, phospho-ERK1/2(Ser202/204), total ERK1/2, and β-tubulin as the loading control. Similar results were observed from a second independent experiment.

AZ12253801 or solvent (0.01% DMSO) for one hour, and in the final 10 minutes with 10nM IGF-1. Phosphorylated and total AKT and ERK1/2 were detected by western blot. Inhibition of IGF-induced activation of AKT showed a similar pattern to inhibition of IGF-1-induced IGF-1R activation, while ERK1/2 activation was more sharply inhibited at 30nM AZ12253801 (Figure 3.3). Taken together, these data show that AZ12253801 was able to inhibit IGF-1-induced AKT and ERK1/2 activation.

3.2.3 Testing effects of IGF-1R inhibition on proliferation of DU145 and MCF-7 cells

Effects of AZ12253801 on cell proliferation and survival were determined in a 96-well-plate CTG assay and in 6-well-plate clonogenic assay. In the 96-well-plate format, DU145 (1000 cells/well) or MCF-7 (2000 cells/well) cells were treated with solvent (0.1% DMSO) or AZ12253801 (0.1nM to 10μM) for 5 days, and cell viability was measured by CTG assay. From the curve-fit of three independent experiments, the GI_{50} was calculated to be 120 nM in DU145 cells and 50 nM in MCF-7 cells (Figure 3.4, A, B). Clonogenic cell survival assays were performed by seeding 1000 cells of each cell line into wells of 6-well plates, and treating with AZ12253801 or solvent. After 10 days, DU145 cells formed visible colonies that were fixed, stained and counted (Figure 3.5, A).

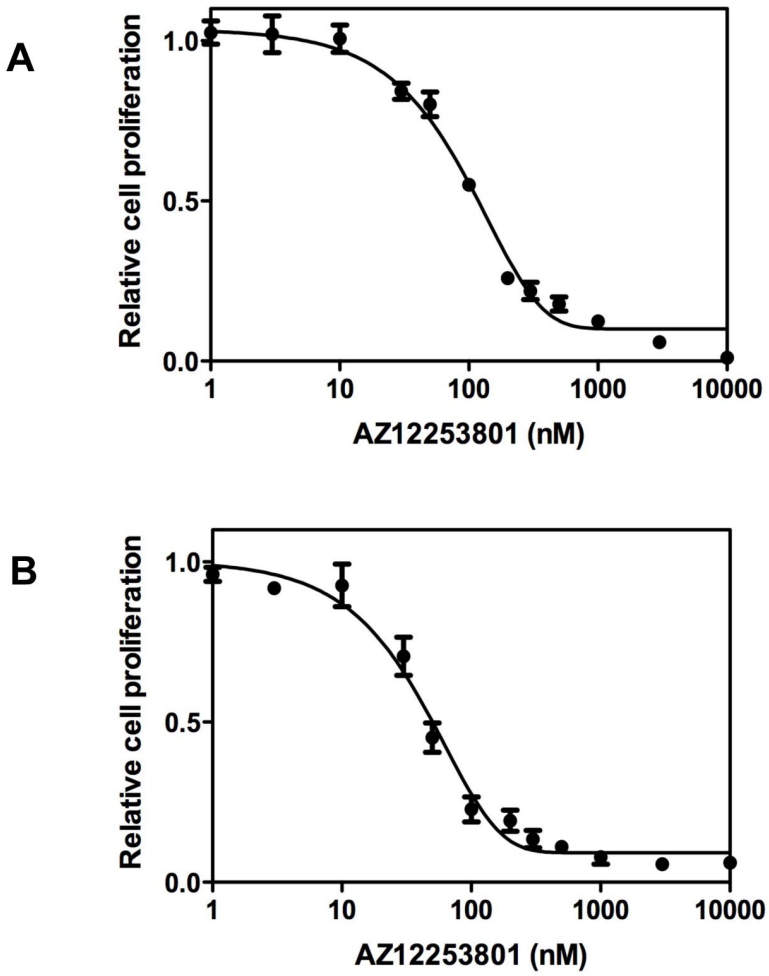

Figure 3.4 Effect of AZ12253801 on cell proliferation. (A) DU145 and (B) MCF-7 cells were treated with DMSO or AZ12253801 (1nM-10μM), and after 5 days, cell viability was quantified using the CTG assay. Graphs show data from three independent experiments, each with triplicate points, expressed as a fraction of viability in solvent-treated cells. Error bars (SEM). The data were curve fitted and GI_{50} values were calculated using GraphPad Prism software. GI_{50} value in DU145 cells, 120nM (A), and in MCF-7, 50nM (B)

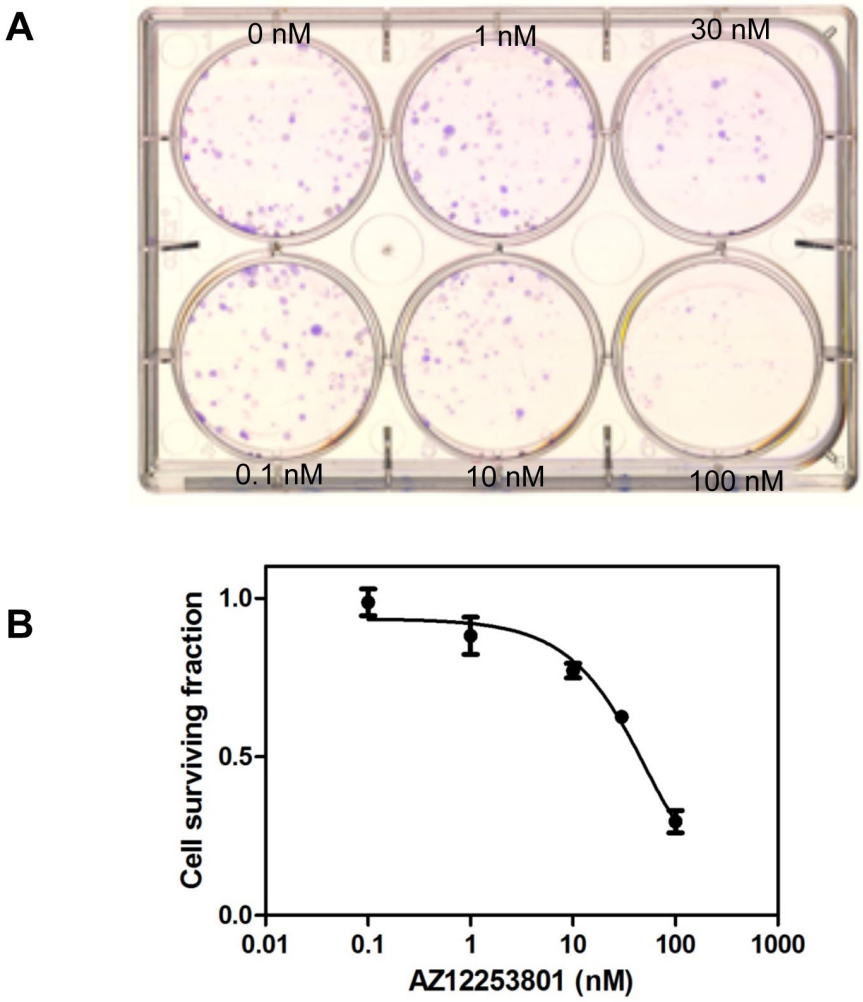

Figure 3.5 AZ12253801 inhibited clonogenic survival of DU145 prostate cancer cells. (A) DU145 cells were treated with solvent (DMSO) or AZ12253801. Colonies surviving after 10 days were fixed, stained and counted. (B) The survival curve represents pooled results from three independent experiments, each with triplicate wells and expressed as a fraction of cell survival in cells not treated with AZ12253801. Error bars represent SEM. The SF_{50} value for AZ12253801 was 45nM in DU145 cells

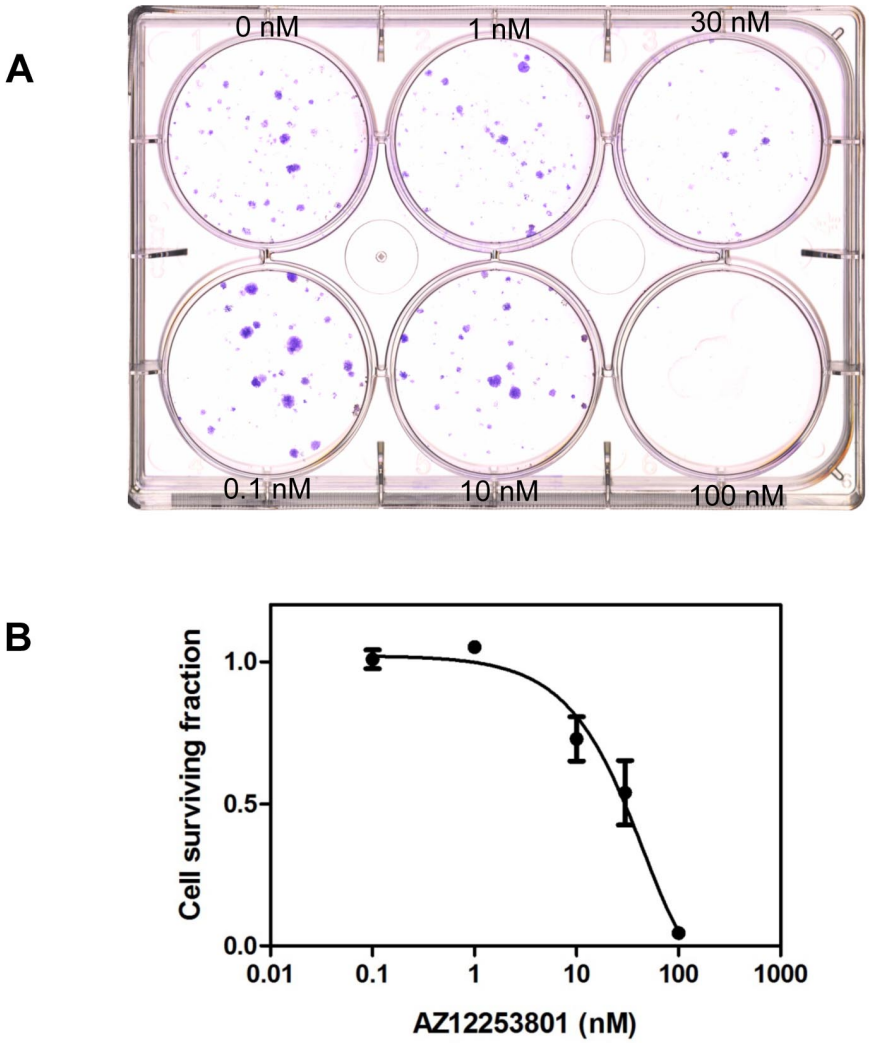

Figure 3.6 AZ12253801 inhibited clonogenic survival of MCF-7 breast cancer cells. (A) MCF-7 cells were treated with solvent (DMSO) or AZ12253801. Colonies surviving after 14 days were fixed, stained and counted. (B) The survival curve represents pooled results from three independent experiments with triplicate wells. Error bars, SEM. The SF_{50} value for AZ12253801 was 30nM in MCF-7 cells.

The concentration required to inhibit survival by 50% of that in solvent-treated wells (SF_{50}) was determined to be 50nM in DU145 cells (Figure 3.5, B). MCF-7 cells took 14 days to form visible colonies (Figure 3.6, A) and the SF_{50} value was determined to be 30nM AZ12253801 (Figure 3.6, B). Thus the IGF-1R inhibitor AZ12253801 was able to block cell growth and survival in DU145 and MCF-7 cells, consistent with the known functions of IGF-1R (Chitnis et al. 2008). While the IC_{50} value for inhibition of receptor phosphorylation was equivalent (2nM) in both cell lines. GI_{50} and SF_{50} values were lower in MCF-7 cells than DU145 cells, perhaps suggesting greater IGF-1R dependence in MCF-7 cells.

3.2.4 Testing effect of overexpression of IGF-1R on sensitivity to AZ12253801

It was reported that IGF-1R expression levels had modest correlation with sensitivity to IGF-1R blockade in NSCLC cell lines (Gong et al. 2009). In clinical trials, level of IGF-1R is a good predictor of resistance to IGF-1R inhibition, but IGF-1R expression levels do not clearly correlate with response (Gualberto et al. 2010; Basu et al. 2011). A pCDNA3.1(+)-IGF-1R-Myc construct was generated (Riedemann et al. 2007) and stably expressed in PC3 prostate cancer cells, and shown to function as endogenous IGF-1R in our group (Tamara Aleksic, unpublished data). Western blot confirmed that the IGF-1R was overexpressed

following IGF-1R-Myc transfection (Figure 3.7, A). However, the IGF-1R overexpressing cells did not show any change in sensitivity to AZ12253801 compared to control transfectants (Figure 3.7, B).

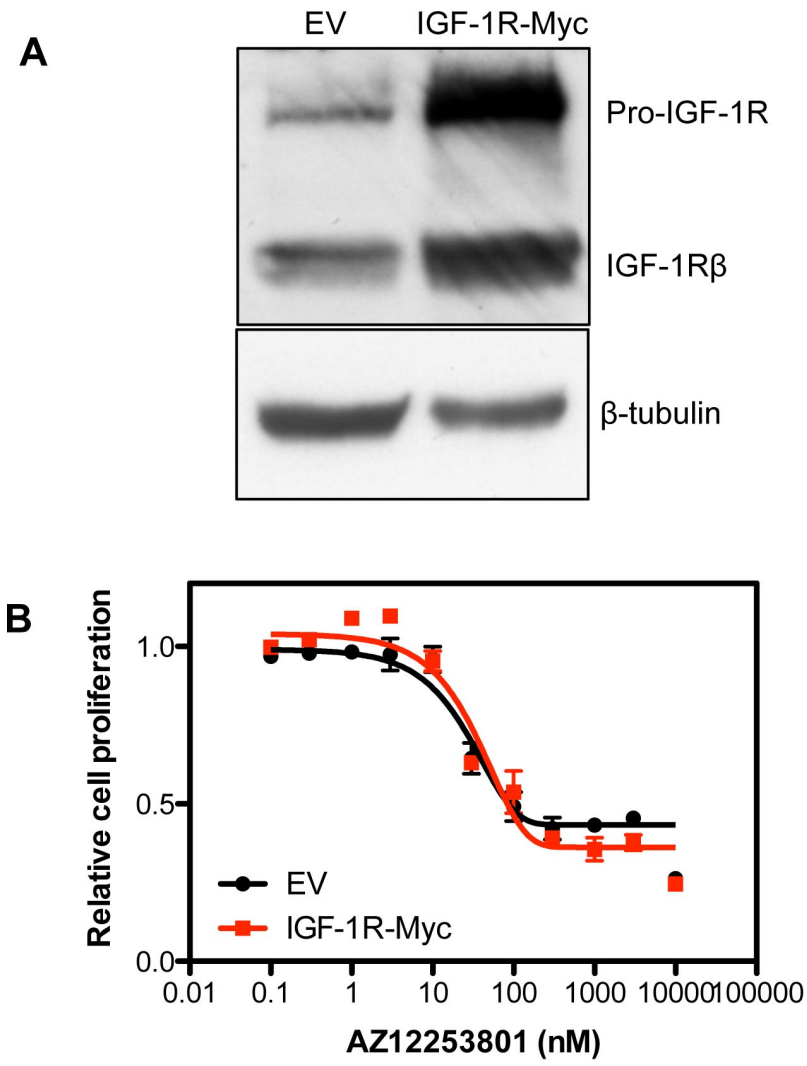

Figure 3.7 Overexpression of IGF-1R did not enhance sensitivity to AZ12253801 in PC3 prostate cancer cells. (A) Lysates of PC3 cells stably transfected with pCDNA3.1 (EV) or pCDNA3.1-IGF-1R-Myc (IGF-1R-Myc) were analyzed by western blot. (B) EV or IGF-1R-Myc transfected cells were treated with DMSO or AZ12253801 (0.1nM-10μM), and after 5 days, cell viability was quantified using the CTG assay. Graphs show data from three independent experiments, each with triplicate points, expressed as a fraction of viability in solvent-treated cells. Error bars (SEM). The data were curve fitted and GI_{50} values were calculated using GraphPad Prism software. GI_{50} value in EV cells, 86nM, and in IGF-1R-Myc, 83nM.

Chapter 4

siRNA screen to identify genes whose silencing influences sensitivity to IGF-1R inhibition

4.1 Introduction

Work in the previous chapter showed that IGF signaling and growth of human breast and prostate cancer cells were inhibited by AZ12253801, but that changing the level of IGF-1R did not affect sensitivity to the inhibitor. The next step was to perform an unbiased siRNA screen to identify proteins that influence sensitivity to IGF-1R inhibition.

4.2 Results and discussion

4.2.1 Optimization of siRNA screen

Initial experiments optimized the reverse transfection protocol that would be used in the screen. The transfection complexes consisting of Dharmafect

reagent plus siRNAs were mixed in 96-well plates, and then cells were added. Initial CTG assays measured the effects of negative control Allstars (AS) siRNA and positive control polo-like kinase 1 (PLK1) siRNA on cell viability (Figure 4.1). Transfection with siRNA targeting PLK1, which is essential for cellular viability, caused a reduction in cell viability of more than 80%, compared to mock transfectants. This indicates that transfection was highly efficient under these conditions. Transfection of DU145 and MCF-7 cells with the non-silencing AS siRNA had only minor effects on cellular viability with reduction of less than 20% compared with mock transfectants. This indicated that these cells could be transfected without excessive non-specific toxicity, which could reduce the sensitivity of the screen. AS negative control siRNA is a highly validated negative control siRNA that has no homology to any known mammalian gene and which has been validated using affymetrix GeneChip arrays. This control has been used in previous work from our group and our collaborators and has been shown to induce minimal nonspecific effects on gene expression and cellular phenotype. (Lord et al. 2008; Aleksic et al. 2010) (https://www.qiagen.com/products/genesilencing/allstarrnaicontrols/allstarsnegativecontrols.aspx.)

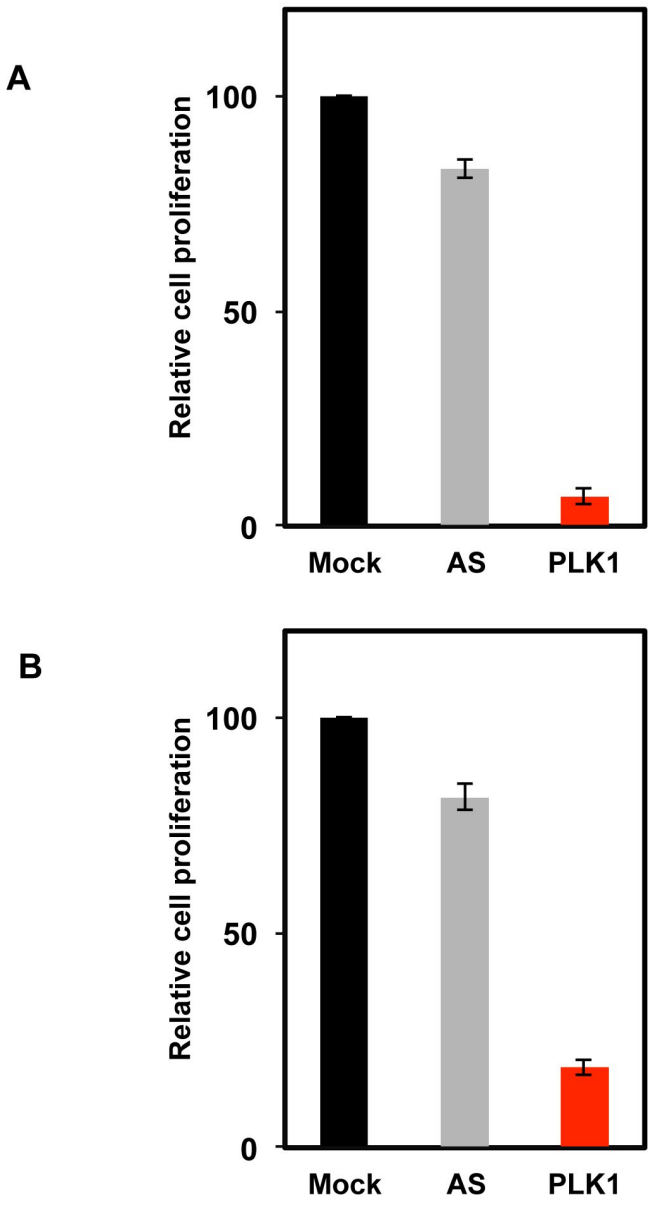

Figure 4.1. Optimization of reverse transfection. (A) DU145 (1000 cells/well) and (B) MCF-7 (2000 cells/well) were reverse transfected with 50nM AS and PLK1 siRNAs. After 7 days, viability was measured by CTG assay. Cell viability was expressed as proportion of viability in mock transfectants (transfection reagent only). Mean and SEM from three independent experiments, each with triplicate wells.

4.2.2 Primary siRNA Screen

4.2.2.1 Screen process

To identify proteins regulating sensitivity to IGF-1R inhibition, an siRNA screen was used, incorporating two different siRNA libraries. The first was a Kinome siRNA library (SMARTpool, Dharmacon) that included 779 known kinase and kinase-associated genes; each gene is targeted by four different siRNAs pooled in the one well (Turner et al. 2008). The second library was the Human DNA Repair Set V1.0 siRNA library (Qiagen UK), which was composed of 230 known and putative genes associated with DNA repair. Each gene was targeted by two different siRNAs which were located in different wells (Lord et al. 2008).

The screen strategy was designed and modified by Dr. Val Macaulay and our collaborator Dr. Chris Lord based on previous screens and is illustrated in figure 4.2 (Lord et al. 2008; Turner et al. 2008). The screen was repeated twice with each library in both cell lines.

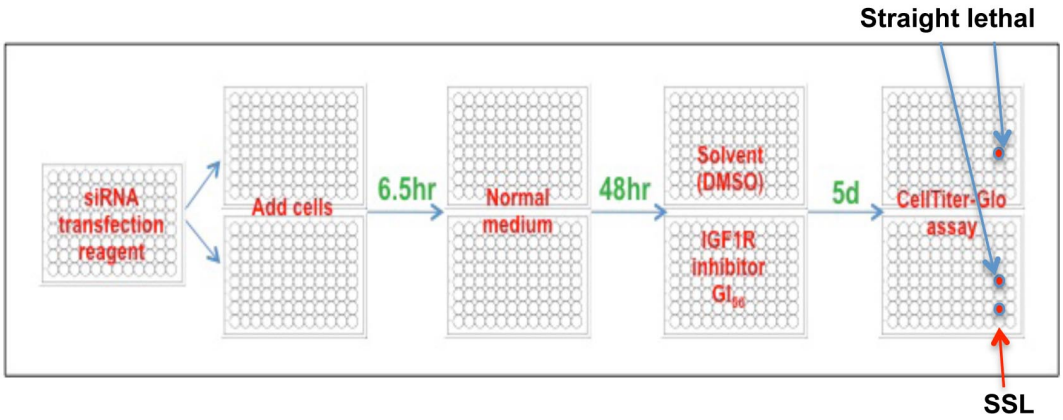

Figure 4.2 Overview of siRNA screen. siRNAs and transfection reagent were mixed and aliquoted into two plates. DU145 or MCF-7 cells were added, and 48 hours later, half of the plates were treated with DMSO vehicle alone and half with AZ12253801 at the GI_{50}. Cell viability was assessed after 5 days using CellTiter-Glo Luminescent Cell Viability Assay. The diagram illustrates a gene whose depletion is straight lethal (kills cells in both solvent and AZ12253801-treated wells) and a second gene whose depletion is toxic only to AZ12253801-treated wells (SSL).

4.2.2.2 Analysis of screen data

It was first necessary to ensure that the screen data met minimum quality standards. The quality of the screen data was measured by calculating Z' scores as shown in chapter 2 (Zhang et al. 1999; Birmingham et al. 2009). The Z' score represents the screen signal window, which is a measure of the distance between the positive and the negative controls. Screens with Z' scores of more than 0.5 are regarded as high quality, and Z' scores of more than 0.2 are acceptable. Screens generating Z' scores of less than 0 are not considered worthy of further analysis, because there is overlap between the positive and negative controls (Zhang et al. 1999; Boutros and Ahringer 2008). The majority of the screens performed in DU145 cells had Z' scores of 0.4-0.6 with none less than 0.2 (Figure 4.3, A and B). The MCF-7 cell screens were less good quality, with Z' scores of 0.03-0.5, and at least one set of data in every screen had a Z' score of less than 0.2 (Table 4.1, A).

Following the initial quality check, all screen data were analyzed as described in chapter 2 and normalized to remove within and between plate variation, to derive Z scores (Boutros et al. 2006). There was a high degree of correlation of Z-scores for cell viability between replicate screens. Comparing replicate DMSO-treated or AZ12253801-treated groups gave correlation coefficients (R^2)

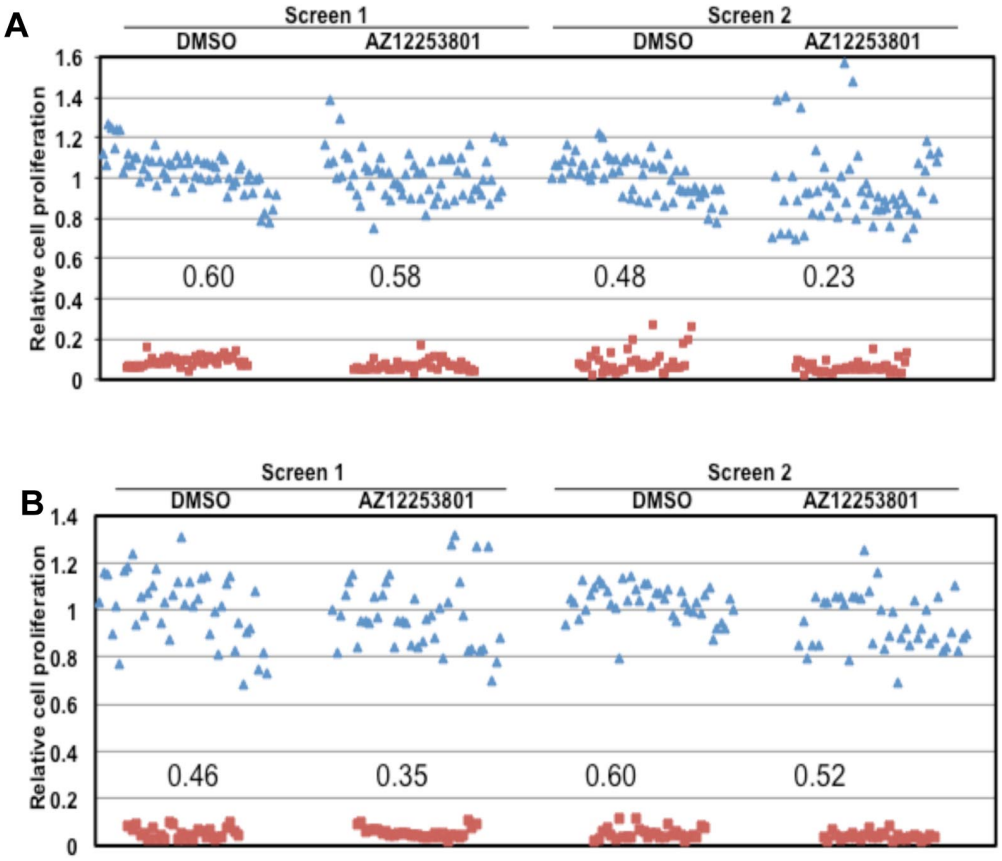

Figure 4.3 Z' scores in primary screens. The plots shows Z' scores from duplicate screens of (A) Kinome and (B) DNA repair-associated siRNAs in DU145 cells. Z' scores were calculated as a measure of the statistical power of the assay to discriminate negative control (blue triangle, AS siRNAs) and positive control (red square, PLK1 siRNAs). The cell viability of every control was calculated as a fraction of the mean cell viability of all mock transfectants.

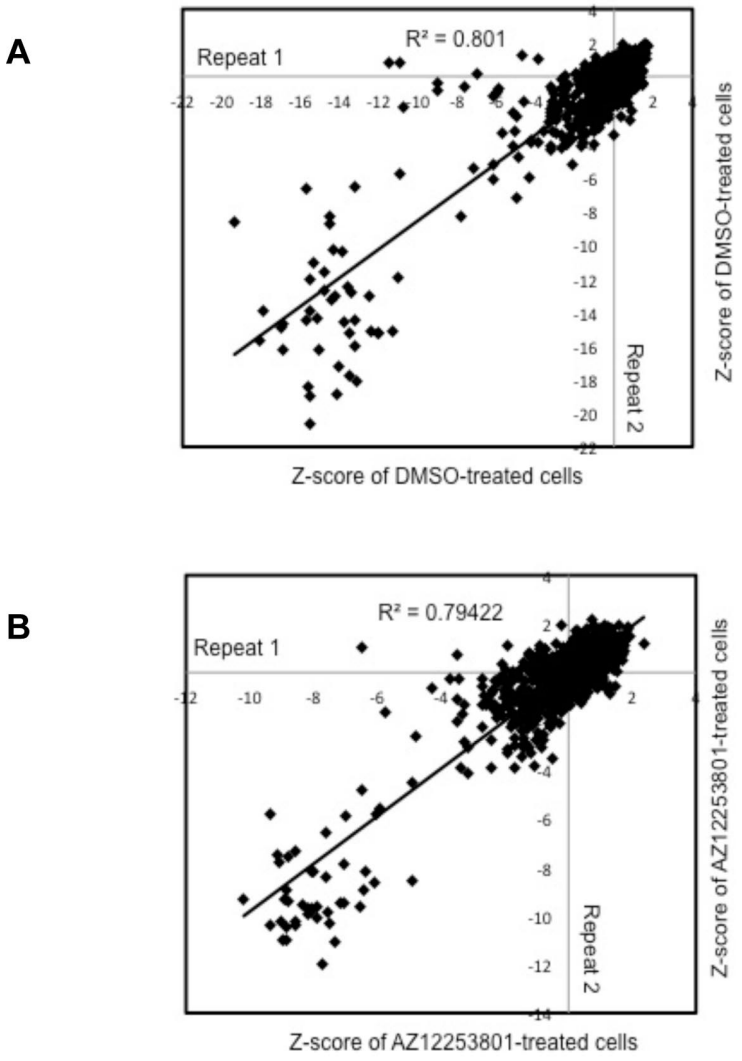

Figure 4.4 The reproducibility of Kinome screens in DU145 cells. Correlation of Z-scores of cell viability in DMSO-treated groups (A) or AZ12235801-treated groups (B) from two replicates of the entire Kinome screen in DU145 cells. (A) DMSO-treated group, spearman correlation coefficient R^2=0.801.（B）R^2=0.7942 in AZ12235801-treated groups.

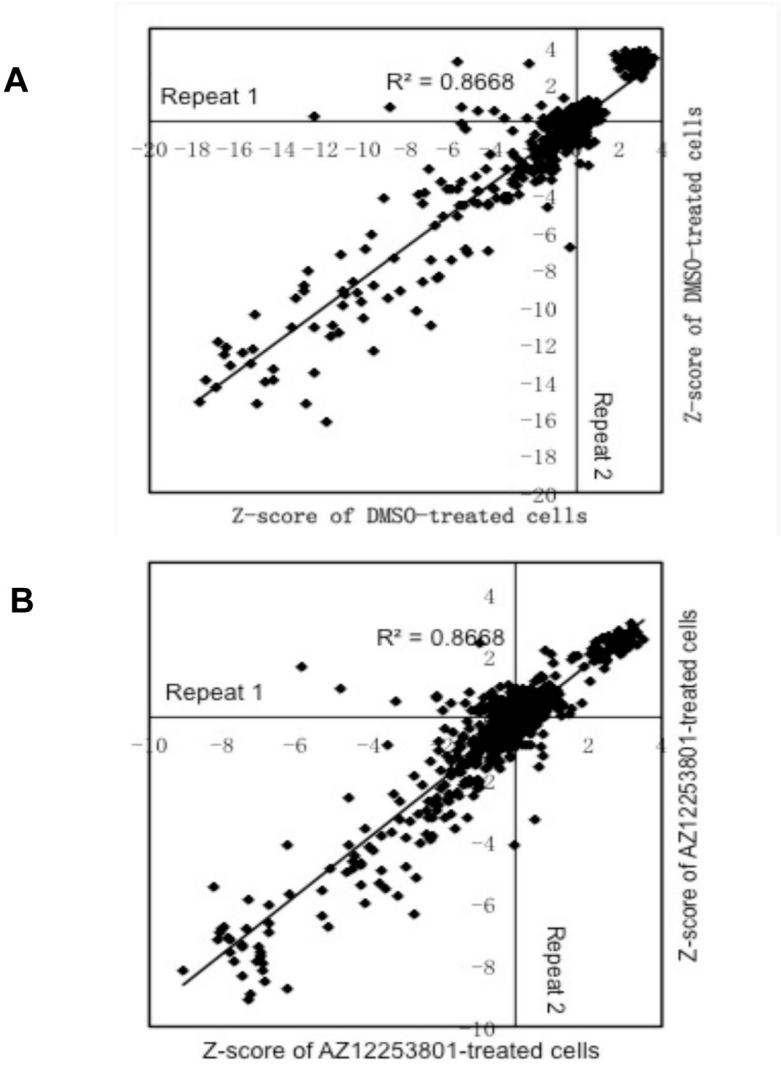

Figure 4.5. The reproducibility of DNA repair-associated screens in DU145 cells. Correlation of Z-scores of cell viability in DMSO-treated groups (A) or AZ12235801-treated groups (B) from two replicates of the DNA repair-associated screen in DU145 cells. (A) DMSO-treated group, R^2=0.8668. (B) R^2=0.8668 in AZ12235801-treated groups.

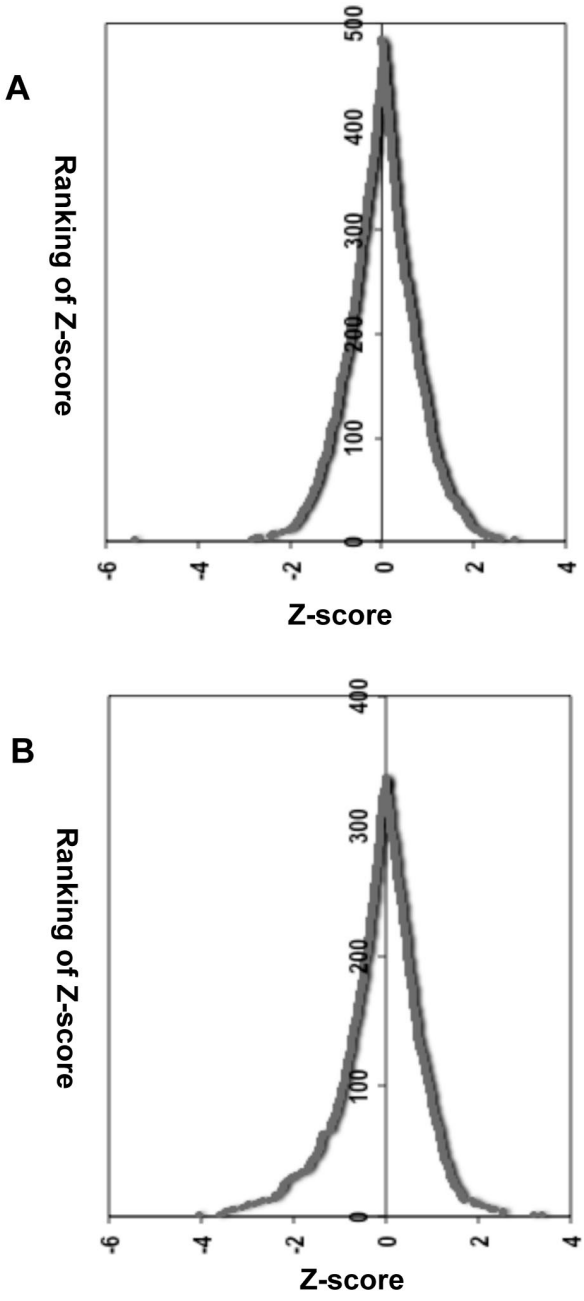

Figure 4.6 Distribution of averaged Z-scores of drug effect in DU145 cells. Graphs show distribution of averaged Z-scores from IGF-1R inhibitor sensitivity screen of (A) Kinome or (B) DNA repair-associated genes.

A

Z'		Kinome	DNA repair
Screen 1	DMSO	0.5	0.18
	AZ12253801	0.28	0.36
Screen 2	DMSO	0.23	0.05
	AZ12253801	0.03	0.04

B

Kinome R^2		Screen 2	
		DMSO	AZ12253801
Screen 1	DMSO	0.38	
	AZ12253801		0.56
DNA repair R^2		Screen 2	
		DMSO	AZ12253801
Screen 1	DMSO	0.51	
	AZ12253801		0.53

Table 4.1 The summary of duplicate screens in MCF-7 cells. (A) Z' scores and (B) spearman correlation coefficient R^2 of cell viability in DMSO-treated groups or AZ12235801-treated groups from Kinome and DNA repair-associated screens in MCF-7 cells.

of 0.80-0.79 in Kinome (Figure 4.4, A and B) and DNA repair-associated screens (Figure 4.5 A and B) in DU145 cells. Equivalent values in MCF-7 cell screens were 0.38-0.56 in MCF-7 cells (Table 4.1, B). This indicated that DU145 screens were highly correlated and reproducible and MCF-7 screens less so. In addition, the average Z-score for inhibitor effect in Kinome and DNA repair-associated screens showed an approximately normal distribution (Figure 4.6, A and B).

4.2.2.3 Results of primary screen

The averaged Z-score of inhibitor effect pooled from two independent experiments in DU145 cells is displayed in Figure 4.7 A and B. Having checked the quality and reproducibility of screen data, criteria were established for selection of potential hits. Given the higher quality of DU145 screen data, most of the hits were selected from DU145 screens. Firstly, any candidate with a Z-score for cell growth in DMSO-treated cells of < -2.0 was excluded, because this indicated that silencing of those genes alone appeared to cause significant cell death in the absence of inhibitor (i.e. straight lethality as illustrated in Figure 4.2). Selection of such candidates for validation has given a high incidence of false positives (Dr. Chris Lord, personal communication). Secondly, any gene with a Z-score for inhibitor effect of < -2.0 in either of the duplicate screens, or

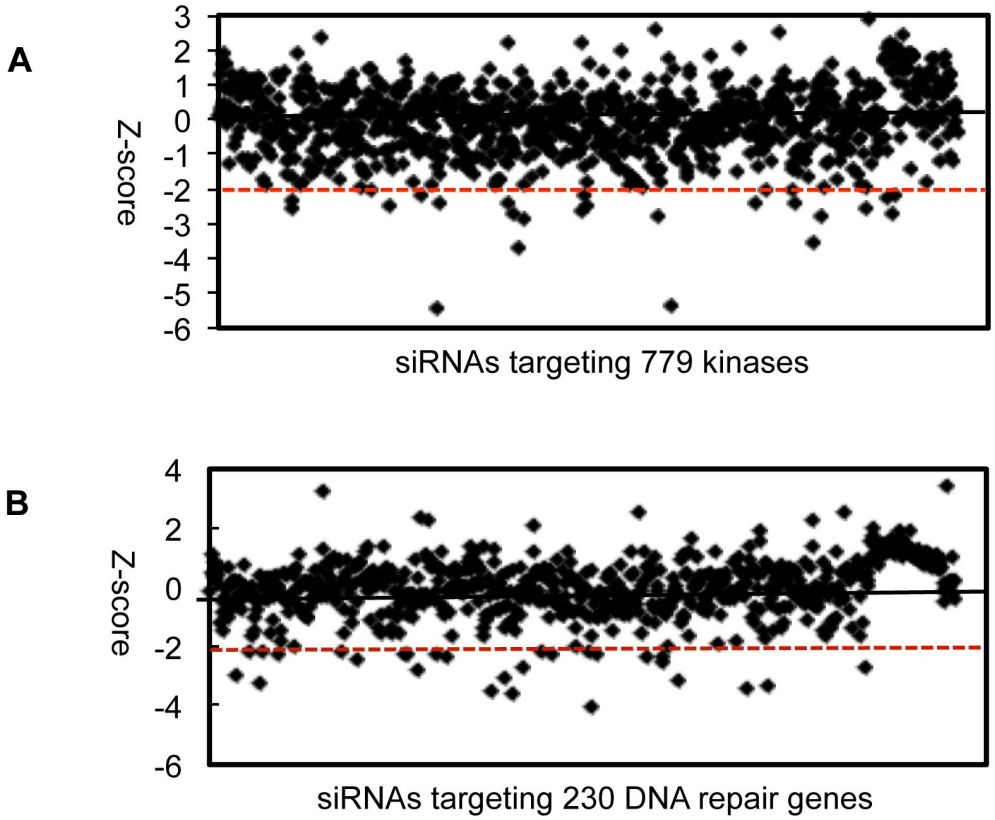

Figure 4.7 Scatter plots of average Z-scores of inhibitor effect. Averaged Z-scores from duplicate IGF-1R inhibitor sensitivity screens of the Kinome (A) and DNA repair-associated (B) libraries in DU145 cells. Red line indicates the -2 cut off for selection of potential hits .

averaged Z-score for inhibitor effect of < -1.8, was included in the next round of screening. Thirdly, we also considered MCF-7 screen data, and included some lower score hits that had predicted interaction with higher score hits. Using these criteria, 30 hits from the Kinome set and 23 hits from the DNA repair-associated library were chosen for the second round screen (Table 4.2).

4.2.3 Validation of primary siRNA screen hits

Interpretation of siRNA screen data can be confounded by false negative results, due to inability of screen siRNA to degrade the mRNA of the target gene. A more significant problem is off target effects of siRNAs, which give rise to false positive screen hits (Turner et al. 2008; Sharma and Rao 2009). Off-target effects can arise in several different ways. Firstly, the interferon response can be activated in mammalian cells by very short siRNA in a sequence-independent way, especially if high siRNA concentrations are used (Sledz and Williams 2004; Sharma and Rao 2009). Secondly, the designed siRNA sequence may be highly homologous or almost identical to another unrelated gene sequence, resulting in the degradation of the mRNA of the unrelated gene. This problem can be avoided by careful design, and siRNA sequences capable of degrading multiple transcripts are being removed from commercial siRNA libraries (Sharma and Rao 2009). Finally, if the central

Kinome

Gene Symbol	Averaged Z-score
DUSP5	-5.395
CDKN2C	-2.811
KIT	-2.742
AKAP1	-2.658
MAP3K10	-2.453
MPP2	-2.422
FLT4	-2.396
LMTK3	-2.389
APEG1	-2.320
MAP4K3	-2.173
TIE	-2.172
LIM	-2.047
PDK4	-2.041
PIK3C2A	-1.984
MYLK	-1.943
CNKSR1	-1.941
DUSP4	-1.889
SGK2	-1.851
CCL4	-1.744
STK39	-1.703
HUNK	-1.605
CDK6	-1.421
LIMK2	-0.942
PLK3	-0.918
CDK4	-0.828
LIMK1	-0.803
CDK3	-0.388
CDC2	2.385
PANK4	2.535
PRKAG3	2.894

DNA repair

Gene Symbol	Averaged Z-score
SOX4	-4.264
MGMT	-3.246
C18orf37	-3.068
RAD23B	-2.525
G22P1	-2.501
XRCC2	-2.465
MPG	-2.423
SND1	-2.421
MCM3	-2.419
LDHA	-2.343
CCT5	-2.229
CDKN3	-2.146
DVL3	-2.143
TREX2	-2.120
Rad51	-1.741
RAD54B	-1.733
BRCA1	-1.635
KIAA0101	-1.604
CKN1	-1.554
DCLRE1A	-1.534
ADPRT	-1.500
LIG4	-1.063
UBE2V2	-0.546

Table 4.2 Results of IGF-1R siRNA primary screens using Kinome and DNA repair-associated siRNAs. Table shows gene names and averaged Z-score. Results of siRNA screen showed as averaged *Z*-score order from duplicate screen with Kinome and DNA repair siRNAs. Potential hits mediating sensitivity to IGF-1R inhibition were selected on those with averaged Z-score < -1.8. Additional hits were included if they had been predicted to interact with higher score hits. The final 3 hits listed from the kinome scree had Z-score > 2.0, suggesting possible resistant to IGF-1R inhibition

region of the siRNA has weak complementarity to the 3' untranslated region of an unrelated mRNA, the siRNA can act like a microRNA to cause depletion of non-target proteins through mRNA degradation or translational block. This problem is intrinsic to RNAi screens and is much more difficult to avoid (Echeverri et al. 2006; Sharma and Rao 2009). Therefore, it is important to perform a second round of screening before selecting hits for final validation.

For second round screening of the kinome library, the SMARTpool siRNAs were deconvoluted into four individual siRNAs. To validate hits in the DNA repair set, a new set of siRNAs was included. These were called Flexitube Genesolution, and consisted of four individual siRNAs targeting one gene located in different wells. The majority of the two original siRNAs from primary screen were included this new set. Therefore, there were 4 siRNAs to target each potential hit listed in table 4.2. In addition, a pool of the four individual siRNAs was tested in the second round screen in both DU145 and MCF-7 cells. In order to qualify as final screen hits, at least two individual siRNAs should have significant effects on cell survival in the presence of AZ12253801, with log2 cell surviving fractions of < -0.2, as described by (Lord et al. 2008). This criterion identified 8 Kinome and 5 DNA repair-associated proteins in the second round screens in DU145 cells (Figure 4.8, A and B). Seven of these hits

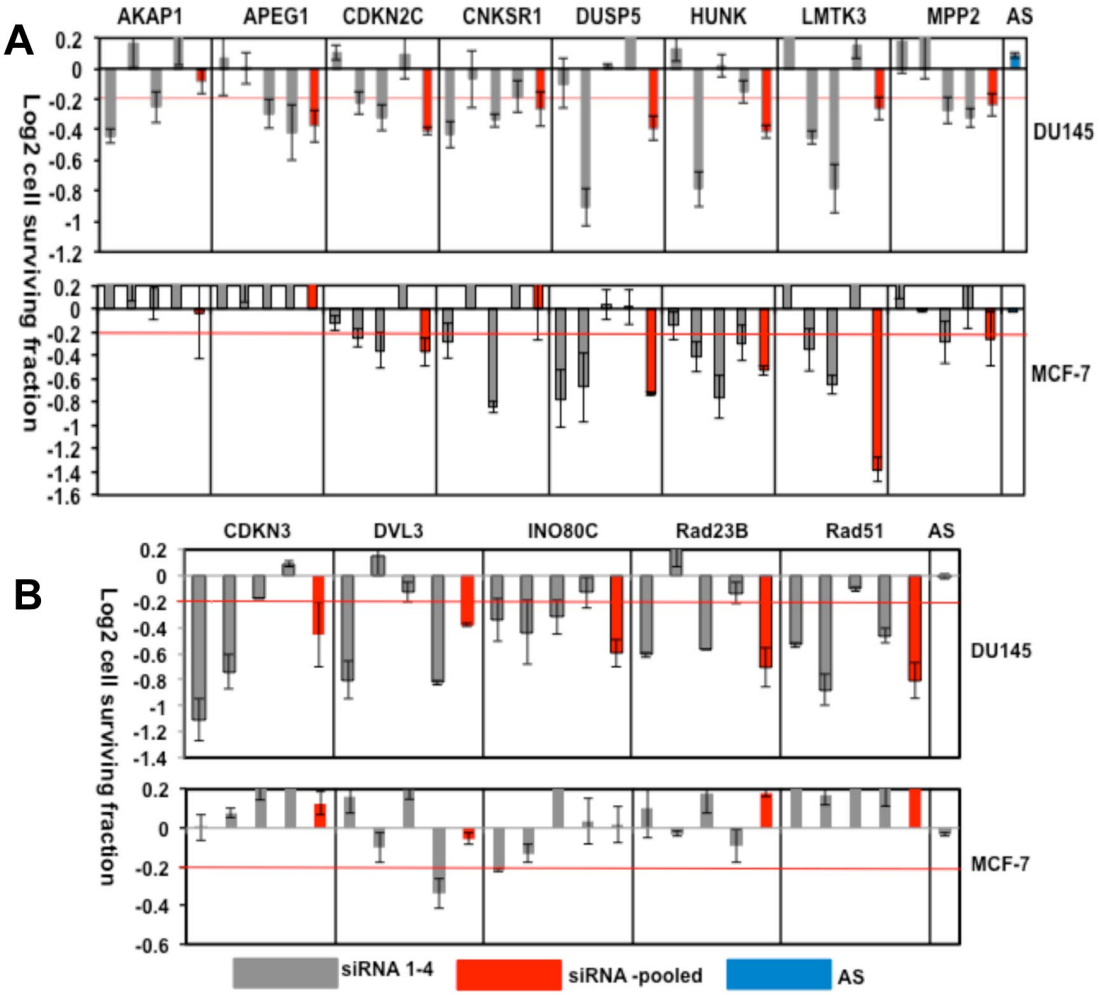

Figure 4.8 Validation of hits from primary screens. (A) Kinome and (B) DNA repair hits were tested in second round screen using 4 individual siRNAs (grey bars) and pooled siRNAs (red bars). The negative AS siRNA (blue bars) was included. The data are shown as mean of triplicate readings (Bars, SD). The score for each target was expressed as log2 cell surviving fraction for AZ12253801 effect in the presence of target gene silencing. Red line shows -0.2 cut-off for hit identification.

were also validated in MCF-7 cells, and these were CDKN2C, CNKSR1, DUSP5, HUNK, LMTK3 and MPP2 with DVL3 as a borderline hit (Figure 4.8, A and B).

4.2.4 Validation of Kinome hits

The eight on-target hits (Figure 4.8, A) from the Kinome screen were A kinase (PRKA) anchor protein 1 (AKAP1, Entrez GeneID 8165); Aortic preferentially expressed gene 1 (APEG1, Entrez GeneID 10290); Cyclin-dependent kinase inhibitor 2C (CDKN2C, Entrez GeneID 1031); Connector enhancer of kinase suppressor of Ras1 (CNKSR1, Entrez GeneID 10250); Dual specificity phosphatase 5 (DUSP5, Entrez GeneID 1847); Hormonally up-regulated Neu-associated kinase (HUNK, Entrez GeneID 30811); Lemur tyrosine kinase 3 (LMTK3, Entrez GeneID 114783), and Membrane protein, palmitoylated 2 (MPP2, Entrez GeneID 4355), all of which were revalidated in the second round screen with at least two individual or pooled siRNAs in DU145 cells. In order to establish effects of depletion of the revalidated on-target hits on sensitivity to the IGF-1R inhibitor, the pooled siRNA was used for further testing in DU145 cells. The efficiency of gene silencing was assessed by qRT-PCR and normalized based on glyceraldehyde 3-phosphate dehydrogenase (GAPDH) (Figure 4.9). Each of the pooled siRNAs induced significant gene silencing,

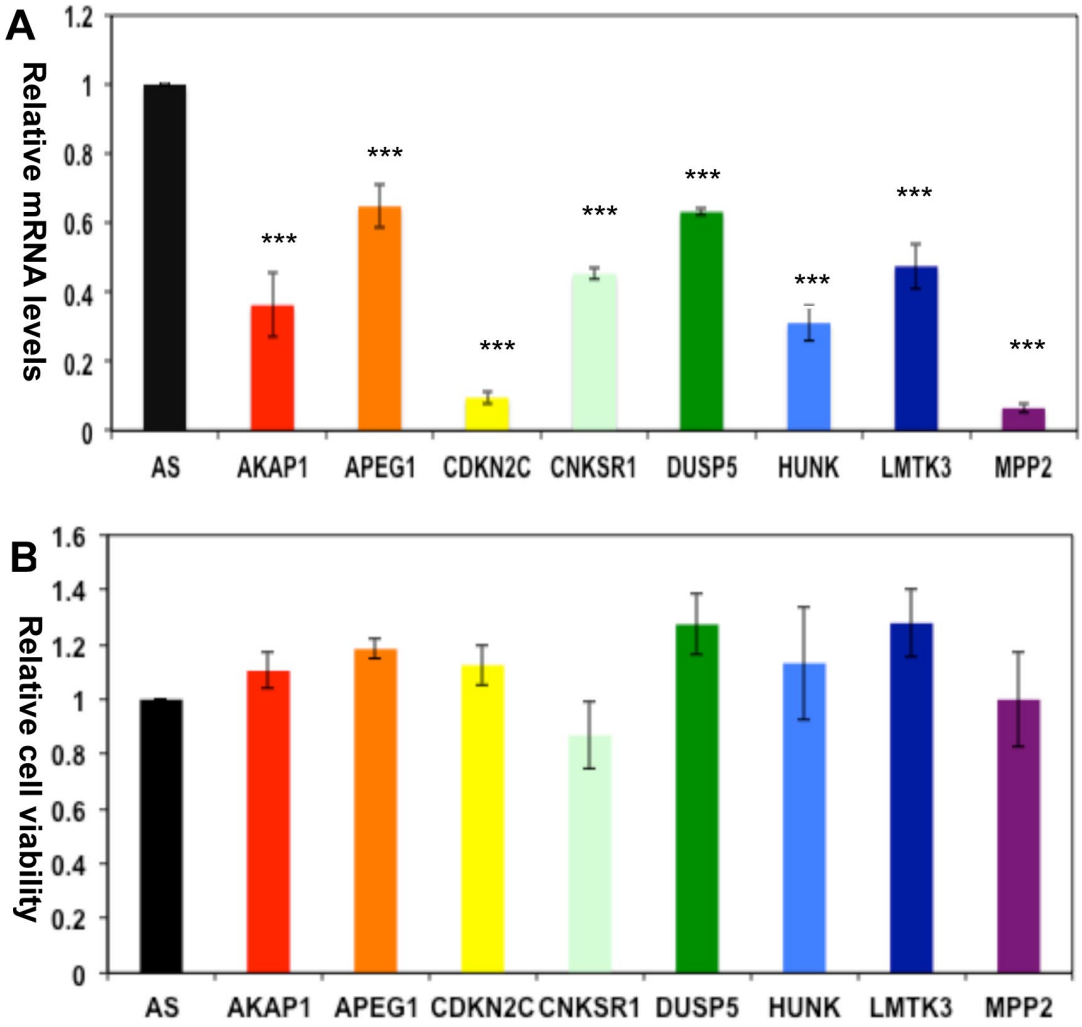

Figure 4.9 Depletion of Kinome hits by screen siRNAs. (A) Gene silencing measured by qRT-PCR. Each pooled siRNA was transfected into DU145 cells, and mRNA was prepared after 48 hrs. After normalizing to GAPDH, the mRNA level of each gene was expressed as percentage of mRNA level of AS-transfected cells. The qPCR was repeated using three independent transfection samples and each qPCR was performed with triplicates. Data represent the mean and SEM. ***, $P<0.001$ (one way ANOVA, compared with AS-transfected cells) (B) Effects on cell viability after depletion. DU145 cells were reverse transfected with AS or gene pooled-siRNAs, and CTG assays were performed 7 days later. Cell viability was expressed as a percentage of the viability of cells transfected with AS siRNA. Column, and bars represent mean and SEM from three independent experiments, each with triplicate wells. None of the pooled siRNAs had any significant effects on cell viability (one way ANOVA, compared with AS-transfected cells).

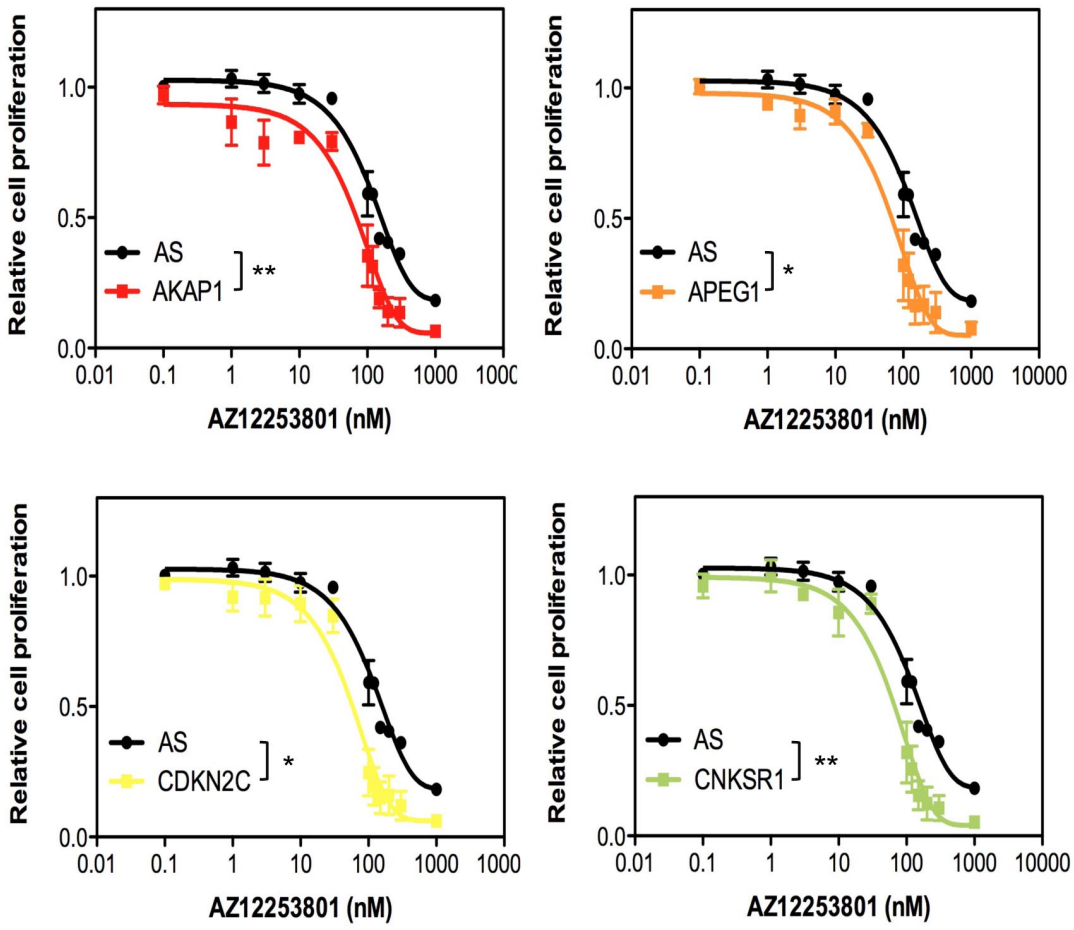

Figure 4.10 See next page for legend

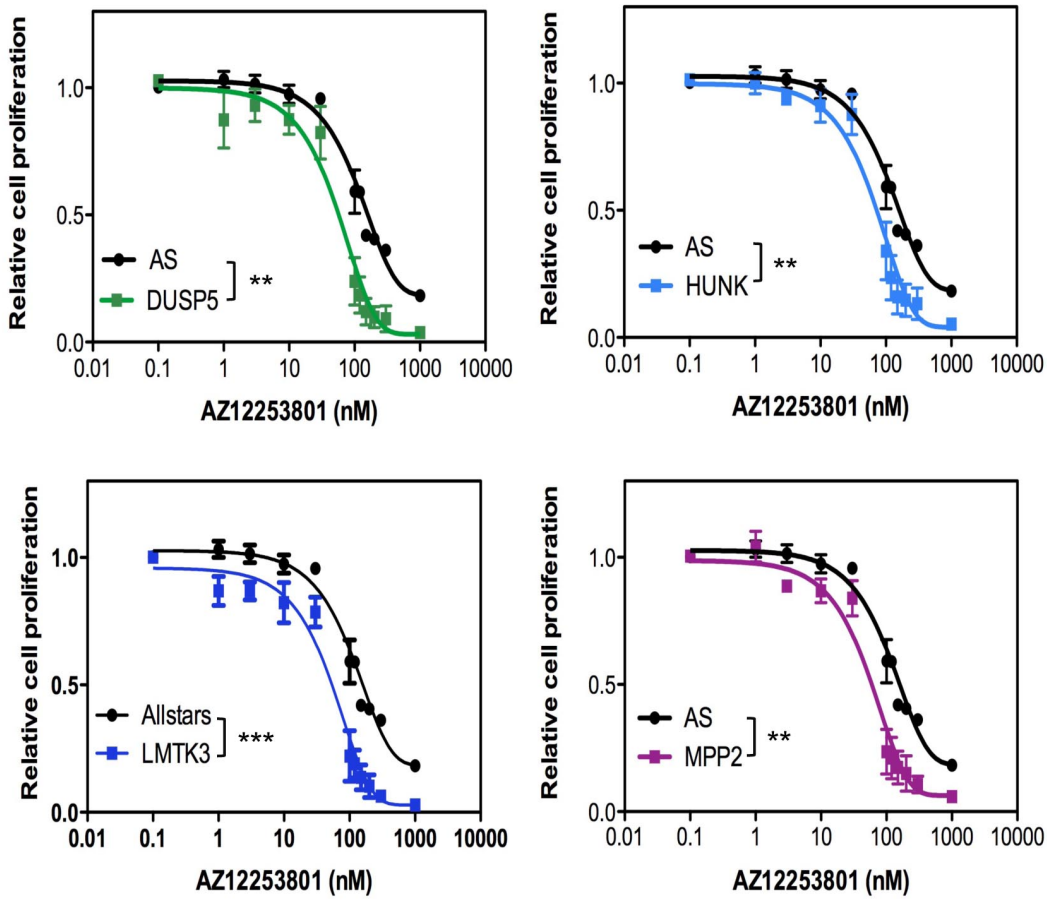

Figure 4.10 Knockdown of Kinome hits sensitized to AZ12253801. Cells were transfected with siRNAs, and after 48 hours were treated with solvent (DMSO) or AZ12253801. After 5 days, cell viability was measured with CTG assay. Graphs show data from three independent experiments, each with triplicate points. Relative proliferation was expressed as a fraction of viability in solvent-treated cells (bars, SEM). The data were curve fitted and GI_{50} values were calculated using GraphPad Prism software. Difference between data sets were determined by two way ANOVA (* $p<0.05$, ** $p<0.01$ or *** $p<0.001$).

Gene/siRNA	GI_{50} (nM)	Fold
AS	159	
AKAP1	69	2.3
APEG1	68	2.3
CDKN2C	59	2.6
CNKSR1	66	2.3
DUSP5	57	2.7
HUNK	72	2.2
LMTK3	54	2.9
MPP2	60	2.6

Table 4.3 Summary of validation hits from Kinome screen. Table shows gene name, GI_{50} values and fold sensitization calculated as ration between GI_{50} for AS transfectants and GI_{50} value for screen hit depletion

although different siRNAs had varying ability to degrade their target transcripts (Figure 4.9, A). Five genes (AKAP1, CDKN2C, CNKSR1, HUNK and MPP2) were silenced to below 50% of control levels, while in the remaining 3, transcript levels were reduced to 50-70% of control levels. Cell viability following siRNA transfection was tested by CTG assay. There were no major effects on cell viability in cells in which hits had been depleted compared with AS-transfected cells (Figure 4.9, B). Next, effects of target gene depletion were tested on sensitivity to AZ12253801. These assays were performed using all Kinome or repair-associated siRNAs in parallel. For clarity, the results are shown as separate graphs in Figure 4.10. In the primary and second round screens, AZ12253801 had been used only at its GI_{50} value. In current experiments, a broad range of concentrations was used. Knockdown of all eight Kinome hits sensitized to AZ12253801 in DU145 cells with 2.2-2.9 fold reduction in GI_{50} values (Figure 4.10 and table 4.3).

4.2.5 Validation of DNA repair-associated hits

The five on-target hits (Figure 4.7, B) were Cyclin-dependent kinase inhibitor 3 (CDKN3, Entrez GeneID 1033); Disheveled (Dsh) homolog 3 (DVL3, Entrez GeneID 1857); INO80 complex subunit C (INO80C, Entrez GeneID 125476);

Rad23 homolog B (Rad23B, Entrez GeneID 5887) and Rad51 homolog (Rad51, Entre GeneID 5888), all of which revalidated with at least two individual siRNAs in DU145 cells (Figure 4.8, B). In order to establish effects of depletion of the revalidated on-target hits on sensitivity to the IGF-1R inhibitor, the individual siRNA achieving the lowest cell survival (Figure 4.8, B) was chosen for further testing. Effects of gene silencing were assessed by qRT-PCR (normalization based on GAPDH) or western blot. Results are shown here for all repair-associated genes except DVL3, which is discussed in more detail in chapter 5 and chapter 6. Knockdown of the remaining 4 target genes was confirmed either by qRT-PCR (Figure 4.11, A) or western blot (Figure 4.11, B and C). The siRNAs induced effective knockdown of CDKN3, Rad23B and Rad51, although the effect of INO80C siRNA was relatively modest (Figure 4.11, A). Effect of hit depletion on cell viability was tested by CTG assay. Compared to controls, there was significant inhibition of cell proliferation that was particularly marked in cells depleted of IN80C and Rad51 (Figure 4.12). Rad51 is required for the strand invasion step of homologous recombination repair, and DU145 cells are defective in mismatch repair (Chen et al. 2003), so defects in DSBs repair after Rad51 loss and mismatch repair may cause significant inhibition of DU145 cell proliferation. Knockdown of each of these four hits sensitized to AZ12253801 in DU145 cells with 2.5-4-fold reduction in GI_{50} values (Figure 4.13 and table 4.4).

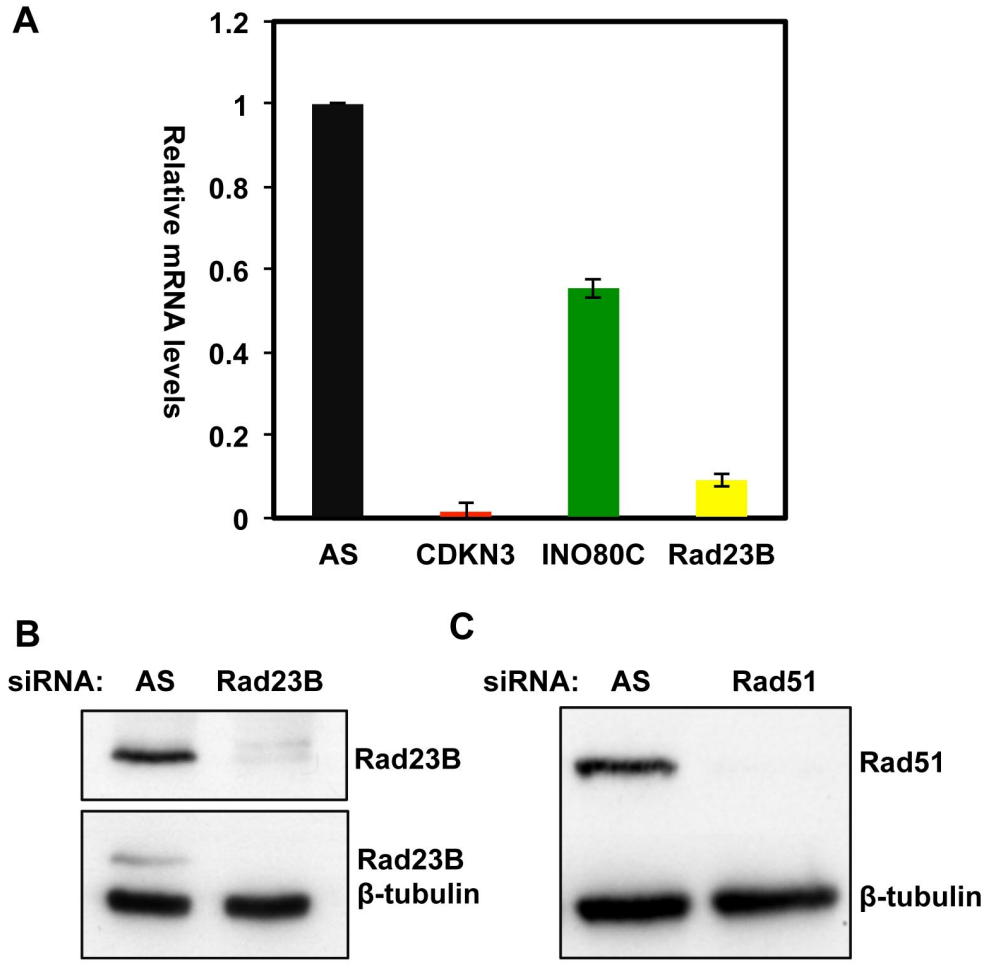

Figure 4.11 Depletion of DNA repair hits was confirmed by qRT-PCR or western blot. (A) RNA was extracted from DU145 cells 48 hours after transfection with siRNA and CDKN3, INO80C and Rad23B mRNA levels were quantified by qRT-PCR. After normalization to GAPDH, the levels of CDKN3, INO80C and Rad23B are shown relative to levels in AS-transfected cells. The qRT-PCR was repeated with three independent samples and each qRT-PCR was performed with triplicates. Error bars (SEM). (B-C) Western blot analysis of lysates prepared from DU145 cells transfected with AS, Rad23B, or Rad51 siRNA. Antibodies recognizing (B) Rad23B and (C) Rad51 were used in western blotting with β-tubulin as a loading control.

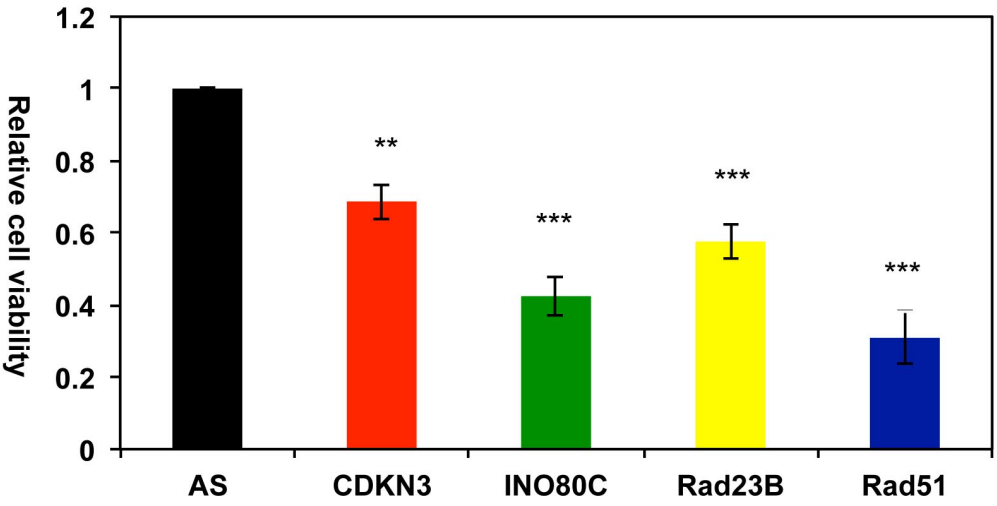

Figure 4.12 Assessment of cell viability after depletion of hits by screen siRNAs. DU145 cells were transfected with AS or gene-specific siRNAs, and CTG assays were performed 7 days later. Cell viability was expressed as a percentage of the viability of cells transfected with AS. The mean and SEM were from three independent experiments, each with triplicate wells. ** P<0.01, *** P<0.001 (one way ANOVA).

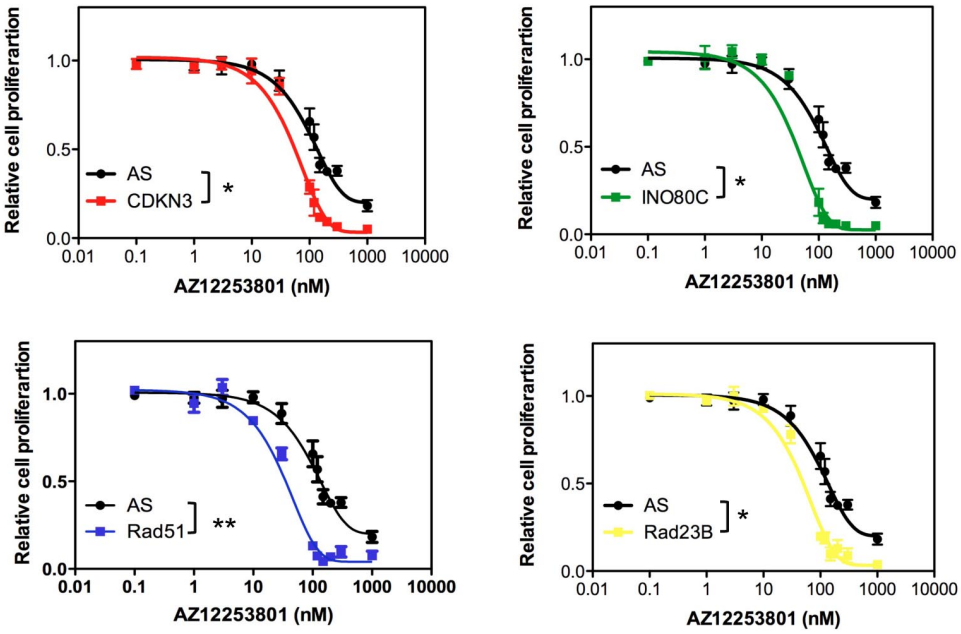

Figure 4.13 Knockdown of DNA repair hits sensitized DU145 cells to AZ12253801. Cells were transfected with siRNAs, and treated with solvent (DMSO) or AZ12253801 48 hours after transfection. After 5 days, cell viability was measured by CTG assay. Graphs represent mean and SEM of data from three independent experiments, each with triplicate wells. The data were curve fitted and GI_{50} values were calculated using GraphPad Prism software. Differences between data sets were analyzed by two way ANOVA (* $p<0.05$, ** $p<0.01$).

Gene/siRNA	GI_{50} (nM)	Fold
AS	148	
CDKN3	60	2.5
INO80C	53	2.8
Rad23B	52	2.8
Rad51	37	3.9

Table 4.4 Summary of validation hits from DNA repair-associated screen. Table shows gene name, GI_{50} values and fold sensitization calculated as ration between GI_{50} for AS transfectants and GI_{50} value for screen hit depletion

In summary, the screen identified 8 kinase-related and 5 DNA repair-associated proteins that appeared to influence sensitivity to IGF-1R inhibition, although the effects are not large (2.2-4 fold changes in GI_{50} values). One of the strongest hits in DU145 cells was DVL3 (Figure 4.8 B), and this became the main focus of the project.

Chapter 5

Investigating DVL3 as a screen hit

5.1 Introduction

The next stage is to investigate hits to elucidate the basis for effects on sensitivity to the IGF-1R inhibitor. Initial experiments are focusing on DVL3, which was identified as a hit in DU145 and MCF-7 cells. DVL3 siRNA was included in the DNA repair-associated library, although it has no known role in DNA repair.

DVL/Dsh was first identified in Drosophila and named because body and wing hairs of mutant flies fail to orient properly (Fahmy and Fahmy 1959). Subsequently it was discovered that this gene had an important role in segment polarity of the early embryo (Perrimon and Mahowald 1987). Three DVL homologs (DVL1, 2 and 3) have been cloned in mice and humans, showing

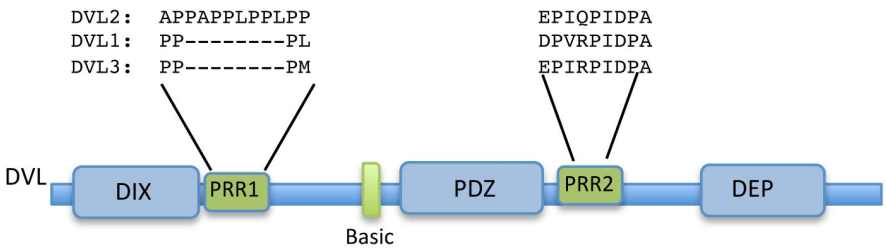

Figure 5.1 Schematic of DVL structure. DVL proteins contain 716 amino acids and consist of conserved DIX, basic region, PDZ, proline-rich region (PRR) and DEP domains. Modified from Crampton et al. 2009)

high sequence homology. The three DVL genes are widely expressed in mouse and xenopus embryonic development, and in various adult tissues, with considerable overlap in expression patterns, indicating that they may have redundant functions (Gao and Chen 2009).

DVL knock-out mice have been generated to study their functions. DVL1 null mice are viable, fertile and stucturally normal. Despite normal brain structure, these mice show abnormal social behaviour (Lijam et al. 1997). Half of DVL2 knock-out mice die in the perinatal period due to cardiac abnormalities. The remaining surviving mutants are predominantly female, indicating a possible function of DVL2 on sexual determination. DVL1 and DVL2 appear to have non-redundant roles in heart morphogenesis, because there is the same ratio of cardiac defects in DVL2 and DVL1:DVL2 mutants. Furthermore, 90% of DVL2 knock-out mice display skeletal malformations, indicating that DVL2 plays a crucial role in skeletal development (Hamblet et al. 2002). DVL3 knock-out mice die at the perinatal stage with cardiac outflow tract abnormalities similar to the phenotype of DVL2-/- mice, but without skeletal defects (Etheridge et al. 2008). Either DVL1 or DVL2 are able to rescue the lethal DVL3-/- heart phenotype, indicating that DVL genes have redundant function in development. Double null mutants and even trans-heterozygotes have more severe phenotypes than any single DVL mutant alone (Etheridge et

al. 2008).

DVL proteins possess three conserved functional domains (Figure 5.1). These are an amino-terminal DIX (DVL, Axin) domain of 80 amino acids, a central PDZ (postsynaptic density 95, Discs Large, Zonula occludens-1) domain of approxmiately 90 amino acids, and a carboxyl-terminal DEP (DVL, Egl-10, Pleckstrin) domain of 80 amino acids. In addition, there are two conserved regions: a basic region which is a cluster of positively charged residues just preceding the PDZ domain, and a proline-rich region (PRR) close to the carboxy-terminus of the PDZ domain. DVL2 has an additional PRR downstream of the DIX domain (Figure 5.1). DVLs interact with other proteins to influence various signalings (Gao and Chen 2009).

5.2 Results and discussion

Given that DVL3 was one of the strongest hits after second round screens in DU145 cells (Figure 4.8, B), and in light of the known crosstalk between the WNT, IGF and mTOR signaling pathways (Playford et al. 2000; Chen et al. 2005; Inoki et al. 2006), the next set of experiments tested whether DVL3 was a valid screen hit. Firstly, expression of DVL isoforms was characterized in

DU145 prostate cancer cells.

5.2.1 Abundant expression of DVL3 in DU145 prostate cancer cells

All three isoforms of DVLs were able to be detected by qRT-PCR, and relative levels of DVL1-3 expression were compared (normalized to GAPDH expression) in DU145 cells (Figure 5.2, A and B). DVL3 appeared to be the dominant isoform among the three homologs and constituted approximately 80% of total pooled DVLs (Figure 5.2, A and B), with DVL1 and DVL2 each constituting approximately 10% (Figure 5.2, B). In contrast, a previous study found that all three DVL isoforms were expressed in mouse F9 and human HEK293 cells, but DVL2 was the dominant isoform, representing more than 80% of the total DVL pool in HEK293 and 95% in F9 cells (Lee et al. 2008).

5.2.2 DVL3 not DVL1 or DVL2 knockdown enhanced sensitivity to IGF-1R inhibiton

5.2.2.1 Isoform-specific DVL3 knockdown enhanced sensitivity to AZ12253801

Two individual screen DVL3 siRNAs (No.1 and 4, see Figure 4.8, B) were

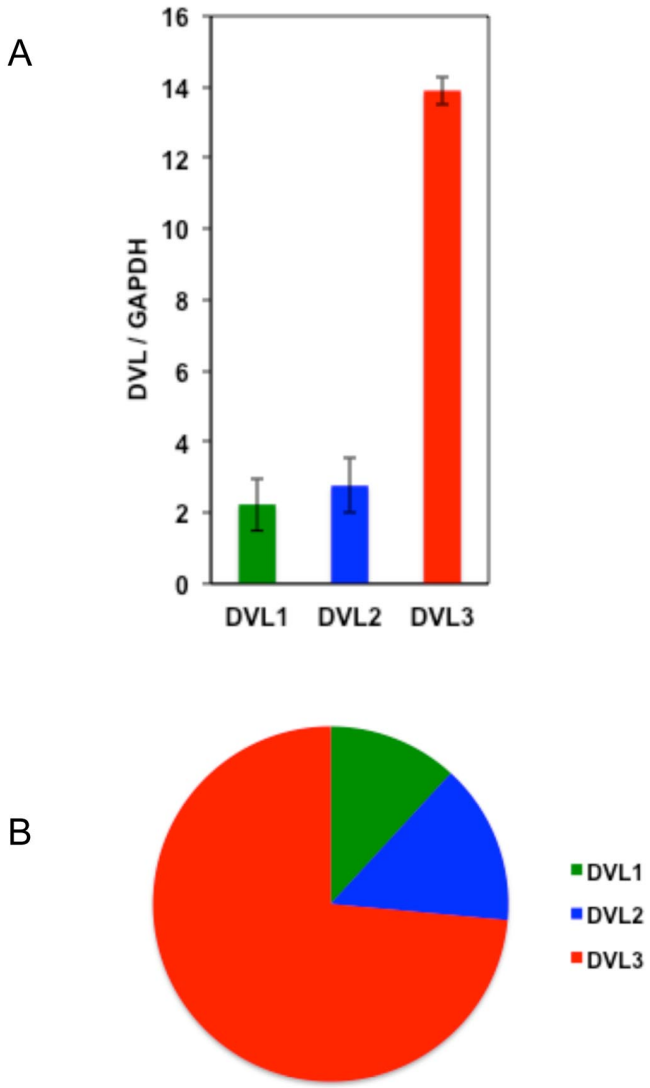

Figure 5.2 Expression of DVL1-3 in DU145 cells. DVL1-3 expression was quantified by qRT-PCR in three independent sets of RNAs. (A) DVL1-3 levels were expressed as ratio of DVL 1-3 to GAPDH (1000 copies). Error bars, SEM from three independent experiments, each with triplicate data points. (B) DVL1-3 expression was expressed as percentage of sum of the total of the three DVL isoforms.

revalidated by testing effects on DVL3 knockdown, which was confirmed by western blot (Figure 5.3, A), with more potent silencing by DVL3 siRNA 4 than siRNA 1. The more potent DVL3 siRNA 4 was used to check the sequence specificity of gene knockdown, in view of the similarity between DVL homologs 1-3. In fact, DVL3 siRNA 4 did not affect expression of DVL2 at the protein level, by comparision with clear knockdown of DVL3 (Figure 5.3, B). There was no good commercial DVL1 antibody available, so it was not possible to test expression of DVL1 at the protein level. At the RNA level, there was significant reduction in DVL3 expression after transfection with DVL3 siRNA 4 compared to control-transfected cells, but DVL1 or DVL2 mRNA levels were not affected (Figure 5.3, C). This suggests that DVL3 siRNA 4 specifically silenced DVL3 and did not affect expression of DVL homologs DVL1 or DVL2.

DVL3 knockdown by siRNA 4 caused modest but statistically significant inhibition of DU145 cell viability (Figure 5.4, A). CTG assays were performed to test effects of DVL3 knockdown on sensitivity to IGF-1R inhibitor AZ12253801 (Figure 5.4, B and C). DVL3 knockdown increased DU145 cell sensitivity to AZ12253801, with 2-fold increase in sensitivity using DVL3 siRNA 1 and 2.7 fold increase in sensitivity using DVL3 siRNA 4, which is consistent with the relative efficacy of DVL3-1 and 4 siRNAs in silencing DVL3 (Figure 5.3, A).

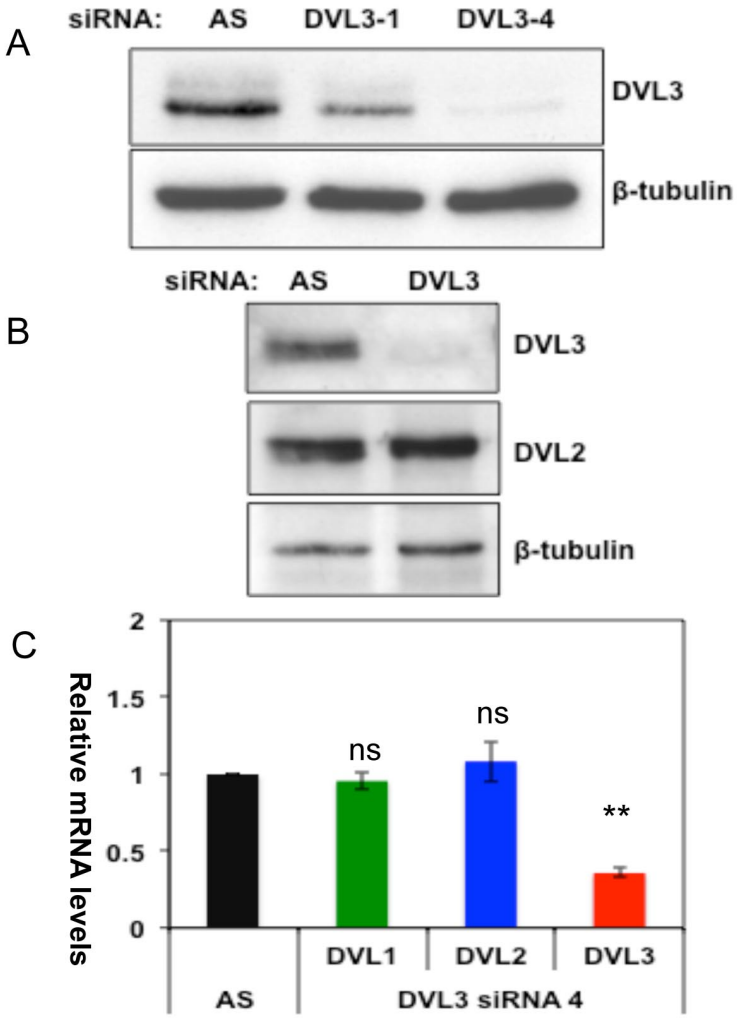

Figure 5.3 DVL3 siRNA 4 specifically silenced its target gene. (A) Western blot analysis of lysates prepared from DU145 cells transfected with AS, DVL3 siRNA 1 or 4. (B) Western blot of lysates from DU145 cells, 48 hours after transfection with DVL3 or AS siRNAs, probed with isoform specific antibodies to DVL2 or 3. There was no validated DVL1 antibody, so expression of this isoform was tested at the mRNA level. (B) DU145 cells were reverse-transfected with DVL3 siRNA 4 and DVL1-3 mRNA levels were quantified by qRT-PCR and normalized to GAPDH. DVL1-3 mRNA level is shown relative to expression in AS-transfected cells. Error bars represent SEM of three independent experiments. Each qRT-PCR included triplicate samples. **, $p<0.01$ (one way ANOVA).

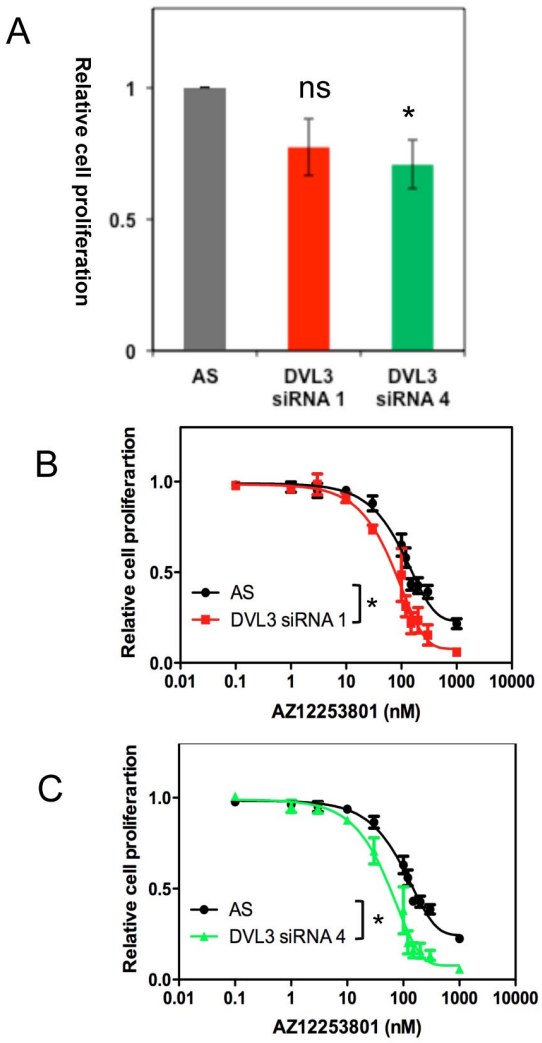

Figure 5.4 DVL3 knockdown enhanced the sensitivity of DU145 cells to AZ12253801. (A) The viability of cells transfected with AS, DVL3 siRNA 1 or 4 was tested in CTG assays after 7 days. Results were normalized to the viability of cells transfected with AS siRNA. The mean and bars (SEM) were from three independent experiments, each with triplicate points. ns (indicating there was no difference between two groups, $p>0.05$), *, $p<0.05$ (one way ANOVA). (B-C) CTG assay in DU145 cells transfected with DVL3-1 or 4 or AS siRNAs, and treated with AZ12253801. The assay was repeated three times, and each assay included triplicate wells. Error bars represent SEM. Curves were fitted to the data points using GraphPad Prism 5 to calculate GI_{50} values: AS siRNA=150nM, DVL siRNA 1=74nM and DVL siRNA 4=58nM. *, $p<0.05$ (two way ANOVA).

5.2.2.2 Knockdown of either DVL1 or DVL2 did not enhance sensitivity to AZ12253801

The siRNA libraries used in the screen had not included DVL1 and 2 siRNA. Therefore, the effects of DVL1 and DVL2 knockdown on AZ12253801 sensitivity were tested, using validated siRNAs targeting DVL1 or DVL2 (QIAgen). According to the results of qRT-PCR, it was clear that each siRNA significantly silenced its target gene and did not affect the other two DVL isoforms (Figure 5.5, A and B). At the protein level, DVL2 was depleted in DU145 cells transfected with DVL2 siRNA, but the DVL3 level did not vary (Figure 5.5, C). As before (Figure 5.4, A), knockdown of DVL3 by siRNA 4 caused modest reduction in DU145 cell proliferation, however, DVL1 and DVL2 knockdown did not have any effect on proliferation of DU145 cells compared to AS-transfected cells (Figure 5.6, A). DVL1 or DVL2 silencing did not enhance sensitivity to AZ12253801, when tested in parallel with DVL3 as positive control (Figure 5.6, B, C, and D). The fold change in GI_{50} values following silencing of DVLs 1-3 was respectively 0.97, 1.07 and 2.78 compared to AS transfectants. There were three possibilities to explain this result. Firstly, the depletion of DVL1 or DVL2 may have been insufficient to trigger the effect on AZ12253801 sensitivity. Secondly, the expression level of DVL1 or DVL2 was lower in DU145 cells compared to DVL3 (Figure 5.2, A and B), suggesting that DU145 cells are less dependent on DVL1 or DVL2. Thirdly, the loss of either DVL1 or

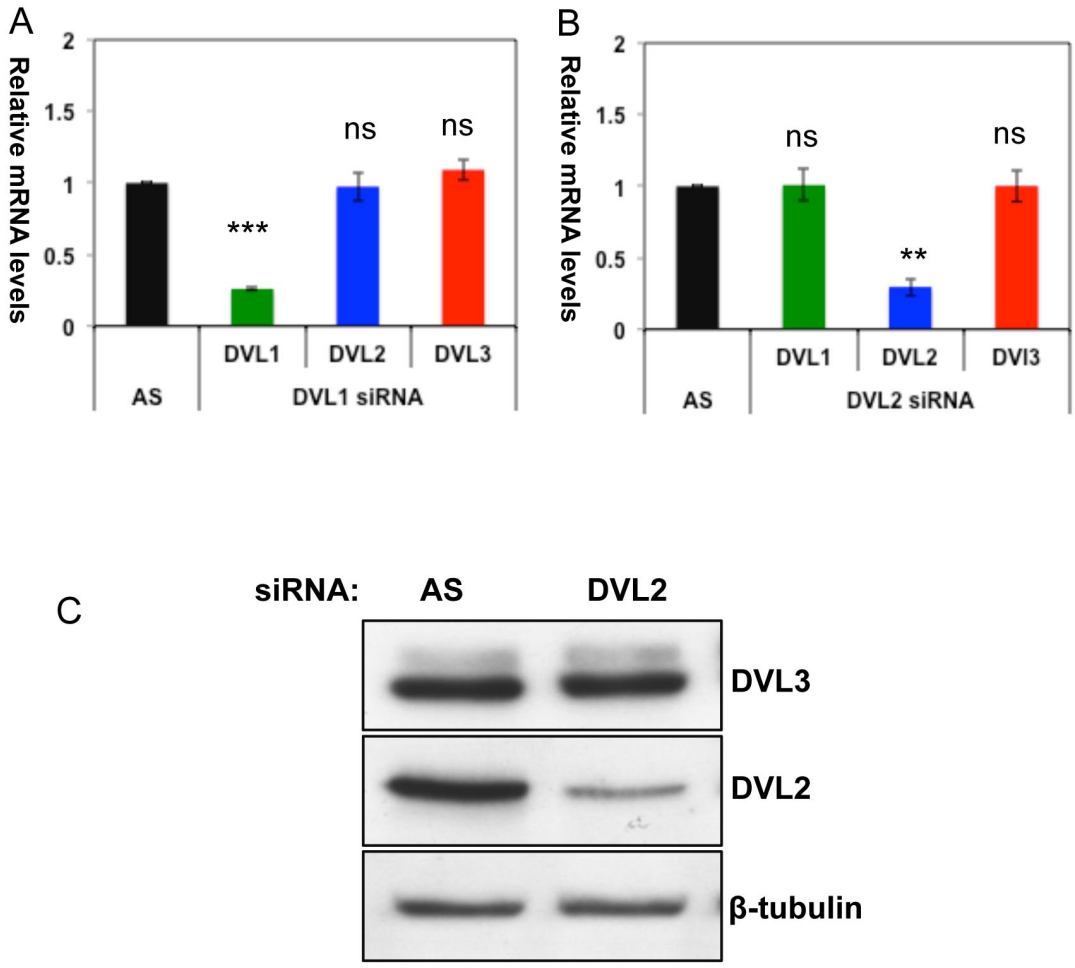

Figure 5.5 Isoform specific gene silencing by DVL1 and DVL2 siRNA. DU145 cells were reverse-transfected with DVL1 siRNA (A) or DVL2 siRNA (B). DVL1-3 mRNA levels were quantified by qRT-PCR, normalized to GAPDH, and are shown relative to expression in AS-transfected cells. Error bars represent SEM from three independent experiments, each with triplicate data points. ns (indicating there was no difference between two groups, $p>0.05$), ***, $p<0.001$, **, $p<0.01$ (one way ANOVA). (C) Western blot of lysates from DU145 cells transfected with DVL2 or AS siRNAs, probed with isoform specific antibodies to DVL2 or 3.

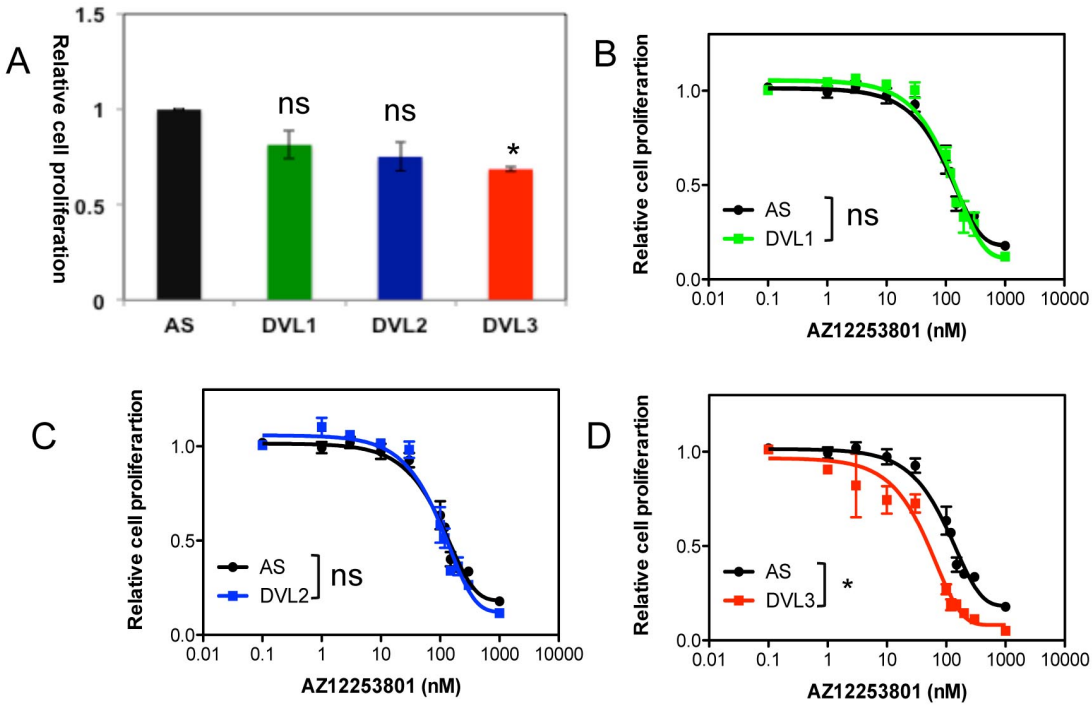

Figure 5.6 DVL1 or DVL2 knockdown did not enhance sensitivity of DU145 cells to AZ12253801. (A) DU145 cells were transfected with AS or DVL siRNAs, and CTG assays were performed 7 days later. Cell viability was expressed as a percentage of the viability of cells transfected with AS. The mean and SEM were from three independent experiments, each with triplicate wells. * $p<0.05$ (one way ANOVA). DU145 cells were transfected with AS or DVL1 (B), DVL2 (C) or DVL3 (D) siRNAs. After 48 hours cells were treated with AZ12253801 and cell viability was measured with CTG assays after five days. Mean ± SEM from three independent CTG assays, each with triplicate points. Curves were fitted to the data points using GraphPad Prism 5 to calculate GI_{50} values: AS siRNA=139nM, DVL1=144nM, DVL2=130nM and DVL3=50nM. ns, not significant, * $p<0.05$ (two way ANOVA).

DVL2 may be compensated by the presence of DVL3.

5.2.2.3 Testing effects of DVL3 silencing on sensitivity to alternative forms of IGF-1R

Small molecule inhibitor may inhibit molecules other than the intended target. To determine whether effects of DVL3 depletion on AZ12253801 sensitivity were related to the ability of AZ12253801 to inhibit IGF-1R, two alternative strategies were used to block the IGF axis. Firstly, double knockdown of IGF1R and DVL3 caused greater inhibition of DU145 cell proliferation compared to IGF-1R or DVL3 knockdown alone (Figure 5.7, A). The depletion of target protein was confirmed by western blot (Figure 5.7, B). Secondly, a specific monoclonal IGF-1R antibody (MAB391, R&D Systems) was combined with DVL3 silencing. The antibody alone did not inhibit DU145 cell growth, but addition of DVL3 depletion caused a significant shift in the dose-response curve (Figure 5.8). Taken together, these data suggested that the ability of DVL3 depletion to sensitize to AZ12253801 is specifically related to the ability of AZ12253801 to inhibit IGF-1R.

In summary, depletion of DVL3 but not DVL1 or 2 appeared to regulate sensitivity of DU145 cells to IGF-1R inhibition or depletion. The effect was

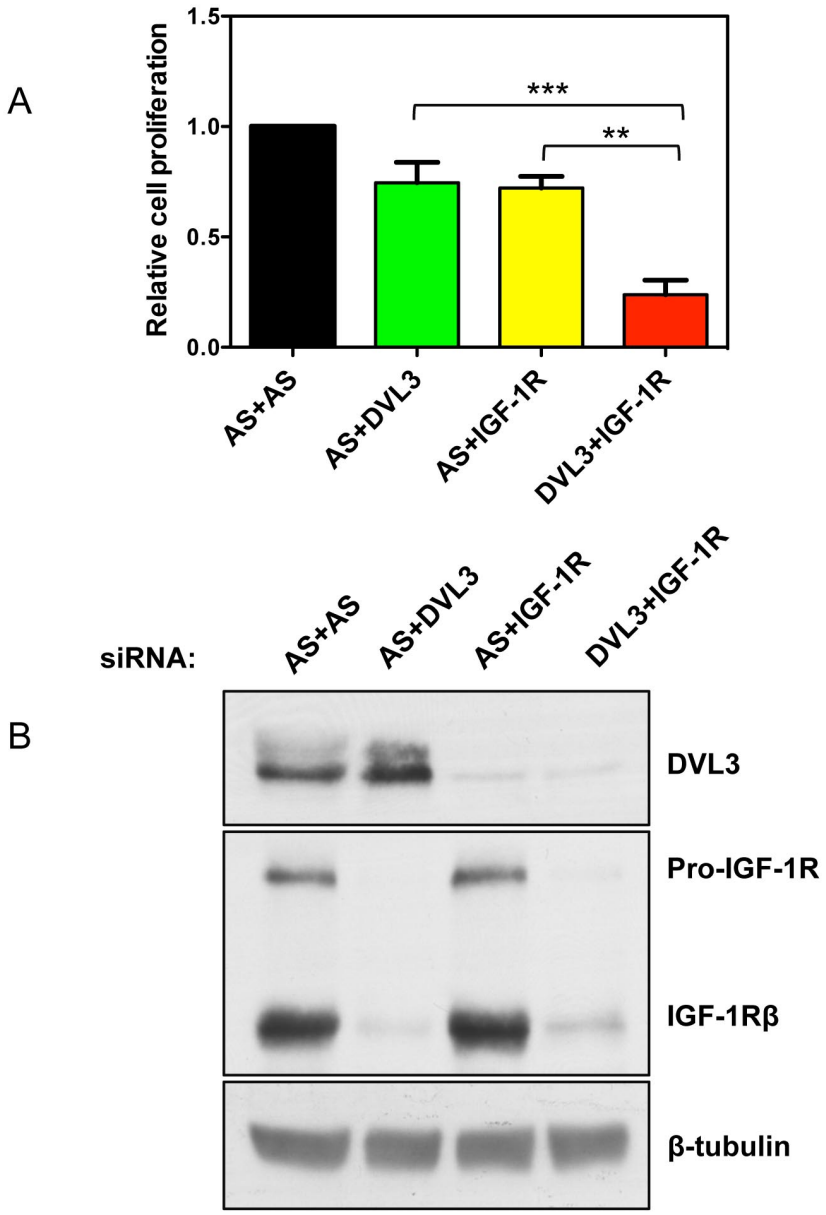

Figure 5.7 DVL3 knockdown enhanced sensitivity to IGF-1R knockdown in DU145 cells. (A) CTG assays were performed 5 days after transfection with AS, DVL3 and/or IGF-1R siRNAs using a total of 100nM siRNA for each transfection. Data represent mean±SEM of three independent experiments, each with triplicate points. ** $p<0.01$, *** $p<0.001$ (one-way ANOVA). (B) Western blot analysis of lysates prepared from DU145 cells transfected with AS, DVL3 and/or IGF-1R siRNAs and probed for DVL3 and IGF-1Rβ with β-tubulin as loading control.

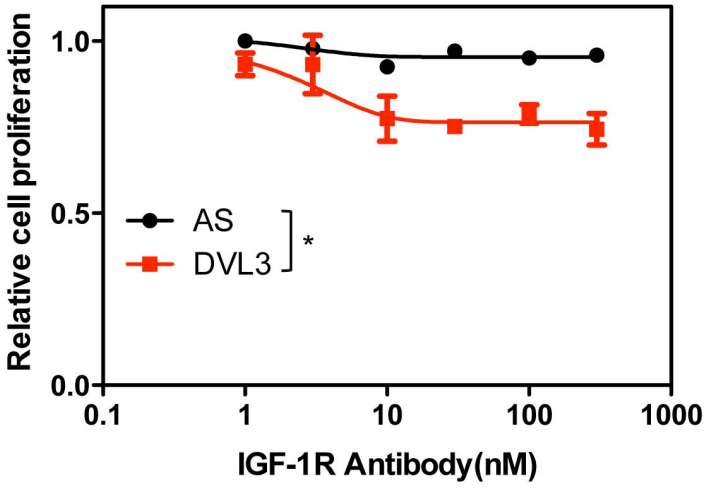

Figure 5.8 DVL3 silencing sensitized DU145 cells to IGF-1R inhibition. DU145 cells were reverse-transfected with AS or DVL3 siRNAs and after 48 hours treated with MAB391 or control (PBS). CTG assays were performed at day 7. Data were curve fitted using GraphPad Prism 5 from two independent experiments, each with duplicate wells. Error bars (SEM), * $p<0.05$ (two way ANOVA).

consistent (compare Figure 5.4 C and 5.6 D), but not large (2-2.8 fold). In deciding whether to pursue investigation of this effect, it was noted that other studies had identified biologically significant results from siRNA screens that initially appeared quite modest. Examples include sensitization of BRCA1/2 null cells to PARP depletion (Farmer et al. 2005) and the inhibitory effects of LMTK3 depletion in MCF7 cells (Giamas et al. 2011), and of GATA2 depletion in KRAS mutant lung cancer (Kumar et al. 2012). Therefore, it was decided to continue with investigation of DVL3 as a screen hit. The priorities were to understand the basis for SLL, and to identify a small molecule drug that could recapitulate effects of DVL3 depletion.

5.2.3 Effects of DVL3 knockdown on IGF WNT and IGF signaling

The next set of experiments assessed the role of DVL3 in cell signaling, and the potential crosstalk with the IGF axis, aiming to identify the mechanism by which DVL3 affects AZ12253801 sensitivity. DVLs play an important role in WNT canonical signaling. In quiescent cells, β-catenin forms a complex with AXIN, GSK3β and APC, which mediates the phosphorylation and destruction of β-catenin. WNT signaling leads to phosphorylation of DVL, and inhibition of β-catenin degradation (Figure 1.2) (Wharton 2003). To test the effect of DVL3

knockdown on WNT canonical signaling, DU145 cells were transfected with AS or DVL3 siRNAs, serum-starved, and treated with IGF-1. Active β-catenin levels were reduced after transfection with DVL3 siRNA compared with control transfectants. These data suggest that DVL3 is a member of the WNT canonical pathway as reported before (Hocevar et al. 2003), although effects on level of active β-catenin were relatively modest (Figure 5.9).

Previously, our lab and others showed that IGF-1R was able to stabilize β-catenin via complexing with IRS-1level, leading to β-catenin nuclear translocation and increasing β-catenin transcriptional activity (Playford et al. 2000; Chen et al. 2005). However, there was no evidence that IGF stimulation (Figure 5.9) affected levels of active β-catenin or levels or phosphorylation of DVL3 in DU145 prostate cancer cells (Figure 5.9). This suggested that IGF signaling does not affect the WNT canonical signaling pathway in these cells.

It then tested whether DVL3 silencing affected signaling via the IGF-1R axis. DU145 cells were DVL3-depleted, serum-starved and IGF-1-treated, to measure effects on activation of IGF axis components. Levels of phospho-IGF-1R and phospho-AKT increased in the presence of IGF-1 as expected. However, DVL3 knockdown did not alter phospho-IGF-1R and

phospho-AKT (Figure, 5.9). The mTOR signaling pathway is an important downstream effector of IGF-1R, activated via PI3K-AKT (Laplante and Sabatini 2009), and is positively regulated by the WNT pathway (Inoki et al. 2006). DVL3 knockdown appeared to inactivate the mTOR pathway, as judged by levels of phosphorylation of mTOR itself and S6 that is an important substrate and indicator of mTOR activity (Inoki et al. 2006) (Figure 5.9). This result is consistent with the reported ability of WNT signaling to activate the mTOR pathway (Inoki et al. 2006). In that report, after WNT 3A stimulation, DVL2 induced the disassociation of GSK3β from the β-catenin destruction complex, reducing sequential phosphorylation by AMPK and GSK3β of TSC2. This process inactivated TSC2 resulting in the activation of mTOR (Inoki et al. 2006). Previously, DVL3 was not implicated in regulation of mTOR, but results in DU145 cells are consistent with the inactivation of the mTOR pathway by DVL3 knockdown (Figure 5.9).

Aside from the PI3K-AKT-mTOR pathway, the second main effector of IGF-1R activation is the RAS-RAF-MEK-ERK pathway. After IGF-1 stimulation, levels of phospho-ERK 1/2 increased as predicted. It was also noted that phospho-ERK levels increased after DVL3 knockdown (Figure 5.9). The activity of ERK1/2 after DVL3 knockdown was enhanced by IGF-1 stimulation

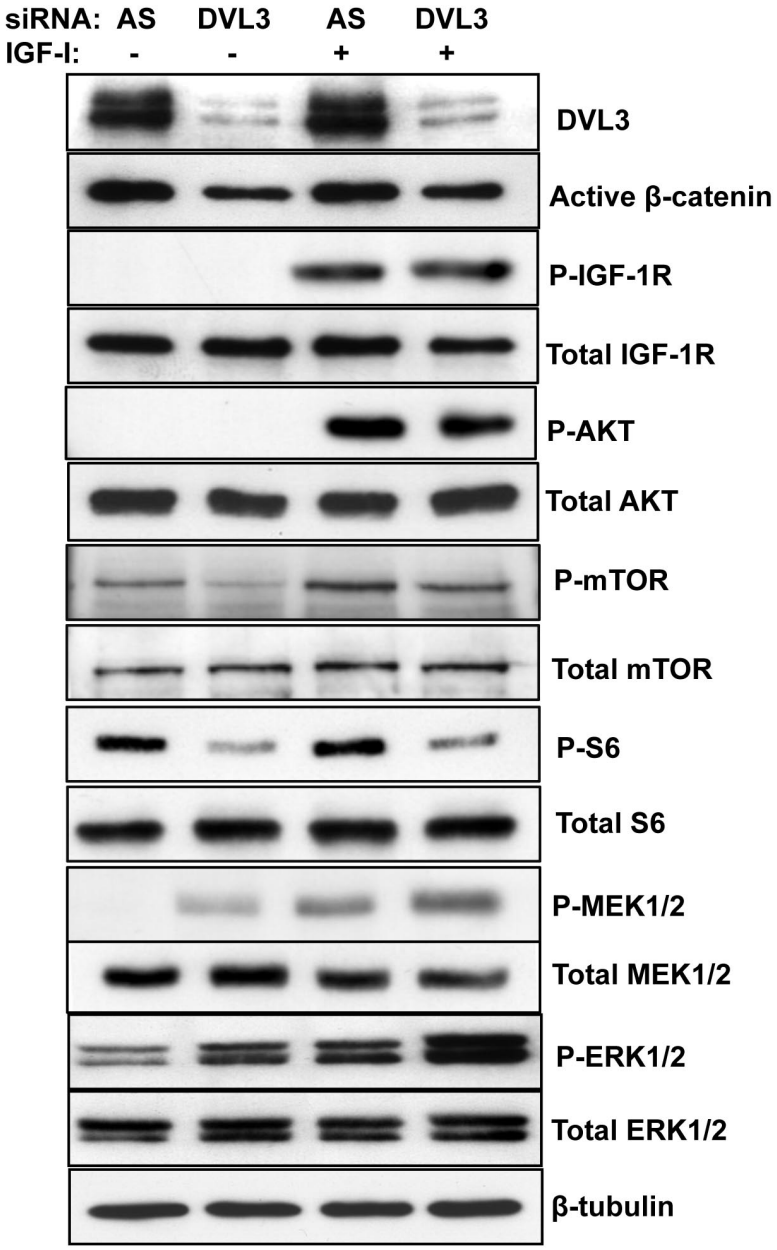

Figure 5.9 Effects of DVL3 knockdown on WNT and IGF signaling in DU145 cells. DU145 cells were transfected with AS or DVL3 siRNAs, after 48 hours serum-starved overnight and treated with 10 nM IGF-1 or solvent for 10 minutes. Cell lysates were analyzed for DVL3, active β-catenin, P-IGF-1R (Tyr1135/1136), IGF-1R, P-AKT（Ser473), P-mTOR (Ser2448), mTOR, P-S6 (Ser240/244), S6, P-MEK1/2 (Ser221), MEK1/2, P-ERK1/2 (Thr202/Tyr204) and ERK1/2 with β-tubulin as loading control. Similar results have been observed from two more independent experiments

compared to DVL3 knockdown or IGF-1 stimulation alone (Figure 5.9). As the upstream kinase of ERK1/2, the activity of MEK1/2 was measured and showed the same pattern as ERK1/2, with increase in the response to IGF-1 stimulation or DVL3 depletion, and more increase after DVL3 depletion responsive to IGF-1 treatment by comparison with IGF-1 stimulation or DVL3 depletion alone (Figure 5.9).

The next experiments assessed whether ERK1/2 activation by DVL3 depletion had effects on ERK1/2 localization and gene expression. ERK1/2 was found to translocate into the nucleus following DVL3 knockdown (Figure 5.10, A), which was consistent with a previous report indicating that ERK1/2 activation is accompanied by ERK1/2 nuclear translocation (Khokhlatchev et al. 1998). So far, there have been more than 160 substrates identified, which are regulated by activated ERK1/2 (Yoon and Seger 2006). These include cyclin D1 and E twenty-six (ETS)-like transcriptional factor (ELK1) (Lavoie et al. 1996; Boros et al. 2009). ELK1 is a transcriptional coactivator and its target genes have been mapped on a genome-wide scale, and include FOS, TATA-binding protein (TBP) and TBP-associated factor 1 (TAF1) (Boros et al. 2009). The expression levels of these genes increased approximately 2 fold after DVL3 knockdown (Figure 5.10, B). These data suggest that ERK1/2 was activated by DVL3 silencing. It is possible that activation of the ERK1/2 pathway and increasing

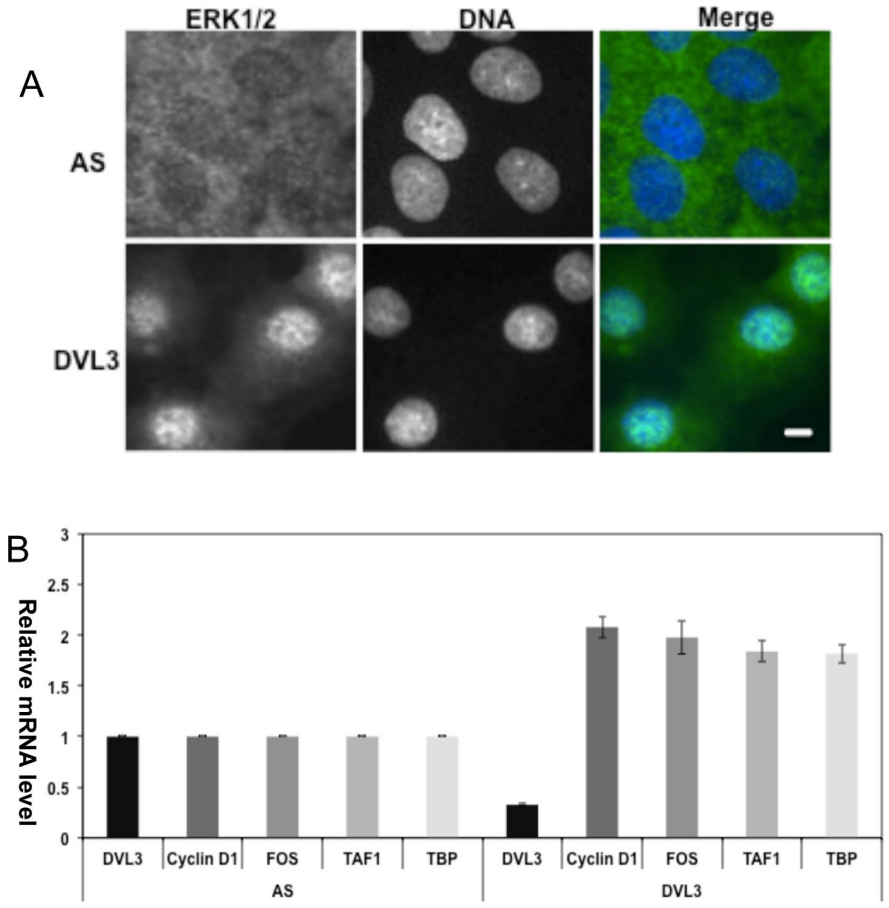

Figure 5.10 ERK1/2 nuclear translocation and functional activation after DVL3 knockdown in DU145 cells. (A) DU145 cells were transfected with AS or DVL3 siRNAs, and serum-starved overnight. Cells were fixed and stained with ERK1/2 antibody (green) and with DAPI to visualize DNA (blue). Similar results have been observed from one more independent experiment. Bar scale, 10μm. (B) DU145 cells were transfected with AS or DVL3 siRNAs, and serum-starved overnight. DVL3, Cyclin D1, FOS, TAF1 and TBP mRNA levels were measured by qRT-PCR and normalized to GAPDH. Data were shown as mean ±SEM of three independent experiments, each with triplicate data points.

sensitivity to IGF ligand may contribute to sensitivity to IGF-1R inhibition after DVL3 silencing.

5.2.4 Overexpressed DVL3 decreased the sensitivity of IGF-1 on ERK1/2 activation

To further investigate the relationship between DVL3 and regulation of ERK1/2 activation, pCDNA3.1(+) Flag-DVL3 human construct was obtained from Addgene, and transfected into DU145 cells. After 48 hours, cells serum-starved and treated with IGF-1. DVL3 antibody was able to detect overexpressed Flag-DVL3 (Figure 5.11). Cells overexpressing Flag-DVL3 showed reduced levels of ERK1/2 phosphorylation in response to IGF-1 stimulation. Flag-DVL3 overexpression also increased the activity of the mTOR pathway as judged by increasing phospho-S6 (Figure 5.11). These results confirm the reported ability of WNT signaling to activate mTOR, and also support a link between DVL3 and regulation of ERK1/2 activation. It is predicted that DVL3 overexpression may reduce sensitivity to AZ12253801, testing this will require production of stable Flag-DVL3 overexpressing cells. These results show that DVL3 suppresses IGF signaling via the MEK-ERK pathway, and may mediates resistance to IGF-1R inhibition.

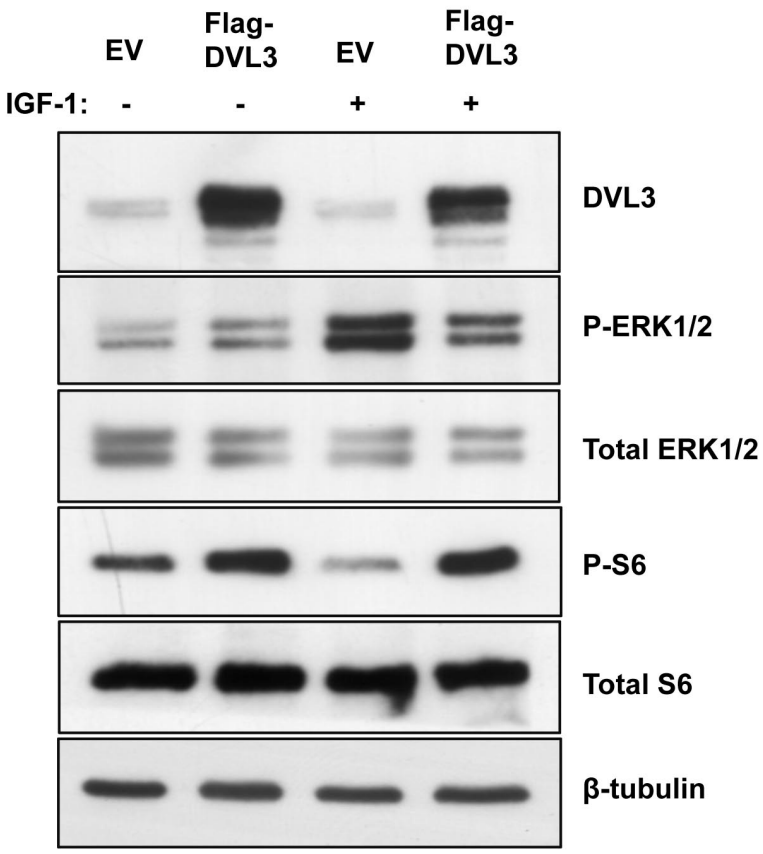

Figure 5.11 Overexpression of FLAG-DVL3 reduced IGF-induced ERK1/2 activation. DU145 cells were transfected with pCDNA3.1 (EV) or pCDNA3.1-Flag-DVL3 (Flag-DVL3), and after 48 hours serum-starved overnight followed by treatment with 10nM IGF-1 for 10 minutes. Lysates were probed with specific DVL3, P-ERK1/2(Thr202/Tyr204), total ERK1/2, P-S6 (Ser240/244) and total S6 antibodies with β-tubulin as loading control. A similar result was obtained from one more independent experiment.

Chapter 6

Testing ability of WNT inhibitors to recapitulate effects of DVL3 depletion

6.1 Introduction

Having identified DVL3 as a mediator of resistance to IGF-1R inhibition, the next step was to try to find a WNT inhibitor that would mimic effects of DVL3 depletion.

6.2 Results and discussion

6.2.1 Testing effects of AXIN stabilization using XAV939

XAV939 is a cell-permeable small molecule inhibitor that inhibits tankyrase 1/2, thus stabilizing axin and stimulating β-catenin degradation. This effect occurs only in cells by the presence of mutated APC (Huang et al. 2009). XAV939 caused dose-dependent inhibition of the growth and survival of DU145 cells

(Figure 6.1, A-C). However, there was no reduction in active β-catenin, probably because DU145 cells harbor wild-type APC and β-catenin (Gerstein et al. 2002). Axin stabilization inactivated the mTOR pathway, shown by reduction of S6 phosphorylation consistent with mTOR regulation by WNT, and probably explaining why the growth of DU145 cells was inhibited by XAV939. XAV939 did not appear to enhance sensitivity to AZ12253801, either in 6-well-plate clonogenic assay or 96-well-plate CTG assay (Figure 6.2, A-C). Furthermore, XAV939 treatment of DU145 cells did not show any change in ERK1/2 phosphorylation compared with solvent-treated cells (Figure 6.2 D).

These findings indicate that both DVL3 knockdown and XAV939 were capable of blocking mTOR, consistent with published data on links between WNT singling and mTOR regulation (Inoki et al. 2006). However, only DVL3 knockdown sensitized to AZ12253801 and increased ERK1/2 phosphorylation. These is a report of negative feedback between ERK1/2 and mTOR that can influence the IGF-1R signaling pathway, which could be involved here (Buck et al. 2008; Li et al. 2011). Given that XAV939 was able to inactivate mTOR and unable to activate ERK1/2, this suggests that ERK1/2 activation by DVL3 knockdown was unlikely to result from its downstream inactivation of mTOR.

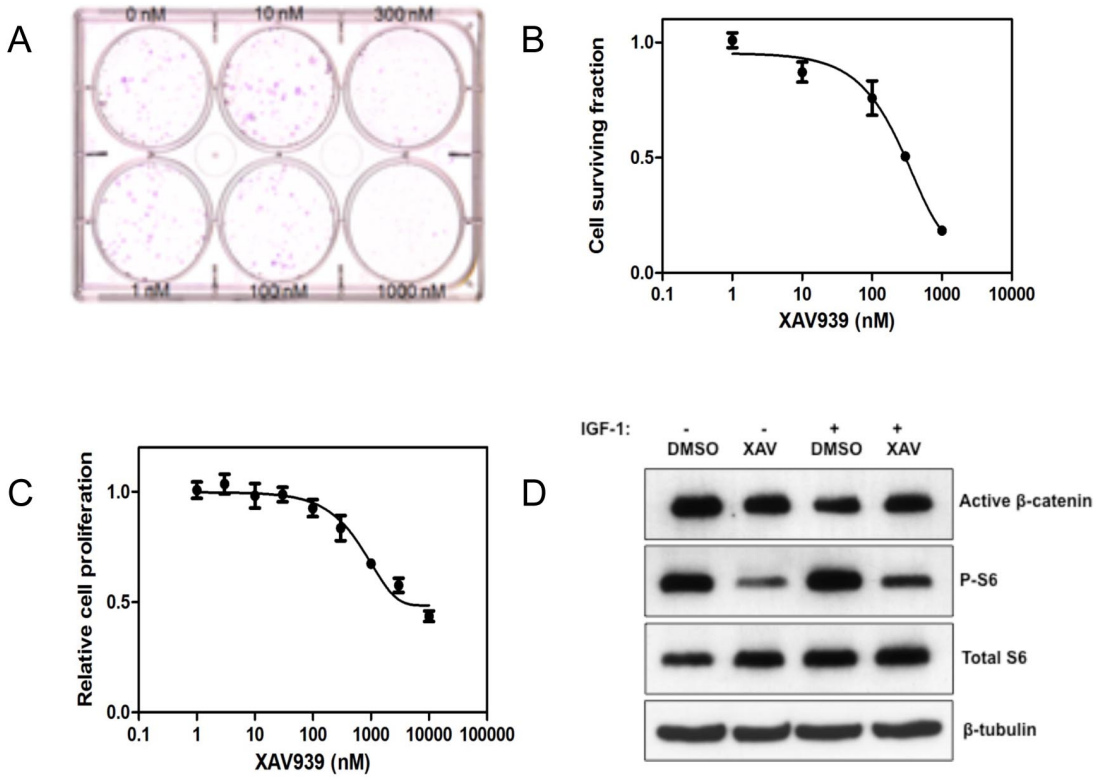

Figure 6.1 XAV939 inhibited the growth of DU145 cells and inactivated the mTOR pathway. (A) DU145 cells (1000 cells per well) were treated with XAV939 or DMSO for 10 days, and colonies were stained and counted. (B) Clonogenic assays as A were repeated 3 times and the results are shown as pooled results of three independent experiments, each with triplicate data points. Error bars represent SEM. (C) DU145 cells were treated with DMSO or XAV939 (1nM-10μM), and were quantified by CTG assay after 5 days. Graph shows data from 3 independent experiments, each with triplicate points and expressed as a fraction of viability of solvent-treated cells (Bars, SEM). (D) DU145 cells were treated with 1μM XAV939 for 16 hours and in the final 10 min with 10nM IGF-1.There was reduction in phospho-S6 but no change in active β-catenin. The same results were obtained using 5μM or 10μM XAV939 for 16 hours, 2 days or 5 days with replacement of fresh inhibitor every 2.5 days (not shown).

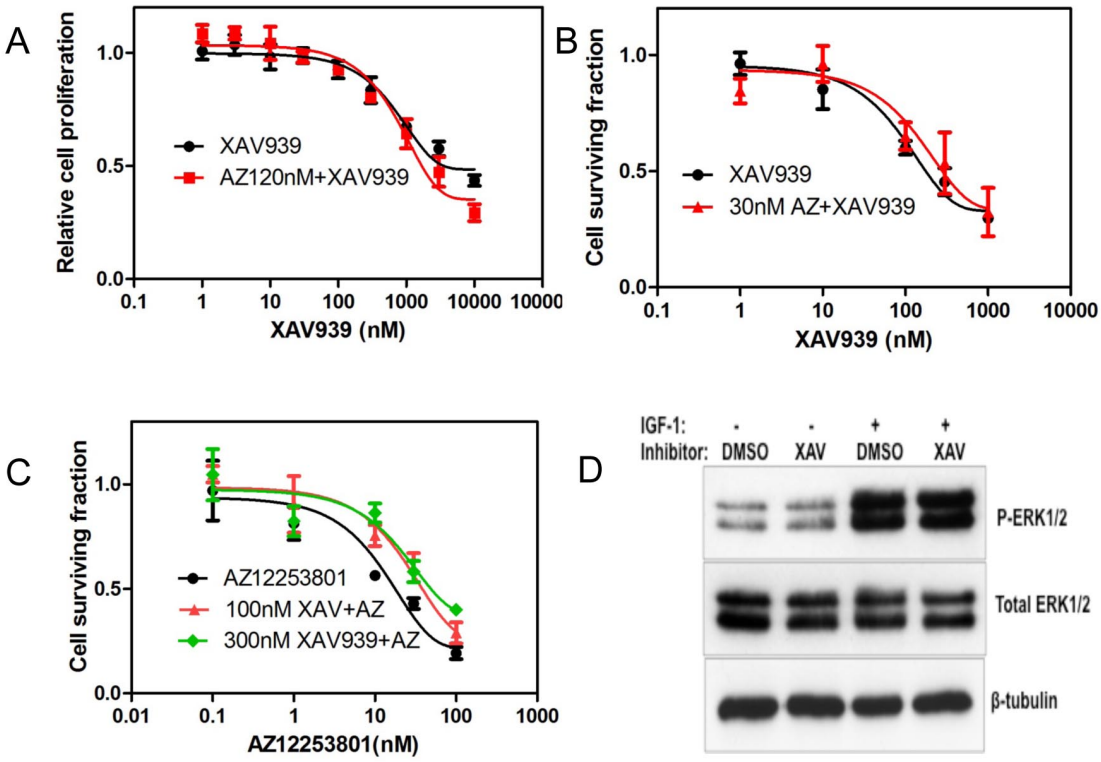

Figure 6.2 XAV939 did not sensitize to IGF-1R inhibition or activate ERK1/2. DU145 cells were treated with A) XAV939 alone or with 120nM AZ12253801, B) XAV939 alone or with 30nM AZ12253801 C) AZ12253801 alone or with XAV939 at 100 or 300nM; in A) Cell viability was quantified after 5 days by CTG assay; in B) and C), clonogenic survival was quantified in 6-well-plate assay. All graphs are mean (N=3) with error bars (SEM). (D) DU145 cells were treated with 1μM XAV939 for 16 hours and treated with solvent or 10nM IGF-1 for 10 min. Lysates were analyzed by western blotting using antibodies to phospho and total ERK1/2 with β-tubulin as the loading control. The same results were obtained using cells treated with 5μM or 10μM of XAV939 for 16 hours, 2 days or 5 days with fresh replacement of inhibitor every 2.5 days.

6.2.2 Effects of DVL3 knockdown were phenocopied by a small molecule DVL inhibitor

A second small molecule WNT inhibitor was obtained, which acts more directly on the function of DVLs. The DVL PDZ domain has a peptide-binding cleft that is involved in transducing signals from the membrane receptor Fz to downstream canonical and non-canonical pathways (Gao and Chen 2009). The DVL PDZ domain has become an attractive pharmaceutical target. A small molecule inhibitor (DVLi) that competitively binds to the cleft of the DVL PDZ domain has been shown to block WNT signaling in Xenopus embryo and PC3 prostate cancer cells (Grandy et al. 2009).

The DVLi was obtained from Calbiochem and tested in DU145 cells. DVLs exist in highly phosphorylated states, visible on western blot as two separated bands (Gonzalez-Sancho et al. 2004). In DU145 cell lysate, DVL3 was detected as two bands, the upper band was abolished by lamda phosphatase, and this effect was abrogated by phosphatase inhibitors (Figure 6.3, A), indicating that the slower mobility band was phosphorylated DVL3. The DVLi was capable of inducing dose-dependent inhibition of DVL3 phosphorylation (Figure 6.3, B). The inhibitor also caused a decrease in active β-catenin, and inactivation of the mTOR pathway as assessed by levels of phosphorylated S6. In contrast, the

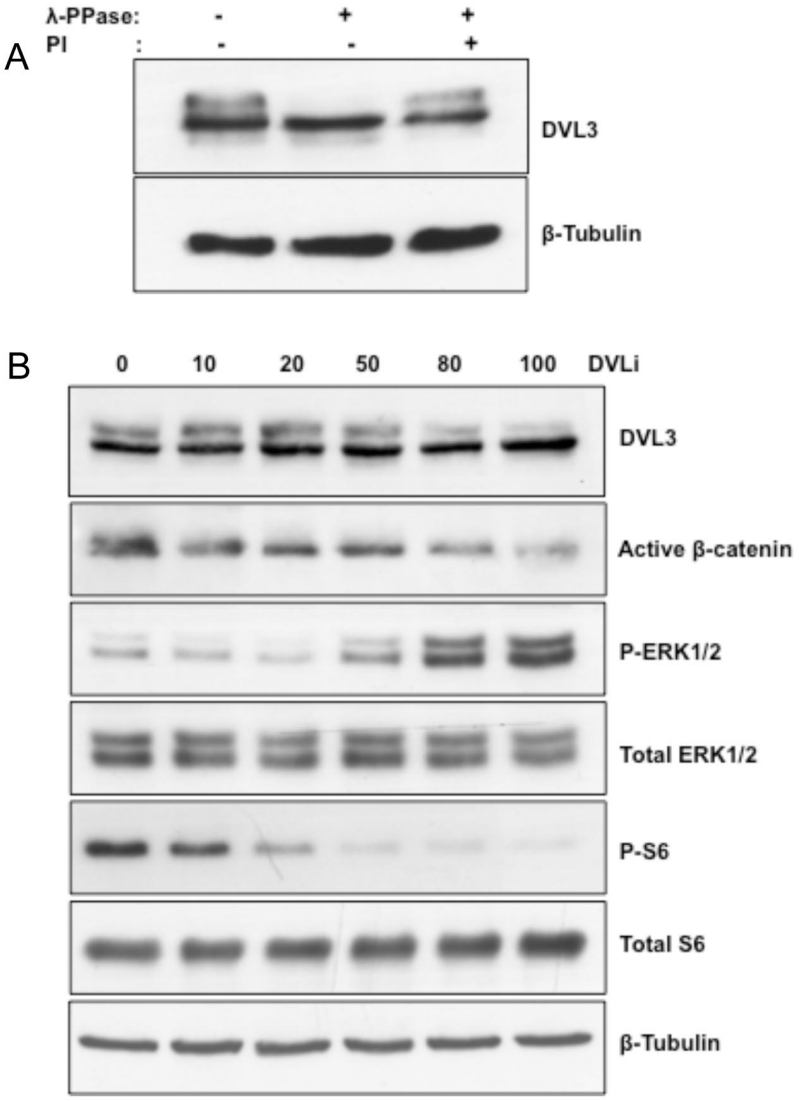

Figure 6.3 Effects of DVLi in DU145 cells. (A) Lysates from DU145 cells were treated with lambda phosphatase (λ-PPase) and/or phosphatase inhibitor (PI). (A) Serum-starved DU145 cells were treated with DVLi at 0-100 μM for 12 hours. Lysates were probed with DVL3, active β-catenin, P-ERK1/2(Thr202/Tyr204) or total ERK1/2 and P-S6 (Ser240/244) and total S6 antibodies with β-Tubulin as loading control. A similar result was obtained from another experiment.

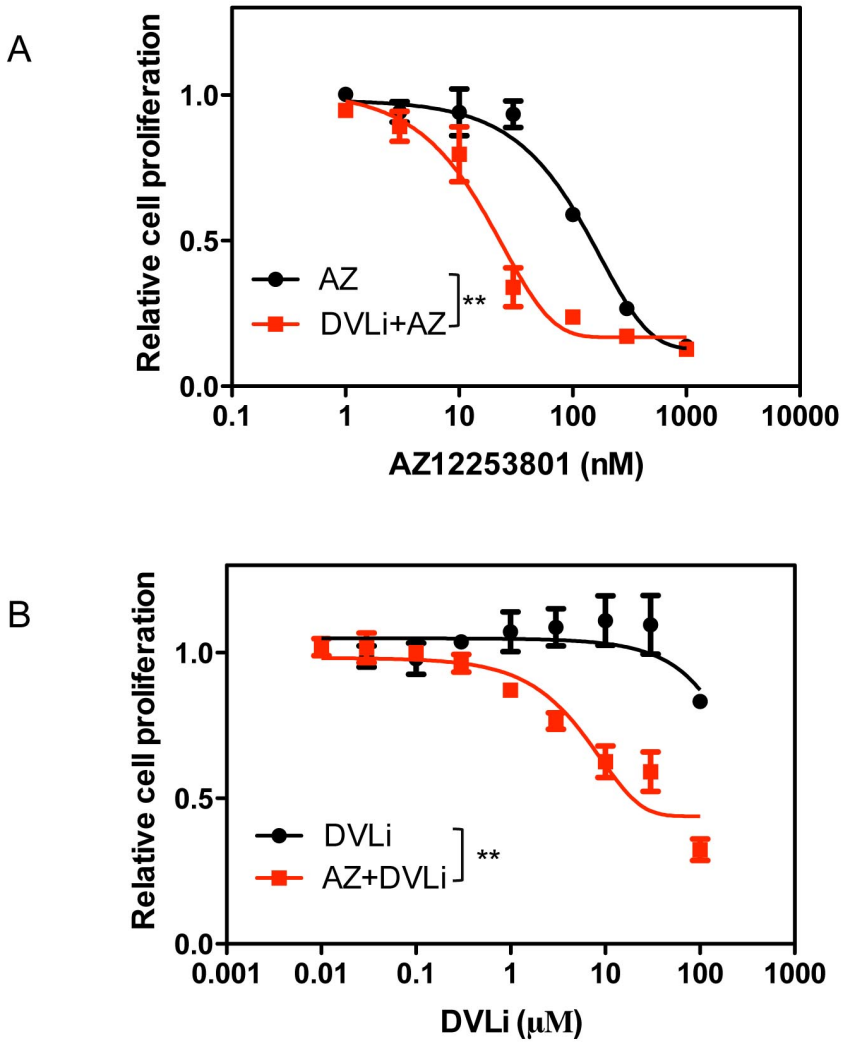

Figure 6.4 Reciprocal sensitization by inhibitors of IGF-1R and DVL. DU145 cells were treated with (A) AZ12253801 alone (AZ) or with DVLi (100μM), GI_{50} values 146 and 23 nM respectively (6.3 fold sensitisation), and (B) DVLi alone or with 120nM AZ12253801, GI_{50} values >100 and 10 μM (>10-fold sensitisation), pooled data from 3 independent experiments. Error bars (SEM). ** $p<0.01$ determined by two way ANOVA

activity of ERK1/2 increased in a dose-dependent manner (Figure 6.3, B). Thus, the DVLi recapitulated effects of DVL3 depletion on cell signaling.

The next experiment tested effects of DVLi on sensitivity to IGF-1R inhibition. The combination of AZ12253801 and DVLi significantly increased the effect of AZ12253801 on the inhibition of DU145 cell proliferation (Figure 6.4, A). There was a significant shift in the dose-response curve with 6.3 fold reduction in GI_{50} compared to AZ12253801 alone. In DU145 cells, the DVLi alone caused negligible effects on proliferation, with less than 20% inhibition in DU145 cells treated with 100μM DVLi. However, the addition of AZ12253801 increased the effect on DU145 cell inhibition compared with DVLi alone (Figure 6.4, B). These experiments indicate that the DVLi phenocopied effects of DVL3 depletion in sensitizing DU145 cells to AZ12253801, with reciprocal sensitization to DVLi by AZ12253801.

6.2.3 DVL inhibition sensitized to IGF-1R inhibition in cells with active ERK1/2

A panel of prostate cancer cell lines (DU145, PC3, LNCaP, LNCaP-LN3 and 22Rv1) was obtained, and cell line identity was verified by STR assay at Cancer Research UK, Clare Hall. Initial assessment checked the expression

status of IGF-1R and WNT signaling pathway components. Both IGF-1R and DVL3 were expressed in all cell lines at different expression levels. AR was absent in DU145 and PC3 (Figure 6.5), consistent with previous reports (Chlenski et al. 2001). PTEN was not detected in PC3, LNCaP and LNCaP-LN3 cells, because PC3 are null for PTEN, and LNCaP and LNCaP-LN3 harbor a 2bp deletion in codon 6 of PTEN, which results in a frame shift (Li et al. 1997). Phospho-AKT and phospho-ERK1/2 expression patterns varied with PTEN status. In cell lines in which PTEN was null or mutated (PC3, LNCaP and LNCaP-LN3), there were high levels of phospho-AKT as expected. In addition, phospho-ERK1/2 was undetectable, which was consistent with other studies (Segawa et al. 2001). Conversely, phospho-AKT was present at lower levels in DU145 and 22Rv1, due to the presence of functional PTEN. These cell lines also had detectable levels of phospho-ERKs, consistent with a previous report that the restoration of functional PTEN not only suppresses phospho-AKT but also activates of ERK1/2 in C4-2 cells, derived from LNCaP cells (Wu et al. 2008). The IGF-1R adaptor IRS-1 was not detected in LNCaP cells, as previously reported (Reiss et al. 2000), but was detected in the subline LNCaP-LN3 (Figure 6.5).

Having characterized the cell line panel, CTG assays were performed to test effects of the DVLi on IGF-1R inhibitor sensitivity. Administration of the DVLi

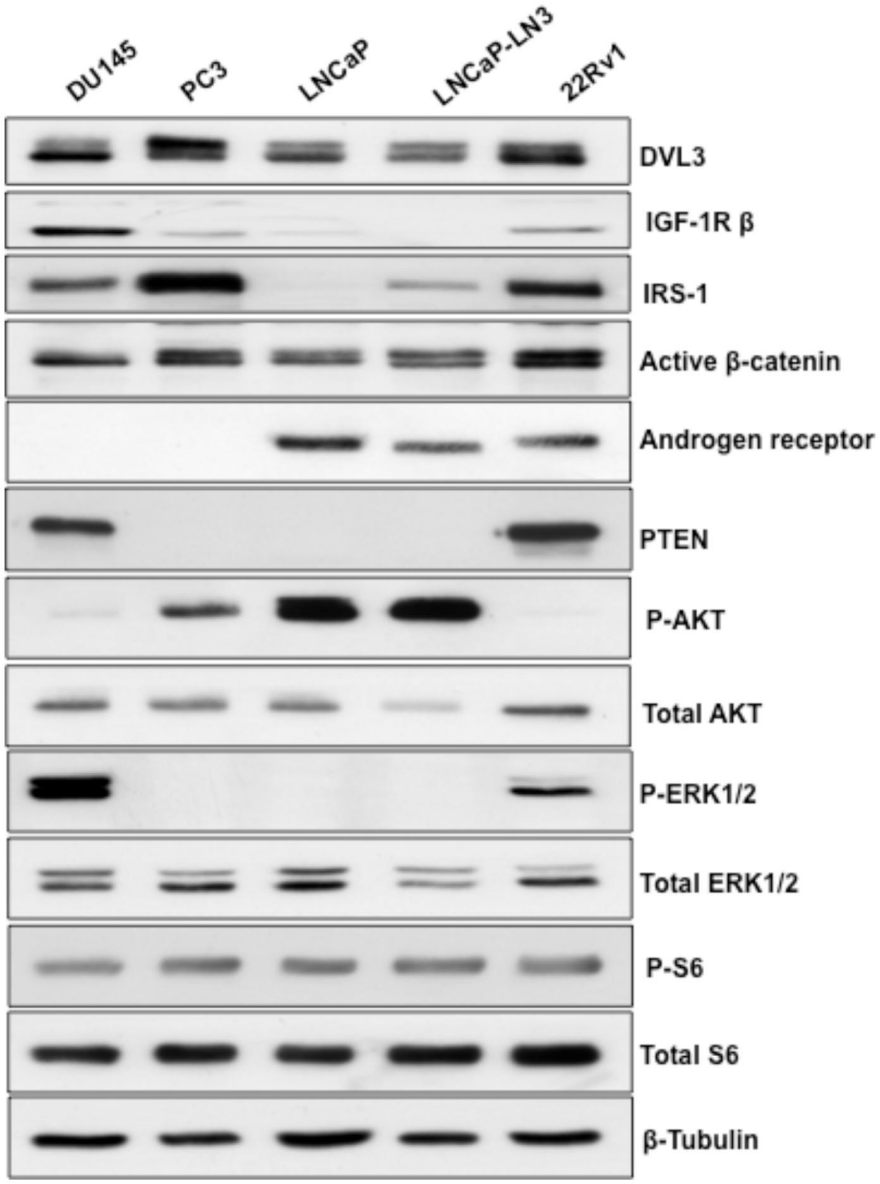

Figure 6.5 Characterization of prostate cancer cell lines. Cell lysates were prepared from culture growing in complete medium (with 10% FCS) and equivalent amounts of protein were analyzed by western blot.

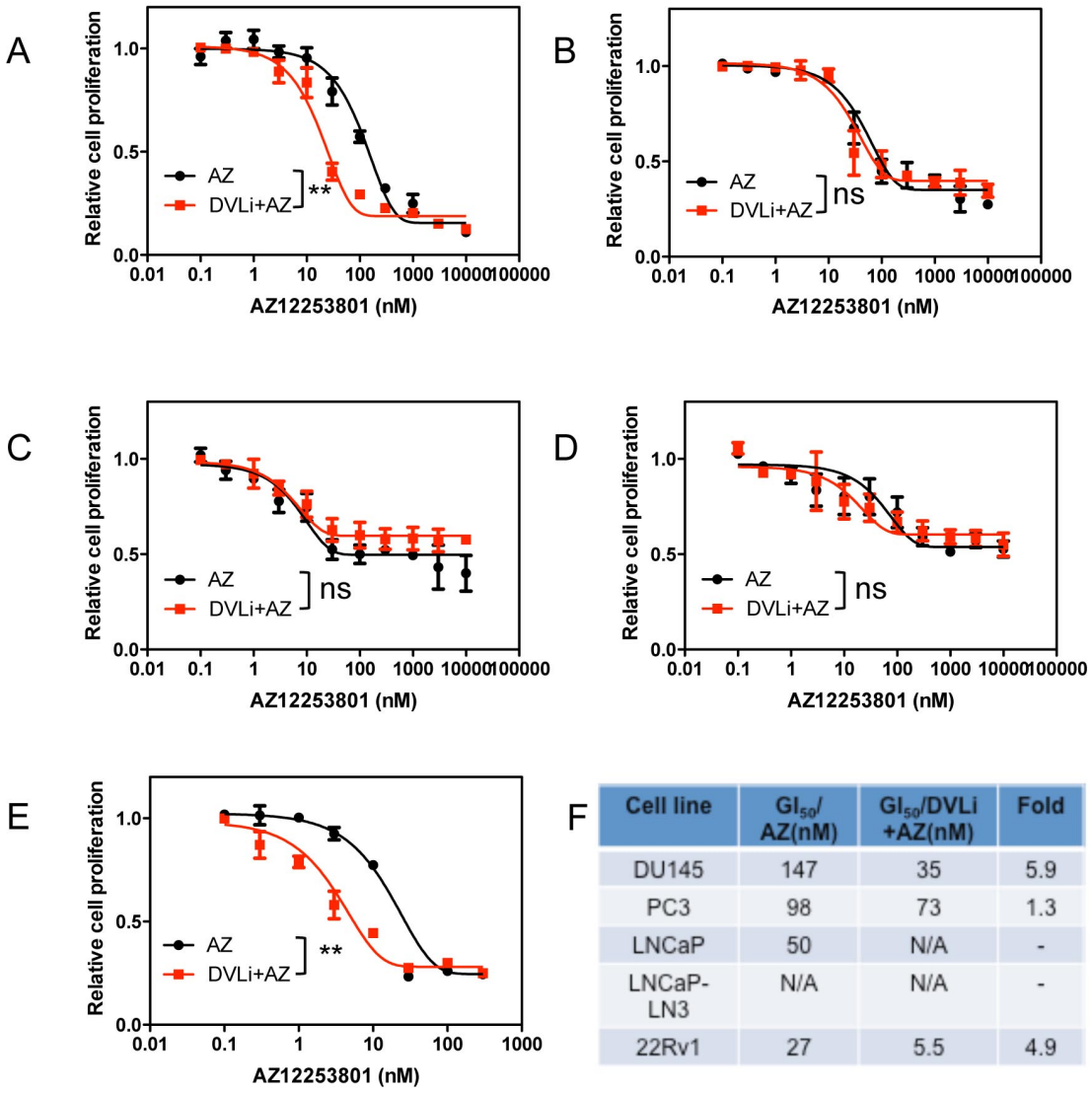

F

Cell line	GI_{50}/ AZ(nM)	GI_{50}/DVLi +AZ(nM)	Fold
DU145	147	35	5.9
PC3	98	73	1.3
LNCaP	50	N/A	-
LNCaP-LN3	N/A	N/A	-
22Rv1	27	5.5	4.9

Figure 6.6 PTEN WT prostate cancer cells are sensitized to AZ12253801 by DVLi. (A) DU145 (1000 cells/well), (B) PC3 (2000 cells/well), (C) LNCaP （5000 cells/well), (D) LNCaP-LN3 (5000 cells/well) and (E) 22Rv1 (5000 cells/well) were treated with AZ12253801 alone or with DVLi (100μM) for 5 days. Graphs show pooled data from 3 independent CTG assays (each assay with triplicate wells) and error bars were SEM. ns, not significant, $p>0.05$; ** $p<0.01$ (two way ANOVA). (F) GI_{50} data for AZ1225380 alone (AZ) or with DVLi (100μM). Table: GI_{50} values, fold sensitization calculated as ratio of GI_{50} values. N/A is not available from curve fit.

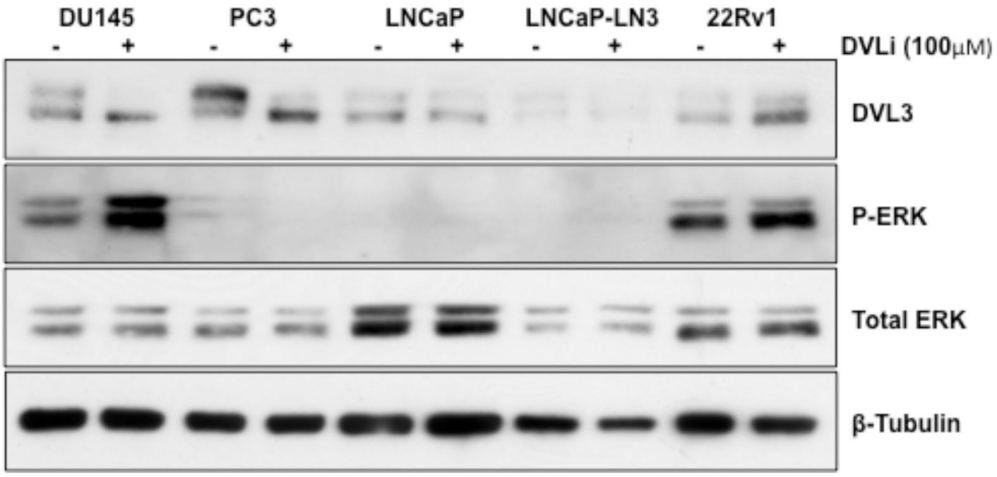

Figure 6.7 ERK1/2 activation by DVLi in DU145 and 22Rv1 cells. Serum-starved cells were treated with 100μM DVLi for 12 hours. Cell lysates were probed with specific DVL3, P-ERK (Thr202/Tyr204) or total ERK1/2 antibodies with β-Tubulin as loading control.

significantly increased the sensitivity to AZ12253801 in DU145 and 22Rv1 cells with respectively 5.9 and 4.9 fold reduction in GI_{50} (Figure 6.6). Also, DVLi induced an increase in phospho-ERK1/2 levels in DU145 and 22Rv1 cells (Figure 6.7). In contrast, DVLi did not sensitize to AZ12253801 in PC3, LNCaP or LNCaP-LN3 cells (Figure 6.6) and phospho-ERK1/2 remained undetectable after treatment with DVLi (Figure 6.7). Phospho-DVL3 was clearly reduced by DVLi in PC3 cells, suggesting that the inhibitor was active (Figure 6.7).

These data provide further circumstantial evidence that the ability to influence ERK activation may be linked to AZ12253801 sensitization, and support an association with PTEN status. As reported before, phospho-ERK1/2 level is highly correlated with PTEN status in prostate cancer cell lines (Segawa et al. 2001; Wu et al. 2008). To explore whether this correlation exists in other cancer cell lines, isogenic PTEN wild-type and knockout (KO22) HCT116 colon cancer cell lines were tested (Mendes-Pereira et al. 2009). It was clear that phospho-AKT was increased in PTEN KO22 cells, which is consistent with loss of PTEN function. However, there was no major difference in levels of phospho-ERK between the two isogenic cell lines (Figure 6.8, A), suggesting that correlation between ERK activity and PTEN status is not invariable. Unexpectedly, it was noted that PTEN KO22 cell proliferation was slower than the wild-type cells (Figure 6.8, B). Both cell lines were sensitized to

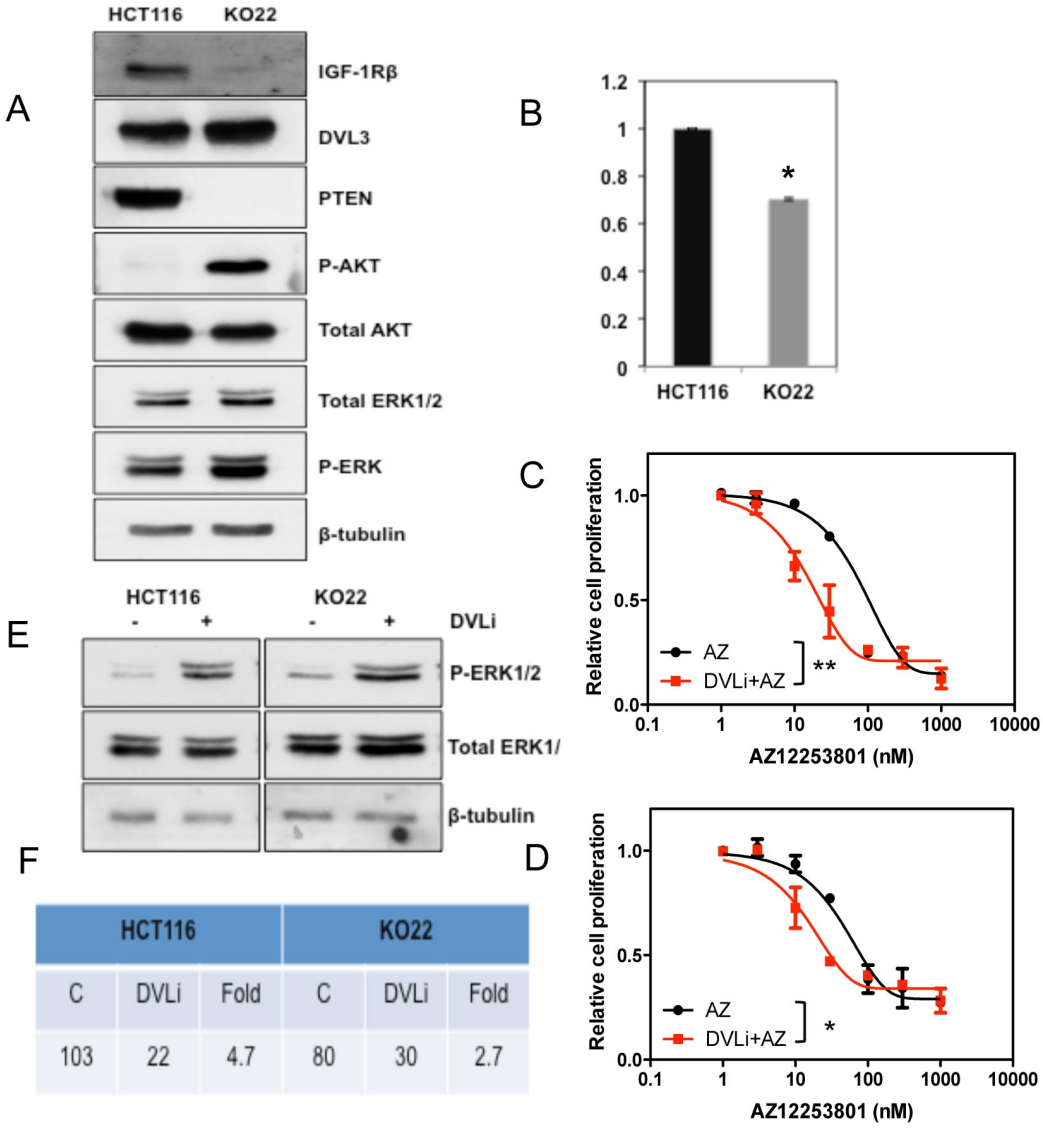

HCT116			KO22		
C	DVLi	Fold	C	DVLi	Fold
103	22	4.7	80	30	2.7

Figure 6.8 HCT166 wild-type or PTEN knockout (KO22) cells sensitized to AZ12253801 by DVLi (A) HCT116 or KO22 lysates were analysed for IGF-1Rβ, DVL3, AKT and ERK status. (B) Proliferation of HCT116 or KO22 (1000 cells/well) was measured by CTG after 5 days. KO22 cell proliferation was expressed as percentage of HCT116 cells. Data were mean (n=2) and error bars (SEM) *, $p<0.05$ determined by student t-test. (C) HCT116 (1000 cells/well) or (D) KO22 (1000 cells/well) were treated with AZ12253801 alone or in combination with DVLi (100μM) for 5 days. Data were from two independent experiments. Error bars (SEM). *, $p<0.05$, **, $p<0.01$ (two way ANOVA). (E) ERK1/2 was activated by DVLi (100μM) either in HCT116 or KO22. (F) Table shown summary of GI_{50} values in cells treated with AZ12253801 plus solvent control (C) or plus DVLi (DVLi) from figure C and D, and sensitization as ratio of GI_{50} values.

AZ12253801 after administration of DVLi (Figure 6.8, C, D and F). Fold sensitization in HCT116 KO22 cells was lower, although it is possible that this could be related to the lower proliferation rate of HCT KO22 cells. Correspondingly, ERK1/2 was activated by DVLi in both HCT116 and HCT116 KO22 cells (Figure 6.8, D). These data are consistent with the previous results, showing AZ12253801 sensitization by DVLi in phospho-ERK1/2 positive prostate cancer cells, but in the HCT116 model, both ERK1/2 phosphorylation and AZ12253801 sensitization by DVLi were PTEN-independent.

6.2.4 DVLi enhanced the sensitivity of MCF-7 cells to IGF-1R inhibition

DVL3 was identified as a borderline hit in second round screen in MCF-7 cells (Figure 4.8, B). DVL1-3 were expressed in MCF-7 cells, and as in DU145 cells, DVL3 was dominant isoform (Figure 6.9, A and B). MCF-7 cells are PTEN wild-type (DeGraffenried et al. 2004), and showed significant increase in sensitivity to AZ12253801 upon DVLi treatment (Figure 6.9, C), together with DVLi induced activation of ERK1/2 (Figure 6.9, D).

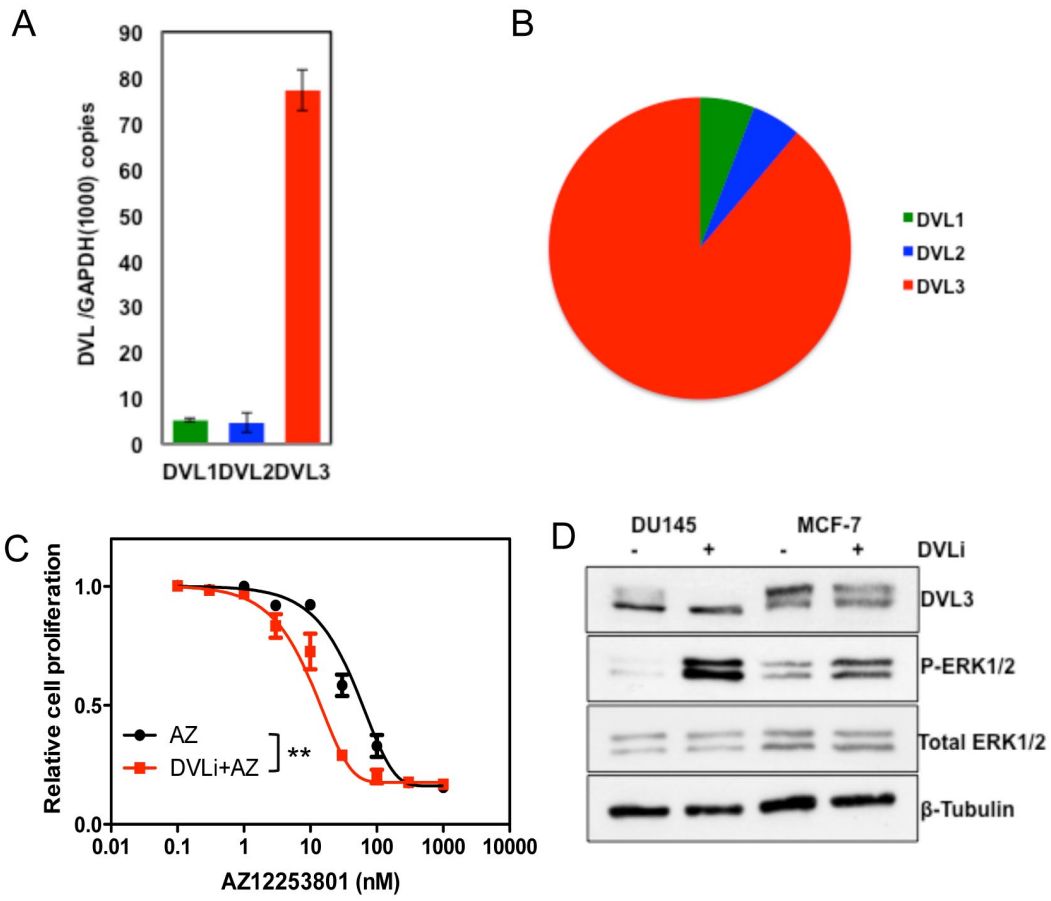

Figure 6.9 Sensitization to AZ12253801 by DVLi in MCF-7 cells. (A-B) Relative expression of DVL1-3 in MCF-7 cells measured by qRT-PCR as Figure 5.4. (C) MCF-7 cells were treated with AZ12253801 alone or combination with DVLi (100μM), CTG assays were performed after 5 days. Graphs shown pooled data from three independent experiments, each with triplicate data points. Error bars (SEM). GI_{50} for AZ12253801-treated cells=60nM and for DVLi with AZ12253801=14nM, giving fold sensitization of 4.3. ** p<0.01 (two way ANOVA). (D) ERK1/2 was activated by DVLi (100μM) in DU145 and MCF-7 cells. A similar result was obtained from a second independent experiment.

6.2.5 Investigating how DVL3 regulates ERK1/2 activation

6.2.5.1 β-arrestin1/2 and IRS-1 knockdown did not abolish DVLi-induced ERK1/2 activation

Signals generated by IGF-1R are integrated by multiple adaptor proteins. Of potential relevance to this project, interaction of DVLs with β-arrestin1/2 has been shown to modify ERK1/2 activity (Bryja et al. 2007; Zheng et al. 2012). The IGF-1R adaptor IRS-1 is a focus for feedback signaling via ERKs and mTOR-S6 kinase (Buck et al. 2008), but is unlikely to be involved in DVL-regulated ERK activation, because WNT inhibitor XAV939 inhibited mTOR but did not activate ERKs or sensitize to AZ12253801. To test involvement of these adaptor proteins, DU145 cells were transfected with siRNA to deplete β-arrestin1/2 or IRS-1. It was clear that β-arrestin1/2 or IRS-1 knockdown did not influence ERK1/2 activation induced by DVLi (Figure 6.10, A and B). Furthermore, endogenous β-arrestin1/2 or IRS-1 failed to co-immunoprecipitate with DVL3 (not shown). These data suggested that DVLi-induced ERK1/2 activation were not mediated by β-arrestin1/2 or IRS-1.

6.2.5.1 GRB2 knockdown abolished ERK1/2 activation induced by DVLi

Previous investigations had shown that DVL3 knockdown activated MEK1/2-ERK1/2, but did not activate the IGF-1R itself (Figure 5.9). RAF is

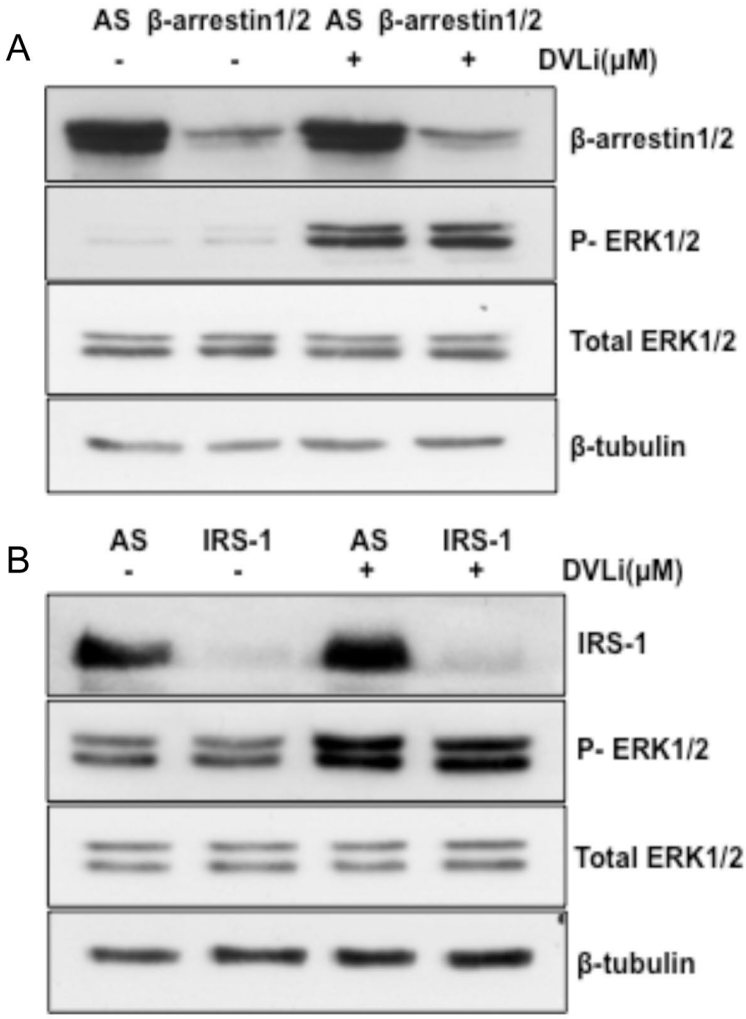

Figure 6.10 knockdown of β-arrestin1/2 or IRS-1 did not abolish DVLi-induced ERK1/2 activation in DU145 cells. DU145 cells were transfected with AS, β-arrestin1/2 (A) or IRS-1 (B) siRNAs, and after 48 hours serum-starved and treated with 100μM DVLi treatment for 16 hours. A similar result was obtained from a second independent experiment.

activated by binding of RAS-GTP (Zhang et al. 1993; Terai and Matsuda 2005), and RAS activity is regulated by the sequential loading of GDP or GTP by guanine exchange factor SOS (Boriack-Sjodin et al. 1998). Effects of DVLi on RAS activity were measured by the ability of the activated form of RAS (RAS-GTP) to bind to the RAS binding domain (RBD) of RAF. More RAS was detected in DVLi-treated lysates compared with solvent-treated lysates. Western blot of the same lysates showed no difference in total level of RAS between DMSO-treated and DVLi-treated samples, and confirmed ERK1/2 activation by DVLi (Figure 6.11, B). These data suggested that RAF and RAS were activated by DVL3 inhibition.

So far, data suggest that ERK1/2 activation by DVL3 knockdown or inhibition was mediated between downstream of IGF-1R and upstream of RAS. GRB2 is a central adaptor protein, which is linked between IGF-1R and WNT signaling and is an important link between receptor tyrosine kinases and RAS activation (Chitnis et al. 2008; Crampton et al. 2009), and therefore the next experiment explored its role in DVL3 regulation of ERK1/2. GRB2 depletion by a validated GRB2 siRNA was capable of abolishing the ERK1/2 activation induced by DVLi, but in contrast, active β-catenin was not affected by GRB2 knockdown (Figure 6.12). Cells treated with DVLi showed reduction in phosphorylated DVL3, and in active β-catenin, which was consistent with the previous results (Figure 6.12,

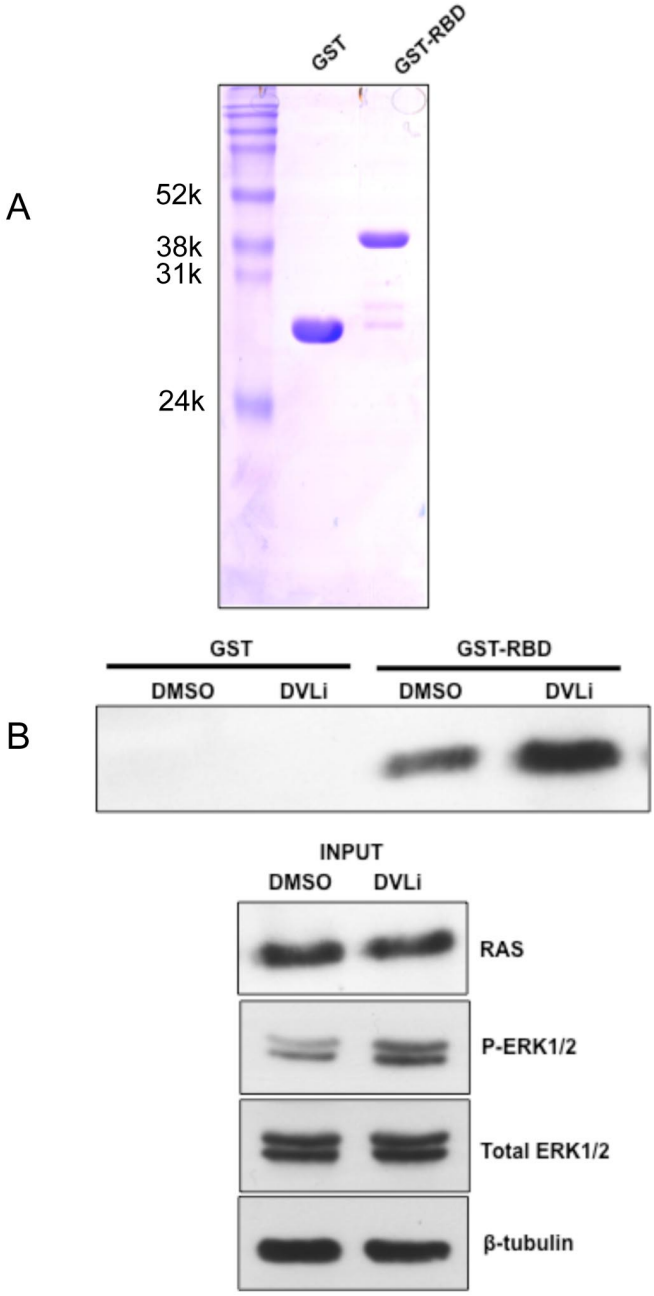

Figure 6.11 RAS was activated by DVLi in DU145 cells. (A) Purified GST and GST-RBD proteins were analyzed by SDS-PAGE and staining with coomassie blue. (B) Purified GST and GST-RBD proteins were incubated with lysates of DU145 cells treated with DMSO or DVLi (100μM) for 16 hours. Binding of activated RAS to RBD was assessed by western blot for RAS. INPUT: total lysates were probed with RAS, P-ERK1/2 (Thr202/ Tyr204) and total ERK1/2 antibodies. Similar results have been observed from two more independent experiments

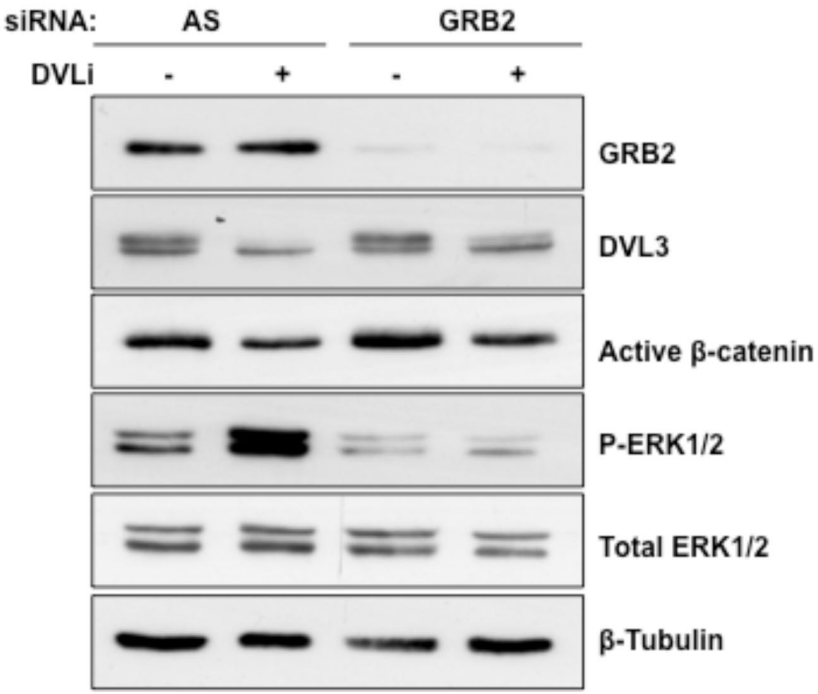

Figure 6.12 DVLi-induced ERK1/2 activation was abolished by GRB2 knockdown in DU145 cells. DU145 cells were transfected with GRB2 siRNA, and after 48 hours serum-starved and treated with 100μM DVLi for 16 hours. A similar result was obtained from a second independent experiment.

compare Figure 6.3). These data suggested that GRB2 is involved in ERK1/2 activation induced by DVLi.

6.2.5.2 Investigating interaction between DVL3, GRB2 and DAB2

GRB2 is a small adaptor protein with two Src homology 3 (SH3) domains, which are respectively in the N- and C-terminus, and a central Src homology 2 (SH2) domain (Figure 6.13, A) (Lowenstein et al. 1992). It has been reported that the N-terminal SH3 domain of GRB2 can directly bind to DVL2 via the PRR that is conserved in DVL1 and DVL3 (Figure 5.1). Furthermore, GRB2 was shown to synergize with DVL2 to induce WNT signaling (Crampton et al. 2009). It has also been reported that N-SH3 domain of GRB2 can directly bind to the C-terminal PRR domain of Disabled homolog 2 (DAB2) (Figure 6.13) (Xu et al. 1998). DAB2 is a tumor suppressor gene, initially reported to be downregulated or absent in ovarian cancer, and subsequently found to show decreased expression in breast cancer, bladder cancer, prostate cancer and metastatic pancreatic cancer (Schwahn and Medina 1998; Tseng et al. 1998; Fazili et al. 1999; Huang et al. 2001; Karam et al. 2007). Furthermore, DAB2 binding to GRB2 has been shown to negatively regulate ERK1/2 activation by disrupting the binding of GRB2 and SOS (Zhou and Hsieh 2001). In addition, the N-terminal phosphotyrosine-binding/interacting domain (PID) of DAB2

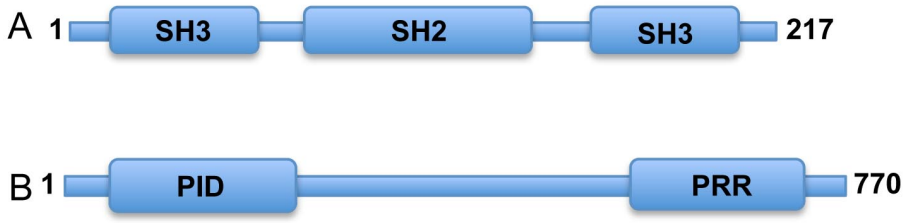

Figure 6.13 Schematic structure of GRB2 and DAB2. (A) GRB2 (217 amino acids) containing two SH3 domains and one SH2. (B) DAB2 (770 amino acids) consists of a phosphotyrosine-binding/ interacting domain (PID) and a prolin-rich region (PRR).

(Figure 6.13) was shown to be capable of binding DEP domain of DVL3 (Figure 5.1) and to negatively regulate the WNT canonical pathway by inhibiting the binding of DVL3 to AXIN (Hocevar et al. 2003).

In light of these reports, experiments were conducted to test interaction between DVL3, GRB2 and DAB2. Immunoprecipitation of DVL3 from DU145 cell extracts revealed that DAB2 was associated with DVL3 (Figure 6.14, A). GRB2 was also present in DVL3 immunoprecipitations, but was also weakly detected in control immnuoprecipiations (Figure 6.14, A). Conversely, endogenous GRB2 was immnuoprecipitated with SOS and SHC but not with DVL3 and DAB2 (Figure 6.14, B). This may be due to poor immunodepletion by the GRB2 antibody affinity we used in immunoprecipitation. To further pursue possible interactions between GRB2, DAB2 and DVL3, purified GST and GST-GRB2 (Figure 6.14, C) pull-down assays were conducted using DU145 cell extracts. Endogenous DVL2, DVL3 and DAB2 were pulled down with GST-GRB2 but not GST, (Figure 6.14, D). However, while a major proportion of SOS was bound to GRB2 (comparing with 10% input in figure 6.14), less amounts of DVL2, DVL3 and DAB2 were detected in GRB2 pull-downs. Additional experiments were performed to test DVL3 and DAB2 binding to different domains of GST-GRB2 (GST-N-SH3, GST-SH2 and GST-C-SH3) (Figure 6.15, A). SOS strongly bound to the N-terminal SH3 domain, weakly

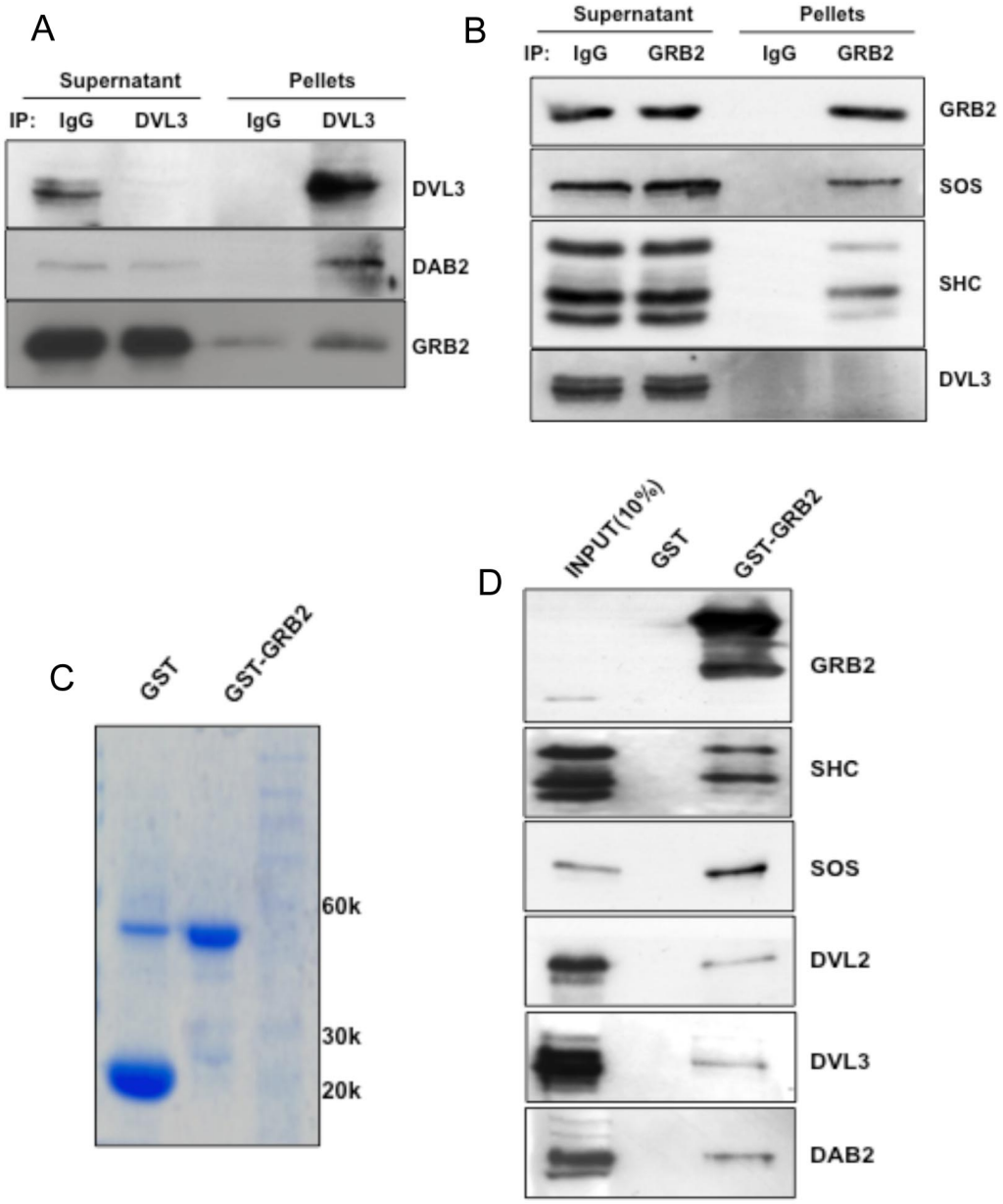

Figure 6.14 Physical interaction between DVL3, GRB2 and DAB2 in DU145 cells. (A) DU145 cell lysates were immnuoprecipitated with control IgG or DVL3 antibodies, and probed for DVL3, DAB2 and GRB2. (B) DU145 cell lysates were immnuoprecipitated with control IgG or GRB2 antibodies, and probeded for GRB2, SOS, SHC and DVL3 (C) Bacterially expressed and purified GST and GST-GRB2 were analyzed by SDS-PAGE. (D) GST or GST-GRB2 were incubated with DU145 cell lysates overnight, and interacting proteins were analyzed by western blot with SOS, SHC, DVL2, DVL3, DAB2 and GRB2 antibodies. A similar result was observed in a second independent experiment.

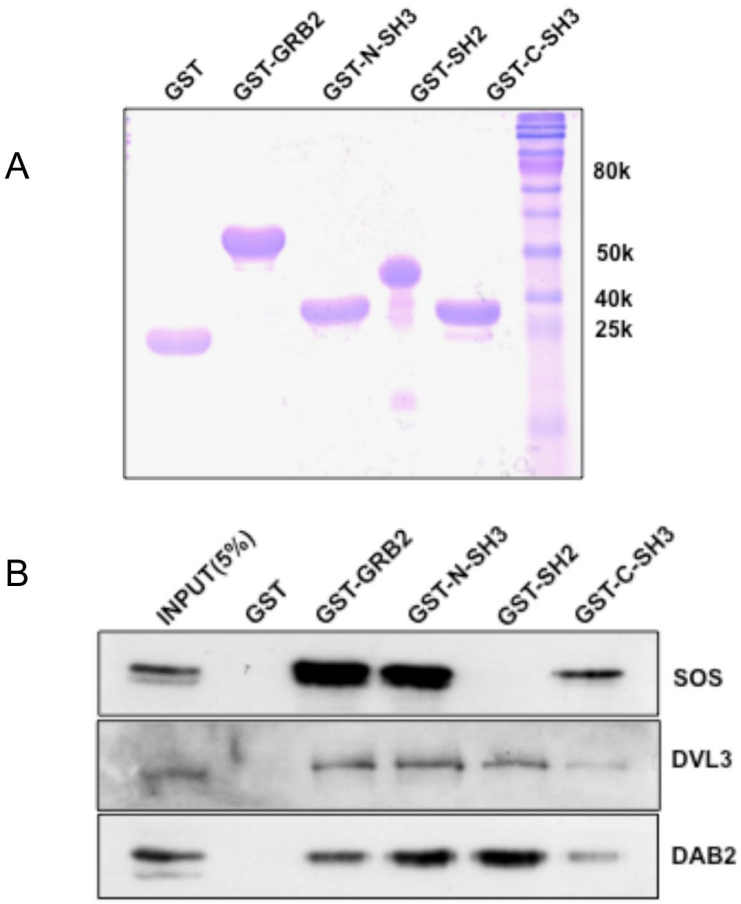

Figure 6.15 DVL3 and DAB2 bind to GRB2 domains in DU145 cells. (A) Bacterially expressed and purified GST, full-length GST-GRB2, GST-N-SH3, GST-SH2 and GST-C-SH3 were analyzed by SDS-PAGE. (A) Bacterially expressed and purified GST and GST-GRB2 were analysed by SDS-PAGE. (B) The above purified proteins were incubated with DU145 cell lysates overnight, and interacting proteins were analyzed by western blot with SOS, DVL3 and DAB2 antibodies. A similar result was observed in a second independent experiment.

bound to the C-terminal SH3 domain and did not bind to the SH2 domain, consistent with a previous study (Xu et al. 1998). DVL3 and DAB2 appeared to primarily bind to the N-SH3 and SH2 domains of GRB2. DAB2 binding to the N-SH3 domain of GRB2, which negatively regulates ERK1/2 activity, was not convincingly demonstrated in previous study (Xu et al. 1998; Zhou and Hsieh 2001). Taken together, these results suggest that DAB2, DVL3 and GRB2 were in the same complex.

6.2.5.3 DAB2 knockdown enhanced sensitization to AZ12253801

To test the contribution of DAB2, DU145 cells were reverse transfected with a validated DAB2 siRNA (QIAgen), which was able to deplete endogenous DAB2 (Figure 6.16, A). It was clear that DAB2 knockdown did not affect DVL3 status but resulted in activation of ERK1/2 consistent with a previous report (Zhou and Hsieh 2001). DAB2 depletion also enhanced the response of DU145 cells to IGF-1 stimulation of ERK1/2 phosphorylation (Figure 6.16, A). In these aspects, DAB2 depletion mimicked effects of DVL3 depletion or inhibition. Similarly, DAB2 depletion reduced active β-catenin levels (Figure 6.16, A), although this would not be expected given a report that DAB2 regulates the binding of DVL3 and Axin to negatively regulate WNT canonical signaling (Hocevar et al. 2003). However, in DU145 cells, the opposite effect was seen, with the reduction in

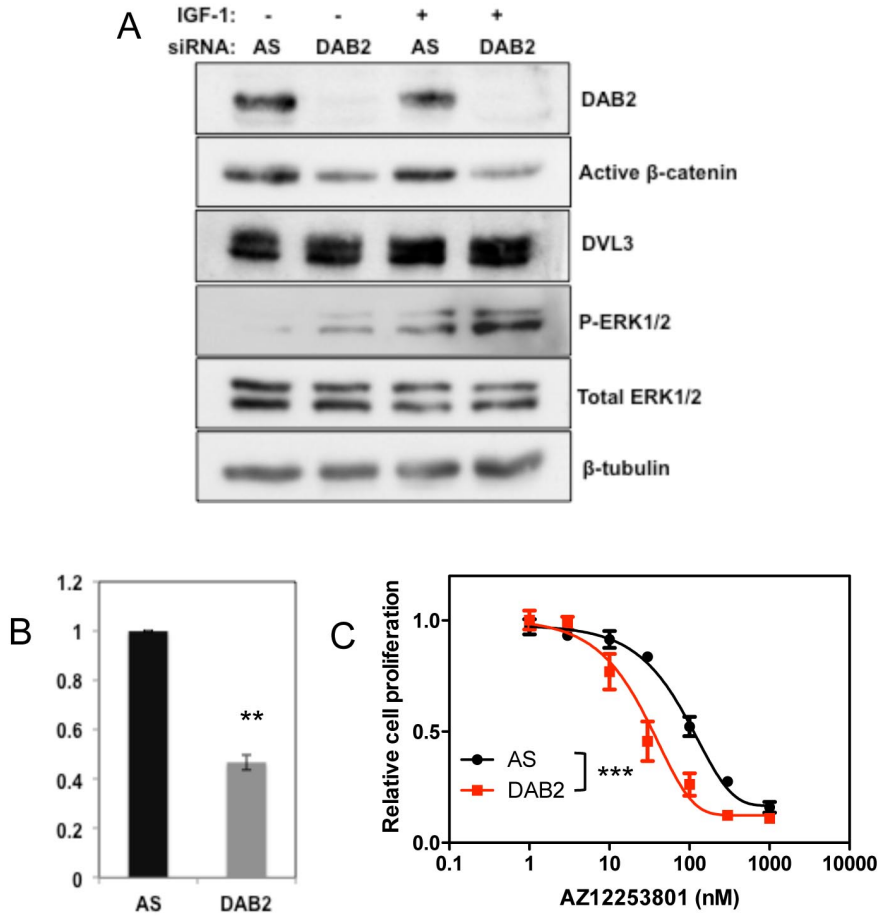

Figure 6.16 DAB2 knockdown activated ERK1/2 and enhanced sensitivity to AZ12253801. (A) DU145 cells were transfected with AS or DAB2 siRNA, and after 48 hours were serum-starved and treated with 10nM IGF-1 for 10 minutes. Lysates were analyzed with antibodies for DAB2, active β-catenin, DVL3, P-ERK1/2(Thr202/Tyr204) and total ERK1/2 with β-Tubulin as loading control. A similar result was obtained from a second experiment. (B) DU145 cells were reverse transfected with AS or DAB2 siRNAs, and CTG assays were performed 7 days later. Cell viability was expressed as a percentage of the viability of cells transfected with AS siRNA. Column, and bars represent mean and SEM from four independent experiments, each with triplicate wells. $p<0.01$(Student's t-test). (C) CTG assays were performed four times, each with triplicate wells. Graph shows data points (mean ± SEM), curve fitted with Prism 5. GI_{50} for AS-transfectants was 113nM and for DAB2 was 35nM, representing 3.2 fold sensitization. *** $p<0.0001$ (two-way ANOVA).

active β-catenin levels after DAB2 depeltion. The reasons for this are not clear, but this may explain why DAB2 knockdown reduced cell viability (Figure 6.16, B). DAB2 silencing increased the sensitivity to AZ12253801 as judged by inhibition of DU145 cell proliferation (Figure 6.16, C).

6.2.5.4 Investigating effects of DVLi on complex of GRB2, DVL3 and DAB2

The results shown in the previous section confirm the reported ability of DAB2 to inhibit ERK1/2 activation, because DAB2 competitively bound to GRB2 to interrupt the interaction between GRB2 and SOS (Zhou and Hsieh 2001). It is possible that ERK1/2 activation by DVL3 depletion or inhibition may result from altered interaction between DAB2 and GRB2, and/or increased association between GRB2 and SOS. To test this, firstly, GRB2 pulldowns were analyzed in DU145 cells treated with DVLi. After DVLi treatment, it was clear that ERK1/2 was activated and phospho-DVL3 was reduced, confirming DVLi bioactivity (Figure 6.17, A and C). However, the physical complex between GRB2, DAB2 and DVL3 was stable with no change in GRB2 binding partners (Figure 6.17, A). Secondly, there was no increase in co-immunoprecipitation between endogenous GRB2 and SOS following DVLi treatment (Figure 6.17, B). This

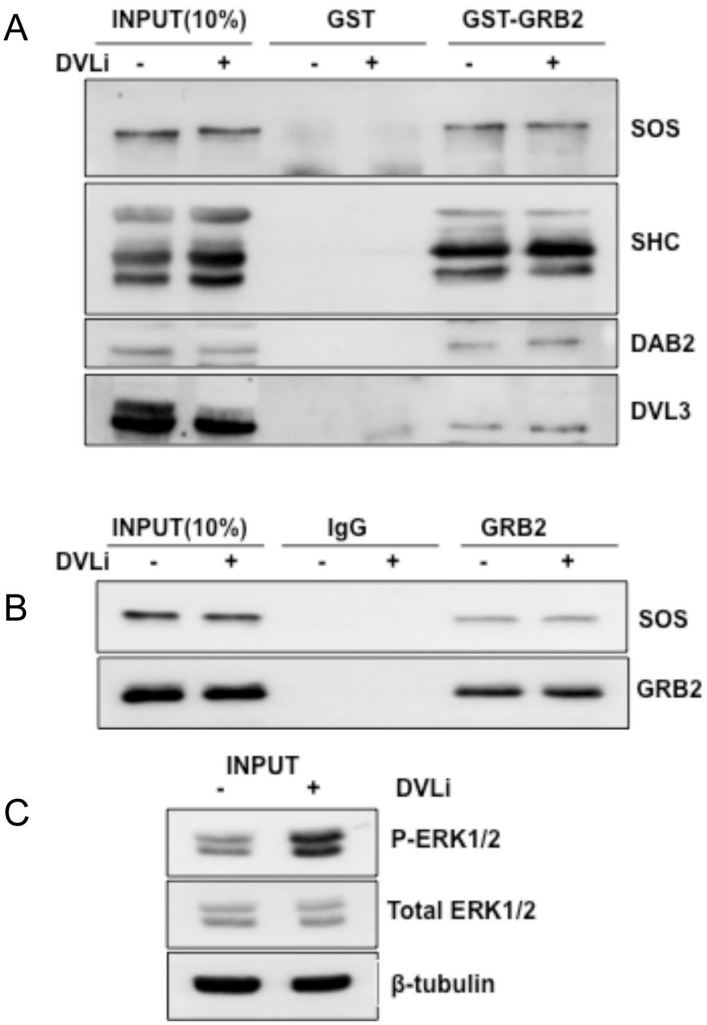

Figure 6.17 DVL inhibition did not influence GRB2 binding partners. (A) Serum-starved DU145 cells were treated with 100μM DVLi for 16 hours. Lysates were incubated with GST or GST-GRB2 and analyzed by western blot with SOS, SHC, DAB2 and DVL3 antibodies. (B) Lysates were prepared as in (A), and GRB2 immunoprecipitats were analyzed by western blot for GRB2 and SOS. (C) Lysates prepared as in (A) were analyzed for P-ERK1/2(Thr202/Tyr204) and total ERK1/2 with β-Tubulin as loading control. Similar results were obtained from one more independent experiment.

suggests that DVLi did not affect the composition of adaptor complexes that link IGF-1R to RAS.

6.2.6 Proposed model for DVL3 regulating sensitivity to IGF-1R inhibition

Taken together, these data show a correlation between the ability of DVL3 to regulate IGF-1R signaling via ERK1/2, and sensitization to AZ12253801 (Figure 6.18). The ability of DVL3 to regulate distal mTOR signaling appears not to contribute to AZ12253801 sensitization, given that AZ12253801 effects were unaffected by XAV939 that inactivated mTOR (Figure 6.1). The DVL protein is an essential component of the WNT pathway, and DVL3 silencing or inhibition led to reduction of active β-catenin and inactivated the mTOR pathway as predicted (Inoki et al. 2006; Gao and Chen 2009). DVL3-induced regulation of IGF signaling via ERK1/2 had not previously been described, and could enhance sensitivity to IGF-1R inhibition, in the same way that EGFR kinase mutants enhance sensitivity to EGF ligand and EGFR inhibition (Paez et al. 2004). These data suggest that IGF-1-induced ERK1/2 activation and AZ12253801 sensitivity are regulated by interruption of WNT signaling at upstream but not downstream step of DVL3. This effect appears to involve in

adaptor protein complexes that assemble downstream of activated IGF-1R, although the precise mechanism is not yet clear.

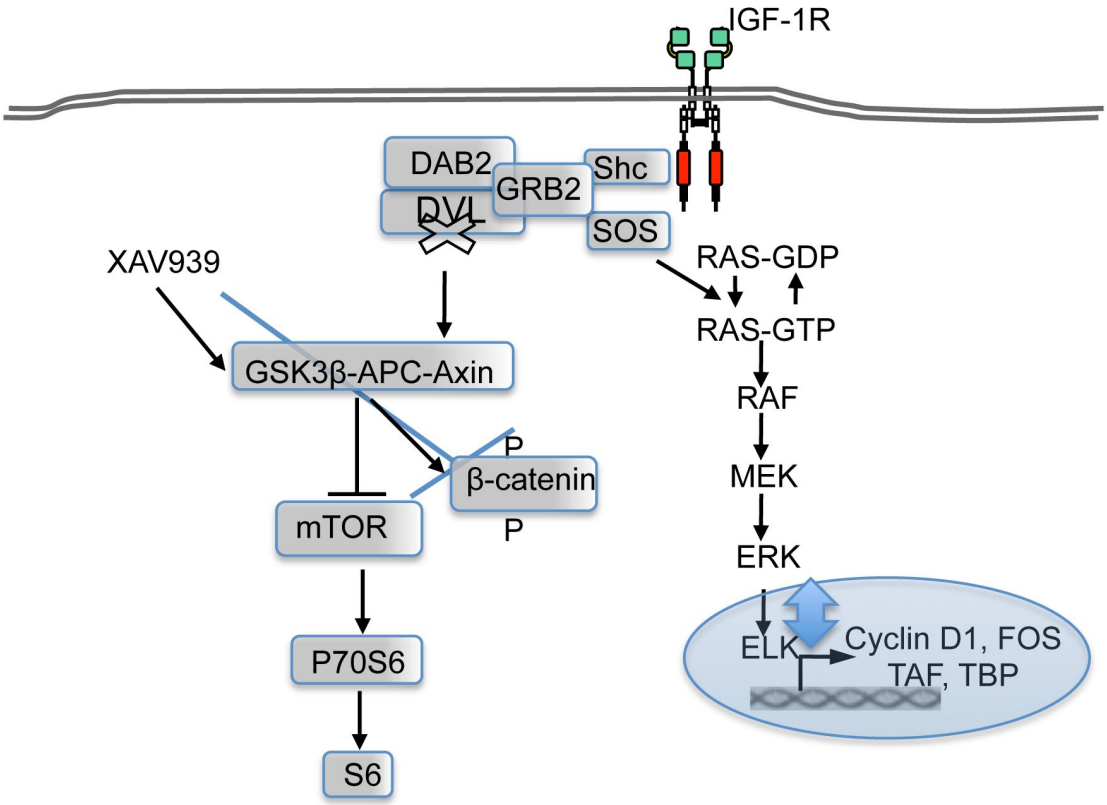

Figure 6.18 Proposed model for interaction between IGF-1R inhibition and DVL3 silencing. DVL3 depletion reduced active β-catenin and also inhibited the mTOR pathway. XAV939 also inactivated mTOR, but did not cause degradation of β-catenin perhaps because of the presence of wild-type APC in DU145 cells. DVL3 silencing activated the Ras-MEK1/2-ERK1/2 pathway, increasing sensitivity to IGF stimulation, and further translocated ERK1/2 into nucleus, leading to increased expression of Cyclin D1 and ELK target genes such as FOS, TAF1 and TBP. DVL3, DAB2 and GRB2 were detected in complex, and GRB2 knockdown abolished the ERK1/2 activation induced by DVLi, and DAB2 knockdown sensitized to AZ12253801.

Chapter 7

Conclusions and future directions

7.1 Conclusions

The major aims of this project were firstly to identify genes whose silencing would influence sensitivity to IGF-1R inhibition, using a small molecule inhibitor provided by AstraZeneca, and secondly to investigate the molecular mechanism underlying interaction between candidate gene silencing and IGF-1R inhibition.

The work presented in **Chapter 3** showed that AZ12253801 was able to inhibit the IGF-1R and its downstream signaling, and also to inhibit the proliferation and survival of DU145 prostate cancer and MCF-7 breast cancer cells. The siRNA screen and validation of 8 Kinome and 5 DNA repair-associated hits were presented in **Chapter 4**.

The final two parts of the project were to investigate interactions between DVL3 silencing and IGF-1R inhibition and to attempt to test small molecule drugs that could mimic effects of DVL3 depletion. As presented in **Chapter 5**, knockdown of DVL3 but not DVL1 or 2 sensitized to IGF-1R inhibition. DVL3 knockdown reduced levels of active β-catenin and inhibited mTOR signaling, consistent with other studies (Logan and Nusse 2004; Inoki et al. 2006). DVL3 knockdown did not affect the activity of IGF-1R or AKT, but did induce clear activation of ERK1/2 accopmained by ERK1/2 nuclear translocation and overexpression of ERK1/2 target genes. Futhermore, the effects of DVL3 knockdown were phenocopied by a PDZ domain inhibitor of DVL (DVLi), as presented in **Chapter 6**. The ability of DVLi to sensitize to IGF-1R inhibition was validated in cell lines with activated ERK1/2, but not in prostate cancer cell lines that had lost functional PTEN and had undetectable phospho-ERK1/2 (Wu et al. 2008). Finally it was shown that DVL3, GRB2 and DAB2 can be detected in a complex, and ERK1/2 activation induced by DVLi was abolished by GRB2 knockdown. Depletion of the adaptor DAB2 also sensitized to AZ12253801, and phenocopied effects of DVL3 depletion on ERK1/2 activation.

Taken together, the work presented here suggests that the siRNA screen successfully identified hits, whose silencing influenced sensitivity to IGF-1R inhibition. Notably, DVL3 silencing enhanced sensitivity to IGF-1R inhibition,

apparently by regulating IGF signaling to ERK1/2.

7.2 Future Directions

IGF-1R inhibition is undergoing clinical trials in various types of cancers, but the encouraging initial results have not so far translated to benefit in later trials of unselected patients (Zha and Lackner 2010; Basu et al. 2011). It has been shown that IGF-1R inhibition can induce tumor shrinkage in Ewing's sarcoma, but has only modest activity in the majority of common cancers (Karp et al. 2009; Olmos et al. 2010). Most Ewing's tumor are characterized by an oncogenic fusion protein, EWS/FLI-1, which requires the IGF-1R for transformation, and downregulates the IGF inhibitory binding protein IGFBP-3 (Toretsky et al. 1997; Prieur et al. 2004). This suggests that high IGF bioactivity may be an important mediator of sensitivity to IGF-1R inhibition. Indeed, NSCLC patients with high circulating IGF-1 levels appear to derive more benefit from treatment with IGF-1R antibodies (Karp et al. 2009; Gualberto et al. 2011). Furthermore, IGF-1R expression levels correlated with sensitivity to IGF-1R blockade in NSCLC and rhabdomyosarcoma cell lines (Cao et al. 2008; Gong et al. 2009), but this correlation is not clearly seen in NSCLC patients (Gualberto et al. 2010). Consistent with this, I found that in PC3 prostate

cancer cells, overexpression of IGF-1R-Myc did not enhance sensitivity to AZ12253801 (Figure 3.7).

Given these uncertainties, we decided to try to identify potential regulators using an unbiased siRNA screen. While this work was in progress, a study was reported using a similar siRNA screen consisting of siRNAs to 88 RTKs, and identified ribosomal protein S6 and macrophage-stimulating 1 receptor tyrosine kinase (MSTR1R) as regulators of sensitivity to IGF-1R inhibitor BMS-536924 in childhood sarcoma cells. Furthermore, MSTR1R silencing was found to block S6 activation and sensitized childhood sarcoma cells to BMS-536924 (Potratz et al. 2010). My screen did not include S6, but my Kinome screen did contain siRNA targeting MTSR1R, although this gene was not identified as a screen hit. In the current study, reducing S6 phosphorylation by XAV939 did not increase sensitivity to AZ12253801, indicating that inactivation of S6 did not regulate IGF-1R inhibitor efficacy in DU145 prostate cancer cells.

According to current research, the human genome contains ~20,000 – 25,000 genes (http://www.ornl.gov/sci/techresources/Human_Genome/faq/genenumber.shtml). Only ~1000 genes were studied in this project, constituting less than 5% of the total whole number of genes. Now that whole genome data are

available, and with development of siRNA or shRNA technology, whole genome siRNA/shRNA HTS is feasible (Karlas et al. 2010; Sims et al. 2011; Mendes-Pereira et al. 2012). It is likely that whole genome siRNA HTS screens may identify more genes that regulate sensitivity to IGF-1R inhibition, and potentially with greater magnitude of effects than was identified for DVL3. This may allow us to build up a picture of a more detailed IGF signaling circuit that regulates sensitivity to the IGF-1R inhibition.

The main focus of this project was DVL3, a member of the WNT signaling axis (Logan and Nusse 2004). The ability of DVL3 to regulate sensitization to AZ12253801 was observed in PTEN wild-type prostate cancer cell lines, but not PTEN-mutated prostate cancer cell lines. I found that lost of PTEN was associated with reduced levels of phospho-ERK1/2, consistent with a previous report that ERK1/2 are activated by restoration of functional PTEN in C4-2 cells (derived from the PTEN-mutant LNCaP cell line) (Wu et al. 2008). Further testing in isogenic C4-2 cells is ongoing.

DVL3, DAB2 and GRB2 were found to be in the same complex, and DAB2 depletion or DVL3 inhibition sensitized DU145 prostate cancer cells to AZ12253801. DAB2 is a tumor suppressor gene and is downregulated in many

cancer types including prostate and breast cancers (Schwahn and Medina 1998; Tseng et al. 1998). Gain of function mutations in oncogenes can be blocked by specific inhibitors or antibodies, but at present it is hard to compensate for the downregulation or loss of tumor suppressor genes. The strategy of searching for SSL may be an appropriate way to treat cancers that have lost known tumor suppressor genes (Brough et al. 2011). Therefore, the results of this study suggest that IGF-1R may be a good target in prostate and breast cancers that have lost DAB2 function, or in which DVL3 is expressed at low level. However, DVL3 was overexpressed in lung cancer tissues (Uematsu et al. 2003) and was highly upregulated at the mRNA level in prostate cancer tissue from publicly available data (www.oncomine.org) deposited by Wallace et.al. (Wallace et al. 2008) (Figure 7.1, A). The results of this study suggest that we should check if DVL3 is highly expressed in cancer tissue of patients entering IGF-1R clinical trials to know whether DVL3 expression is really associated with clinical response in future. Dr. Val Macaulay is involved in two Phase I trials of IGF-1R therapeutics in Oxford University, the first an IGF-1R antibody, and the second a recently completed study of IGF-1R tyrosine kinase inhibitor (TKI). This is providing an opportunity to study relevant clinical patients samples. Initial staining of tumors from 3 TKI trial patients showed similarly expressed IGF-1R (immunohistochemistry performed by Dr. Tamara Aleksic, not shown). DVL3 immunohistochemistry has been optimized in DU145 cells

using as control. DVL3 showed stronger staining in AS-transfected DU145 cells than in DVL3 siRNA-transfected cells (Figure 7.1, B). There was granular cytoplasmic DVL3 staining in a prostate cancer of a patient who experienced early progression (Figure 7.1, C, a and b), and negligible DVL3 in tumors of two patients achieving durable partial response (PR) (Figure 7.1, C, c-f). These initial data support our hypothesis that DVL3 levels correlate with sensitivity to IGF-1R inhibition. More samples are being collected and assessed.

A very recent study has shown that WNT signaling blockade suppressed mammary tumor growth by inducing expression of IGFBP5, which inhibited the ability of IGFs to activate IGF-1R in mouse mammary tumors. It was further confirmed that the IGF-1R inhibitor PPP could also inhibit WNT1-mediated tumor growth (Liu et al. 2012). These results are consistent with findings of this project, although Liu et.al used a more upstream approach to block WNT signaling, via expression of soluble extracellular domain of Fz, leading to blockade of WNT, and achieving similar results as the DVLi used in this project. Together with our collaborators Professor Alan Ashworth and Dr. Chris Lord, we are currently testing the combination of DVLi and AZ12253801 in xenograft models.

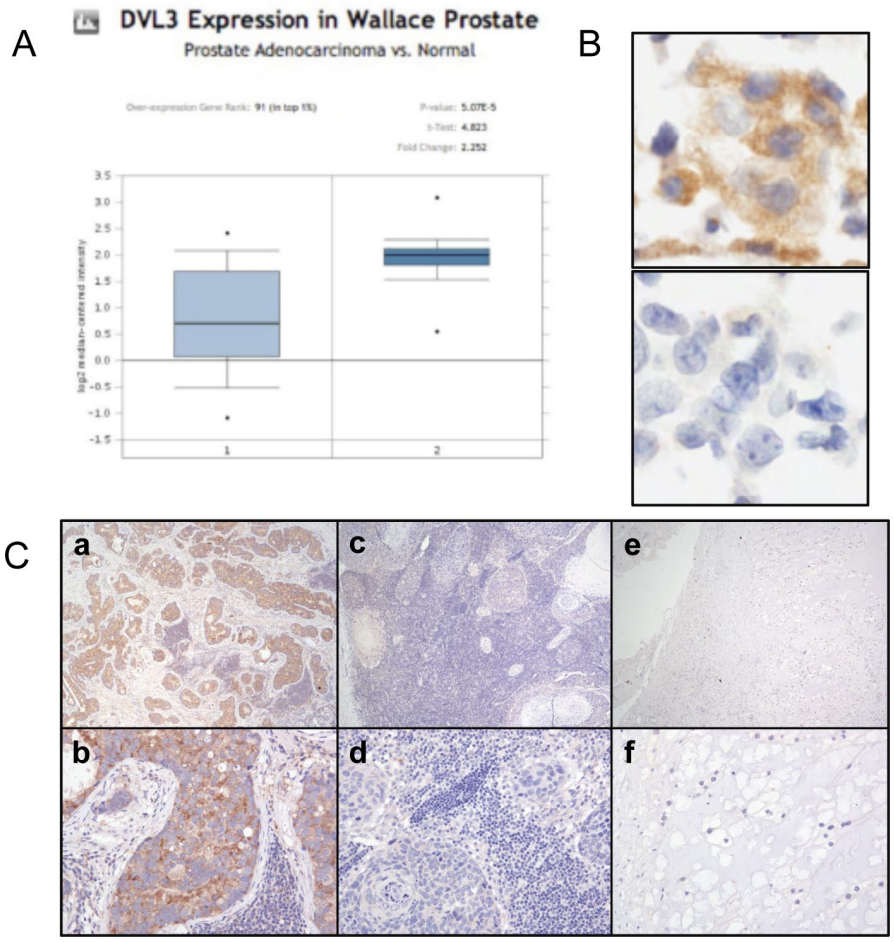

Figure 7.1 DVL3 expression in cancers. (A) DVL3 mRNA levels in prostate cancers. Output from Oncomine (www.oncomine.org) showing DVL3 expression in benign prostate (n=20) and prostate cancer (n=69). DVL3 is overexpressed 2.5 fold in cancers ($p=5.07x10^{-5}$). Data analysed and figure generated by Mr. Steve Taylor, Bioinformatics, WIMM, Oxford University. (B) Optimization of DVL3 immunohistochemistry in DU145 cells. DU145 cells were reverse-transfected with AS (upper panel) or DVL3 siRNA (lower panel), collected after 48 hours, fixed and stained with DVL3 antibody. (C) DVL3 immunohistochemistry in tumours of patients treated with IGF-1R TKI. a, b: prostate cancer from non-responder; c, d squamous cancer, achieved PR; e, f spinal chordoma, durable (3 year) PR. All slides were from the same staining run. Original magnification a, c, e x4; b, d, f x20 (Staining performed by Ms. Debbie Bailey and assessed by Dr. Clare Verrill and Dr. Lisa Browning, Department of Pathology, John Radcliffe Hospital, Oxford University).

Several recent studies have shown that some of the hits identified here could be linked to the IGF axis. LMTK3 has been shown to regulate WNT signaling in colon cancer, to increase survival of leukemia cells, and was an important regulator of sensitivity to ERα inhibition in breast cancer (Naik et al. 2009; Tyner et al. 2009; Giamas et al. 2011). Notably, LMTK3 was found to negatively regulate AKT phosphorylation (Giamas et al. 2011). It is plausible that this effect could contribute to SLL between LMTK3 and IGF-1R. Finally, gemcitabine treatment of human NSCLC cells was shown to activate AKT and ERK1/2, and up-regulate Rad51 protein, effects that could be reversed by Rad51 gene silencing, with consequent sensitization to gemcitabine (Tsai et al. 2010). This study also raises the concept of combining targeted treatments, such as AZ12253801 in combination with a second agent to enhance IGF-1R inhibitor efficacy. The combination with DNA damage is clinically relevant given that our group showed that IGF-1R depletion delays repair of damage in prostate cancer cells (Turney et al. 2012).

HUNK is a serine/threonine kinase that is expressed in breast cancer, and has been reported to be associated with metastasis. However, there is conflict between two significant publications, one indicating that HUNK is essential for metastasis, and the other reporting that HUNK represses metastasis by binding PP2A to prevent dephosphorylation of cofilin (Wertheim et al. 2009;

Quintela-Fandino et al. 2010). Of note, HUNK has been identified as a binding partner of GRB2 (Bisson et al. 2011) and also as protein that influences sensitivity to EGFR inhibition (Komurov et al. 2010). In a preliminary experiment, effects of HUNK knockdown on IGF-1R signaling were tested. HUNK-depleted cells did not show changes in ERK1/2 activity, but did show enhancement of IGF-1-induced IGF-1R autophosphorylation and AKT activation (Figure 7.2), similar to the report that HUNK silencing increases EGFR activity (Komurov et al. 2010). It will be interesting in future work to explore how HUNK silencing contributes to IGF axis activation, especially as HUNK kinase activity has not been assigned any definite role as yet.

In summary, it is clear that further studies are need to fully understand the function of IGF-1R, and the clinical application of IGF-1R inhibitory drugs. This study has established a basis for identifying regulators of sensitivity to IGF-1R inhibition, and paved the way for the future application of IGF-1R inhibition in preclinical testing and clinical trials.

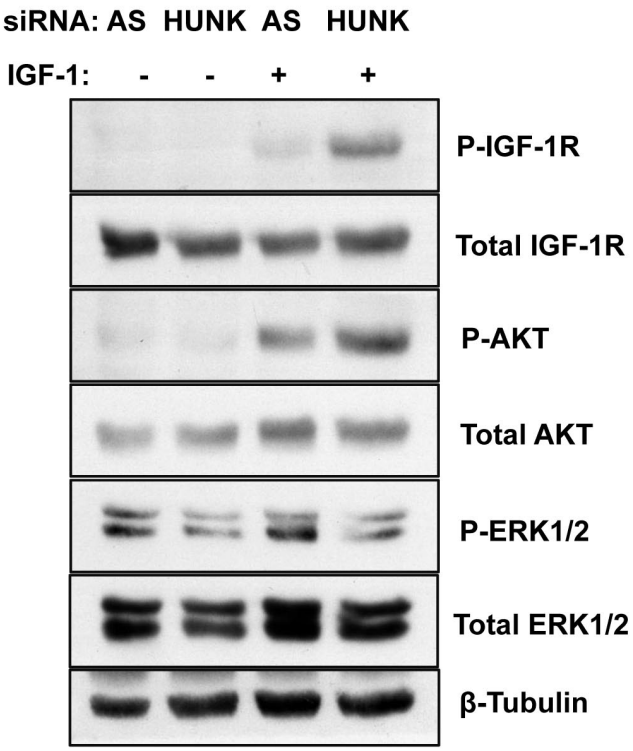

Figure 7.2 HUNK knockdown enhances IGF-1 response of IGF-1R and AKT. DU145 cells were reverse-transfected with AS or HUNK siRNAs, after 48 hours serum-starved overnight and treated with 10nM IGF-I for 10min. Lysates were probed with specific P-IGF-1R, IGF-1R, P-AKT, AKT, P-ERK1/2 and ERK1/2 antibodies with β-Tubulin as loading control.

Bibliography

Abuzzahab, M. J., A. Schneider, A. Goddard, F. Grigorescu, C. Lautier, E. Keller, W. Kiess, J. Klammt, J. Kratzsch, D. Osgood, R. Pfaffle, K. Raile, B. Seidel, R. J. Smith and S. D. Chernausek (2003). "IGF-I receptor mutations resulting in intrauterine and postnatal growth retardation." The New England journal of medicine **349**(23): 2211-2222.

Aleksic, T., M. M. Chitnis, O. V. Perestenko, S. Gao, P. H. Thomas, G. D. Turner, A. S. Protheroe, M. Howarth and V. M. Macaulay (2010). "Type 1 insulin-like growth factor receptor translocates to the nucleus of human tumor cells." Cancer Res **70**(16): 6412-6419.

All-Ericsson, C., L. Girnita, S. Seregard, A. Bartolazzi, M. J. Jager and O. Larsson (2002). "Insulin-like growth factor-1 receptor in uveal melanoma: a predictor for metastatic disease and a potential therapeutic target." Invest Ophthalmol Vis Sci **43**(1): 1-8.

Allen, G. W., C. Saba, E. A. Armstrong, S. M. Huang, S. Benavente, D. L. Ludwig, D. J. Hicklin and P. M. Harari (2007). "Insulin-like growth factor-I receptor signaling blockade combined with radiation." Cancer research **67**(3): 1155-1162.

Almeida, R. and R. C. Allshire (2005). "RNA silencing and genome regulation." Trends Cell Biol **15**(5): 251-258.

Audeh, M. W., J. Carmichael, R. T. Penson, M. Friedlander, B. Powell, K. M. Bell-McGuinn, C. Scott, J. N. Weitzel, A. Oaknin, N. Loman, K. Lu, R. K. Schmutzler, U. Matulonis, M. Wickens and A. Tutt (2010). "Oral poly(ADP-ribose) polymerase inhibitor olaparib in patients with BRCA1 or BRCA2 mutations and recurrent ovarian cancer: a proof-of-concept trial." Lancet **376**(9737): 245-251.

Baserga, R. (1995). "The Insulin-Like Growth-Factor-I Receptor - a Key to Tumor-Growth." Cancer Research **55**(2): 249-252.

Baserga, R. (1999). "The IGF-I receptor in cancer research." Experimental cell research **253**(1): 1-6.

Baserga, R. (2009). "The insulin receptor substrate-1: A biomarker for cancer?" Experimental Cell Research **315**(5): 727-732.

Baserga, R., F. Peruzzi and K. Reiss (2003). "The IGF-1 receptor in cancer biology." Int J Cancer **107**(6): 873-877.

Basu, B., D. Olmos and J. S. de Bono (2011). "Targeting IGF-1R: throwing out the baby with the bathwater?" British Journal of Cancer **104**(1): 1-3.

Belfiore, A., F. Frasca, G. Pandini, L. Sciacca and R. Vigneri (2009). "Insulin receptor isoforms and insulin receptor/insulin-like growth factor receptor hybrids in physiology and disease." Endocr Rev **30**(6): 586-623.

Bernstein, E., A. A. Caudy, S. M. Hammond and G. J. Hannon (2001). "Role for a bidentate ribonuclease in the initiation step of RNA interference." Nature **409**(6818): 363-366.

Birmingham, A., L. M. Selfors, T. Forster, D. Wrobel, C. J. Kennedy, E. Shanks, J. Santoyo-Lopez, D. J. Dunican, A. Long, D. Kelleher, Q. Smith, R. L. Beijersbergen, P. Ghazal and C. E. Shamu (2009). "Statistical methods for analysis of high-throughput RNA interference screens." Nat Methods **6**(8): 569-575.

Bisson, N., D. A. James, G. Ivosev, S. A. Tate, R. Bonner, L. Taylor and T. Pawson (2011). "Selected reaction monitoring mass spectrometry reveals the dynamics of signaling through the GRB2 adaptor." Nature Biotechnology **29**(7): 653-U138.

Bjorndahl, M., R. Cao, L. J. Nissen, S. Clasper, L. A. Johnson, Y. Xue, Z. Zhou, D. Jackson, A. J. Hansen and Y. Cao (2005). "Insulin-like growth factors 1 and 2 induce lymphangiogenesis in vivo." Proc Natl Acad Sci U S A **102**(43): 15593-15598.

Boriack-Sjodin, P. A., S. M. Margarit, D. Bar-Sagi and J. Kuriyan (1998). "The structural basis of the activation of Ras by Sos." Nature **394**(6691): 337-343.

Boros, J., I. J. Donaldson, A. O'Donnell, Z. A. Odrowaz, L. Zeef, M. Lupien, C. A. Meyer, X. S. Liu, M. Brown and A. D. Sharrocks (2009). "Elucidation of the ELK1 target gene network reveals a role in the coordinate regulation of core components of the gene regulation machinery." Genome research **19**(11): 1963-1973.

Boutros, M. and J. Ahringer (2008). "The art and design of genetic screens: RNA interference." Nat Rev Genet **9**(7): 554-566.

Boutros, M., L. P. Bras and W. Huber (2006). "Analysis of cell-based RNAi screens." Genome Biol **7**(7): R66.

Brough, R., J. R. Frankum, S. Costa-Cabral, C. J. Lord and A. Ashworth (2011). "Searching for synthetic lethality in cancer." Curr Opin Genet Dev **21**(1): 34-41.

Brunet, A., A. Bonni, M. J. Zigmond, M. Z. Lin, P. Juo, L. S. Hu, M. J. Anderson, K. C. Arden, J. Blenis and M. E. Greenberg (1999). "Akt promotes cell survival by phosphorylating and inhibiting a Forkhead transcription factor." Cell **96**(6): 857-868.

Bryant, H. E., N. Schultz, H. D. Thomas, K. M. Parker, D. Flower, E. Lopez, S. Kyle, M. Meuth, N. J. Curtin and T. Helleday (2005). "Specific killing of BRCA2-deficient tumours with inhibitors of poly(ADP-ribose) polymerase." Nature **434**(7035): 913-917.

Bryja, V., D. Gradl, A. Schambony, E. Arenas and G. Schulte (2007). "Beta-arrestin is a necessary component of Wnt/beta-catenin signaling in vitro and in vivo." Proceedings of the National Academy of Sciences of the United States of America **104**(16): 6690-6695.

Buck, E., A. Eyzaguirre, M. Rosenfeld-Franklin, S. Thomson, M. Mulvihill, S. Barr, E. Brown, M. O'Connor, Y. Yao, J. Pachter, M. Miglarese, D. Epstein, K. K. Iwata, J. D. Haley, N. W. Gibson and Q. S. Ji (2008). "Feedback mechanisms promote cooperativity for small molecule inhibitors of epidermal and insulin-like growth factor receptors." Cancer research **68**(20): 8322-8332.

Burgaud, J. L. and R. Baserga (1996). "Intracellular transactivation of the insulin-like growth factor I receptor by an epidermal growth factor receptor."

Experimental Cell Research **223**(2): 412-419.

Campbell, R. A., P. Bhat-Nakshatri, N. M. Patel, D. Constantinidou, S. Ali and H. Nakshatri (2001). "Phosphatidylinositol 3-kinase/AKT-mediated activation of estrogen receptor alpha: a new model for anti-estrogen resistance." The Journal of biological chemistry **276**(13): 9817-9824.

Cao, L., Y. Yu, I. Darko, D. Currier, L. H. Mayeenuddin, X. Wan, C. Khanna and L. J. Helman (2008). "Addiction to elevated insulin-like growth factor I receptor and initial modulation of the AKT pathway define the responsiveness of rhabdomyosarcoma to the targeting antibody." Cancer research **68**(19): 8039-8048.

Cardozo, C. P., Y. Wu, W. D. Zhao, J. B. Zhao, J. P. Pan, Q. Q. Wu, Y. F. Zhang and W. A. Bauman (2007). "Identification of androgen response elements in the insulin-like growth factor I upstream promoter." Endocrinology **148**(6): 2984-2993.

Carmeliet, P. and R. K. Jain (2000). "Angiogenesis in cancer and other diseases." Nature **407**(6801): 249-257.

Carney, D. N., A. F. Gazdar and J. D. Minna (1980). "Positive correlation between histological tumor involvement and generation of tumor cell colonies in agarose in specimens taken directly from patients with small-cell carcinoma of the lung." Cancer research **40**(6): 1820-1823.

Chan, J. M., M. J. Stampfer, E. Giovannucci, P. H. Gann, J. Ma, P. Wilkinson, C. H. Hennekens and M. Pollak (1998). "Plasma insulin-like growth factor-I and prostate cancer risk: a prospective study." Science **279**(5350): 563-566.

Chen, J., A. Wu, H. Sun, R. Drakas, C. Garofalo, S. Cascio, E. Surmacz and R. Baserga (2005). "Functional significance of type 1 insulin-like growth factor-mediated nuclear translocation of the insulin receptor substrate-1 and beta-catenin." The Journal of biological chemistry **280**(33): 29912-29920.

Chen, Y., J. Wang, M. M. Fraig, K. Henderson, N. K. Bissada, D. K. Watson and C. W. Schweinfest (2003). "Alterations in PMS2, MSH2 and MLH1 expression in human prostate cancer." International journal of oncology **22**(5):

1033-1043.

Chitnis, M. M., J. S. Yuen, A. S. Protheroe, M. Pollak and V. M. Macaulay (2008). "The type 1 insulin-like growth factor receptor pathway." Clin Cancer Res **14**(20): 6364-6370.

Chlenski, A., K. Nakashiro, K. V. Ketels, G. I. Korovaitseva and R. Oyasu (2001). "Androgen receptor expression in androgen-independent prostate cancer cell lines." The Prostate **47**(1): 66-75.

Clemmons, D. R. (2007). "Modifying IGF1 activity: an approach to treat endocrine disorders, atherosclerosis and cancer." Nature reviews. Drug discovery **6**(10): 821-833.

Collett-Solberg, P. F. and P. Cohen (1996). "The role of the insulin-like growth factor binding proteins and the IGFBP proteases in modulating IGF action." Endocrinol Metab Clin North Am **25**(3): 591-614.

Coppola, D., B. Saunders, L. Fu, W. Mao and S. V. Nicosia (1999). "The insulin-like growth factor 1 receptor induces transformation and tumorigenicity of ovarian mesothelial cells and down-regulates their Fas-receptor expression." Cancer Res **59**(13): 3264-3270.

Crampton, S. P., B. B. Wu, E. J. Park, J. H. Kim, C. Solomon, M. L. Waterman and C. C. W. Hughes (2009). "Integration of the beta-Catenin-Dependent Wnt Pathway with Integrin Signaling through the Adaptor Molecule Grb2." Plos One **4**(11).

D'Ambrosio, C., A. Ferber, M. Resnicoff and R. Baserga (1996). "A soluble insulin-like growth factor I receptor that induces apoptosis of tumor cells in vivo and inhibits tumorigenesis." Cancer Res **56**(17): 4013-4020.

Dambrosio, C., S. R. Keller, A. Morrione, G. E. Lienhard, R. Baserga and E. Surmacz (1995). "Transforming Potential of the Insulin-Receptor Substrate-1." Cell Growth & Differentiation **6**(5): 557-562.

DeAngelis, T., J. Chen, A. Wu, M. Prisco and R. Baserga (2006). "Transformation by the simian virus 40 T antigen is regulated by IGF-I receptor

and IRS-1 signaling." Oncogene **25**(1): 32-42.

DeChiara, T. M., A. Efstratiadis and E. J. Robertson (1990). "A growth-deficiency phenotype in heterozygous mice carrying an insulin-like growth factor II gene disrupted by targeting." Nature **345**(6270): 78-80.

DeGraffenried, L. A., L. Fulcher, W. E. Friedrichs, V. Grunwald, R. B. Ray and M. Hidalgo (2004). "Reduced PTEN expression in breast cancer cells confers susceptibility to inhibitors of the PI3 kinase/Akt pathway." Annals of oncology : official journal of the European Society for Medical Oncology / ESMO **15**(10): 1510-1516.

Denley, A., L. J. Cosgrove, G. W. Booker, J. C. Wallace and B. E. Forbes (2005). "Molecular interactions of the IGF system." Cytokine Growth Factor Rev **16**(4-5): 421-439.

Desbois-Mouthon, C., A. Cadoret, M. J. Blivet-Van Eggelpoel, F. Bertrand, G. Cherqui, C. Perret and J. Capeau (2001). "Insulin and IGF-1 stimulate the beta-catenin pathway through two signalling cascades involving GSK-3 beta inhibition and Ras activation." Oncogene **20**(2): 252-259.

Dobzhansky, T. (1946). "Genetics of Natural Populations. Xiii. Recombination and Variability in Populations of Drosophila Pseudoobscura." Genetics **31**(3): 269-290.

Du, K. Y. and M. Montminy (1998). "CREB is a regulatory target for the protein kinase Akt/PKB." Journal of Biological Chemistry **273**(49): 32377-32379.

Dunn, S. E., R. A. Hardman, F. W. Kari and J. C. Barrett (1997). "Insulin-like growth factor 1 (IGF-1) alters drug sensitivity of HBL100 human breast cancer cells by inhibition of apoptosis induced by diverse anticancer drugs." Cancer Res **57**(13): 2687-2693.

Dupont, J. and D. Le Roith (2001). "Insulin-like growth factor 1 and oestradiol promote cell proliferation of MCF-7 breast cancer cells: new insights into their synergistic effects." Journal of Clinical Pathology-Molecular Pathology **54**(3): 149-154.

Echeverri, C. J., P. A. Beachy, B. Baum, M. Boutros, F. Buchholz, S. K. Chanda, J. Downward, J. Ellenberg, A. G. Fraser, N. Hacohen, W. C. Hahn, A. L. Jackson, A. Kiger, P. S. Linsley, L. Lum, Y. Ma, B. Mathey-Prevot, D. E. Root, D. M. Sabatini, J. Taipale, N. Perrimon and R. Bernards (2006). "Minimizing the risk of reporting false positives in large-scale RNAi screens." Nature Methods **3**(10): 777-779.

Echeverri, C. J. and N. Perrimon (2006). "High-throughput RNAi screening in cultured cells: a user's guide." Nat Rev Genet **7**(5): 373-384.

Edwards, S. L., R. Brough, C. J. Lord, R. Natrajan, R. Vatcheva, D. A. Levine, J. Boyd, J. S. Reis-Filho and A. Ashworth (2008). "Resistance to therapy caused by intragenic deletion in BRCA2." Nature **451**(7182): 1111-1115.

Elbashir, S. M., J. Harborth, W. Lendeckel, A. Yalcin, K. Weber and T. Tuschl (2001). "Duplexes of 21-nucleotide RNAs mediate RNA interference in cultured mammalian cells." Nature **411**(6836): 494-498.

Elmore, S. (2007). "Apoptosis: a review of programmed cell death." Toxicol Pathol **35**(4): 495-516.

Etheridge, S. L., S. Ray, S. Li, N. S. Hamblet, N. Lijam, M. Tsang, J. Greer, N. Kardos, J. Wang, D. J. Sussman, P. Chen and A. Wynshaw-Boris (2008). "Murine dishevelled 3 functions in redundant pathways with dishevelled 1 and 2 in normal cardiac outflow tract, cochlea, and neural tube development." PLoS genetics **4**(11): e1000259.

Fagan, D. and D. Yee (2008). "Crosstalk Between IGF1R and Estrogen Receptor Signaling in Breast Cancer." Journal of Mammary Gland Biology and Neoplasia **13**(4): 423-429.

Fahmy, O. G. and M. J. Fahmy (1959). "Differential Gene Response to Mutagens in Drosophila Melanogaster." Genetics **44**(6): 1149-1171.

Farmer, H., N. McCabe, C. J. Lord, A. N. Tutt, D. A. Johnson, T. B. Richardson, M. Santarosa, K. J. Dillon, I. Hickson, C. Knights, N. M. Martin, S. P. Jackson, G. C. Smith and A. Ashworth (2005). "Targeting the DNA repair defect in BRCA mutant cells as a therapeutic strategy." Nature **434**(7035): 917-921.

Fazili, Z., W. P. Sun, S. Mittelstaedt, C. Cohen and X. X. Xu (1999). "Disabled-2 inactivation is an early step in ovarian tumorigenicity." Oncogene **18**(20): 3104-3113.

Feldser, D., F. Agani, N. V. Iyer, B. Pak, G. Ferreira and G. L. Semenza (1999). "Reciprocal positive regulation of hypoxia-inducible factor 1alpha and insulin-like growth factor 2." Cancer Res **59**(16): 3915-3918.

Ferrara, N. (2002). "VEGF and the quest for tumour angiogenesis factors." Nat Rev Cancer **2**(10): 795-803.

Ferrari, E., C. Lucca and M. Foiani (2010). "A lethal combination for cancer cells: synthetic lethality screenings for drug discovery." Eur J Cancer **46**(16): 2889-2895.

Fire, A., S. Xu, M. K. Montgomery, S. A. Kostas, S. E. Driver and C. C. Mello (1998). "Potent and specific genetic interference by double-stranded RNA in Caenorhabditis elegans." Nature **391**(6669): 806-811.

Fong, P. C., D. S. Boss, T. A. Yap, A. Tutt, P. Wu, M. Mergui-Roelvink, P. Mortimer, H. Swaisland, A. Lau, M. J. O'Connor, A. Ashworth, J. Carmichael, S. B. Kaye, J. H. Schellens and J. S. de Bono (2009). "Inhibition of poly(ADP-ribose) polymerase in tumors from BRCA mutation carriers." N Engl J Med **361**(2): 123-134.

Fukuda, R., K. Hirota, F. Fan, Y. Do Jung, L. M. Ellis and G. L. Semenza (2002). "Insulin-like growth factor 1 induces hypoxia-inducible factor 1-mediated vascular endothelial growth factor expression, which is dependent on MAP kinase and phosphatidylinositol 3-kinase signaling in colon cancer cells." Journal of Biological Chemistry **277**(41): 38205-38211.

Gao, C. and Y. G. Chen (2009). "Dishevelled: The hub of Wnt signaling." Cell Signal **22**(5): 717-727.

Gao, W. Q. (2010). "Androgen receptor as a therapeutic target." Advanced Drug Delivery Reviews **62**(13): 1277-1284.

Gerstein, A. V., T. A. Almeida, G. Zhao, E. Chess, M. Shih Ie, K. Buhler, K.

Pienta, M. A. Rubin, R. Vessella and N. Papadopoulos (2002). "APC/CTNNB1 (beta-catenin) pathway alterations in human prostate cancers." Genes Chromosomes Cancer **34**(1): 9-16.

Giamas, G., A. Filipovic, J. Jacob, W. Messier, H. Zhang, D. Y. Yang, W. Zhang, B. A. Shifa, A. Photiou, C. Tralau-Stewart, L. Castellano, A. R. Green, R. C. Coombes, I. O. Ellis, S. Ali, H. J. Lenz and J. Stebbing (2011). "Kinome screening for regulators of the estrogen receptor identifies LMTK3 as a new therapeutic target in breast cancer." Nature Medicine **17**(6): 715-U105.

Girnita, L., A. Girnita and O. Larsson (2003). "Mdm2-dependent ubiquitination and degradation of the insulin-like growth factor 1 receptor." Proceedings of the National Academy of Sciences of the United States of America **100**(14): 8247-8252.

Gong, Y., E. Yao, R. Shen, A. Goel, M. Arcila, J. Teruya-Feldstein, M. F. Zakowski, S. Frankel, M. Peifer, R. K. Thomas, M. Ladanyi and W. Pao (2009). "High expression levels of total IGF-1R and sensitivity of NSCLC cells in vitro to an anti-IGF-1R antibody (R1507)." PloS one **4**(10): e7273.

Gonzalez-Sancho, J. M., K. R. Brennan, L. A. Castelo-Soccio and A. M. Brown (2004). "Wnt proteins induce dishevelled phosphorylation via an LRP5/6-independent mechanism, irrespective of their ability to stabilize beta-catenin." Molecular and cellular biology **24**(11): 4757-4768.

Gordon, M. D. and R. Nusse (2006). "Wnt signaling: Multiple pathways, multiple receptors, and multiple transcription factors." Journal of Biological Chemistry **281**(32): 22429-22433.

Grandy, D., J. Shan, X. Zhang, S. Rao, S. Akunuru, H. Li, Y. Zhang, I. Alpatov, X. A. Zhang, R. A. Lang, D. L. Shi and J. J. Zheng (2009). "Discovery and characterization of a small molecule inhibitor of the PDZ domain of dishevelled." The Journal of Biological Chemistry **284**(24): 16256-16263.

Gualberto, A., M. Dolled-Filhart, M. Gustavson, J. Christiansen, Y. F. Wang, M. L. Hixon, J. Reynolds, S. McDonald, A. Ang, D. L. Rimm, C. J. Langer, J. Blakely, L. Garland, L. G. Paz-Ares, D. D. Karp and A. V. Lee (2010). "Molecular analysis of non-small cell lung cancer identifies subsets with

different sensitivity to insulin-like growth factor I receptor inhibition." Clinical Cancer Research **16**(18): 4654-4665.

Gualberto, A., M. L. Hixon, D. D. Karp, D. Li, S. Green, M. Dolled-Filhart, L. G. Paz-Ares, S. Novello, J. Blakely, C. J. Langer and M. N. Pollak (2011). "Pre-treatment levels of circulating free IGF-1 identify NSCLC patients who derive clinical benefit from figitumumab." British Journal of Cancer **104**(1): 68-74.

Gualberto, A. and M. Pollak (2009). "Emerging role of insulin-like growth factor receptor inhibitors in oncology: early clinical trial results and future directions." Oncogene **28**(34): 3009-3021.

Guo, S. and K. J. Kemphues (1995). "Par-1, a Gene Required for Establishing Polarity in C-Elegans Embryos, Encodes a Putative Ser/Thr Kinase That Is Asymmetrically Distributed." Cell **81**(4): 611-620.

Hamblet, N. S., N. Lijam, P. Ruiz-Lozano, J. Wang, Y. Yang, Z. Luo, L. Mei, K. R. Chien, D. J. Sussman and A. Wynshaw-Boris (2002). "Dishevelled 2 is essential for cardiac outflow tract development, somite segmentation and neural tube closure." Development **129**(24): 5827-5838.

Hanahan, D. and R. A. Weinberg (2000). "The hallmarks of cancer." Cell **100**(1): 57-70.

Hanahan, D. and R. A. Weinberg (2011). "Hallmarks of cancer: the next generation." Cell **144**(5): 646-674.

Hankinson, S. E., W. C. Willett, G. A. Colditz, D. J. Hunter, D. S. Michaud, B. Deroo, B. Rosner, F. E. Speizer and M. Pollak (1998). "Circulating concentrations of insulin-like growth factor-I and risk of breast cancer." Lancet **351**(9113): 1393-1396.

Hannon, G. J. (2002). "RNA interference." Nature **418**(6894): 244-251.

Hartman, J. L. t., B. Garvik and L. Hartwell (2001). "Principles for the buffering of genetic variation." Science **291**(5506): 1001-1004.

Harzatark (2007). "A phase I trial of nordihydroguareacetic acid (NDGA) in patients with non-metastatic prostate cancer and rising PSA." J Clin Oncol (Meeting Abstracts).

Hellawell, G. O., G. D. Turner, D. R. Davies, R. Poulsom, S. F. Brewster and V. M. Macaulay (2002). "Expression of the type 1 insulin-like growth factor receptor is up-regulated in primary prostate cancer and commonly persists in metastatic disease." Cancer Res **62**(10): 2942-2950.

Hocevar, B. A., F. Mou, J. L. Rennolds, S. M. Morris, J. A. Cooper and P. H. Howe (2003). "Regulation of the Wnt signaling pathway by disabled-2 (Dab2)." The EMBO journal **22**(12): 3084-3094.

Huang, S. M., Y. M. Mishina, S. Liu, A. Cheung, F. Stegmeier, G. A. Michaud, O. Charlat, E. Wiellette, Y. Zhang, S. Wiessner, M. Hild, X. Shi, C. J. Wilson, C. Mickanin, V. Myer, A. Fazal, R. Tomlinson, F. Serluca, W. Shao, H. Cheng, M. Shultz, C. Rau, M. Schirle, J. Schlegl, S. Ghidelli, S. Fawell, C. Lu, D. Curtis, M. W. Kirschner, C. Lengauer, P. M. Finan, J. A. Tallarico, T. Bouwmeester, J. A. Porter, A. Bauer and F. Cong (2009). "Tankyrase inhibition stabilizes axin and antagonizes Wnt signalling." Nature **461**(7264): 614-620.

Huang, Y., H. Friess, J. Kleeff, I. Esposito, Z. W. Zhu, S. L. Liu, S. C. Mok, A. Zimmermann and M. W. Buchler (2001). "DOC-2/hDab2 expression is up-regulated in primary pancreatic cancer but reduced in metastasis." Laboratory Investigation **81**(6): 863-873.

Huesken, D., J. Lange, C. Mickanin, J. Weiler, F. Asselbergs, J. Warner, B. Meloon, S. Engel, A. Rosenberg, D. Cohen, M. Labow, M. Reinhardt, F. Natt and J. Hall (2005). "Design of a genome-wide siRNA library using an artificial neural network." Nature Biotechnology **23**(8): 995-1001.

Hwa, V., Y. Oh and R. G. Rosenfeld (1999). "The insulin-like growth factor-binding protein (IGFBP) superfamily." Endocr Rev **20**(6): 761-787.

Igney, F. H. and P. H. Krammer (2002). "Death and anti-death: tumour resistance to apoptosis." Nat Rev Cancer **2**(4): 277-288.

Inoki, K., H. Ouyang, T. Zhu, C. Lindvall, Y. Wang, X. Zhang, Q. Yang, C.

Bennett, Y. Harada, K. Stankunas, C. Y. Wang, X. He, O. A. MacDougald, M. You, B. O. Williams and K. L. Guan (2006). "TSC2 integrates Wnt and energy signals via a coordinated phosphorylation by AMPK and GSK3 to regulate cell growth." Cell **126**(5): 955-968.

Iorns, E., N. C. Turner, R. Elliott, N. Syed, O. Garrone, M. Gasco, A. N. Tutt, T. Crook, C. J. Lord and A. Ashworth (2008). "Identification of CDK10 as an important determinant of resistance to endocrine therapy for breast cancer." Cancer cell **13**(2): 91-104.

Iwasa, T., I. Okamoto, M. Suzuki, E. Hatashita, Y. Yamada, M. Fukuoka, K. Ono and K. Nakagawa (2009). "Inhibition of insulin-like growth factor 1 receptor by CP-751,871 radiosensitizes non-small cell lung cancer cells." Clinical cancer research : an official journal of the American Association for Cancer Research **15**(16): 5117-5125.

Jassem, J., Langer, CJ, Karp, DD, Mok T, Benner RJ, Green SJ, Park K, Novello S, Strausz J, Gualberto A (2010). "Randomized, open label, phase III trial of figitumumab in combination with paclitaxel and carboplatin versus paclitaxel and carboplatin in patients with non-small cell lung cancer (NSCLC)." J Clin Oncol **(Meet Abstr)** (28(Suppl 15): 7500).

Javle, M., G. R. Varadhachary, D. R. Fogelman, R. T. Shroff, M. J. Overman, L. Ukegbu, B. N. Bekele, S. P. Kar, R. A. Wolff, J. L. Abbruzzese (2011). "Randomized phase II study of gemcitabine (G) plus anti-IGF-1R antibody MK-0646, G plus erlotinib (E) plus MK-0646 and G plus E for advanced pancreatic cancer." J Clin Oncol **29**(suppl; abstr 4026).

Jernberg-Wiklund, H. and K. Nilsson (2007). "Control of apoptosis in human multiple myeloma by insulin-like growth factor I (IGF-I)." Adv Cancer Res **97**: 139-165.

Joshi, R. L., B. Lamothe, N. Cordonnier, K. Mesbah, E. Monthioux, J. Jami and D. Bucchini (1996). "Targeted disruption of the insulin receptor gene in the mouse results in neonatal lethality." Embo Journal **15**(7): 1542-1547.

Kahlert, S., S. Nuedling, M. van Eickels, H. Vetter, R. Meyer and C. Grohe (2000). "Estrogen receptor alpha rapidly activates the IGF-1 receptor pathway."

J Biol Chem **275**(24): 18447-18453.

Kang, S., A. G. Bader and P. K. Vogt (2005). "Phosphatidylinositol 3-kinase mutations identified in human cancer are oncogenic." Proceedings of the National Academy of Sciences of the United States of America **102**(3): 802-807.

Kanter-Lewensohn, L., A. Dricu, M. Wang, J. Wejde, R. Kiessling and O. Larsson (1998). "Expression of the insulin-like growth factor-1 receptor and its anti-apoptotic effect in malignant melanoma: a potential therapeutic target." Melanoma Research **8**(5): 389-397.

Karam, J. A., S. F. Shariat, H. Y. Huang, R. C. Pong, R. Ashfaq, E. Shapiro, Y. Lotan, A. I. Sagalowsky, X. R. Wu and J. T. Hsieh (2007). "Decreased DOC-2/DAB2 expression in urothelial carcinoma of the bladder." Clinical Cancer Research **13**(15 Pt 1): 4400-4406.

Karasic, T. B., T. K. Hei and V. N. Ivanov (2010). "Disruption of IGF-1R signaling increases TRAIL-induced apoptosis: a new potential therapy for the treatment of melanoma." Exp Cell Res **316**(12): 1994-2007.

Karlas, A., N. Machuy, Y. Shin, K. P. Pleissner, A. Artarini, D. Heuer, D. Becker, H. Khalil, L. A. Ogilvie, S. Hess, A. P. Maurer, E. Muller, T. Wolff, T. Rudel and T. F. Meyer (2010). "Genome-wide RNAi screen identifies human host factors crucial for influenza virus replication." Nature **463**(7282): 818-822.

Karp, D. D., L. G. Paz-Ares, S. Novello, P. Haluska, L. Garland, F. Cardenal, L. J. Blakely, P. D. Eisenberg, C. J. Langer, G. Blumenschein, F. M. Johnson, S. Green and A. Gualberto (2009). "Phase II Study of the Anti-Insulin-Like Growth Factor Type 1 Receptor Antibody CP-751,871 in Combination With Paclitaxel and Carboplatin in Previously Untreated, Locally Advanced, or Metastatic Non-Small-Cell Lung Cancer." Journal of Clinical Oncology **27**(15): 2516-2522.

Kato, S., H. Endoh, Y. Masuhiro, T. Kitamoto, S. Uchiyama, H. Sasaki, S. Masushige, Y. Gotoh, E. Nishida, H. Kawashima, D. Metzger and P. Chambon (1995). "Activation of the Estrogen-Receptor through Phosphorylation by Mitogen-Activated Protein-Kinase." Science **270**(5241): 1491-1494.

Key, T. J., P. N. Appleby, G. K. Reeves, A. W. Roddam and T. E. H. Breast (2010). "Insulin-like growth factor 1 (IGF1), IGF binding protein 3 (IGFBP3), and breast cancer risk: pooled individual data analysis of 17 prospective studies." Lancet Oncology **11**(6): 530-542.

Khokhlatchev, A. V., B. Canagarajah, J. Wilsbacher, M. Robinson, M. Atkinson, E. Goldsmith and M. H. Cobb (1998). "Phosphorylation of the MAP kinase ERK2 promotes its homodimerization and nuclear translocation." Cell **93**(4): 605-615.

Kim, D. H. and J. J. Rossi (2007). "Strategies for silencing human disease using RNA interference." Nature Reviews Genetics **8**(3): 173-184.

Kim, S. O., J. G. Park and Y. I. Lee (1996). "Increased expression of the insulin-like growth factor I (IGF-I) receptor gene in hepatocellular carcinoma cell lines: implications of IGF-I receptor gene activation by hepatitis B virus X gene product." Cancer Research **56**(16): 3831-3836.

Kimura, G., J. Kasuya, S. Giannini, Y. Honda, S. Mohan, M. Kawachi, M. Akimoto and Y. Fujita-Yamaguchi (1996). "Insulin-like growth factor (IGF) system components in human prostatic cancer cell-lines: LNCaP, DU145, and PC-3 cells." Int J Urol **3**(1): 39-46.

Kleiner, D. E. and W. G. Stetler-Stevenson (1999). "Matrix metalloproteinases and metastasis." Cancer Chemother Pharmacol **43 Suppl**: S42-51.

Komurov, K., D. Padron, T. Cheng, M. Roth, K. P. Rosenblatt and M. A. White (2010). "Comprehensive mapping of the human kinome to epidermal growth factor receptor signaling." The Journal of Biological Chemistry **285**(27): 21134-21142.

Kondo, T., D. Vicent, K. Suzuma, M. Yanagisawa, G. L. King, M. Holzenberger and C. R. Kahn (2003). "Knockout of insulin and IGF-1 receptors on vascular endothelial cells protects against retinal neovascularization." J Clin Invest **111**(12): 1835-1842.

Kooijman, R. (2006). "Regulation of apoptosis by insulin-like growth factor (IGF)-I." Cytokine Growth Factor Rev **17**(4): 305-323.

Kroemer, G., L. Galluzzi, P. Vandenabeele, J. Abrams, E. S. Alnemri, E. H. Baehrecke, M. V. Blagosklonny, W. S. El-Deiry, P. Golstein, D. R. Green, M. Hengartner, R. A. Knight, S. Kumar, S. A. Lipton, W. Malorni, G. Nunez, M. E. Peter, J. Tschopp, J. Yuan, M. Piacentini, B. Zhivotovsky and G. Melino (2009). "Classification of cell death: recommendations of the Nomenclature Committee on Cell Death 2009." Cell Death Differ **16**(1): 3-11.

Kumar, M. S., D. C. Hancock, M. Molina-Arcas, M. Steckel, P. East, M. Diefenbacher, E. Armenteros-Monterroso, F. Lassailly, N. Matthews, E. Nye, G. Stamp, A. Behrens and J. Downward (2012). "The GATA2 Transcriptional Network Is Requisite for RAS Oncogene-Driven Non-Small Cell Lung Cancer." Cell **149**(3): 642-655.

Laplante, M. and D. M. Sabatini (2009). "mTOR signaling at a glance." Journal of Cell Science **122**(20): 3589-3594.

Larsson, O., A. Girnita and L. Girnita (2005). "Role of insulin-like growth factor 1 receptor signalling in cancer." Br J Cancer **92**(12): 2097-2101.

Lavoie, J. N., G. LAllemain, A. Brunet, R. Muller and J. Pouyssegur (1996). "Cyclin D1 expression is regulated positively by the p42/p44(MAPK) and negatively by the p38/HOG(MAPK) pathway." Journal of Biological Chemistry **271**(34): 20608-20616.

Lawen, A. (2003). "Apoptosis-an introduction." Bioessays **25**(9): 888-896.

Lee, A. V., C. N. Weng, J. G. Jackson and D. Yee (1997). "Activation of estrogen receptor-mediated gene transcription by IGF-I in human breast cancer cells." J Endocrinol **152**(1): 39-47.

Lee, O. H., S. K. Bae, M. H. Bae, Y. M. Lee, E. J. Moon, H. J. Cha, Y. G. Kwon and K. W. Kim (2000). "Identification of angiogenic properties of insulin-like growth factor II in in vitro angiogenesis models." Br J Cancer **82**(2): 385-391.

Lee, Y. N., Y. Gao and H. Y. Wang (2008). "Differential mediation of the Wnt canonical pathway by mammalian Dishevelleds-1, -2, and -3." Cellular Signalling **20**(2): 443-452.

Lemmon, M. A. and J. Schlessinger (2010). "Cell signaling by receptor tyrosine kinases." Cell **141**(7): 1117-1134.

Li, J., J. Liu, J. Song, X. Wang, H. L. Weiss, C. M. Townsend, Jr., T. Gao and B. M. Evers (2011). "mTORC1 inhibition increases neurotensin secretion and gene expression through activation of the MEK/ERK/c-Jun pathway in the human endocrine cell line BON." American Journal of Physiology. Cell physiology **301**(1): C213-226.

Li, J., C. Yen, D. Liaw, K. Podsypanina, S. Bose, S. I. Wang, J. Puc, C. Miliaresis, L. Rodgers, R. McCombie, S. H. Bigner, B. C. Giovanella, M. Ittmann, B. Tycko, H. Hibshoosh, M. H. Wigler and R. Parsons (1997). "PTEN, a putative protein tyrosine phosphatase gene mutated in human brain, breast, and prostate cancer." Science **275**(5308): 1943-1947.

Li, J. and J. Yuan (2008). "Caspases in apoptosis and beyond." Oncogene **27**(48): 6194-6206.

Lijam, N., R. Paylor, M. P. McDonald, J. N. Crawley, C. X. Deng, K. Herrup, K. E. Stevens, G. Maccaferri, C. J. McBain, D. J. Sussman and A. Wynshaw-Boris (1997). "Social interaction and sensorimotor gating abnormalities in mice lacking Dvl1." Cell **90**(5): 895-905.

Liu, B. Y., I. Soloviev, X. Huang, P. Chang, J. A. Ernst, P. Polakis and C. Sakanaka (2012). "Mammary tumor regression elicited by Wnt signaling inhibitor requires IGFBP5." Cancer Research. **72**(6):1568-1578

Liu, J. L., V. A. Blakesley, J. S. Gutkind and D. LeRoith (1997). "The constitutively active mutant Galpha13 transforms mouse fibroblast cells deficient in insulin-like growth factor-I receptor." J Biol Chem **272**(47): 29438-29441.

Liu, J. P., J. Baker, A. S. Perkins, E. J. Robertson and A. Efstratiadis (1993). "Mice carrying null mutations of the genes encoding insulin-like growth factor I (Igf-1) and type 1 IGF receptor (Igf1r)." Cell **75**(1): 59-72.

Logan, C. Y. and R. Nusse (2004). "The Wnt signaling pathway in development and disease." Annual Review of Cell and Developmental Biology **20**: 781-810.

Long, L., R. Rubin and P. Brodt (1998). "Enhanced invasion and liver colonization by lung carcinoma cells overexpressing the type 1 insulin-like growth factor receptor." Exp Cell Res **238**(1): 116-121.

Lopez, T. and D. Hanahan (2002). "Elevated levels of IGF-1 receptor convey invasive and metastatic capability in a mouse model of pancreatic islet tumorigenesis." Cancer Cell **1**(4): 339-353.

Lord, C. J. and A. Ashworth (2012). "The DNA damage response and cancer therapy." Nature **481**(7381): 287-294.

Lord, C. J., S. McDonald, S. Swift, N. C. Turner and A. Ashworth (2008). "A high-throughput RNA interference screen for DNA repair determinants of PARP inhibitor sensitivity." DNA Repair **7**(12): 2010-2019.

Lowenstein, E. J., R. J. Daly, A. G. Batzer, W. Li, B. Margolis, R. Lammers, A. Ullrich, E. Y. Skolnik, D. Bar-Sagi and J. Schlessinger (1992). "The SH2 and SH3 domain-containing protein GRB2 links receptor tyrosine kinases to ras signaling." Cell **70**(3): 431-442.

Lucchesi, J. C. (1968). "Synthetic Lethality and Semi-Lethality among Functionally Related Mutants of Drosophila Melanogaster." Genetics **59**(1): 37-&.

Luo, J., M. J. Emanuele, D. Li, C. J. Creighton, M. R. Schlabach, T. F. Westbrook, K. K. Wong and S. J. Elledge (2009a). "A genome-wide RNAi screen identifies multiple synthetic lethal interactions with the Ras oncogene." Cell **137**(5): 835-848.

Luo, J., N. L. Solimini and S. J. Elledge (2009b). "Principles of Cancer Therapy: Oncogene and Non-oncogene Addiction." Cell **136**(5): 823-837.

Macaulay, V. M., A. J. Salisbury, E. A. Bohula, M. P. Playford, N. I. Smorodinsky and Y. Shiloh (2001). "Downregulation of the type 1 insulin-like growth factor receptor in mouse melanoma cells is associated with enhanced radiosensitivity and impaired activation of Atm kinase." Oncogene **20**(30): 4029-4040.

Malaguarnera, R., A. Sacco, C. Voci, G. Pandini, R. Vigneri and A. Belfiore (2012). "Proinsulin binds with high affinity the insulin receptor isoform a and predominantly activates the mitogenic pathway." Endocrinology **153**(5): 2152-2163.

Manning, B. D. and L. C. Cantley (2007). "AKT/PKB signaling: Navigating downstream." Cell **129**(7): 1261-1274.

Marsden, V. S., L. O'Connor, L. A. O'Reilly, J. Silke, D. Metcalf, P. G. Ekert, D. C. Huang, F. Cecconi, K. Kuida, K. J. Tomaselli, S. Roy, D. W. Nicholson, D. L. Vaux, P. Bouillet, J. M. Adams and A. Strasser (2002). "Apoptosis initiated by Bcl-2-regulated caspase activation independently of the cytochrome c/Apaf-1/caspase-9 apoptosome." Nature **419**(6907): 634-637.

Martin, S. A., M. Hewish, D. Sims, C. J. Lord and A. Ashworth (2011). "Parallel High Throughput RNA interference Screens Identify PINK1 as a Potential Therapeutic Target for the Treatment of DNA Mismatch Repair Deficient Cancers." Cancer Res. **71**(5): 1836-1848.

Martinez, J., A. Patkaniowska, H. Urlaub, R. Luhrmann and T. Tuschl (2002). "Single-stranded antisense siRNAs guide target RNA cleavage in RNAi." Cell **110**(5): 563-574.

Mathews, L. S., G. Norstedt and R. D. Palmiter (1986). "Regulation of insulin-like growth factor I gene expression by growth hormone." Proc Natl Acad Sci U S A **83**(24): 9343-9347.

McCabe, N., C. J. Lord, A. N. Tutt, N. M. Martin, G. C. Smith and A. Ashworth (2005). "BRCA2-deficient CAPAN-1 cells are extremely sensitive to the inhibition of Poly (ADP-Ribose) polymerase: an issue of potency." Cancer Biol Ther **4**(9): 934-936.

McDonnell, D. P. and J. D. Norris (2002). "Connections and regulation of the human estrogen receptor." Science **296**(5573): 1642-1644.

Mendes-Pereira, A. M., S. A. Martin, R. Brough, A. McCarthy, J. R. Taylor, J. S. Kim, T. Waldman, C. J. Lord and A. Ashworth (2009). "Synthetic lethal targeting of PTEN mutant cells with PARP inhibitors." EMBO Molecular Medicine **1**(6-7):

315-322.

Mendes-Pereira, A. M., D. Sims, T. Dexter, K. Fenwick, I. Assiotis, I. Kozarewa, C. Mitsopoulos, J. Hakas, M. Zvelebil, C. J. Lord and A. Ashworth (2012). "Genome-wide functional screen identifies a compendium of genes affecting sensitivity to tamoxifen." Proceedings of the National Academy of Sciences of the United States of America **109**(8): 2730-2735.

Meyer, G., B. Kim, C. van Golen and E. L. Feldman (2005). "Cofilin activity during insulin-like growth factor I-stimulated neuroblastoma cell motility." Cell Mol Life Sci **62**(4): 461-470.

Michael, D. and M. Oren (2003). "The p53-Mdm2 module and the ubiquitin system." Seminars in Cancer Biology **13**(1): 49-58.

Minuto, F., P. Delmonte, A. Barreca, P. Fortini, G. Cariola, G. Catrambone and G. Giordano (1986). "Evidence for an Increased Somatomedin-C/Insulin-Like Growth Factor-I Content in Primary Human-Lung Tumors." Cancer Research **46**(2): 985-988.

Mok, T. S., Y. L. Wu, S. Thongprasert, C. H. Yang, D. T. Chu, N. Saijo, P. Sunpaweravong, B. Han, B. Margono, Y. Ichinose, Y. Nishiwaki, Y. Ohe, J. J. Yang, B. Chewaskulyong, H. Jiang, E. L. Duffield, C. L. Watkins, A. A. Armour and M. Fukuoka (2009). "Gefitinib or carboplatin-paclitaxel in pulmonary adenocarcinoma." The New England Journal of Medicine **361**(10): 947-957.

Morrione, A., T. DeAngelis and R. Baserga (1995). "Failure of the bovine papillomavirus to transform mouse embryo fibroblasts with a targeted disruption of the insulin-like growth factor I receptor genes." J Virol **69**(9): 5300-5303.

Moschos, S. J. and C. S. Mantzoros (2002). "The role of the IGF system in cancer: from basic to clinical studies and clinical applications." Oncology **63**(4): 317-332.

Moser, C., P. Schachtschneider, S. A. Lang, A. Gaumann, A. Mori, J. Zimmermann, H. J. Schlitt, E. K. Geissler and O. Stoeltzing (2008). "Inhibition of insulin-like growth factor-I receptor (IGF-IR) using NVP-AEW541, a small molecule kinase inhibitor, reduces orthotopic pancreatic cancer growth and

angiogenesis." European Journal of Cancer **44**(11): 1577-1586.

Muise-Helmericks, R. C., H. L. Grimes, A. Bellacosa, S. E. Malstrom, P. N. Tsichlis and N. Rosen (1998). "Cyclin D expression is controlled post-transcriptionally via a phosphatidylinositol 3-kinase/Akt-dependent pathway." The Journal of Biological Chemistry **273**(45): 29864-29872.

Munshi, A., M. Hobbs and R. E. Meyn (2005). "Clonogenic cell survival assay." Methods Mol Med **110**: 21-28.

Nahta, R., L. X. Yuan, B. Zhang, R. Kobayashi and F. J. Esteva (2005). "Insulin-like growth factor-I receptor/human epidermal growth factor receptor 2 heterodimerization contributes to trastuzumab resistance of breast cancer cells." Cancer Research **65**(23): 11118-11128.

Naik, S., R. S. Dothager, J. Marasa, C. L. Lewis and D. Piwnica-Worms (2009). "Vascular Endothelial Growth Factor Receptor-1 Is Synthetic Lethal to Aberrant beta-Catenin Activation in Colon Cancer." Clinical Cancer Research **15**(24): 7529-7537.

Napoli, C., C. Lemieux and R. Jorgensen (1990). "Introduction of a Chimeric Chalcone Synthase Gene into Petunia Results in Reversible Co-Suppression of Homologous Genes in Trans." Plant Cell **2**(4): 279-289.

Nguyen, D. X., P. D. Bos and J. Massague (2009). "Metastasis: from dissemination to organ-specific colonization." Nat Rev Cancer **9**(4): 274-284.

Nishida, Y., H. Miyamori, E. W. Thompson, T. Takino, Y. Endo and H. Sato (2008). "Activation of Matrix Metalloproteinase-2 (MMP-2) by Membrane Type 1 Matrix Metalloproteinase through an Artificial Receptor for ProMMP-2 Generates Active MMP-2." Cancer Research **68**(21): 9096-9104.

Normanno, N., A. De Luca, C. Bianco, L. Strizzi, M. Mancino, M. R. Maiello, A. Carotenuto, G. De Feo, F. Caponigro and D. S. Salomon (2006). "Epidermal growth factor receptor (EGFR) signaling in cancer." Gene **366**(1): 2-16.

O'Connor, R., A. Kauffmann-Zeh, Y. Liu, S. Lehar, G. I. Evan, R. Baserga and W. A. Blattler (1997). "Identification of domains of the insulin-like growth factor I

receptor that are required for protection from apoptosis." Molecular and Cellular Biology **17**(1): 427-435.

OConnor, R., A. KauffmannZeh, Y. M. Liu, S. Lehar, G. I. Evan, R. Baserga and W. A. Blattler (1997). "Identification of domains of the insulin-like growth factor I receptor that are required for protection from apoptosis." Molecular and Cellular Biology **17**(1): 427-435.

Ohlsson, C., N. Kley, H. Werner and D. LeRoith (1998). "p53 regulates insulin-like growth factor-I (IGF-I) receptor expression and IGF-I-induced tyrosine phosphorylation in an osteosarcoma cell line: Interaction between p53 and Sp1." Endocrinology **139**(3): 1101-1107.

Oliver, G. and M. Detmar (2002). "The rediscovery of the lymphatic system: old and new insights into the development and biological function of the lymphatic vasculature." Genes & Development **16**(7): 773-783.

Olmos, D., S. Postel-Vinay, L. R. Molife, S. H. Okuno, S. M. Schuetze, M. L. Paccagnella, G. N. Batzel, D. Yin, K. Pritchard-Jones, I. Judson, F. P. Worden, A. Gualberto, M. Scurr, J. S. de Bono and P. Haluska (2010). "Safety, pharmacokinetics, and preliminary activity of the anti-IGF-1R antibody figitumumab (CP-751,871) in patients with sarcoma and Ewing's sarcoma: a phase 1 expansion cohort study." The Lancet Oncology **11**(2): 129-135.

Paez, J. G., P. A. Janne, J. C. Lee, S. Tracy, H. Greulich, S. Gabriel, P. Herman, F. J. Kaye, N. Lindeman, T. J. Boggon, K. Naoki, H. Sasaki, Y. Fujii, M. J. Eck, W. R. Sellers, B. E. Johnson and M. Meyerson (2004). "EGFR mutations in lung cancer: correlation with clinical response to gefitinib therapy." Science **304**(5676): 1497-1500.

Pantel, K. and R. H. Brakenhoff (2004). "Dissecting the metastatic cascade." Nat Rev Cancer **4**(6): 448-456.

Pavelic, K., D. Bukovic and J. Pavelic (2002). "The role of insulin-like growth factor 2 and its receptors in human tumors." Mol Med **8**(12): 771-780.

Perrimon, N. and A. P. Mahowald (1987). "Multiple functions of segment polarity genes in Drosophila." Developmental Biology **119**(2): 587-600.

Peruzzi, F., M. Prisco, M. Dews, P. Salomoni, E. Grassilli, G. Romano, B. Calabretta and R. Baserga (1999). "Multiple signaling pathways of the insulin-like growth factor 1 receptor in protection from apoptosis." Mol Cell Biol **19**(10): 7203-7215.

Playford, M. P., D. Bicknell, W. F. Bodmer and V. M. Macaulay (2000). "Insulin-like growth factor 1 regulates the location, stability, and transcriptional activity of beta-catenin." Proceedings of the National Academy of Sciences of the United States of America **97**(22): 12103-12108.

Pollak, M. (2008). "Insulin and insulin-like growth factor signalling in neoplasia." Nat Rev Cancer **8**(12): 915-928.

Pollak, M. (2012). "The insulin and insulin-like growth factor receptor family in neoplasia: an update." Nature Reviews. Cancer **12**(3): 159-169.

Potratz, J. C., D. N. Saunders, D. H. Wai, T. L. Ng, S. E. McKinney, J. M. Carboni, M. M. Gottardis, T. J. Triche, H. Jurgens, M. N. Pollak, S. A. Aparicio and P. H. B. Sorensen (2010). "Synthetic Lethality Screens Reveal RPS6 and MST1R as Modifiers of Insulin-like Growth Factor-1 Receptor Inhibitor Activity in Childhood Sarcomas." Cancer Research **70**(21): 8770-8781.

Powell-Braxton, L., P. Hollingshead, C. Warburton, M. Dowd, S. Pitts-Meek, D. Dalton, N. Gillett and T. A. Stewart (1993). "IGF-I is required for normal embryonic growth in mice." Genes & Development **7**(12B): 2609-2617.

Prieur, A., F. Tirode, P. Cohen and O. Delattre (2004). "EWS/FLI-1 silencing and gene profiling of Ewing cells reveal downstream oncogenic pathways and a crucial role for repression of insulin-like growth factor binding protein 3." Molecular and Cellular Biology **24**(16): 7275-7283.

Pugazhenthi, S., E. Millers, C. Sable, P. Young, K. A. Heidenreich, L. M. Boxer and J. E. B. Reusch (1999). "Insulin-like growth factor-I induces bcl-2 promoter through the transcription factor cAMP-response element-binding protein." Journal of Biological Chemistry **274**(39): 27529-27535.

Pugazhenthi, S., A. Nesterova, C. Sable, K. A. Heidenreich, L. M. Boxer, L. E. Heasley and J. E. B. Reusch (2000). "Akt/protein kinase B up-regulates Bcl-2

expression through cAMP-response element-binding protein." Journal of Biological Chemistry **275**(15): 10761-10766.

Quintela-Fandino, M., E. Arpaia, D. Brenner, T. Goh, F. A. Yeung, H. Blaser, R. Alexandrova, E. F. Lind, M. W. Tusche, A. Wakeham, P. S. Ohashi and T. W. Mak (2010). "HUNK suppresses metastasis of basal type breast cancers by disrupting the interaction between PP2A and cofilin-1." Proceedings of the National Academy of Sciences of the United States of America **107**(6): 2622-2627.

Rehman, F. L., C. J. Lord and A. Ashworth (2010). "Synthetic lethal approaches to breast cancer therapy." Nat Rev Clin Oncol **7**(12): 718-724.

Reiss, K., A. Ferber, S. Travali, P. Porcu, P. D. Phillips and R. Baserga (1991). "The protooncogene c-myb increases the expression of insulin-like growth factor 1 and insulin-like growth factor 1 receptor messenger RNAs by a transcriptional mechanism." Cancer Research **51**(21): 5997-6000.

Reiss, K., J. Y. Wang, G. Romano, F. B. Furnari, W. K. Cavenee, A. Morrione, X. Tu and R. Baserga (2000). "IGF-I receptor signaling in a prostatic cancer cell line with a PTEN mutation." Oncogene **19**(22): 2687-2694.

Resnicoff, M., D. Coppola, C. Sell, R. Rubin, S. Ferrone and R. Baserga (1994). "Growth inhibition of human melanoma cells in nude mice by antisense strategies to the type 1 insulin-like growth factor receptor." Cancer Research **54**(18): 4848-4850.

Reya, T. and H. Clevers (2005). "Wnt signalling in stem cells and cancer." Nature **434**(7035): 843-850.

Reynolds, A., E. M. Anderson, A. Vermeulen, Y. Fedorov, K. Robinson, D. Leake, J. Karpilow, W. S. Marshall and A. Khvorova (2006). "Induction of the interferon response by siRNA is cell type- and duplex length-dependent." RNA-a Publication of the RNA Society **12**(6): 988-993.

Riedemann, J., M. Takiguchi, M. Sohail and V. M. Macaulay (2007). "The EGF receptor interacts with the type 1 IGF receptor and regulates its stability." Biochem Biophys Res Commun **355**(3): 707-714.

Riesterer, O., Q. Yang, U. Raju, M. Torres, D. Molkentine, N. Patel, D. Valdecanas, L. Milas and K. K. Ang (2011). "Combination of anti-IGF-1R antibody A12 and ionizing radiation in upper respiratory tract cancers." International Journal of Radiation Oncology, Biology, Physics **79**(4): 1179-1187.

Rinaldi, S., R. Cleveland, T. Norat, C. Biessy, S. Rohrmann, J. Linseisen, H. Boeing, T. Pischon, S. Panico, C. Agnoli, D. Palli, R. Tumino, P. Vineis, P. H. Peeters, C. H. van Gils, B. H. Bueno-de-Mesquita, A. Vrieling, N. E. Allen, A. Roddam, S. Bingham, K. T. Khaw, J. Manjer, S. Borgquist, V. Dumeaux, I. Torhild Gram, E. Lund, A. Trichopoulou, G. Makrygiannis, V. Benetou, E. Molina, I. Donate Suarez, A. Barricarte Gurrea, C. A. Gonzalez, M. J. Tormo, J. M. Altzibar, A. Olsen, A. Tjonneland, H. Gronbaek, K. Overvad, F. Clavel-Chapelon, M. C. Boutron-Ruault, S. Morois, N. Slimani, P. Boffetta, M. Jenab, E. Riboli and R. Kaaks (2010). "Serum levels of IGF-I, IGFBP-3 and colorectal cancer risk: results from the EPIC cohort, plus a meta-analysis of prospective studies." Int J Cancer **126**(7): 1702-1715.

Rochester, M. A., N. Patel, B. W. Turney, D. R. Davies, I. S. Roberts, J. Crew, A. Protheroe and V. M. Macaulay (2007). "The type 1 insulin-like growth factor receptor is over-expressed in bladder cancer." BJU Int **100**(6): 1396-1401.

Rochester, M. A., J. Riedemann, G. O. Hellawell, S. F. Brewster and V. M. Macaulay (2005). "Silencing of the IGF1R gene enhances sensitivity to DNA-damaging agents in both PTEN wild-type and mutant human prostate cancer." Cancer Gene Therapy **12**(1): 90-100.

Roddam, A. W., N. E. Allen, P. Appleby, T. J. Key, L. Ferrucci, H. B. Carter, E. J. Metter, C. Chen, N. S. Weiss, A. Fitzpatrick, A. W. Hsing, J. V. Lacey, K. Helzlsouer, S. Rinaldi, E. Riboli, R. Kaaks, J. A. M. J. L. Janssen, M. F. Wildhagen, F. H. Schroder, E. A. Platz, M. Pollak, E. Giovannucci, C. Schaefer, C. P. Quesenberry, J. H. Vogelman, G. Severi, D. R. English, G. G. Giles, P. Stattin, G. Hallmans, M. Johansson, J. M. Chan, P. Gann, S. E. Oliver, J. M. Holly, J. Donovan, F. Meyer, I. Bairati and P. Galan (2008). "Insulin-like growth factors, their binding proteins, and prostate cancer risk: Analysis of individual patient data from 12 prospective studies." Annals of Internal Medicine **149**(7): 461-W488.

Rosenthal, S. M. and Z. Q. Cheng (1995). "Opposing early and late effects of

insulin-like growth factor I on differentiation and the cell cycle regulatory retinoblastoma protein in skeletal myoblasts." Proceedings of the National Academy of Sciences of the United States of America **92**(22): 10307-10311.

Sachdev, D. and D. Yee (2001). "The IGF system and breast cancer." Endocr Relat Cancer **8**(3): 197-209.

Saikali, Z., H. Setya, G. Singh and S. Persad (2008). "Role of IGF-1/IGF-1R in regulation of invasion in DU145 prostate cancer cells." Cancer Cell Int **8**: 10.

Saltiel, A. R. and C. R. Kahn (2001). "Insulin signalling and the regulation of glucose and lipid metabolism." Nature **414**(6865): 799-806.

Samani, A. A., S. Yakar, D. LeRoith and P. Brodt (2007). "The role of the IGF system in cancer growth and metastasis: overview and recent insights." Endocr Rev **28**(1): 20-47.

Sawyers, C. L., B. S. Carver, C. Chapinski, J. Wongvipat, H. Hieronymus, Y. Chen, S. Chandarlapaty, V. K. Arora, C. Le, J. Koutcher, H. Scher, P. T. Scardino and N. Rosen (2011). "Reciprocal Feedback Regulation of PI3K and Androgen Receptor Signaling in PTEN-Deficient Prostate Cancer." Cancer Cell **19**(5): 575-586.

Schwahn, D. J. and D. Medina (1998). "p96, a MAPK-related protein, is consistently downregulated during mouse mammary carcinogenesis." Oncogene **17**(9): 1173-1178.

Segawa, N., M. Nakamura, Y. Nakamura, I. Mori, Y. Katsuoka and K. Kakudo (2001). "Phosphorylation of mitogen-activated protein kinase is inhibited by calcitonin in DU145 prostate cancer cells." Cancer Research **61**(16): 6060-6063.

Sehat, B., S. Andersson, R. Vasilcanu, L. Girnita and O. Larsson (2007). "Role of ubiquitination in IGF-1 receptor signaling and degradation." PloS One **2**(4): e340.

Sehat, B., A. Tofigh, Y. B. Lin, E. Trocme, U. Liljedahl, J. Lagergren and O. Larsson (2010). "SUMOylation Mediates the Nuclear Translocation and

Signaling of the IGF-1 Receptor." Science Signaling **3**(108).

Sell, C., G. Dumenil, C. Deveaud, M. Miura, D. Coppola, T. DeAngelis, R. Rubin, A. Efstratiadis and R. Baserga (1994). "Effect of a null mutation of the insulin-like growth factor I receptor gene on growth and transformation of mouse embryo fibroblasts." Mol Cell Biol **14**(6): 3604-3612.

Sell, C., M. Rubini, R. Rubin, J. P. Liu, A. Efstratiadis and R. Baserga (1993). "Simian Virus-40 Large Tumor-Antigen Is Unable to Transform Mouse Embryonic Fibroblasts Lacking Type-1 Insulin-Like Growth-Factor Receptor." Proceedings of the National Academy of Sciences of the United States of America **90**(23): 11217-11221.

Semenov, M. V., R. Habas, B. T. Macdonald and X. He (2007). "SnapShot: Noncanonical Wnt Signaling Pathways." Cell **131**(7): 1378.

Sharma, S. and A. Rao (2009). "RNAi screening: tips and techniques." Nat Immunol **10**(8): 799-804.

Shigematsu, S., K. Yamauchi, K. Nakajima, S. Iijima, T. Aizawa and K. Hashizume (1999). "IGF-1 regulates migration and angiogenesis of human endothelial cells." Endocr J **46 Suppl**: S59-62.

Shimasaki, S. and N. Ling (1991). "Identification and molecular characterization of insulin-like growth factor binding proteins (IGFBP-1, -2, -3, -4, -5 and -6)." Prog Growth Factor Res **3**(4): 243-266.

Shin, S. I., V. H. Freedman, R. Risser and R. Pollack (1975). "Tumorigenicity of virus-transformed cells in nude mice is correlated specifically with anchorage independent growth in vitro." Proceedings of the National Academy of Sciences of the United States of America **72**(11): 4435-4439.

Sims, D., A. M. Mendes-Pereira, J. Frankum, D. Burgess, M. A. Cerone, C. Lombardelli, C. Mitsopoulos, J. Hakas, N. Murugaesu, C. M. Isacke, K. Fenwick, I. Assiotis, I. Kozarewa, M. Zvelebil, A. Ashworth and C. J. Lord (2011). "High-throughput RNA interference screening using pooled shRNA libraries and next generation sequencing." Genome Biology **12**(10): R104.

Skolnik, E. Y., A. Batzer, N. Li, C. H. Lee, E. Lowenstein, M. Mohammadi, B. Margolis and J. Schlessinger (1993). "The function of GRB2 in linking the insulin receptor to Ras signaling pathways." Science **260**(5116): 1953-1955.

Sledz, C. A. and B. R. G. Williams (2004). "RNA interference and double-stranded-RNA-activated pathways." Biochemical Society Transactions **32**: 952-956.

Stambolic, V., A. Suzuki, J. L. de la Pompa, G. M. Brothers, C. Mirtsos, T. Sasaki, J. Ruland, J. M. Penninger, D. P. Siderovski and T. W. Mak (1998). "Negative regulation of PKB/Akt-dependent cell survival by the tumor suppressor PTEN." Cell **95**(1): 29-39.

Stratikopoulos, E., M. Szabolcs, I. Dragatsis, A. Klinakis and A. Efstratiadis (2008). "The hormonal action of IGF1 in postnatal mouse growth." Proceedings of the National Academy of Sciences of the United States of America **105**(49): 19378-19383.

Stromberg, T., S. Ekman, L. Girnita, L. Y. Dimberg, O. Larsson, M. Axelson, J. Lennartsson, U. Hellman, K. Carlson, A. Osterborg, K. Vanderkerken, K. Nilsson and H. Jernberg-Wiklund (2006). "IGF-1 receptor tyrosine kinase inhibition by the cyclolignan PPP induces G2/M-phase accumulation and apoptosis in multiple myeloma cells." Blood **107**(2): 669-678.

Tang, Y., D. Zhang, L. Fallavollita and P. Brodt (2003). "Vascular endothelial growth factor C expression and lymph node metastasis are regulated by the type I insulin-like growth factor receptor." Cancer Res **63**(6): 1166-1171.

Terai, K. and M. Matsuda (2005). "Ras binding opens c-Raf to expose the docking site for mitogen-activated protein kinase kinase." EMBO Reports **6**(3): 251-255.

Tolcher, A. W., J. Sarantopoulos, A. Patnaik, K. Papadopoulos, C. C. Lin, J. Rodon, B. Murphy, B. Roth, I. McCaffery, K. S. Gorski, B. Kaiser, M. Zhu, H. J. Deng, G. Friberg and I. Puzanov (2009). "Phase I, Pharmacokinetic, and Pharmacodynamic Study of AMG 479, a Fully Human Monoclonal Antibody to Insulin-Like Growth Factor Receptor 1." Journal of Clinical Oncology **27**(34): 5800-5807.

Toretsky, J. A., T. Kalebic, V. Blakesley, D. LeRoith and L. J. Helman (1997). "The insulin-like growth factor-I receptor is required for EWS/FLI-1 transformation of fibroblasts." Journal of Biological Chemistry **272**(49): 30822-30827.

Tricoli, J. V., L. B. Rall, C. P. Karakousis, L. Herrera, N. J. Petrelli, G. I. Bell and T. B. Shows (1986). "Enhanced Levels of Insulin-Like Growth-Factor Messenger-Rna in Human-Colon Carcinomas and Liposarcomas." Cancer Research **46**(12): 6169-6173.

Trojanek, J., T. Ho, L. Del Valle, M. Nowicki, J. Y. Wang, A. Lassak, F. Peruzzi, K. Khalili, T. Skorski and K. Reiss (2003). "Role of the insulin-like growth factor I/insulin receptor substrate 1 axis in Rad51 trafficking and DNA repair by homologous recombination." Molecular and Cellular Biology **23**(21): 7510-7524.

Tsai, M. S., Y. H. Kuo, Y. F. Chiu, Y. C. Su and Y. W. Lin (2010). "Down-regulation of Rad51 expression overcomes drug resistance to gemcitabine in human non-small-cell lung cancer cells." The Journal of Pharmacology and Experimental Therapeutics **335**(3): 830-840.

Tseng, C. P., B. D. Ely, Y. M. Li, R. C. Pong and J. T. Hsieh (1998). "Regulation of rat DOC-2 gene during castration-induced rat ventral prostate degeneration and its growth inhibitory function in human prostatic carcinoma cells." Endocrinology **139**(8): 3542-3553.

Turner, B. C., B. G. Haffty, L. Narayanan, J. Yuan, P. A. Havre, A. A. Gumbs, L. Kaplan, J. L. Burgaud, D. Carter, R. Baserga and P. M. Glazer (1997). "Insulin-like growth factor-I receptor overexpression mediates cellular radioresistance and local breast cancer recurrence after lumpectomy and radiation." Cancer Research **57**(15): 3079-3083.

Turner, N. C., C. J. Lord, E. Iorns, R. Brough, S. Swift, R. Elliott, S. Rayter, A. N. Tutt and A. Ashworth (2008). "A synthetic lethal siRNA screen identifying genes mediating sensitivity to a PARP inhibitor." EMBO J **27**(9): 1368-1377.

Turney, B. W., M. Kerr, M. M. Chitnis, K. Lodhia, Y. Wang, J. Riedemann, M. Rochester, A. S. Protheroe, S. F. Brewster and V. M. Macaulay (2012).

"Depletion of the type 1 IGF receptor delays repair of radiation-induced DNA double strand breaks." Radiotherapy and Oncology (In press).

Tutt, A., M. Robson, J. E. Garber, S. M. Domchek, M. W. Audeh, J. N. Weitzel, M. Friedlander, B. Arun, N. Loman, R. K. Schmutzler, A. Wardley, G. Mitchell, H. Earl, M. Wickens and J. Carmichael (2010). "Oral poly(ADP-ribose) polymerase inhibitor olaparib in patients with BRCA1 or BRCA2 mutations and advanced breast cancer: a proof-of-concept trial." Lancet **376**(9737): 235-244.

Tyner, J. W., M. W. Deininger, M. M. Loriaux, B. H. Chang, J. R. Gotlib, S. G. Willis, H. Erickson, T. Kovacsovics, T. O'Hare, M. C. Heinrich and B. J. Druker (2009). "RNAi screen for rapid therapeutic target identification in leukemia patients." Proceedings of the National Academy of Sciences of the United States of America **106**(21): 8695-8700.

Uematsu, K., B. He, L. You, Z. Xu, F. McCormick and D. M. Jablons (2003). "Activation of the Wnt pathway in non small cell lung cancer: evidence of dishevelled overexpression." Oncogene **22**(46): 7218-7221.

Ullrich, A., A. Gray, A. W. Tam, T. Yangfeng, M. Tsubokawa, C. Collins, W. Henzel, T. Lebon, S. Kathuria, E. Chen, S. Jacobs, U. Francke, J. Ramachandran and Y. Fujitayamaguchi (1986). "Insulin-Like Growth Factor-I Receptor Primary Structure - Comparison with Insulin-Receptor Suggests Structural Determinants That Define Functional Specificity." Embo Journal **5**(10): 2503-2512.

Underwood, L. E., J. P. Thissen, S. Lemozy, J. M. Ketelslegers and D. R. Clemmons (1994). "Hormonal and nutritional regulation of IGF-I and its binding proteins." Horm Res **42**(4-5): 145-151.

Valentinis, B., A. Morrione, S. J. Taylor and R. Baserga (1997). "Insulin-like growth factor I receptor signaling in transformation by src oncogenes." Mol Cell Biol **17**(7): 3744-3754.

van der Veeken, J., S. Oliveira, R. M. Schiffelers, G. Storm, P. M. P. V. E. Henegouwen and R. C. Roovers (2009). "Crosstalk Between Epidermal Growth Factor Receptor- and Insulin-Like Growth Factor-1 Receptor Signaling: Implications for Cancer Therapy." Current Cancer Drug Targets **9**(6): 748-760.

Vert, G. and J. Chory (2011). "Crosstalk in cellular signaling: background noise or the real thing?" Developmental Cell **21**(6): 985-991.

Vojtek, A. B., S. M. Hollenberg and J. A. Cooper (1993). "Mammalian Ras interacts directly with the serine/threonine kinase Raf." Cell **74**(1): 205-214.

Walenkamp, M. J., H. J. van der Kamp, A. M. Pereira, S. G. Kant, H. A. van Duyvenvoorde, M. F. Kruithof, M. H. Breuning, J. A. Romijn, M. Karperien and J. M. Wit (2006). "A variable degree of intrauterine and postnatal growth retardation in a family with a missense mutation in the insulin-like growth factor I receptor." J Clin Endocrinol Metab **91**(8): 3062-3070.

Wallace, T. A., R. L. Prueitt, M. Yi, T. M. Howe, J. W. Gillespie, H. G. Yfantis, R. M. Stephens, N. E. Caporaso, C. A. Loffredo and S. Ambs (2008). "Tumor immunobiological differences in prostate cancer between African-American and European-American men." Cancer Research **68**(3): 927-936.

Wang, Q., X. Wang, A. Hernandez, M. R. Hellmich, Z. Gatalica and B. M. Evers (2002). "Regulation of TRAIL expression by the phosphatidylinositol 3-kinase/Akt/GSK-3 pathway in human colon cancer cells." J Biol Chem **277**(39): 36602-36610.

Warsito, D., S. Sjostrom, S. Andersson, O. Larsson and B. Sehat (2012). "Nuclear IGF1R is a transcriptional co-activator of LEF1/TCF." EMBO Reports **13**(3): 244-250.

Wertheim, G. B. W., T. W. Yang, T. C. Pan, A. Ramne, Z. D. Liu, H. P. Gardner, K. D. Dugan, P. Kristel, B. Kreike, M. J. van de Vijver, R. D. Cardiff, C. Reynolds and L. A. Chodosh (2009). "The Snf1-related kinase, Hunk, is essential for mammary tumor metastasis." Proceedings of the National Academy of Sciences of the United States of America **106**(37): 15855-15860.

Wharton, K. A. (2003). "Runnin' with the Dvl: Proteins that associate with Dsh/Dvl and their significance to Wnt signal transduction." Developmental Biology **253**(1): 1-17.

Woods, K. A., C. CamachoHubner, M. O. Savage and A. J. L. Clark (1996). "Intrauterine growth retardation and postnatal growth failure associated with

deletion of the insulin-like growth factor I gene." New England Journal of Medicine **335**(18): 1363-1367.

Wu, Z., D. Gioeli, M. Conaway, M. J. Weber and D. Theodorescu (2008). "Restoration of PTEN expression alters the sensitivity of prostate cancer cells to EGFR inhibitors." The Prostate **68**(9): 935-944.

Wylie, A. A., D. J. Pulford, A. J. McVie-Wylie, R. A. Waterland, H. K. Evans, Y. T. Chen, C. M. Nolan, T. C. Orton and R. L. Jirtle (2003). "Tissue-specific inactivation of murine M6P/IGF2R." Am J Pathol **162**(1): 321-328.

Xie, Y., B. Skytting, G. Nilsson, B. Brodin and O. Larsson (1999). "Expression of insulin-like growth factor-1 receptor in synovial sarcoma: association with an aggressive phenotype." Cancer Res **59**(15): 3588-3591.

Xu, X. X., T. L. Yi, B. Tang and J. D. Lambeth (1998). "Disabled-2 (Dab2) is an SH3 domain-binding partner of Grb2." Oncogene **16**(12): 1561-1569.

Yang, D., H. Liu, A. Goga, S. Kim, M. Yuneva and J. M. Bishop (2010). "Therapeutic potential of a synthetic lethal interaction between the MYC proto-oncogene and inhibition of aurora-B kinase." Proceedings of the National Academy of Sciences of the United States of America **107**(31): 13836-13841.

Yang, J., X. Liu, K. Bhalla, C. N. Kim, A. M. Ibrado, J. Cai, T. I. Peng, D. P. Jones and X. Wang (1997). "Prevention of apoptosis by Bcl-2: release of cytochrome c from mitochondria blocked." Science **275**(5303): 1129-1132.

Yarden, Y. (2001). "The EGFR family and its ligands in human cancer. signalling mechanisms and therapeutic opportunities." Eur J Cancer **37 Suppl 4**: S3-8.

Yardy, G. W. and S. F. Brewster (2005). "Wnt signalling and prostate cancer." Prostate Cancer and Prostatic Diseases **8**(2): 119-126.

Yoon, S. and R. Seger (2006). "The extracellular signal-regulated kinase: multiple substrates regulate diverse cellular functions." Growth Factors **24**(1): 21-44.

Yu, H., J. Mistry, M. J. Nicar, M. J. Khosravi, A. Diamandis, J. van Doorn and A. Juul (1999a). "Insulin-like growth factors (IGF-I, free IGF-I and IGF-II) and insulin-like growth factor binding proteins (IGFBP-2, IGFBP-3, IGFBP-6, and ALS) in blood circulation." J Clin Lab Anal **13**(4): 166-172.

Yu, H., M. R. Spitz, J. Mistry, J. Gu, W. K. Hong and X. Wu (1999b). "Plasma levels of insulin-like growth factor-I and lung cancer risk: a case-control analysis." J Natl Cancer Inst **91**(2): 151-156.

Yuen, J. S., M. E. Cockman, M. Sullivan, A. Protheroe, G. D. Turner, I. S. Roberts, C. W. Pugh, H. Werner and V. M. Macaulay (2007). "The VHL tumor suppressor inhibits expression of the IGF1R and its loss induces IGF1R upregulation in human clear cell renal carcinoma." Oncogene **26**(45): 6499-6508.

Yuen, J. S. and V. M. Macaulay (2008). "Targeting the type 1 insulin-like growth factor receptor as a treatment for cancer." Expert Opin Ther Targets **12**(5): 589-603.

Zha, J. and M. R. Lackner (2010). "Targeting the insulin-like growth factor receptor-1R pathway for cancer therapy." Clin Cancer Res **16**(9): 2512-2517.

Zhang, D. and P. Brodt (2003). "Type 1 insulin-like growth factor regulates MT1-MMP synthesis and tumor invasion via PI 3-kinase/Akt signaling." Oncogene **22**(7): 974-982.

Zhang, D., A. A. Samani and P. Brodt (2003). "The role of the IGF-I receptor in the regulation of matrix metalloproteinases, tumor invasion and metastasis." Horm Metab Res **35**(11-12): 802-808.

Zhang, J. H., T. D. Y. Chung and K. R. Oldenburg (1999). "A simple statistical parameter for use in evaluation and validation of high throughput screening assays." Journal of Biomolecular Screening **4**(2): 67-73.

Zhang, X. F., J. Settleman, J. M. Kyriakis, E. Takeuchi-Suzuki, S. J. Elledge, M. S. Marshall, J. T. Bruder, U. R. Rapp and J. Avruch (1993). "Normal and oncogenic p21ras proteins bind to the amino-terminal regulatory domain of c-Raf-1." Nature **364**(6435): 308-313.

Zheng, H., C. Worrall, H. Shen, T. Issad, S. Seregard, A. Girnita and L. Girnita (2012). "Selective recruitment of G protein-coupled receptor kinases (GRKs) controls signaling of the insulin-like growth factor 1 receptor." Proceedings of the National Academy of Sciences of the United States of America. **109**(18):7055-7060

Zhou, J. and J. T. Hsieh (2001). "The inhibitory role of DOC-2/DAB2 in growth factor receptor-mediated signal cascade. DOC-2/DAB2-mediated inhibition of ERK phosphorylation via binding to Grb2." The Journal of Biological Chemistry **276**(30): 27793-27798.

Zong, C. S., J. Chan, D. E. Levy, C. Horvath, H. B. Sadowski and L. H. Wang (2000). "Mechanism of STAT3 activation by insulin-like growth factor I receptor." The Journal of Biological Chemistry **275**(20): 15099-15105.

Appendix

Table S1 Kinase siRNA library. Gene symbol and siRNA catalog

Plate	Well	Pool Catalog	Duplex	Gene Symbol
Plate 1	A02	M-004105-00	D-004105-01	TTK
Plate 1	A02	M-004105-00	D-004105-02	TTK
Plate 1	A02	M-004105-00	D-004105-03	TTK
Plate 1	A02	M-004105-00	D-004105-04	TTK
Plate 1	A03	M-003176-03	D-003176-02	SYK
Plate 1	A03	M-003176-03	D-003176-05	SYK
Plate 1	A03	M-003176-03	D-003176-06	SYK
Plate 1	A03	M-003176-03	D-003176-08	SYK
Plate 1	A04	M-003120-03	D-003120-09	EPHA8
Plate 1	A04	M-003120-03	D-003120-22	EPHA8
Plate 1	A04	M-003120-03	D-003120-23	EPHA8
Plate 1	A04	M-003120-03	D-003120-24	EPHA8
Plate 1	A05	M-004637-01	D-004637-02	DMPK
Plate 1	A05	M-004637-01	D-004637-03	DMPK
Plate 1	A05	M-004637-01	D-004637-04	DMPK
Plate 1	A05	M-004637-01	D-004637-17	DMPK
Plate 1	A06	M-006751-00	D-006751-01	COASY
Plate 1	A06	M-006751-00	D-006751-02	COASY
Plate 1	A06	M-006751-00	D-006751-03	COASY
Plate 1	A06	M-006751-00	D-006751-04	COASY
Plate 1	A07	M-004863-01	D-004863-01	MYO3B
Plate 1	A07	M-004863-01	D-004863-02	MYO3B
Plate 1	A07	M-004863-01	D-004863-03	MYO3B
Plate 1	A07	M-004863-01	D-004863-04	MYO3B
Plate 1	A08	M-005363-01	D-005363-01	PRKWNK2
Plate 1	A08	M-005363-01	D-005363-02	PRKWNK2
Plate 1	A08	M-005363-01	D-005363-04	PRKWNK2
Plate 1	A08	M-005363-01	D-005363-05	PRKWNK2
Plate 1	A09	M-003164-02	D-003164-05	PTK2
Plate 1	A09	M-003164-02	D-003164-07	PTK2
Plate 1	A09	M-003164-02	D-003164-08	PTK2
Plate 1	A09	M-003164-02	D-003164-09	PTK2
Plate 1	A10	M-003129-02	D-003129-05	FER
Plate 1	A10	M-003129-02	D-003129-06	FER
Plate 1	A10	M-003129-02	D-003129-07	FER
Plate 1	A10	M-003129-02	D-003129-08	FER
Plate 1	A11	M-004943-04	D-004943-01	CAMK2B
Plate 1	A11	M-004943-04	D-004943-02	CAMK2B
Plate 1	A11	M-004943-04	D-004943-06	CAMK2B
Plate 1	A11	M-004943-04	D-004943-22	CAMK2B
Plate 1	B02	M-005302-03	D-005302-01	ACVRL1
Plate 1	B02	M-005302-03	D-005302-03	ACVRL1
Plate 1	B02	M-005302-03	D-005302-05	ACVRL1
Plate 1	B02	M-005302-03	D-005302-06	ACVRL1
Plate 1	B03	M-003153-04	D-003153-03	LYN
Plate 1	B03	M-003153-04	D-003153-13	LYN
Plate 1	B03	M-003153-04	D-003153-27	LYN
Plate 1	B03	M-003153-04	D-003153-28	LYN
Plate 1	B04	M-007736-01	D-007736-01	PAPSS1
Plate 1	B04	M-007736-01	D-007736-02	PAPSS1
Plate 1	B04	M-007736-01	D-007736-04	PAPSS1
Plate 1	B04	M-007736-01	D-007736-05	PAPSS1
Plate 1	B05	M-003593-04	D-003593-01	MAPK4
Plate 1	B05	M-003593-04	D-003593-02	MAPK4
Plate 1	B05	M-003593-04	D-003593-04	MAPK4
Plate 1	B05	M-003593-04	D-003593-06	MAPK4
Plate 1	B06	M-004020-03	D-004020-02	MASTL
Plate 1	B06	M-004020-03	D-004020-05	MASTL
Plate 1	B06	M-004020-03	D-004020-06	MASTL
Plate 1	B06	M-004020-03	D-004020-07	MASTL
Plate 1	B07	M-003633-01	D-003633-01	TRIB1
Plate 1	B07	M-003633-01	D-003633-03	TRIB1
Plate 1	B07	M-003633-01	D-003633-05	TRIB1
Plate 1	B07	M-003633-01	D-003633-06	TRIB1
Plate 1	B08	M-004936-01	D-004936-02	BRD3
Plate 1	B08	M-004936-01	D-004936-03	BRD3
Plate 1	B08	M-004936-01	D-004936-04	BRD3
Plate 1	B08	M-004936-01	D-004936-17	BRD3
Plate 1	B09	M-005326-00	D-005326-01	FLJ34389
Plate 1	B09	M-005326-00	D-005326-02	FLJ34389
Plate 1	B09	M-005326-00	D-005326-03	FLJ34389
Plate 1	B09	M-005326-00	D-005326-04	FLJ34389
Plate 1	B10	M-006820-01	D-006820-01	HK1
Plate 1	B10	M-006820-01	D-006820-03	HK1
Plate 1	C02	M-005306-02	D-005306-05	ALS2CR2
Plate 1	C02	M-005306-02	D-005306-06	ALS2CR2
Plate 1	C02	M-005306-02	D-005306-07	ALS2CR2
Plate 1	C02	M-005306-02	D-005306-20	ALS2CR2
Plate 1	C03	M-006815-01	D-006815-01	CARKL
Plate 1	C03	M-006815-01	D-006815-02	CARKL
Plate 1	C03	M-006815-01	D-006815-03	CARKL
Plate 1	C03	M-006815-01	D-006815-17	CARKL
Plate 1	C04	M-004733-02	D-004733-02	ADK
Plate 1	C04	M-004733-02	D-004733-03	ADK
Plate 1	C04	M-004733-02	D-004733-04	ADK
Plate 1	C04	M-004733-02	D-004733-05	ADK
Plate 1	C05	M-003101-02	D-003101-05	ABL2
Plate 1	C05	M-003101-02	D-003101-06	ABL2
Plate 1	C05	M-003101-02	D-003101-07	ABL2
Plate 1	C05	M-003101-02	D-003101-08	ABL2
Plate 1	C06	M-003290-01	D-003290-05	PLK1
Plate 1	C06	M-003290-01	D-003290-06	PLK1
Plate 1	C06	M-003290-01	D-003290-07	PLK1
Plate 1	C06	M-003290-01	D-003290-08	PLK1
Plate 1	C07	M-004861-03	D-004861-02	MINK
Plate 1	C07	M-004861-03	D-004861-09	MINK
Plate 1	C07	M-004861-03	D-004861-10	MINK
Plate 1	C07	M-004861-03	D-004861-11	MINK
Plate 1	C08	M-004798-00	D-004798-01	CDKL3
Plate 1	C08	M-004798-00	D-004798-02	CDKL3
Plate 1	C08	M-004798-00	D-004798-03	CDKL3
Plate 1	C08	M-004798-00	D-004798-04	CDKL3
Plate 1	C09	M-003580-04	D-003580-10	MAP3K14
Plate 1	C09	M-003580-04	D-003580-11	MAP3K14
Plate 1	C09	M-003580-04	D-003580-12	MAP3K14
Plate 1	C09	M-003580-04	D-003580-26	MAP3K14
Plate 1	C10	M-003790-06	D-003790-16	MAP3K7
Plate 1	C10	M-003790-06	D-003790-17	MAP3K7
Plate 1	C10	M-003790-06	D-003790-18	MAP3K7
Plate 1	C10	M-003790-06	D-003790-31	MAP3K7
Plate 1	C11	M-006706-01	D-006706-01	CKB
Plate 1	C11	M-006706-01	D-006706-02	CKB
Plate 1	C11	M-006706-01	D-006706-03	CKB
Plate 1	C11	M-006706-01	D-006706-05	CKB
Plate 1	D02	M-003224-03	D-003224-09	CDC2
Plate 1	D02	M-003224-03	D-003224-10	CDC2
Plate 1	D02	M-003224-03	D-003224-11	CDC2
Plate 1	D02	M-003224-03	D-003224-12	CDC2
Plate 1	D03	M-005359-00	D-005359-01	PIM2
Plate 1	D03	M-005359-00	D-005359-02	PIM2
Plate 1	D03	M-005359-00	D-005359-03	PIM2
Plate 1	D03	M-005359-00	D-005359-04	PIM2
Plate 1	D04	M-006323-02	D-006323-01	LRRK2
Plate 1	D04	M-006323-02	D-006323-02	LRRK2
Plate 1	D04	M-006323-02	D-006323-03	LRRK2
Plate 1	D04	M-006323-02	D-006323-04	LRRK2
Plate 1	D05	M-006735-01	D-006735-02	HK2
Plate 1	D05	M-006735-01	D-006735-03	HK2
Plate 1	D05	M-006735-01	D-006735-04	HK2
Plate 1	D05	M-006735-01	D-006735-05	HK2
Plate 1	D06	M-006724-00	D-006724-01	FN3K
Plate 1	D06	M-006724-00	D-006724-02	FN3K
Plate 1	D06	M-006724-00	D-006724-03	FN3K
Plate 1	D06	M-006724-00	D-006724-04	FN3K
Plate 1	D07	M-008492-00	D-008492-01	CRIM1
Plate 1	D07	M-008492-00	D-008492-02	CRIM1
Plate 1	D07	M-008492-00	D-008492-03	CRIM1
Plate 1	D07	M-008492-00	D-008492-04	CRIM1
Plate 1	D08	M-006776-04	D-006776-02	PIK4CA
Plate 1	D08	M-006776-04	D-006776-03	PIK4CA
Plate 1	D08	M-006776-04	D-006776-09	PIK4CA
Plate 1	D08	M-006776-04	D-006776-25	PIK4CA
Plate 1	D09	M-005034-01	D-005034-01	SSTK
Plate 1	D09	M-005034-01	D-005034-02	SSTK
Plate 1	D09	M-005034-01	D-005034-03	SSTK
Plate 1	D09	M-005034-01	D-005034-04	SSTK
Plate 1	D10	M-004171-03	D-004171-13	TAO1
Plate 1	D10	M-004171-03	D-004171-14	TAO1

Plate 1	E02	M-009859-01	D-009859-01	PRKAG3
Plate 1	E02	M-009859-01	D-009859-02	PRKAG3
Plate 1	E02	M-009859-01	D-009859-03	PRKAG3
Plate 1	E02	M-009859-01	D-009859-05	PRKAG3
Plate 1	E03	M-004626-01	D-004626-01	GRK5
Plate 1	E03	M-004626-01	D-004626-02	GRK5
Plate 1	E03	M-004626-01	D-004626-03	GRK5
Plate 1	E03	M-004626-01	D-004626-04	GRK5
Plate 1	E04	M-007730-02	D-007730-01	LIMK1
Plate 1	E04	M-007730-02	D-007730-04	LIMK1
Plate 1	E04	M-007730-02	D-007730-05	LIMK1
Plate 1	E04	M-007730-02	D-007730-18	LIMK1
Plate 1	E05	M-005077-00	D-005077-01	UMPK
Plate 1	E05	M-005077-00	D-005077-02	UMPK
Plate 1	E05	M-005077-00	D-005077-03	UMPK
Plate 1	E05	M-005077-00	D-005077-04	UMPK
Plate 1	E06	M-016140-01	D-016140-01	C7ORF2
Plate 1	E06	M-016140-01	D-016140-02	C7ORF2
Plate 1	E06	M-016140-01	D-016140-03	C7ORF2
Plate 1	E06	M-016140-01	D-016140-04	C7ORF2
Plate 1	E07	M-003570-02	D-003570-01	KSR
Plate 1	E07	M-003570-02	D-003570-03	KSR
Plate 1	E07	M-003570-02	D-003570-04	KSR
Plate 1	E07	M-003570-02	D-003570-05	KSR
Plate 1	E08	M-003971-02	D-003971-05	MAP4K4
Plate 1	E08	M-003971-02	D-003971-06	MAP4K4
Plate 1	E08	M-003971-02	D-003971-08	MAP4K4
Plate 1	E08	M-003971-02	D-003971-09	MAP4K4
Plate 1	E09	M-005029-01	D-005029-02	PRKCN
Plate 1	E09	M-005029-01	D-005029-04	PRKCN
Plate 1	E09	M-005029-01	D-005029-05	PRKCN
Plate 1	E09	M-005029-01	D-005029-06	PRKCN
Plate 1	E10	M-004680-02	D-004680-01	TTBK1
Plate 1	E10	M-004680-02	D-004680-03	TTBK1
Plate 1	E10	M-004680-02	D-004680-05	TTBK1
Plate 1	E10	M-004680-02	D-004680-18	TTBK1
Plate 1	E11	M-003536-02	D-003536-01	ROCK1
Plate 1	E11	M-003536-02	D-003536-02	ROCK1
Plate 1	E11	M-003536-02	D-003536-03	ROCK1
Plate 1	E11	M-003536-02	D-003536-05	ROCK1
Plate 1	F02	M-003178-03	D-003178-05	TEK
Plate 1	F02	M-003178-03	D-003178-07	TEK
Plate 1	F02	M-003178-03	D-003178-08	TEK
Plate 1	F02	M-003178-03	D-003178-09	TEK
Plate 1	F03	M-004057-02	D-004057-02	PANK1
Plate 1	F03	M-004057-02	D-004057-06	PANK1
Plate 1	F03	M-004057-02	D-004057-07	PANK1
Plate 1	F03	M-004057-02	D-004057-08	PANK1
Plate 1	F04	M-004679-03	D-004679-02	CSNK1G3
Plate 1	F04	M-004679-03	D-004679-05	CSNK1G3
Plate 1	F04	M-004679-03	D-004679-06	CSNK1G3
Plate 1	F04	M-004679-03	D-004679-07	CSNK1G3
Plate 1	F05	M-007678-00	D-007678-01	CKS2
Plate 1	F05	M-007678-00	D-007678-02	CKS2
Plate 1	F05	M-007678-00	D-007678-03	CKS2
Plate 1	F05	M-007678-00	D-007678-04	CKS2
Plate 1	F06	M-004881-02	D-004881-02	PHKG2
Plate 1	F06	M-004881-02	D-004881-03	PHKG2
Plate 1	F06	M-004881-02	D-004881-04	PHKG2
Plate 1	F06	M-004881-02	D-004881-25	PHKG2
Plate 1	F07	M-003513-02	D-003513-01	MAPK7
Plate 1	F07	M-003513-02	D-003513-03	MAPK7
Plate 1	F07	M-003513-02	D-003513-04	MAPK7
Plate 1	F07	M-003513-02	D-003513-06	MAPK7
Plate 1	F08	M-006238-01	D-006238-02	KCNH8
Plate 1	F08	M-006238-01	D-006238-03	KCNH8
Plate 1	F08	M-006238-01	D-006238-04	KCNH8
Plate 1	F08	M-006238-01	D-006238-05	KCNH8
Plate 1	F09	M-004042-02	D-004042-02	CAMK2D
Plate 1	F09	M-004042-02	D-004042-03	CAMK2D
Plate 1	F09	M-004042-02	D-004042-04	CAMK2D
Plate 1	F09	M-004042-02	D-004042-05	CAMK2D
Plate 1	F10	M-003589-02	D-003589-01	MAP4K5
Plate 1	F10	M-003589-02	D-003589-06	MAP4K5
Plate 1	F10	M-003589-02	D-003589-07	MAP4K5
Plate 1	F10	M-003589-02	D-003589-08	MAP4K5
Plate 1	F11	M-004647-01	D-004647-05	PKN3
Plate 1	F11	M-004647-01	D-004647-06	PKN3
Plate 1	F11	M-004647-01	D-004647-07	PKN3
Plate 1	F11	M-004647-01	D-004647-08	PKN3

Plate 1	G02	M-003201-04	D-003201-27	ATM
Plate 1	G02	M-003201-04	D-003201-28	ATM
Plate 1	G02	M-003201-04	D-003201-29	ATM
Plate 1	G02	M-003201-04	D-003201-30	ATM
Plate 1	G03	M-007669-00	D-007669-01	PHKA2
Plate 1	G03	M-007669-00	D-007669-02	PHKA2
Plate 1	G03	M-007669-00	D-007669-03	PHKA2
Plate 1	G03	M-007669-00	D-007669-04	PHKA2
Plate 1	G04	M-007256-02	D-007256-01	MULK
Plate 1	G04	M-007256-02	D-007256-02	MULK
Plate 1	G04	M-007256-02	D-007256-03	MULK
Plate 1	G04	M-007256-02	D-007256-04	MULK
Plate 1	G05	M-004627-02	D-004627-02	GRK6
Plate 1	G05	M-004627-02	D-004627-05	GRK6
Plate 1	G05	M-004627-02	D-004627-19	GRK6
Plate 1	G05	M-004627-02	D-004627-20	GRK6
Plate 1	G06	M-004934-01	D-004934-01	BMPR1B
Plate 1	G06	M-004934-01	D-004934-03	BMPR1B
Plate 1	G06	M-004934-01	D-004934-04	BMPR1B
Plate 1	G06	M-004934-01	D-004934-05	BMPR1B
Plate 1	G07	M-005383-02	D-005383-03	STK33
Plate 1	G07	M-005383-02	D-005383-04	STK33
Plate 1	G07	M-005383-02	D-005383-05	STK33
Plate 1	G07	M-005383-02	D-005383-06	STK33
Plate 1	G08	M-005350-02	D-005350-02	MIDORI
Plate 1	G08	M-005350-02	D-005350-03	MIDORI
Plate 1	G08	M-005350-02	D-005350-04	MIDORI
Plate 1	G08	M-005350-02	D-005350-05	MIDORI
Plate 1	G09	M-005032-01	D-005032-02	RNASEL
Plate 1	G09	M-005032-01	D-005032-03	RNASEL
Plate 1	G09	M-005032-01	D-005032-05	RNASEL
Plate 1	G09	M-005032-01	D-005032-06	RNASEL
Plate 1	G10	M-004054-01	D-004054-01	STK16
Plate 1	G10	M-004054-01	D-004054-02	STK16
Plate 1	G10	M-004054-01	D-004054-03	STK16
Plate 1	G10	M-004054-01	D-004054-04	STK16
Plate 1	G11	M-004662-01	D-004662-01	GRK1
Plate 1	G11	M-004662-01	D-004662-02	GRK1
Plate 1	G11	M-004662-01	D-004662-03	GRK1
Plate 1	G11	M-004662-01	D-004662-04	GRK1
Plate 1	H02	M-006552-01	D-006552-01	RFP
Plate 1	H02	M-006552-01	D-006552-02	RFP
Plate 1	H02	M-006552-01	D-006552-03	RFP
Plate 1	H02	M-006552-01	D-006552-04	RFP
Plate 1	H03	M-008770-00	D-008770-01	PIP5KL1
Plate 1	H03	M-008770-00	D-008770-02	PIP5KL1
Plate 1	H03	M-008770-00	D-008770-03	PIP5KL1
Plate 1	H03	M-008770-00	D-008770-04	PIP5KL1
Plate 1	H04	M-021702-03	D-021702-04	NEK5
Plate 1	H04	M-021702-03	D-021702-05	NEK5
Plate 1	H04	M-021702-03	D-021702-06	NEK5
Plate 1	H04	M-021702-03	D-021702-19	NEK5
Plate 1	H05	M-003325-05	D-003325-26	PLK2
Plate 1	H05	M-003325-05	D-003325-27	PLK2
Plate 1	H05	M-003325-05	D-003325-28	PLK2
Plate 1	H05	M-003325-05	D-003325-29	PLK2
Plate 1	H06	M-004678-01	D-004678-01	CSNK1G2
Plate 1	H06	M-004678-01	D-004678-02	CSNK1G2
Plate 1	H06	M-004678-01	D-004678-03	CSNK1G2
Plate 1	H06	M-004678-01	D-004678-04	CSNK1G2
Plate 1	H07	M-004260-02	D-004260-02	MARK2
Plate 1	H07	M-004260-02	D-004260-03	MARK2
Plate 1	H07	M-004260-02	D-004260-04	MARK2
Plate 1	H07	M-004260-02	D-004260-05	MARK2
Plate 1	H08	M-004542-03	D-004542-03	TNIK
Plate 1	H08	M-004542-03	D-004542-04	TNIK
Plate 1	H08	M-004542-03	D-004542-07	TNIK
Plate 1	H08	M-004542-03	D-004542-09	TNIK
Plate 1	H09	M-019939-02	D-019939-01	CALM3
Plate 1	H09	M-019939-02	D-019939-03	CALM3
Plate 1	H09	M-019939-02	D-019939-04	CALM3
Plate 1	H09	M-019939-02	D-019939-05	CALM3
Plate 1	H10	M-006781-02	D-006781-01	PKM2
Plate 1	H10	M-006781-02	D-006781-05	PKM2
Plate 1	H10	M-006781-02	D-006781-18	PKM2
Plate 1	H10	M-006781-02	D-006781-19	PKM2
Plate 1	H11	M-004799-03	D-004799-01	CDKL5
Plate 1	H11	M-004799-03	D-004799-02	CDKL5
Plate 1	H11	M-004799-03	D-004799-06	CDKL5
Plate 1	H11	M-004799-03	D-004799-19	CDKL5

Plate 2	A02	M-003018-03	D-003018-07	PIK3CA
Plate 2	A02	M-003018-03	D-003018-08	PIK3CA
Plate 2	A02	M-003018-03	D-003018-24	PIK3CA
Plate 2	A02	M-003018-03	D-003018-25	PIK3CA
Plate 2	A03	M-004063-03	D-004063-02	KIAA1804
Plate 2	A03	M-004063-03	D-004063-04	KIAA1804
Plate 2	A03	M-004063-03	D-004063-23	KIAA1804
Plate 2	A03	M-004063-03	D-004063-24	KIAA1804
Plate 2	A04	M-006750-01	D-006750-01	NAGK
Plate 2	A04	M-006750-01	D-006750-03	NAGK
Plate 2	A04	M-006750-01	D-006750-04	NAGK
Plate 2	A04	M-006750-01	D-006750-17	NAGK
Plate 2	A05	M-004760-03	D-004760-01	IRAK1
Plate 2	A05	M-004760-03	D-004760-03	IRAK1
Plate 2	A05	M-004760-03	D-004760-04	IRAK1
Plate 2	A05	M-004760-03	D-004760-07	IRAK1
Plate 2	A06	M-004950-01	D-004950-01	EEF2K
Plate 2	A06	M-004950-01	D-004950-02	EEF2K
Plate 2	A06	M-004950-01	D-004950-03	EEF2K
Plate 2	A06	M-004950-01	D-004950-04	EEF2K
Plate 2	A07	M-004930-01	D-004930-01	ANKK1
Plate 2	A07	M-004930-01	D-004930-02	ANKK1
Plate 2	A07	M-004930-01	D-004930-04	ANKK1
Plate 2	A07	M-004930-01	D-004930-05	ANKK1
Plate 2	A08	M-003584-02	D-003584-01	MAP3K5
Plate 2	A08	M-003584-02	D-003584-03	MAP3K5
Plate 2	A08	M-003584-02	D-003584-04	MAP3K5
Plate 2	A08	M-003584-02	D-003584-09	MAP3K5
Plate 2	A09	M-005027-02	D-005027-01	PRKAA1
Plate 2	A09	M-005027-02	D-005027-02	PRKAA1
Plate 2	A09	M-005027-02	D-005027-03	PRKAA1
Plate 2	A09	M-005027-02	D-005027-05	PRKAA1
Plate 2	A10	M-004664-01	D-004664-01	RPS6KA4
Plate 2	A10	M-004664-01	D-004664-02	RPS6KA4
Plate 2	A10	M-004664-01	D-004664-03	RPS6KA4
Plate 2	A10	M-004664-01	D-004664-04	RPS6KA4
Plate 2	A11	M-017646-01	D-017646-01	CALM1
Plate 2	A11	M-017646-01	D-017646-02	CALM1
Plate 2	A11	M-017646-01	D-017646-03	CALM1
Plate 2	A11	M-017646-01	D-017646-04	CALM1
Plate 2	B02	M-004052-02	D-004052-08	FLJ32685
Plate 2	B02	M-004052-02	D-004052-09	FLJ32685
Plate 2	B02	M-004052-02	D-004052-10	FLJ32685
Plate 2	B02	M-004052-02	D-004052-11	FLJ32685
Plate 2	B03	M-006744-01	D-006744-05	ITPKC
Plate 2	B03	M-006744-01	D-006744-06	ITPKC
Plate 2	B03	M-006744-01	D-006744-07	ITPKC
Plate 2	B03	M-006744-01	D-006744-08	ITPKC
Plate 2	B04	M-005315-03	D-005315-01	EPHA5
Plate 2	B04	M-005315-03	D-005315-02	EPHA5
Plate 2	B04	M-005315-03	D-005315-03	EPHA5
Plate 2	B04	M-005315-03	D-005315-20	EPHA5
Plate 2	B05	M-005342-04	D-005342-01	MLCK
Plate 2	B05	M-005342-04	D-005342-05	MLCK
Plate 2	B05	M-005342-04	D-005342-07	MLCK
Plate 2	B05	M-005342-04	D-005342-08	MLCK
Plate 2	B06	M-005365-01	D-005365-01	PSKH1
Plate 2	B06	M-005365-01	D-005365-02	PSKH1
Plate 2	B06	M-005365-01	D-005365-04	PSKH1
Plate 2	B06	M-005365-01	D-005365-17	PSKH1
Plate 2	B07	M-019573-04	D-019573-01	AURKC
Plate 2	B07	M-019573-04	D-019573-02	AURKC
Plate 2	B07	M-019573-04	D-019573-03	AURKC
Plate 2	B07	M-019573-04	D-019573-05	AURKC
Plate 2	B08	M-004653-02	D-004653-01	PRKCE
Plate 2	B08	M-004653-02	D-004653-02	PRKCE
Plate 2	B08	M-004653-02	D-004653-03	PRKCE
Plate 2	B08	M-004653-02	D-004653-18	PRKCE
Plate 2	B09	M-006811-03	D-006811-01	AK1
Plate 2	B09	M-006811-03	D-006811-05	AK1
Plate 2	B09	M-006811-03	D-006811-06	AK1
Plate 2	B09	M-006811-03	D-006811-19	AK1
Plate 2	B10	M-005048-01	D-005048-01	TRPM6
Plate 2	B10	M-005048-01	D-005048-02	TRPM6
Plate 2	B10	M-005048-01	D-005048-03	TRPM6
Plate 2	B10	M-005048-01	D-005048-05	TRPM6
Plate 2	B11	M-004800-01	D-004800-01	CLK1
Plate 2	B11	M-004800-01	D-004800-02	CLK1
Plate 2	B11	M-004800-01	D-004800-03	CLK1
Plate 2	B11	M-004800-01	D-004800-04	CLK1

Plate 2	C02	M-006760-02	D-006760-01	PAPSS2
Plate 2	C02	M-006760-02	D-006760-02	PAPSS2
Plate 2	C02	M-006760-02	D-006760-03	PAPSS2
Plate 2	C02	M-006760-02	D-006760-05	PAPSS2
Plate 2	C03	M-004671-01	D-004671-01	RPS6KB2
Plate 2	C03	M-004671-01	D-004671-02	RPS6KB2
Plate 2	C03	M-004671-01	D-004671-03	RPS6KB2
Plate 2	C03	M-004671-01	D-004671-04	RPS6KB2
Plate 2	C04	M-004837-01	D-004837-01	PFTK1
Plate 2	C04	M-004837-01	D-004837-02	PFTK1
Plate 2	C04	M-004837-01	D-004837-03	PFTK1
Plate 2	C04	M-004837-01	D-004837-05	PFTK1
Plate 2	C05	M-006754-00	D-006754-01	NME5
Plate 2	C05	M-006754-00	D-006754-02	NME5
Plate 2	C05	M-006754-00	D-006754-03	NME5
Plate 2	C05	M-006754-00	D-006754-04	NME5
Plate 2	C06	M-003175-03	D-003175-05	SRC
Plate 2	C06	M-003175-03	D-003175-06	SRC
Plate 2	C06	M-003175-03	D-003175-07	SRC
Plate 2	C06	M-003175-03	D-003175-12	SRC
Plate 2	C07	M-003519-02	D-003519-01	NEK4
Plate 2	C07	M-003519-02	D-003519-02	NEK4
Plate 2	C07	M-003519-02	D-003519-03	NEK4
Plate 2	C07	M-003519-02	D-003519-05	NEK4
Plate 2	C08	M-004666-02	D-004666-05	CSNK1G1
Plate 2	C08	M-004666-02	D-004666-06	CSNK1G1
Plate 2	C08	M-004666-02	D-004666-07	CSNK1G1
Plate 2	C08	M-004666-02	D-004666-08	CSNK1G1
Plate 2	C09	M-005368-01	D-005368-01	RIOK1
Plate 2	C09	M-005368-01	D-005368-02	RIOK1
Plate 2	C09	M-005368-01	D-005368-05	RIOK1
Plate 2	C09	M-005368-01	D-005368-06	RIOK1
Plate 2	C10	M-003000-03	D-003000-05	AKT1
Plate 2	C10	M-003000-03	D-003000-07	AKT1
Plate 2	C10	M-003000-03	D-003000-08	AKT1
Plate 2	C10	M-003000-03	D-003000-22	AKT1
Plate 2	C11	M-004322-05	D-004322-01	SNRK
Plate 2	C11	M-004322-05	D-004322-04	SNRK
Plate 2	C11	M-004322-05	D-004322-17	SNRK
Plate 2	C11	M-004322-05	D-004322-18	SNRK
Plate 2	D02	M-004619-02	D-004619-05	KIAA1811
Plate 2	D02	M-004619-02	D-004619-06	KIAA1811
Plate 2	D02	M-004619-02	D-004619-07	KIAA1811
Plate 2	D02	M-004619-02	D-004619-21	KIAA1811
Plate 2	D03	M-005020-00	D-005020-01	PDK2
Plate 2	D03	M-005020-00	D-005020-02	PDK2
Plate 2	D03	M-005020-00	D-005020-03	PDK2
Plate 2	D03	M-005020-00	D-005020-04	PDK2
Plate 2	D04	M-005352-02	D-005352-01	MYLK2
Plate 2	D04	M-005352-02	D-005352-02	MYLK2
Plate 2	D04	M-005352-02	D-005352-05	MYLK2
Plate 2	D04	M-005352-02	D-005352-06	MYLK2
Plate 2	D05	M-004865-02	D-004865-01	NEK11
Plate 2	D05	M-004865-02	D-004865-02	NEK11
Plate 2	D05	M-004865-02	D-004865-03	NEK11
Plate 2	D05	M-004865-02	D-004865-05	NEK11
Plate 2	D06	M-004846-03	D-004846-01	KIAA1361
Plate 2	D06	M-004846-03	D-004846-02	KIAA1361
Plate 2	D06	M-004846-03	D-004846-04	KIAA1361
Plate 2	D06	M-004846-03	D-004846-05	KIAA1361
Plate 2	D07	M-003959-05	D-003959-02	SNF1LK
Plate 2	D07	M-003959-05	D-003959-03	SNF1LK
Plate 2	D07	M-003959-05	D-003959-08	SNF1LK
Plate 2	D07	M-003959-05	D-003959-26	SNF1LK
Plate 2	D08	M-003168-03	D-003168-05	PTK9
Plate 2	D08	M-003168-03	D-003168-09	PTK9
Plate 2	D08	M-003168-03	D-003168-10	PTK9
Plate 2	D08	M-003168-03	D-003168-12	PTK9
Plate 2	D09	M-004632-00	D-004632-01	LATS1
Plate 2	D09	M-004632-00	D-004632-02	LATS1
Plate 2	D09	M-004632-00	D-004632-03	LATS1
Plate 2	D09	M-004632-00	D-004632-04	LATS1
Plate 2	D10	M-010253-01	D-010253-01	PFKP
Plate 2	D10	M-010253-01	D-010253-02	PFKP
Plate 2	D10	M-010253-01	D-010253-03	PFKP
Plate 2	D10	M-010253-01	D-010253-05	PFKP
Plate 2	D11	M-004658-04	D-004658-01	PRKG1
Plate 2	D11	M-004658-04	D-004658-03	PRKG1
Plate 2	D11	M-004658-04	D-004658-04	PRKG1
Plate 2	D11	M-004658-04	D-004658-09	PRKG1

Plate 2	E02	M-005002-00	D-005002-01	RIOK2
Plate 2	E02	M-005002-00	D-005002-02	RIOK2
Plate 2	E02	M-005002-00	D-005002-03	RIOK2
Plate 2	E02	M-005002-00	D-005002-04	RIOK2
Plate 2	E03	M-003008-03	D-003008-05	FRAP1
Plate 2	E03	M-003008-03	D-003008-06	FRAP1
Plate 2	E03	M-003008-03	D-003008-08	FRAP1
Plate 2	E03	M-003008-03	D-003008-23	FRAP1
Plate 2	E04	M-010529-00	D-010529-01	PDGFRL
Plate 2	E04	M-010529-00	D-010529-02	PDGFRL
Plate 2	E04	M-010529-00	D-010529-03	PDGFRL
Plate 2	E04	M-010529-00	D-010529-04	PDGFRL
Plate 2	E05	M-007257-01	D-007257-01	AK7
Plate 2	E05	M-007257-01	D-007257-02	AK7
Plate 2	E05	M-007257-01	D-007257-03	AK7
Plate 2	E05	M-007257-01	D-007257-04	AK7
Plate 2	E06	M-005325-01	D-005325-13	EPHA10
Plate 2	E06	M-005325-01	D-005325-14	EPHA10
Plate 2	E06	M-005325-01	D-005325-15	EPHA10
Plate 2	E06	M-005325-01	D-005325-16	EPHA10
Plate 2	E07	M-004051-01	D-004051-01	STK17B
Plate 2	E07	M-004051-01	D-004051-02	STK17B
Plate 2	E07	M-004051-01	D-004051-03	STK17B
Plate 2	E07	M-004051-01	D-004051-05	STK17B
Plate 2	E08	M-005355-02	D-005355-02	NPR2
Plate 2	E08	M-005355-02	D-005355-05	NPR2
Plate 2	E08	M-005355-02	D-005355-06	NPR2
Plate 2	E08	M-005355-02	D-005355-07	NPR2
Plate 2	E09	M-010633-01	D-010633-01	GOLGA5
Plate 2	E09	M-010633-01	D-010633-04	GOLGA5
Plate 2	E09	M-010633-01	D-010633-05	GOLGA5
Plate 2	E09	M-010633-01	D-010633-06	GOLGA5
Plate 2	E10	M-004872-03	D-004872-05	STK24
Plate 2	E10	M-004872-03	D-004872-21	STK24
Plate 2	E10	M-004872-03	D-004872-22	STK24
Plate 2	E10	M-004872-03	D-004872-23	STK24
Plate 2	E11	M-006712-01	D-006712-01	DGKB
Plate 2	E11	M-006712-01	D-006712-02	DGKB
Plate 2	E11	M-006712-01	D-006712-04	DGKB
Plate 2	E11	M-006712-01	D-006712-05	DGKB
Plate 2	F02	M-004873-01	D-004873-02	STK25
Plate 2	F02	M-004873-01	D-004873-03	STK25
Plate 2	F02	M-004873-01	D-004873-04	STK25
Plate 2	F02	M-004873-01	D-004873-17	STK25
Plate 2	F03	M-003234-02	D-003234-06	CDC7
Plate 2	F03	M-003234-02	D-003234-07	CDC7
Plate 2	F03	M-003234-02	D-003234-08	CDC7
Plate 2	F03	M-003234-02	D-003234-09	CDC7
Plate 2	F04	M-004536-01	D-004536-01	CAMK2G
Plate 2	F04	M-004536-01	D-004536-03	CAMK2G
Plate 2	F04	M-004536-01	D-004536-05	CAMK2G
Plate 2	F04	M-004536-01	D-004536-06	CAMK2G
Plate 2	F05	M-006792-01	D-006792-01	URKL1
Plate 2	F05	M-006792-01	D-006792-02	URKL1
Plate 2	F05	M-006792-01	D-006792-03	URKL1
Plate 2	F05	M-006792-01	D-006792-04	URKL1
Plate 2	F06	M-003585-03	D-003585-02	MAP3K9
Plate 2	F06	M-003585-03	D-003585-05	MAP3K9
Plate 2	F06	M-003585-03	D-003585-06	MAP3K9
Plate 2	F06	M-003585-03	D-003585-07	MAP3K9
Plate 2	F07	M-005329-02	D-005329-02	GUCY2D
Plate 2	F07	M-005329-02	D-005329-03	GUCY2D
Plate 2	F07	M-005329-02	D-005329-05	GUCY2D
Plate 2	F07	M-005329-02	D-005329-18	GUCY2D
Plate 2	F08	M-004842-02	D-004842-06	CAMKK2
Plate 2	F08	M-004842-02	D-004842-07	CAMKK2
Plate 2	F08	M-004842-02	D-004842-21	CAMKK2
Plate 2	F08	M-004842-02	D-004842-22	CAMKK2
Plate 2	F09	M-005336-00	D-005336-01	KIAA1639
Plate 2	F09	M-005336-00	D-005336-02	KIAA1639
Plate 2	F09	M-005336-00	D-005336-03	KIAA1639
Plate 2	F09	M-005336-00	D-005336-04	KIAA1639
Plate 2	F10	M-017896-01	D-017896-01	CAMKIINALP
Plate 2	F10	M-017896-01	D-017896-02	CAMKIINALP
Plate 2	F10	M-017896-01	D-017896-03	CAMKIINALP
Plate 2	F10	M-017896-01	D-017896-04	CAMKIINALP
Plate 2	F11	M-003150-02	D-003150-05	KIT
Plate 2	F11	M-003150-02	D-003150-06	KIT
Plate 2	F11	M-003150-02	D-003150-07	KIT
Plate 2	F11	M-003150-02	D-003150-08	KIT

Plate 2	G02	M-004175-02	D-004175-09	PRKCL1
Plate 2	G02	M-004175-02	D-004175-10	PRKCL1
Plate 2	G02	M-004175-02	D-004175-11	PRKCL1
Plate 2	G02	M-004175-02	D-004175-12	PRKCL1
Plate 2	G03	M-003602-02	D-003602-01	RIPK2
Plate 2	G03	M-003602-02	D-003602-02	RIPK2
Plate 2	G03	M-003602-02	D-003602-03	RIPK2
Plate 2	G03	M-003602-02	D-003602-04	RIPK2
Plate 2	G04	M-006708-01	D-006708-01	CKMT1B
Plate 2	G04	M-006708-01	D-006708-02	CKMT1B
Plate 2	G04	M-006708-01	D-006708-04	CKMT1B
Plate 2	G04	M-006708-01	D-006708-17	CKMT1B
Plate 2	G05	M-004908-02	D-004908-01	MKNK2
Plate 2	G05	M-004908-02	D-004908-02	MKNK2
Plate 2	G05	M-004908-02	D-004908-04	MKNK2
Plate 2	G05	M-004908-02	D-004908-05	MKNK2
Plate 2	G06	M-005013-01	D-005013-03	TNNI3K
Plate 2	G06	M-005013-01	D-005013-05	TNNI3K
Plate 2	G06	M-005013-01	D-005013-06	TNNI3K
Plate 2	G06	M-005013-01	D-005013-07	TNNI3K
Plate 2	G07	M-004685-01	D-004685-01	ALS2CR7
Plate 2	G07	M-004685-01	D-004685-02	ALS2CR7
Plate 2	G07	M-004685-01	D-004685-05	ALS2CR7
Plate 2	G07	M-004685-01	D-004685-06	ALS2CR7
Plate 2	G08	M-003141-03	D-003141-10	HCK
Plate 2	G08	M-003141-03	D-003141-11	HCK
Plate 2	G08	M-003141-03	D-003141-12	HCK
Plate 2	G08	M-003141-03	D-003141-25	HCK
Plate 2	G09	M-004586-01	D-004586-01	CKS1B
Plate 2	G09	M-004586-01	D-004586-03	CKS1B
Plate 2	G09	M-004586-01	D-004586-04	CKS1B
Plate 2	G09	M-004586-01	D-004586-05	CKS1B
Plate 2	G10	M-005071-01	D-005071-01	BMP2K
Plate 2	G10	M-005071-01	D-005071-02	BMP2K
Plate 2	G10	M-005071-01	D-005071-03	BMP2K
Plate 2	G10	M-005071-01	D-005071-17	BMP2K
Plate 2	G11	M-007674-01	D-007674-02	PHKB
Plate 2	G11	M-007674-01	D-007674-03	PHKB
Plate 2	G11	M-007674-01	D-007674-04	PHKB
Plate 2	G11	M-007674-01	D-007674-05	PHKB
Plate 2	H02	M-005047-00	D-005047-01	TRIO
Plate 2	H02	M-005047-00	D-005047-02	TRIO
Plate 2	H02	M-005047-00	D-005047-03	TRIO
Plate 2	H02	M-005047-00	D-005047-04	TRIO
Plate 2	H03	M-006721-03	D-006721-22	ETNK1
Plate 2	H03	M-006721-03	D-006721-23	ETNK1
Plate 2	H03	M-006721-03	D-006721-24	ETNK1
Plate 2	H03	M-006721-03	D-006721-25	ETNK1
Plate 2	H04	M-004807-02	D-004807-01	ERK8
Plate 2	H04	M-004807-02	D-004807-02	ERK8
Plate 2	H04	M-004807-02	D-004807-04	ERK8
Plate 2	H04	M-004807-02	D-004807-05	ERK8
Plate 2	H05	M-006809-00	D-006809-01	ADP-GK
Plate 2	H05	M-006809-00	D-006809-02	ADP-GK
Plate 2	H05	M-006809-00	D-006809-03	ADP-GK
Plate 2	H05	M-006809-00	D-006809-04	ADP-GK
Plate 2	H06	M-005274-02	D-005274-03	PIK3CG
Plate 2	H06	M-005274-02	D-005274-04	PIK3CG
Plate 2	H06	M-005274-02	D-005274-05	PIK3CG
Plate 2	H06	M-005274-02	D-005274-06	PIK3CG
Plate 2	H07	M-003133-01	D-003133-05	FGFR3
Plate 2	H07	M-003133-01	D-003133-06	FGFR3
Plate 2	H07	M-003133-01	D-003133-07	FGFR3
Plate 2	H07	M-003133-01	D-003133-08	FGFR3
Plate 2	H08	M-003302-01	D-003302-01	IRAK4
Plate 2	H08	M-003302-01	D-003302-02	IRAK4
Plate 2	H08	M-003302-01	D-003302-05	IRAK4
Plate 2	H08	M-003302-01	D-003302-06	IRAK4
Plate 2	H09	M-004836-02	D-004836-01	PCTK3
Plate 2	H09	M-004836-02	D-004836-02	PCTK3
Plate 2	H09	M-004836-02	D-004836-03	PCTK3
Plate 2	H09	M-004836-02	D-004836-06	PCTK3
Plate 2	H10	M-004673-01	D-004673-05	SGK2
Plate 2	H10	M-004673-01	D-004673-06	SGK2
Plate 2	H10	M-004673-01	D-004673-07	SGK2
Plate 2	H10	M-004673-01	D-004673-08	SGK2
Plate 2	H11	M-004732-01	D-004732-01	DYRK4
Plate 2	H11	M-004732-01	D-004732-03	DYRK4
Plate 2	H11	M-004732-01	D-004732-04	DYRK4
Plate 2	H11	M-004732-01	D-004732-05	DYRK4

Plate 3	A02	M-003582-04	D-003582-03	MAP3K2
Plate 3	A02	M-003582-04	D-003582-06	MAP3K2
Plate 3	A02	M-003582-04	D-003582-26	MAP3K2
Plate 3	A02	M-003582-04	D-003582-27	MAP3K2
Plate 3	A03	M-003865-02	D-003865-01	LATS2
Plate 3	A03	M-003865-02	D-003865-02	LATS2
Plate 3	A03	M-003865-02	D-003865-03	LATS2
Plate 3	A03	M-003865-02	D-003865-04	LATS2
Plate 3	A04	M-020619-01	D-020619-01	P101-PI3K
Plate 3	A04	M-020619-01	D-020619-02	P101-PI3K
Plate 3	A04	M-020619-01	D-020619-03	P101-PI3K
Plate 3	A04	M-020619-01	D-020619-04	P101-PI3K
Plate 3	A05	M-006715-01	D-006715-01	DGKG
Plate 3	A05	M-006715-01	D-006715-02	DGKG
Plate 3	A05	M-006715-01	D-006715-03	DGKG
Plate 3	A05	M-006715-01	D-006715-04	DGKG
Plate 3	A06	M-004046-02	D-004046-01	MAST3
Plate 3	A06	M-004046-02	D-004046-02	MAST3
Plate 3	A06	M-004046-02	D-004046-03	MAST3
Plate 3	A06	M-004046-02	D-004046-04	MAST3
Plate 3	A07	M-019190-02	D-019190-01	EFNA3
Plate 3	A07	M-019190-02	D-019190-03	EFNA3
Plate 3	A07	M-019190-02	D-019190-05	EFNA3
Plate 3	A07	M-019190-02	D-019190-18	EFNA3
Plate 3	A08	M-004932-01	D-004932-02	BCKDK
Plate 3	A08	M-004932-01	D-004932-03	BCKDK
Plate 3	A08	M-004932-01	D-004932-04	BCKDK
Plate 3	A08	M-004932-01	D-004932-17	BCKDK
Plate 3	A09	M-006742-02	D-006742-04	ITPKA
Plate 3	A09	M-006742-02	D-006742-05	ITPKA
Plate 3	A09	M-006742-02	D-006742-06	ITPKA
Plate 3	A09	M-006742-02	D-006742-20	ITPKA
Plate 3	A10	M-004166-01	D-004166-01	NEK6
Plate 3	A10	M-004166-01	D-004166-02	NEK6
Plate 3	A10	M-004166-01	D-004166-04	NEK6
Plate 3	A10	M-004166-01	D-004166-05	NEK6
Plate 3	A11	M-003105-03	D-003105-07	BLK
Plate 3	A11	M-003105-03	D-003105-08	BLK
Plate 3	A11	M-003105-03	D-003105-09	BLK
Plate 3	A11	M-003105-03	D-003105-10	BLK
Plate 3	B02	M-024694-01	D-024694-01	DGKK
Plate 3	B02	M-024694-01	D-024694-02	DGKK
Plate 3	B02	M-024694-01	D-024694-04	DGKK
Plate 3	B02	M-024694-01	D-024694-17	DGKK
Plate 3	B03	M-009729-01	D-009729-01	MPP2
Plate 3	B03	M-009729-01	D-009729-02	MPP2
Plate 3	B03	M-009729-01	D-009729-03	MPP2
Plate 3	B03	M-009729-01	D-009729-04	MPP2
Plate 3	B04	M-004102-01	D-004102-01	BUB1
Plate 3	B04	M-004102-01	D-004102-02	BUB1
Plate 3	B04	M-004102-01	D-004102-03	BUB1
Plate 3	B04	M-004102-01	D-004102-04	BUB1
Plate 3	B05	M-003981-04	D-003981-01	UHMK1
Plate 3	B05	M-003981-04	D-003981-05	UHMK1
Plate 3	B05	M-003981-04	D-003981-06	UHMK1
Plate 3	B05	M-003981-04	D-003981-07	UHMK1
Plate 3	B06	M-005028-02	D-005028-01	PRKCM
Plate 3	B06	M-005028-02	D-005028-02	PRKCM
Plate 3	B06	M-005028-02	D-005028-03	PRKCM
Plate 3	B06	M-005028-02	D-005028-21	PRKCM
Plate 3	B07	M-006777-03	D-006777-02	PIK4CB
Plate 3	B07	M-006777-03	D-006777-03	PIK4CB
Plate 3	B07	M-006777-03	D-006777-06	PIK4CB
Plate 3	B07	M-006777-03	D-006777-21	PIK4CB
Plate 3	B08	M-007882-02	D-007882-01	DLG4
Plate 3	B08	M-007882-02	D-007882-02	DLG4
Plate 3	B08	M-007882-02	D-007882-05	DLG4
Plate 3	B08	M-007882-02	D-007882-18	DLG4
Plate 3	B09	M-003107-01	D-003107-05	BTK
Plate 3	B09	M-003107-01	D-003107-06	BTK
Plate 3	B09	M-003107-01	D-003107-07	BTK
Plate 3	B09	M-003107-01	D-003107-08	BTK
Plate 3	B10	M-004847-02	D-004847-01	MAP3K15
Plate 3	B10	M-004847-02	D-004847-02	MAP3K15
Plate 3	B10	M-004847-02	D-004847-03	MAP3K15
Plate 3	B10	M-004847-02	D-004847-04	MAP3K15
Plate 3	B11	M-003009-01	D-003009-05	GSK3A
Plate 3	B11	M-003009-01	D-003009-06	GSK3A
Plate 3	B11	M-003009-01	D-003009-07	GSK3A
Plate 3	B11	M-003009-01	D-003009-08	GSK3A

Plate 3	C02	M-003479-01	D-003479-01	CSNK1E
Plate 3	C02	M-003479-01	D-003479-02	CSNK1E
Plate 3	C02	M-003479-01	D-003479-04	CSNK1E
Plate 3	C02	M-003479-01	D-003479-05	CSNK1E
Plate 3	C03	M-003533-02	D-003533-03	RELA
Plate 3	C03	M-003533-02	D-003533-04	RELA
Plate 3	C03	M-003533-02	D-003533-05	RELA
Plate 3	C03	M-003533-02	D-003533-18	RELA
Plate 3	C04	M-004686-02	D-004686-01	CCRK
Plate 3	C04	M-004686-02	D-004686-02	CCRK
Plate 3	C04	M-004686-02	D-004686-04	CCRK
Plate 3	C04	M-004686-02	D-004686-05	CCRK
Plate 3	C05	M-003505-02	D-003505-05	MAPK9
Plate 3	C05	M-003505-02	D-003505-06	MAPK9
Plate 3	C05	M-003505-02	D-003505-07	MAPK9
Plate 3	C05	M-003505-02	D-003505-09	MAPK9
Plate 3	C06	M-003102-04	D-003102-10	TNK2
Plate 3	C06	M-003102-04	D-003102-11	TNK2
Plate 3	C06	M-003102-04	D-003102-12	TNK2
Plate 3	C06	M-003102-04	D-003102-13	TNK2
Plate 3	C07	M-005011-03	D-005011-01	PDIK1L
Plate 3	C07	M-005011-03	D-005011-03	PDIK1L
Plate 3	C07	M-005011-03	D-005011-04	PDIK1L
Plate 3	C07	M-005011-03	D-005011-05	PDIK1L
Plate 3	C08	M-003104-03	D-003104-06	AXL
Plate 3	C08	M-003104-03	D-003104-07	AXL
Plate 3	C08	M-003104-03	D-003104-08	AXL
Plate 3	C08	M-003104-03	D-003104-09	AXL
Plate 3	C09	M-005308-03	D-005308-02	ANKRD3
Plate 3	C09	M-005308-03	D-005308-05	ANKRD3
Plate 3	C09	M-005308-03	D-005308-20	ANKRD3
Plate 3	C09	M-005308-03	D-005308-21	ANKRD3
Plate 3	C10	M-004445-02	D-004445-03	RIPK1
Plate 3	C10	M-004445-02	D-004445-04	RIPK1
Plate 3	C10	M-004445-02	D-004445-05	RIPK1
Plate 3	C10	M-004445-02	D-004445-06	RIPK1
Plate 3	C11	M-004075-02	D-004075-02	CDC42BPB
Plate 3	C11	M-004075-02	D-004075-03	CDC42BPB
Plate 3	C11	M-004075-02	D-004075-04	CDC42BPB
Plate 3	C11	M-004075-02	D-004075-05	CDC42BPB
Plate 3	D02	M-003147-01	D-003147-05	JAK3
Plate 3	D02	M-003147-01	D-003147-06	JAK3
Plate 3	D02	M-003147-01	D-003147-07	JAK3
Plate 3	D02	M-003147-01	D-003147-08	JAK3
Plate 3	D03	M-005038-02	D-005038-05	STK22D
Plate 3	D03	M-005038-02	D-005038-07	STK22D
Plate 3	D03	M-005038-02	D-005038-08	STK22D
Plate 3	D03	M-005038-02	D-005038-09	STK22D
Plate 3	D04	M-003131-03	D-003131-09	FGFR1
Plate 3	D04	M-003131-03	D-003131-22	FGFR1
Plate 3	D04	M-003131-03	D-003131-23	FGFR1
Plate 3	D04	M-003131-03	D-003131-24	FGFR1
Plate 3	D05	M-006783-02	D-006783-03	PNKP
Plate 3	D05	M-006783-02	D-006783-04	PNKP
Plate 3	D05	M-006783-02	D-006783-05	PNKP
Plate 3	D05	M-006783-02	D-006783-06	PNKP
Plate 3	D06	M-003126-04	D-003126-05	ERBB2
Plate 3	D06	M-003126-04	D-003126-06	ERBB2
Plate 3	D06	M-003126-04	D-003126-07	ERBB2
Plate 3	D06	M-003126-04	D-003126-08	ERBB2
Plate 3	D07	M-009056-01	D-009056-01	PRKAG1
Plate 3	D07	M-009056-01	D-009056-02	PRKAG1
Plate 3	D07	M-009056-01	D-009056-03	PRKAG1
Plate 3	D07	M-009056-01	D-009056-17	PRKAG1
Plate 3	D08	M-005078-00	D-005078-01	FLJ10761
Plate 3	D08	M-005078-00	D-005078-02	FLJ10761
Plate 3	D08	M-005078-00	D-005078-03	FLJ10761
Plate 3	D08	M-005078-00	D-005078-04	FLJ10761
Plate 3	D09	M-003012-05	D-003012-06	IGF1R
Plate 3	D09	M-003012-05	D-003012-08	IGF1R
Plate 3	D09	M-003012-05	D-003012-17	IGF1R
Plate 3	D09	M-003012-05	D-003012-18	IGF1R
Plate 3	D10	M-004869-01	D-004869-01	NEK9
Plate 3	D10	M-004869-01	D-004869-04	NEK9
Plate 3	D10	M-004869-01	D-004869-05	NEK9
Plate 3	D10	M-004869-01	D-004869-06	NEK9
Plate 3	D11	M-005321-00	D-005321-01	FLJ23356
Plate 3	D11	M-005321-00	D-005321-02	FLJ23356
Plate 3	D11	M-005321-00	D-005321-03	FLJ23356
Plate 3	D11	M-005321-00	D-005321-04	FLJ23356

Plate 3	E02	M-003137-02	D-003137-05	FLT3
Plate 3	E02	M-003137-02	D-003137-06	FLT3
Plate 3	E02	M-003137-02	D-003137-07	FLT3
Plate 3	E02	M-003137-02	D-003137-08	FLT3
Plate 3	E03	M-006778-01	D-006778-01	PIP5K2A
Plate 3	E03	M-006778-01	D-006778-02	PIP5K2A
Plate 3	E03	M-006778-01	D-006778-04	PIP5K2A
Plate 3	E03	M-006778-01	D-006778-17	PIP5K2A
Plate 3	E04	M-004417-03	D-004417-02	DAPK1
Plate 3	E04	M-004417-03	D-004417-04	DAPK1
Plate 3	E04	M-004417-03	D-004417-07	DAPK1
Plate 3	E04	M-004417-03	D-004417-21	DAPK1
Plate 3	E05	M-005317-02	D-005317-01	FASTK
Plate 3	E05	M-005317-02	D-005317-02	FASTK
Plate 3	E05	M-005317-02	D-005317-04	FASTK
Plate 3	E05	M-005317-02	D-005317-06	FASTK
Plate 3	E06	M-004659-00	D-004659-01	PRKG2
Plate 3	E06	M-004659-00	D-004659-02	PRKG2
Plate 3	E06	M-004659-00	D-004659-03	PRKG2
Plate 3	E06	M-004659-00	D-004659-04	PRKG2
Plate 3	E07	M-010252-00	D-010252-01	MPP1
Plate 3	E07	M-010252-00	D-010252-02	MPP1
Plate 3	E07	M-010252-00	D-010252-03	MPP1
Plate 3	E07	M-010252-00	D-010252-04	MPP1
Plate 3	E08	M-005006-00	D-005006-01	HSPB8
Plate 3	E08	M-005006-00	D-005006-02	HSPB8
Plate 3	E08	M-005006-00	D-005006-03	HSPB8
Plate 3	E08	M-005006-00	D-005006-04	HSPB8
Plate 3	E09	M-003109-03	D-003109-06	CSF1R
Plate 3	E09	M-003109-03	D-003109-07	CSF1R
Plate 3	E09	M-003109-03	D-003109-09	CSF1R
Plate 3	E09	M-003109-03	D-003109-22	CSF1R
Plate 3	E10	M-004730-03	D-004730-01	DYRK2
Plate 3	E10	M-004730-03	D-004730-02	DYRK2
Plate 3	E10	M-004730-03	D-004730-03	DYRK2
Plate 3	E10	M-004730-03	D-004730-05	DYRK2
Plate 3	E11	M-004612-03	D-004612-03	PRKCL2
Plate 3	E11	M-004612-03	D-004612-09	PRKCL2
Plate 3	E11	M-004612-03	D-004612-10	PRKCL2
Plate 3	E11	M-004612-03	D-004612-11	PRKCL2
Plate 3	F02	M-003026-02	D-003026-05	RPS6KA3
Plate 3	F02	M-003026-02	D-003026-06	RPS6KA3
Plate 3	F02	M-003026-02	D-003026-07	RPS6KA3
Plate 3	F02	M-003026-02	D-003026-08	RPS6KA3
Plate 3	F03	M-006858-01	D-006858-01	EFNA4
Plate 3	F03	M-006858-01	D-006858-02	EFNA4
Plate 3	F03	M-006858-01	D-006858-03	EFNA4
Plate 3	F03	M-006858-01	D-006858-05	EFNA4
Plate 3	F04	M-005303-03	D-005303-01	ADCK1
Plate 3	F04	M-005303-03	D-005303-05	ADCK1
Plate 3	F04	M-005303-03	D-005303-07	ADCK1
Plate 3	F04	M-005303-03	D-005303-20	ADCK1
Plate 3	F05	M-003511-03	D-003511-07	MAP3K8
Plate 3	F05	M-003511-03	D-003511-08	MAP3K8
Plate 3	F05	M-003511-03	D-003511-09	MAP3K8
Plate 3	F05	M-003511-03	D-003511-10	MAP3K8
Plate 3	F06	M-003242-02	D-003242-05	CDK8
Plate 3	F06	M-003242-02	D-003242-06	CDK8
Plate 3	F06	M-003242-02	D-003242-07	CDK8
Plate 3	F06	M-003242-02	D-003242-08	CDK8
Plate 3	F07	M-004879-02	D-004879-03	MKNK1
Plate 3	F07	M-004879-02	D-004879-05	MKNK1
Plate 3	F07	M-004879-02	D-004879-06	MKNK1
Plate 3	F07	M-004879-02	D-004879-20	MKNK1
Plate 3	F08	M-006773-01	D-006773-01	PIK3C2G
Plate 3	F08	M-006773-01	D-006773-02	PIK3C2G
Plate 3	F08	M-006773-01	D-006773-03	PIK3C2G
Plate 3	F08	M-006773-01	D-006773-04	PIK3C2G
Plate 3	F09	M-003238-02	D-003238-05	CDK4
Plate 3	F09	M-003238-02	D-003238-06	CDK4
Plate 3	F09	M-003238-02	D-003238-07	CDK4
Plate 3	F09	M-003238-02	D-003238-08	CDK4
Plate 3	F10	M-003923-00	D-003923-01	PIM1
Plate 3	F10	M-003923-00	D-003923-02	PIM1
Plate 3	F10	M-003923-00	D-003923-03	PIM1
Plate 3	F10	M-003923-00	D-003923-04	PIM1
Plate 3	F11	M-005079-02	D-005079-03	DGKQ
Plate 3	F11	M-005079-02	D-005079-04	DGKQ
Plate 3	F11	M-005079-02	D-005079-06	DGKQ
Plate 3	F11	M-005079-02	D-005079-07	DGKQ

Plate 3	G02	M-003312-02	D-003312-05	MAP3K12
Plate 3	G02	M-003312-02	D-003312-08	MAP3K12
Plate 3	G02	M-003312-02	D-003312-09	MAP3K12
Plate 3	G02	M-003312-02	D-003312-10	MAP3K12
Plate 3	G03	M-004050-02	D-004050-05	STK22C
Plate 3	G03	M-004050-02	D-004050-06	STK22C
Plate 3	G03	M-004050-02	D-004050-07	STK22C
Plate 3	G03	M-004050-02	D-004050-08	STK22C
Plate 3	G04	M-006770-02	D-006770-02	PI4KII
Plate 3	G04	M-006770-02	D-006770-03	PI4KII
Plate 3	G04	M-006770-02	D-006770-05	PI4KII
Plate 3	G04	M-006770-02	D-006770-18	PI4KII
Plate 3	G05	M-005385-03	D-005385-01	TAF1L
Plate 3	G05	M-005385-03	D-005385-07	TAF1L
Plate 3	G05	M-005385-03	D-005385-08	TAF1L
Plate 3	G05	M-005385-03	D-005385-09	TAF1L
Plate 3	G06	M-004941-01	D-004941-01	CAMK1G
Plate 3	G06	M-004941-01	D-004941-02	CAMK1G
Plate 3	G06	M-004941-01	D-004941-03	CAMK1G
Plate 3	G06	M-004941-01	D-004941-05	CAMK1G
Plate 3	G07	M-007691-03	D-007691-02	HSMDPKIN
Plate 3	G07	M-007691-03	D-007691-05	HSMDPKIN
Plate 3	G07	M-007691-03	D-007691-06	HSMDPKIN
Plate 3	G07	M-007691-03	D-007691-23	HSMDPKIN
Plate 3	G08	M-004168-01	D-004168-05	STK10
Plate 3	G08	M-004168-01	D-004168-06	STK10
Plate 3	G08	M-004168-01	D-004168-07	STK10
Plate 3	G08	M-004168-01	D-004168-08	STK10
Plate 3	G09	M-012456-01	D-012456-01	AIP1
Plate 3	G09	M-012456-01	D-012456-03	AIP1
Plate 3	G09	M-012456-01	D-012456-04	AIP1
Plate 3	G09	M-012456-01	D-012456-17	AIP1
Plate 3	G10	M-003100-02	D-003100-05	ABL1
Plate 3	G10	M-003100-02	D-003100-07	ABL1
Plate 3	G10	M-003100-02	D-003100-08	ABL1
Plate 3	G10	M-003100-02	D-003100-21	ABL1
Plate 3	G11	M-004338-02	D-004338-02	PAK6
Plate 3	G11	M-004338-02	D-004338-03	PAK6
Plate 3	G11	M-004338-02	D-004338-05	PAK6
Plate 3	G11	M-004338-02	D-004338-06	PAK6
Plate 3	H02	M-006817-00	D-006817-01	FN3KRP
Plate 3	H02	M-006817-00	D-006817-02	FN3KRP
Plate 3	H02	M-006817-00	D-006817-03	FN3KRP
Plate 3	H02	M-006817-00	D-006817-04	FN3KRP
Plate 3	H03	M-003001-02	D-003001-05	AKT2
Plate 3	H03	M-003001-02	D-003001-07	AKT2
Plate 3	H03	M-003001-02	D-003001-08	AKT2
Plate 3	H03	M-003001-02	D-003001-21	AKT2
Plate 3	H04	M-004779-03	D-004779-01	KIAA0999
Plate 3	H04	M-004779-03	D-004779-05	KIAA0999
Plate 3	H04	M-004779-03	D-004779-06	KIAA0999
Plate 3	H04	M-004779-03	D-004779-20	KIAA0999
Plate 3	H05	M-005036-02	D-005036-02	PLK4
Plate 3	H05	M-005036-02	D-005036-04	PLK4
Plate 3	H05	M-005036-02	D-005036-05	PLK4
Plate 3	H05	M-005036-02	D-005036-06	PLK4
Plate 3	H06	M-004810-02	D-004810-01	HIPK3
Plate 3	H06	M-004810-02	D-004810-02	HIPK3
Plate 3	H06	M-004810-02	D-004810-03	HIPK3
Plate 3	H06	M-004810-02	D-004810-04	HIPK3
Plate 3	H07	M-003183-02	D-003183-06	TYRO3
Plate 3	H07	M-003183-02	D-003183-07	TYRO3
Plate 3	H07	M-003183-02	D-003183-08	TYRO3
Plate 3	H07	M-003183-02	D-003183-09	TYRO3
Plate 3	H08	M-003592-03	D-003592-01	MAPK3
Plate 3	H08	M-003592-03	D-003592-02	MAPK3
Plate 3	H08	M-003592-03	D-003592-06	MAPK3
Plate 3	H08	M-003592-03	D-003592-19	MAPK3
Plate 3	H09	M-003184-03	D-003184-05	YES1
Plate 3	H09	M-003184-03	D-003184-07	YES1
Plate 3	H09	M-003184-03	D-003184-08	YES1
Plate 3	H09	M-003184-03	D-003184-09	YES1
Plate 3	H10	M-007733-00	D-007733-01	NYD-SP25
Plate 3	H10	M-007733-00	D-007733-02	NYD-SP25
Plate 3	H10	M-007733-00	D-007733-03	NYD-SP25
Plate 3	H10	M-007733-00	D-007733-04	NYD-SP25
Plate 3	H11	M-007732-00	D-007732-01	CDADC1
Plate 3	H11	M-007732-00	D-007732-02	CDADC1
Plate 3	H11	M-007732-00	D-007732-03	CDADC1
Plate 3	H11	M-007732-00	D-007732-04	CDADC1

Plate 4	A02	M-005382-01	D-005382-01	STK31
Plate 4	A02	M-005382-01	D-005382-03	STK31
Plate 4	A02	M-005382-01	D-005382-04	STK31
Plate 4	A02	M-005382-01	D-005382-17	STK31
Plate 4	A03	M-003002-02	D-003002-09	AKT3
Plate 4	A03	M-003002-02	D-003002-10	AKT3
Plate 4	A03	M-003002-02	D-003002-11	AKT3
Plate 4	A03	M-003002-02	D-003002-12	AKT3
Plate 4	A04	M-004763-01	D-004763-03	NLK
Plate 4	A04	M-004763-01	D-004763-04	NLK
Plate 4	A04	M-004763-01	D-004763-05	NLK
Plate 4	A04	M-004763-01	D-004763-06	NLK
Plate 4	A05	M-006763-01	D-006763-01	PFKFB3
Plate 4	A05	M-006763-01	D-006763-02	PFKFB3
Plate 4	A05	M-006763-01	D-006763-03	PFKFB3
Plate 4	A05	M-006763-01	D-006763-17	PFKFB3
Plate 4	A06	M-005044-01	D-005044-01	TESK2
Plate 4	A06	M-005044-01	D-005044-02	TESK2
Plate 4	A06	M-005044-01	D-005044-04	TESK2
Plate 4	A06	M-005044-01	D-005044-17	TESK2
Plate 4	A07	M-003119-02	D-003119-06	EPHA7
Plate 4	A07	M-003119-02	D-003119-07	EPHA7
Plate 4	A07	M-003119-02	D-003119-08	EPHA7
Plate 4	A07	M-003119-02	D-003119-21	EPHA7
Plate 4	A08	M-005384-01	D-005384-01	STK35
Plate 4	A08	M-005384-01	D-005384-02	STK35
Plate 4	A08	M-005384-01	D-005384-04	STK35
Plate 4	A08	M-005384-01	D-005384-17	STK35
Plate 4	A09	M-005035-02	D-005035-01	STK11
Plate 4	A09	M-005035-02	D-005035-03	STK11
Plate 4	A09	M-005035-02	D-005035-05	STK11
Plate 4	A09	M-005035-02	D-005035-06	STK11
Plate 4	A10	M-003146-02	D-003146-06	JAK2
Plate 4	A10	M-003146-02	D-003146-07	JAK2
Plate 4	A10	M-003146-02	D-003146-09	JAK2
Plate 4	A10	M-003146-02	D-003146-10	JAK2
Plate 4	A11	M-004935-02	D-004935-01	BRD2
Plate 4	A11	M-004935-02	D-004935-02	BRD2
Plate 4	A11	M-004935-02	D-004935-04	BRD2
Plate 4	A11	M-004935-02	D-004935-18	BRD2
Plate 4	B02	M-003246-01	D-003246-05	CDKN2C
Plate 4	B02	M-003246-01	D-003246-06	CDKN2C
Plate 4	B02	M-003246-01	D-003246-07	CDKN2C
Plate 4	B02	M-003246-01	D-003246-08	CDKN2C
Plate 4	B03	M-003509-03	D-003509-02	MAP2K3
Plate 4	B03	M-003509-03	D-003509-04	MAP2K3
Plate 4	B03	M-003509-03	D-003509-05	MAP2K3
Plate 4	B03	M-003509-03	D-003509-06	MAP2K3
Plate 4	B04	M-003151-02	D-003151-05	LCK
Plate 4	B04	M-003151-02	D-003151-06	LCK
Plate 4	B04	M-003151-02	D-003151-07	LCK
Plate 4	B04	M-003151-02	D-003151-08	LCK
Plate 4	B05	M-012230-00	D-012230-01	CIB2
Plate 4	B05	M-012230-00	D-012230-02	CIB2
Plate 4	B05	M-012230-00	D-012230-03	CIB2
Plate 4	B05	M-012230-00	D-012230-04	CIB2
Plate 4	B06	M-005300-01	D-005300-01	AAK1
Plate 4	B06	M-005300-01	D-005300-02	AAK1
Plate 4	B06	M-005300-01	D-005300-03	AAK1
Plate 4	B06	M-005300-01	D-005300-04	AAK1
Plate 4	B07	M-003021-03	D-003021-05	PIK3R2
Plate 4	B07	M-003021-03	D-003021-07	PIK3R2
Plate 4	B07	M-003021-03	D-003021-08	PIK3R2
Plate 4	B07	M-003021-03	D-003021-26	PIK3R2
Plate 4	B08	M-004761-01	D-004761-01	IRAK2
Plate 4	B08	M-004761-01	D-004761-03	IRAK2
Plate 4	B08	M-004761-01	D-004761-04	IRAK2
Plate 4	B08	M-004761-01	D-004761-17	IRAK2
Plate 4	B09	M-004929-02	D-004929-03	ACVR1C
Plate 4	B09	M-004929-02	D-004929-05	ACVR1C
Plate 4	B09	M-004929-02	D-004929-18	ACVR1C
Plate 4	B09	M-004929-02	D-004929-19	ACVR1C
Plate 4	B10	M-004925-01	D-004925-01	ACVR1B
Plate 4	B10	M-004925-01	D-004925-03	ACVR1B
Plate 4	B10	M-004925-01	D-004925-05	ACVR1B
Plate 4	B10	M-004925-01	D-004925-06	ACVR1B
Plate 4	B11	M-011550-00	D-011550-01	CPNE3
Plate 4	B11	M-011550-00	D-011550-02	CPNE3
Plate 4	B11	M-011550-00	D-011550-03	CPNE3
Plate 4	B11	M-011550-00	D-011550-04	CPNE3

Plate 4	C02	M-004940-00	D-004940-01	CAMK1
Plate 4	C02	M-004940-00	D-004940-02	CAMK1
Plate 4	C02	M-004940-00	D-004940-03	CAMK1
Plate 4	C02	M-004940-00	D-004940-04	CAMK1
Plate 4	C03	M-003517-03	D-003517-02	MARK3
Plate 4	C03	M-003517-03	D-003517-03	MARK3
Plate 4	C03	M-003517-03	D-003517-04	MARK3
Plate 4	C03	M-003517-03	D-003517-10	MARK3
Plate 4	C04	M-005016-01	D-005016-01	MGC42105
Plate 4	C04	M-005016-01	D-005016-03	MGC42105
Plate 4	C04	M-005016-01	D-005016-04	MGC42105
Plate 4	C04	M-005016-01	D-005016-05	MGC42105
Plate 4	C05	M-003255-04	D-003255-06	CHEK1
Plate 4	C05	M-003255-04	D-003255-07	CHEK1
Plate 4	C05	M-003255-04	D-003255-08	CHEK1
Plate 4	C05	M-003255-04	D-003255-26	CHEK1
Plate 4	C06	M-011505-02	D-011505-01	SCAP1
Plate 4	C06	M-011505-02	D-011505-03	SCAP1
Plate 4	C06	M-011505-02	D-011505-05	SCAP1
Plate 4	C06	M-011505-02	D-011505-06	SCAP1
Plate 4	C07	M-181567-01	D-181567-09	CDC2L2
Plate 4	C07	M-181567-01	D-181567-10	CDC2L2
Plate 4	C07	M-181567-01	D-181567-11	CDC2L2
Plate 4	C07	M-181567-01	D-181567-12	CDC2L2
Plate 4	C08	M-004874-02	D-004874-01	STK3
Plate 4	C08	M-004874-02	D-004874-04	STK3
Plate 4	C08	M-004874-02	D-004874-05	STK3
Plate 4	C08	M-004874-02	D-004874-18	STK3
Plate 4	C09	M-003138-02	D-003138-05	FLT4
Plate 4	C09	M-003138-02	D-003138-06	FLT4
Plate 4	C09	M-003138-02	D-003138-07	FLT4
Plate 4	C09	M-003138-02	D-003138-08	FLT4
Plate 4	C10	M-004687-02	D-004687-02	CDC2L1
Plate 4	C10	M-004687-02	D-004687-03	CDC2L1
Plate 4	C10	M-004687-02	D-004687-04	CDC2L1
Plate 4	C10	M-004687-02	D-004687-05	CDC2L1
Plate 4	C11	M-004016-01	D-004016-02	MAP2K7
Plate 4	C11	M-004016-01	D-004016-04	MAP2K7
Plate 4	C11	M-004016-01	D-004016-05	MAP2K7
Plate 4	C11	M-004016-01	D-004016-06	MAP2K7
Plate 4	D02	M-003125-02	D-003125-05	EPHB6
Plate 4	D02	M-003125-02	D-003125-06	EPHB6
Plate 4	D02	M-003125-02	D-003125-07	EPHB6
Plate 4	D02	M-003125-02	D-003125-08	EPHB6
Plate 4	D03	M-004259-03	D-004259-01	MARK1
Plate 4	D03	M-004259-03	D-004259-02	MARK1
Plate 4	D03	M-004259-03	D-004259-03	MARK1
Plate 4	D03	M-004259-03	D-004259-07	MARK1
Plate 4	D04	M-007671-01	D-007671-01	PRKAR2A
Plate 4	D04	M-007671-01	D-007671-02	PRKAR2A
Plate 4	D04	M-007671-01	D-007671-03	PRKAR2A
Plate 4	D04	M-007671-01	D-007671-17	PRKAR2A
Plate 4	D05	M-004030-02	D-004030-02	PINK1
Plate 4	D05	M-004030-02	D-004030-03	PINK1
Plate 4	D05	M-004030-02	D-004030-04	PINK1
Plate 4	D05	M-004030-02	D-004030-05	PINK1
Plate 4	D06	M-003158-01	D-003158-05	MUSK
Plate 4	D06	M-003158-01	D-003158-06	MUSK
Plate 4	D06	M-003158-01	D-003158-07	MUSK
Plate 4	D06	M-003158-01	D-003158-08	MUSK
Plate 4	D07	M-005396-01	D-005396-01	ULK2
Plate 4	D07	M-005396-01	D-005396-03	ULK2
Plate 4	D07	M-005396-01	D-005396-04	ULK2
Plate 4	D07	M-005396-01	D-005396-05	ULK2
Plate 4	D08	M-005349-02	D-005349-01	MGC8407
Plate 4	D08	M-005349-02	D-005349-04	MGC8407
Plate 4	D08	M-005349-02	D-005349-06	MGC8407
Plate 4	D08	M-005349-02	D-005349-19	MGC8407
Plate 4	D09	M-003545-10	D-003545-02	AURKA
Plate 4	D09	M-003545-10	D-003545-05	AURKA
Plate 4	D09	M-003545-10	D-003545-18	AURKA
Plate 4	D09	M-003545-10	D-003545-35	AURKA
Plate 4	D10	M-003615-03	D-003615-03	PAK4
Plate 4	D10	M-003615-03	D-003615-05	PAK4
Plate 4	D10	M-003615-03	D-003615-06	PAK4
Plate 4	D10	M-003615-03	D-003615-07	PAK4
Plate 4	D11	M-003555-04	D-003555-01	MAPK1
Plate 4	D11	M-003555-04	D-003555-03	MAPK1
Plate 4	D11	M-003555-04	D-003555-04	MAPK1
Plate 4	D11	M-003555-04	D-003555-09	MAPK1

Plate 4	E02	M-031608-01	D-031608-03	MAST4
Plate 4	E02	M-031608-01	D-031608-17	MAST4
Plate 4	E02	M-031608-01	D-031608-18	MAST4
Plate 4	E02	M-031608-01	D-031608-19	MAST4
Plate 4	E03	M-006709-01	D-006709-01	CKMT2
Plate 4	E03	M-006709-01	D-006709-02	CKMT2
Plate 4	E03	M-006709-01	D-006709-03	CKMT2
Plate 4	E03	M-006709-01	D-006709-04	CKMT2
Plate 4	E04	M-019546-00	D-019546-01	PIK3R3
Plate 4	E04	M-019546-00	D-019546-02	PIK3R3
Plate 4	E04	M-019546-00	D-019546-03	PIK3R3
Plate 4	E04	M-019546-00	D-019546-04	PIK3R3
Plate 4	E05	M-004926-02	D-004926-01	ACVR2
Plate 4	E05	M-004926-02	D-004926-02	ACVR2
Plate 4	E05	M-004926-02	D-004926-03	ACVR2
Plate 4	E05	M-004926-02	D-004926-05	ACVR2
Plate 4	E06	M-005364-03	D-005364-04	PRKWNK3
Plate 4	E06	M-005364-03	D-005364-05	PRKWNK3
Plate 4	E06	M-005364-03	D-005364-06	PRKWNK3
Plate 4	E06	M-005364-03	D-005364-07	PRKWNK3
Plate 4	E07	M-003526-04	D-003526-10	PRKCZ
Plate 4	E07	M-003526-04	D-003526-11	PRKCZ
Plate 4	E07	M-003526-04	D-003526-12	PRKCZ
Plate 4	E07	M-003526-04	D-003526-13	PRKCZ
Plate 4	E08	M-003144-03	D-003144-09	ITK
Plate 4	E08	M-003144-03	D-003144-11	ITK
Plate 4	E08	M-003144-03	D-003144-12	ITK
Plate 4	E08	M-003144-03	D-003144-25	ITK
Plate 4	E09	M-004912-01	D-004912-01	CAMKK1
Plate 4	E09	M-004912-01	D-004912-02	CAMKK1
Plate 4	E09	M-004912-01	D-004912-04	CAMKK1
Plate 4	E09	M-004912-01	D-004912-17	CAMKK1
Plate 4	E10	M-005039-02	D-005039-05	STK36
Plate 4	E10	M-005039-02	D-005039-06	STK36
Plate 4	E10	M-005039-02	D-005039-07	STK36
Plate 4	E10	M-005039-02	D-005039-21	STK36
Plate 4	E11	M-003514-04	D-003514-13	MAPK8
Plate 4	E11	M-003514-04	D-003514-15	MAPK8
Plate 4	E11	M-003514-04	D-003514-16	MAPK8
Plate 4	E11	M-003514-04	D-003514-29	MAPK8
Plate 4	F02	M-003929-02	D-003929-05	TGFBR1
Plate 4	F02	M-003929-02	D-003929-06	TGFBR1
Plate 4	F02	M-003929-02	D-003929-07	TGFBR1
Plate 4	F02	M-003929-02	D-003929-08	TGFBR1
Plate 4	F03	M-008885-00	D-008885-01	CDK5R2
Plate 4	F03	M-008885-00	D-008885-02	CDK5R2
Plate 4	F03	M-008885-00	D-008885-03	CDK5R2
Plate 4	F03	M-008885-00	D-008885-04	CDK5R2
Plate 4	F04	M-005341-02	D-005341-01	LOC91461
Plate 4	F04	M-005341-02	D-005341-02	LOC91461
Plate 4	F04	M-005341-02	D-005341-05	LOC91461
Plate 4	F04	M-005341-02	D-005341-06	LOC91461
Plate 4	F05	M-025870-01	D-025870-01	DKFZP761P0
Plate 4	F05	M-025870-01	D-025870-02	DKFZP761P0
Plate 4	F05	M-025870-01	D-025870-03	DKFZP761P0
Plate 4	F05	M-025870-01	D-025870-04	DKFZP761P0
Plate 4	F06	M-004049-03	D-004049-01	DUSTYPK
Plate 4	F06	M-004049-03	D-004049-02	DUSTYPK
Plate 4	F06	M-004049-03	D-004049-03	DUSTYPK
Plate 4	F06	M-004049-03	D-004049-04	DUSTYPK
Plate 4	F07	M-005321-00	D-005321-01	FLJ23356
Plate 4	F07	M-005321-00	D-005321-02	FLJ23356
Plate 4	F07	M-005321-00	D-005321-03	FLJ23356
Plate 4	F07	M-005321-00	D-005321-04	FLJ23356
Plate 4	F08	M-005021-02	D-005021-02	PDK3
Plate 4	F08	M-005021-02	D-005021-03	PDK3
Plate 4	F08	M-005021-02	D-005021-05	PDK3
Plate 4	F08	M-005021-02	D-005021-06	PDK3
Plate 4	F09	M-006711-03	D-006711-05	DGKA
Plate 4	F09	M-006711-03	D-006711-06	DGKA
Plate 4	F09	M-006711-03	D-006711-19	DGKA
Plate 4	F09	M-006711-03	D-006711-20	DGKA
Plate 4	F10	M-006703-03	D-006703-01	C9ORF12
Plate 4	F10	M-006703-03	D-006703-03	C9ORF12
Plate 4	F10	M-006703-03	D-006703-05	C9ORF12
Plate 4	F10	M-006703-03	D-006703-06	C9ORF12
Plate 4	F11	M-003166-02	D-003166-05	PTK6
Plate 4	F11	M-003166-02	D-003166-06	PTK6
Plate 4	F11	M-003166-02	D-003166-07	PTK6
Plate 4	F11	M-003166-02	D-003166-21	PTK6

Plate 4	G02	M-003521-04	D-003521-03	PAK1
Plate 4	G02	M-003521-04	D-003521-05	PAK1
Plate 4	G02	M-003521-04	D-003521-07	PAK1
Plate 4	G02	M-003521-04	D-003521-21	PAK1
Plate 4	G03	M-003174-03	D-003174-05	RYK
Plate 4	G03	M-003174-03	D-003174-08	RYK
Plate 4	G03	M-003174-03	D-003174-09	RYK
Plate 4	G03	M-003174-03	D-003174-22	RYK
Plate 4	G04	M-005070-02	D-005070-01	PDXK
Plate 4	G04	M-005070-02	D-005070-02	PDXK
Plate 4	G04	M-005070-02	D-005070-04	PDXK
Plate 4	G04	M-005070-02	D-005070-05	PDXK
Plate 4	G05	M-004866-00	D-004866-01	NEK8
Plate 4	G05	M-004866-00	D-004866-02	NEK8
Plate 4	G05	M-004866-00	D-004866-03	NEK8
Plate 4	G05	M-004866-00	D-004866-04	NEK8
Plate 4	G06	M-006727-00	D-006727-01	GK
Plate 4	G06	M-006727-00	D-006727-02	GK
Plate 4	G06	M-006727-00	D-006727-03	GK
Plate 4	G06	M-006727-00	D-006727-04	GK
Plate 4	G07	M-005322-02	D-005322-01	KSR2
Plate 4	G07	M-005322-02	D-005322-02	KSR2
Plate 4	G07	M-005322-02	D-005322-03	KSR2
Plate 4	G07	M-005322-02	D-005322-05	KSR2
Plate 4	G08	M-007670-02	D-007670-02	PRKAR1A
Plate 4	G08	M-007670-02	D-007670-04	PRKAR1A
Plate 4	G08	M-007670-02	D-007670-05	PRKAR1A
Plate 4	G08	M-007670-02	D-007670-18	PRKAR1A
Plate 4	G09	M-012468-01	D-012468-01	NUP62
Plate 4	G09	M-012468-01	D-012468-03	NUP62
Plate 4	G09	M-012468-01	D-012468-04	NUP62
Plate 4	G09	M-012468-01	D-012468-17	NUP62
Plate 4	G10	M-003172-01	D-003172-05	ROR2
Plate 4	G10	M-003172-01	D-003172-06	ROR2
Plate 4	G10	M-003172-01	D-003172-07	ROR2
Plate 4	G10	M-003172-01	D-003172-08	ROR2
Plate 4	G11	M-004535-00	D-004535-01	PIP5K2C
Plate 4	G11	M-004535-00	D-004535-02	PIP5K2C
Plate 4	G11	M-004535-00	D-004535-03	PIP5K2C
Plate 4	G11	M-004535-00	D-004535-04	PIP5K2C
Plate 4	H02	M-004924-02	D-004924-01	ACVR1
Plate 4	H02	M-004924-02	D-004924-02	ACVR1
Plate 4	H02	M-004924-02	D-004924-03	ACVR1
Plate 4	H02	M-004924-02	D-004924-18	ACVR1
Plate 4	H03	M-004650-00	D-004650-01	PRKACB
Plate 4	H03	M-004650-00	D-004650-02	PRKACB
Plate 4	H03	M-004650-00	D-004650-03	PRKACB
Plate 4	H03	M-004650-00	D-004650-04	PRKACB
Plate 4	H04	M-004875-02	D-004875-01	STK39
Plate 4	H04	M-004875-02	D-004875-02	STK39
Plate 4	H04	M-004875-02	D-004875-04	STK39
Plate 4	H04	M-004875-02	D-004875-05	STK39
Plate 4	H05	M-003154-04	D-003154-01	MATK
Plate 4	H05	M-003154-04	D-003154-07	MATK
Plate 4	H05	M-003154-04	D-003154-08	MATK
Plate 4	H05	M-003154-04	D-003154-09	MATK
Plate 4	H06	M-003616-03	D-003616-09	RPS6KB1
Plate 4	H06	M-003616-03	D-003616-10	RPS6KB1
Plate 4	H06	M-003616-03	D-003616-11	RPS6KB1
Plate 4	H06	M-003616-03	D-003616-12	RPS6KB1
Plate 4	H07	M-007260-01	D-007260-01	RFK
Plate 4	H07	M-007260-01	D-007260-02	RFK
Plate 4	H07	M-007260-01	D-007260-03	RFK
Plate 4	H07	M-007260-01	D-007260-04	RFK
Plate 4	H08	M-004682-01	D-004682-01	TTBK2
Plate 4	H08	M-004682-01	D-004682-02	TTBK2
Plate 4	H08	M-004682-01	D-004682-03	TTBK2
Plate 4	H08	M-004682-01	D-004682-04	TTBK2
Plate 4	H09	M-003814-04	D-003814-01	CDC42BPA
Plate 4	H09	M-003814-04	D-003814-04	CDC42BPA
Plate 4	H09	M-003814-04	D-003814-08	CDC42BPA
Plate 4	H09	M-003814-04	D-003814-09	CDC42BPA
Plate 4	H10	M-005327-01	D-005327-01	GSG2
Plate 4	H10	M-005327-01	D-005327-02	GSG2
Plate 4	H10	M-005327-01	D-005327-03	GSG2
Plate 4	H10	M-005327-01	D-005327-04	GSG2
Plate 4	H11	M-004809-03	D-004809-06	HIPK1
Plate 4	H11	M-004809-03	D-004809-21	HIPK1
Plate 4	H11	M-004809-03	D-004809-22	HIPK1
Plate 4	H11	M-004809-03	D-004809-23	HIPK1

Plate 5	A02	M-003577-03	D-003577-02	MAP3K11
Plate 5	A02	M-003577-03	D-003577-03	MAP3K11
Plate 5	A02	M-003577-03	D-003577-05	MAP3K11
Plate 5	A02	M-003577-03	D-003577-07	MAP3K11
Plate 5	A03	M-003326-08	D-003326-07	AURKB
Plate 5	A03	M-003326-08	D-003326-08	AURKB
Plate 5	A03	M-003326-08	D-003326-09	AURKB
Plate 5	A03	M-003326-08	D-003326-10	AURKB
Plate 5	A04	M-003311-03	D-003311-06	LIMK2
Plate 5	A04	M-003311-03	D-003311-07	LIMK2
Plate 5	A04	M-003311-03	D-003311-08	LIMK2
Plate 5	A04	M-003311-03	D-003311-09	LIMK2
Plate 5	A05	M-004625-01	D-004625-01	GRK4
Plate 5	A05	M-004625-01	D-004625-02	GRK4
Plate 5	A05	M-004625-01	D-004625-03	GRK4
Plate 5	A05	M-004625-01	D-004625-04	GRK4
Plate 5	A06	M-027171-02	D-027171-01	LOC340156
Plate 5	A06	M-027171-02	D-027171-02	LOC340156
Plate 5	A06	M-027171-02	D-027171-03	LOC340156
Plate 5	A06	M-027171-02	D-027171-04	LOC340156
Plate 5	A07	M-004660-02	D-004660-04	PRKX
Plate 5	A07	M-004660-02	D-004660-05	PRKX
Plate 5	A07	M-004660-02	D-004660-06	PRKX
Plate 5	A07	M-004660-02	D-004660-07	PRKX
Plate 5	A08	M-006729-00	D-006729-01	GNE
Plate 5	A08	M-006729-00	D-006729-02	GNE
Plate 5	A08	M-006729-00	D-006729-03	GNE
Plate 5	A08	M-006729-00	D-006729-04	GNE
Plate 5	A09	M-030847-01	D-030847-05	PRKAR1B
Plate 5	A09	M-030847-01	D-030847-06	PRKAR1B
Plate 5	A09	M-030847-01	D-030847-07	PRKAR1B
Plate 5	A09	M-030847-01	D-030847-08	PRKAR1B
Plate 5	A10	M-006749-00	D-006749-01	MVK
Plate 5	A10	M-006749-00	D-006749-02	MVK
Plate 5	A10	M-006749-00	D-006749-03	MVK
Plate 5	A10	M-006749-00	D-006749-04	MVK
Plate 5	A11	M-008224-01	D-008224-02	PKIB
Plate 5	A11	M-008224-01	D-008224-04	PKIB
Plate 5	A11	M-008224-01	D-008224-05	PKIB
Plate 5	A11	M-008224-01	D-008224-06	PKIB
Plate 5	B02	M-003239-01	D-003239-05	CDK5
Plate 5	B02	M-003239-01	D-003239-06	CDK5
Plate 5	B02	M-003239-01	D-003239-07	CDK5
Plate 5	B02	M-003239-01	D-003239-08	CDK5
Plate 5	B03	M-005305-01	D-005305-01	ADCK4
Plate 5	B03	M-005305-01	D-005305-02	ADCK4
Plate 5	B03	M-005305-01	D-005305-04	ADCK4
Plate 5	B03	M-005305-01	D-005305-05	ADCK4
Plate 5	B04	M-005007-00	D-005007-01	HRI
Plate 5	B04	M-005007-00	D-005007-02	HRI
Plate 5	B04	M-005007-00	D-005007-03	HRI
Plate 5	B04	M-005007-00	D-005007-04	HRI
Plate 5	B05	M-005014-01	D-005014-01	MAPKAPK3
Plate 5	B05	M-005014-01	D-005014-04	MAPKAPK3
Plate 5	B05	M-005014-01	D-005014-05	MAPKAPK3
Plate 5	B05	M-005014-01	D-005014-06	MAPKAPK3
Plate 5	B06	M-004927-01	D-004927-01	ACVR2B
Plate 5	B06	M-004927-01	D-004927-02	ACVR2B
Plate 5	B06	M-004927-01	D-004927-04	ACVR2B
Plate 5	B06	M-004927-01	D-004927-17	ACVR2B
Plate 5	B07	M-003114-03	D-003114-06	EGFR
Plate 5	B07	M-003114-03	D-003114-08	EGFR
Plate 5	B07	M-003114-03	D-003114-22	EGFR
Plate 5	B07	M-003114-03	D-003114-23	EGFR
Plate 5	B08	M-003173-01	D-003173-05	ROS1
Plate 5	B08	M-003173-01	D-003173-06	ROS1
Plate 5	B08	M-003173-01	D-003173-07	ROS1
Plate 5	B08	M-003173-01	D-003173-08	ROS1
Plate 5	B09	M-006736-00	D-006736-01	HK3
Plate 5	B09	M-006736-00	D-006736-02	HK3
Plate 5	B09	M-006736-00	D-006736-03	HK3
Plate 5	B09	M-006736-00	D-006736-04	HK3
Plate 5	B10	M-003112-04	D-003112-06	DDR2
Plate 5	B10	M-003112-04	D-003112-09	DDR2
Plate 5	B10	M-003112-04	D-003112-23	DDR2
Plate 5	B10	M-003112-04	D-003112-24	DDR2
Plate 5	B11	M-004418-03	D-004418-01	DAPK2
Plate 5	B11	M-004418-03	D-004418-03	DAPK2
Plate 5	B11	M-004418-03	D-004418-04	DAPK2
Plate 5	B11	M-004418-03	D-004418-05	DAPK2

Plate 5	C02	M-006741-00	D-006741-01	ITPK1
Plate 5	C02	M-006741-00	D-006741-02	ITPK1
Plate 5	C02	M-006741-00	D-006741-03	ITPK1
Plate 5	C02	M-006741-00	D-006741-04	ITPK1
Plate 5	C03	M-027180-01	D-027180-01	ILK-2
Plate 5	C03	M-027180-01	D-027180-02	ILK-2
Plate 5	C03	M-027180-01	D-027180-03	ILK-2
Plate 5	C03	M-027180-01	D-027180-05	ILK-2
Plate 5	C04	M-003116-02	D-003116-06	EPHA2
Plate 5	C04	M-003116-02	D-003116-08	EPHA2
Plate 5	C04	M-003116-02	D-003116-21	EPHA2
Plate 5	C04	M-003116-02	D-003116-22	EPHA2
Plate 5	C05	M-005023-02	D-005023-01	PHKG1
Plate 5	C05	M-005023-02	D-005023-02	PHKG1
Plate 5	C05	M-005023-02	D-005023-04	PHKG1
Plate 5	C05	M-005023-02	D-005023-05	PHKG1
Plate 5	C06	M-007255-01	D-007255-01	FUK
Plate 5	C06	M-007255-01	D-007255-02	FUK
Plate 5	C06	M-007255-01	D-007255-03	FUK
Plate 5	C06	M-007255-01	D-007255-04	FUK
Plate 5	C07	M-006700-02	D-006700-02	AK3
Plate 5	C07	M-006700-02	D-006700-03	AK3
Plate 5	C07	M-006700-02	D-006700-04	AK3
Plate 5	C07	M-006700-02	D-006700-05	AK3
Plate 5	C08	M-004752-00	D-004752-01	CSNK2A2
Plate 5	C08	M-004752-00	D-004752-02	CSNK2A2
Plate 5	C08	M-004752-00	D-004752-03	CSNK2A2
Plate 5	C08	M-004752-00	D-004752-04	CSNK2A2
Plate 5	C09	M-004684-02	D-004684-02	VRK2
Plate 5	C09	M-004684-02	D-004684-04	VRK2
Plate 5	C09	M-004684-02	D-004684-05	VRK2
Plate 5	C09	M-004684-02	D-004684-06	VRK2
Plate 5	C10	M-010019-00	D-010019-01	KALRN
Plate 5	C10	M-010019-00	D-010019-02	KALRN
Plate 5	C10	M-010019-00	D-010019-03	KALRN
Plate 5	C10	M-010019-00	D-010019-04	KALRN
Plate 5	C11	M-003563-03	D-003563-04	ARAF1
Plate 5	C11	M-003563-03	D-003563-06	ARAF1
Plate 5	C11	M-003563-03	D-003563-07	ARAF1
Plate 5	C11	M-003563-03	D-003563-08	ARAF1
Plate 5	D02	M-003875-05	D-003875-02	BCR
Plate 5	D02	M-003875-05	D-003875-03	BCR
Plate 5	D02	M-003875-05	D-003875-06	BCR
Plate 5	D02	M-003875-05	D-003875-13	BCR
Plate 5	D03	M-006710-00	D-006710-01	DCK
Plate 5	D03	M-006710-00	D-006710-02	DCK
Plate 5	D03	M-006710-00	D-006710-03	DCK
Plate 5	D03	M-006710-00	D-006710-04	DCK
Plate 5	D04	M-005346-00	D-005346-01	MGC16169
Plate 5	D04	M-005346-00	D-005346-02	MGC16169
Plate 5	D04	M-005346-00	D-005346-03	MGC16169
Plate 5	D04	M-005346-00	D-005346-04	MGC16169
Plate 5	D05	M-005038-02	D-005038-05	STK22D
Plate 5	D05	M-005038-02	D-005038-07	STK22D
Plate 5	D05	M-005038-02	D-005038-08	STK22D
Plate 5	D05	M-005038-02	D-005038-09	STK22D
Plate 5	D06	M-019716-01	D-019716-01	SRP72
Plate 5	D06	M-019716-01	D-019716-02	SRP72
Plate 5	D06	M-019716-01	D-019716-03	SRP72
Plate 5	D06	M-019716-01	D-019716-17	SRP72
Plate 5	D07	M-006717-01	D-006717-01	DGKI
Plate 5	D07	M-006717-01	D-006717-03	DGKI
Plate 5	D07	M-006717-01	D-006717-05	DGKI
Plate 5	D07	M-006717-01	D-006717-06	DGKI
Plate 5	D08	M-003110-02	D-003110-06	CSK
Plate 5	D08	M-003110-02	D-003110-07	CSK
Plate 5	D08	M-003110-02	D-003110-08	CSK
Plate 5	D08	M-003110-02	D-003110-09	CSK
Plate 5	D09	M-009371-00	D-009371-01	IKBKAP
Plate 5	D09	M-009371-00	D-009371-02	IKBKAP
Plate 5	D09	M-009371-00	D-009371-03	IKBKAP
Plate 5	D09	M-009371-00	D-009371-04	IKBKAP
Plate 5	D10	M-004326-02	D-004326-01	ADRBK2
Plate 5	D10	M-004326-02	D-004326-02	ADRBK2
Plate 5	D10	M-004326-02	D-004326-03	ADRBK2
Plate 5	D10	M-004326-02	D-004326-21	ADRBK2
Plate 5	D11	M-004811-02	D-004811-02	ICK
Plate 5	D11	M-004811-02	D-004811-03	ICK
Plate 5	D11	M-004811-02	D-004811-04	ICK
Plate 5	D11	M-004811-02	D-004811-05	ICK

Plate 5	E02	M-005304-01	D-005304-02	ADCK2
Plate 5	E02	M-005304-01	D-005304-03	ADCK2
Plate 5	E02	M-005304-01	D-005304-04	ADCK2
Plate 5	E02	M-005304-01	D-005304-05	ADCK2
Plate 5	E03	M-006769-01	D-006769-01	PI4K2B
Plate 5	E03	M-006769-01	D-006769-03	PI4K2B
Plate 5	E03	M-006769-01	D-006769-04	PI4K2B
Plate 5	E03	M-006769-01	D-006769-05	PI4K2B
Plate 5	E04	M-003754-01	D-003754-05	TRIB3
Plate 5	E04	M-003754-01	D-003754-06	TRIB3
Plate 5	E04	M-003754-01	D-003754-07	TRIB3
Plate 5	E04	M-003754-01	D-003754-08	TRIB3
Plate 5	E05	M-004843-01	D-004843-01	FLJ23074
Plate 5	E05	M-004843-01	D-004843-03	FLJ23074
Plate 5	E05	M-004843-01	D-004843-04	FLJ23074
Plate 5	E05	M-004843-01	D-004843-17	FLJ23074
Plate 5	E06	M-003266-03	D-003266-06	HIPK2
Plate 5	E06	M-003266-03	D-003266-07	HIPK2
Plate 5	E06	M-003266-03	D-003266-08	HIPK2
Plate 5	E06	M-003266-03	D-003266-09	HIPK2
Plate 5	E07	M-006784-00	D-006784-01	PRPS1
Plate 5	E07	M-006784-00	D-006784-02	PRPS1
Plate 5	E07	M-006784-00	D-006784-03	PRPS1
Plate 5	E07	M-006784-00	D-006784-04	PRPS1
Plate 5	E08	M-003478-00	D-003478-01	CSNK1D
Plate 5	E08	M-003478-00	D-003478-02	CSNK1D
Plate 5	E08	M-003478-00	D-003478-03	CSNK1D
Plate 5	E08	M-003478-00	D-003478-04	CSNK1D
Plate 5	E09	M-004731-01	D-004731-01	DYRK3
Plate 5	E09	M-004731-01	D-004731-02	DYRK3
Plate 5	E09	M-004731-01	D-004731-03	DYRK3
Plate 5	E09	M-004731-01	D-004731-04	DYRK3
Plate 5	E10	M-003182-02	D-003182-06	TYK2
Plate 5	E10	M-003182-02	D-003182-07	TYK2
Plate 5	E10	M-003182-02	D-003182-08	TYK2
Plate 5	E10	M-003182-02	D-003182-21	TYK2
Plate 5	E11	M-004862-01	D-004862-01	MYO3A
Plate 5	E11	M-004862-01	D-004862-02	MYO3A
Plate 5	E11	M-004862-01	D-004862-03	MYO3A
Plate 5	E11	M-004862-01	D-004862-04	MYO3A
Plate 5	F02	M-004172-03	D-004172-22	SPHK1
Plate 5	F02	M-004172-03	D-004172-23	SPHK1
Plate 5	F02	M-004172-03	D-004172-24	SPHK1
Plate 5	F02	M-004172-03	D-004172-25	SPHK1
Plate 5	F03	M-004165-02	D-004165-01	ASK
Plate 5	F03	M-004165-02	D-004165-03	ASK
Plate 5	F03	M-004165-02	D-004165-06	ASK
Plate 5	F03	M-004165-02	D-004165-22	ASK
Plate 5	F04	M-003163-03	D-003163-05	PDGFRB
Plate 5	F04	M-003163-03	D-003163-06	PDGFRB
Plate 5	F04	M-003163-03	D-003163-07	PDGFRB
Plate 5	F04	M-003163-03	D-003163-09	PDGFRB
Plate 5	F05	M-003135-03	D-003135-05	FGR
Plate 5	F05	M-003135-03	D-003135-06	FGR
Plate 5	F05	M-003135-03	D-003135-08	FGR
Plate 5	F05	M-003135-03	D-003135-22	FGR
Plate 5	F06	M-003171-02	D-003171-08	ROR1
Plate 5	F06	M-003171-02	D-003171-21	ROR1
Plate 5	F06	M-003171-02	D-003171-22	ROR1
Plate 5	F06	M-003171-02	D-003171-23	ROR1
Plate 5	F07	M-004031-03	D-004031-01	CRK7
Plate 5	F07	M-004031-03	D-004031-02	CRK7
Plate 5	F07	M-004031-03	D-004031-04	CRK7
Plate 5	F07	M-004031-03	D-004031-06	CRK7
Plate 5	F08	M-003472-00	D-003472-01	CDKN1B
Plate 5	F08	M-003472-00	D-003472-02	CDKN1B
Plate 5	F08	M-003472-00	D-003472-03	CDKN1B
Plate 5	F08	M-003472-00	D-003472-04	CDKN1B
Plate 5	F09	M-007735-00	D-007735-01	PACSIN1
Plate 5	F09	M-007735-00	D-007735-02	PACSIN1
Plate 5	F09	M-007735-00	D-007735-03	PACSIN1
Plate 5	F09	M-007735-00	D-007735-04	PACSIN1
Plate 5	F10	M-004947-00	D-004947-01	DAPK3
Plate 5	F10	M-004947-00	D-004947-02	DAPK3
Plate 5	F10	M-004947-00	D-004947-03	DAPK3
Plate 5	F10	M-004947-00	D-004947-04	DAPK3
Plate 5	F11	M-003020-04	D-003020-10	PIK3R1
Plate 5	F11	M-003020-04	D-003020-11	PIK3R1
Plate 5	F11	M-003020-04	D-003020-26	PIK3R1
Plate 5	F11	M-003020-04	D-003020-27	PIK3R1

Plate 5	G02	M-004661-03	D-004661-08	PRKY
Plate 5	G02	M-004661-03	D-004661-09	PRKY
Plate 5	G02	M-004661-03	D-004661-22	PRKY
Plate 5	G02	M-004661-03	D-004661-23	PRKY
Plate 5	G03	M-003575-02	D-003575-02	MAP3K1
Plate 5	G03	M-003575-02	D-003575-03	MAP3K1
Plate 5	G03	M-003575-02	D-003575-04	MAP3K1
Plate 5	G03	M-003575-02	D-003575-05	MAP3K1
Plate 5	G04	M-005398-04	D-005398-09	ZAP70
Plate 5	G04	M-005398-04	D-005398-13	ZAP70
Plate 5	G04	M-005398-04	D-005398-14	ZAP70
Plate 5	G04	M-005398-04	D-005398-15	ZAP70
Plate 5	G05	M-004840-03	D-004840-07	STK23
Plate 5	G05	M-004840-03	D-004840-08	STK23
Plate 5	G05	M-004840-03	D-004840-09	STK23
Plate 5	G05	M-004840-03	D-004840-22	STK23
Plate 5	G06	M-003167-03	D-003167-09	PTK7
Plate 5	G06	M-003167-03	D-003167-10	PTK7
Plate 5	G06	M-003167-03	D-003167-11	PTK7
Plate 5	G06	M-003167-03	D-003167-25	PTK7
Plate 5	G07	M-005372-01	D-005372-01	RPS6KL1
Plate 5	G07	M-005372-01	D-005372-02	RPS6KL1
Plate 5	G07	M-005372-01	D-005372-03	RPS6KL1
Plate 5	G07	M-005372-01	D-005372-04	RPS6KL1
Plate 5	G08	M-004670-01	D-004670-01	RPS6KA6
Plate 5	G08	M-004670-01	D-004670-02	RPS6KA6
Plate 5	G08	M-004670-01	D-004670-03	RPS6KA6
Plate 5	G08	M-004670-01	D-004670-04	RPS6KA6
Plate 5	G09	M-003982-02	D-003982-02	SRPK1
Plate 5	G09	M-003982-02	D-003982-04	SRPK1
Plate 5	G09	M-003982-02	D-003982-05	SRPK1
Plate 5	G09	M-003982-02	D-003982-07	SRPK1
Plate 5	G10	M-004649-01	D-004649-01	PRKACA
Plate 5	G10	M-004649-01	D-004649-02	PRKACA
Plate 5	G10	M-004649-01	D-004649-03	PRKACA
Plate 5	G10	M-004649-01	D-004649-17	PRKACA
Plate 5	G11	M-003165-03	D-003165-05	PTK2B
Plate 5	G11	M-003165-03	D-003165-06	PTK2B
Plate 5	G11	M-003165-03	D-003165-07	PTK2B
Plate 5	G11	M-003165-03	D-003165-13	PTK2B
Plate 5	H02	M-003155-02	D-003155-05	MERTK
Plate 5	H02	M-003155-02	D-003155-06	MERTK
Plate 5	H02	M-003155-02	D-003155-21	MERTK
Plate 5	H02	M-003155-02	D-003155-22	MERTK
Plate 5	H03	M-004061-02	D-004061-01	CERK
Plate 5	H03	M-004061-02	D-004061-02	CERK
Plate 5	H03	M-004061-02	D-004061-03	CERK
Plate 5	H03	M-004061-02	D-004061-04	CERK
Plate 5	H04	M-014208-01	D-014208-01	NUCKS
Plate 5	H04	M-014208-01	D-014208-02	NUCKS
Plate 5	H04	M-014208-01	D-014208-03	NUCKS
Plate 5	H04	M-014208-01	D-014208-04	NUCKS
Plate 5	H05	M-004613-00	D-004613-01	CIT
Plate 5	H05	M-004613-00	D-004613-02	CIT
Plate 5	H05	M-004613-00	D-004613-03	CIT
Plate 5	H05	M-004613-00	D-004613-04	CIT
Plate 5	H06	M-022660-01	D-022660-01	CDKL4
Plate 5	H06	M-022660-01	D-022660-02	CDKL4
Plate 5	H06	M-022660-01	D-022660-03	CDKL4
Plate 5	H06	M-022660-01	D-022660-17	CDKL4
Plate 5	H07	M-005339-01	D-005339-01	KIAA2002
Plate 5	H07	M-005339-01	D-005339-02	KIAA2002
Plate 5	H07	M-005339-01	D-005339-03	KIAA2002
Plate 5	H07	M-005339-01	D-005339-04	KIAA2002
Plate 5	H08	M-004870-02	D-004870-01	OSR1
Plate 5	H08	M-004870-02	D-004870-02	OSR1
Plate 5	H08	M-004870-02	D-004870-03	OSR1
Plate 5	H08	M-004870-02	D-004870-18	OSR1
Plate 5	H09	M-004838-01	D-004838-05	RAGE
Plate 5	H09	M-004838-01	D-004838-06	RAGE
Plate 5	H09	M-004838-01	D-004838-07	RAGE
Plate 5	H09	M-004838-01	D-004838-08	RAGE
Plate 5	H10	M-005309-03	D-005309-03	BMPR2
Plate 5	H10	M-005309-03	D-005309-05	BMPR2
Plate 5	H10	M-005309-03	D-005309-07	BMPR2
Plate 5	H10	M-005309-03	D-005309-20	BMPR2
Plate 5	H11	M-005340-02	D-005340-02	NRBP2
Plate 5	H11	M-005340-02	D-005340-05	NRBP2
Plate 5	H11	M-005340-02	D-005340-06	NRBP2
Plate 5	H11	M-005340-02	D-005340-07	NRBP2

Plate 6	A02	M-003574-02	D-003574-01	MAP2K4
Plate 6	A02	M-003574-02	D-003574-03	MAP2K4
Plate 6	A02	M-003574-02	D-003574-05	MAP2K4
Plate 6	A02	M-003574-02	D-003574-06	MAP2K4
Plate 6	A03	M-006318-01	D-006318-01	FLJ13052
Plate 6	A03	M-006318-01	D-006318-02	FLJ13052
Plate 6	A03	M-006318-01	D-006318-03	FLJ13052
Plate 6	A03	M-006318-01	D-006318-04	FLJ13052
Plate 6	A04	M-005389-02	D-005389-01	TLK2
Plate 6	A04	M-005389-02	D-005389-03	TLK2
Plate 6	A04	M-005389-02	D-005389-04	TLK2
Plate 6	A04	M-005389-02	D-005389-05	TLK2
Plate 6	A05	M-009932-02	D-009932-01	TJP2
Plate 6	A05	M-009932-02	D-009932-03	TJP2
Plate 6	A05	M-009932-02	D-009932-05	TJP2
Plate 6	A05	M-009932-02	D-009932-18	TJP2
Plate 6	A06	M-018919-00	D-018919-01	ADCK5
Plate 6	A06	M-018919-00	D-018919-02	ADCK5
Plate 6	A06	M-018919-00	D-018919-03	ADCK5
Plate 6	A06	M-018919-00	D-018919-04	ADCK5
Plate 6	A07	M-003972-03	D-003972-07	MAPK11
Plate 6	A07	M-003972-03	D-003972-08	MAPK11
Plate 6	A07	M-003972-03	D-003972-09	MAPK11
Plate 6	A07	M-003972-03	D-003972-10	MAPK11
Plate 6	A08	M-006768-02	D-006768-03	PGK2
Plate 6	A08	M-006768-02	D-006768-04	PGK2
Plate 6	A08	M-006768-02	D-006768-05	PGK2
Plate 6	A08	M-006768-02	D-006768-18	PGK2
Plate 6	A09	M-004101-02	D-004101-01	BUB1B
Plate 6	A09	M-004101-02	D-004101-02	BUB1B
Plate 6	A09	M-004101-02	D-004101-03	BUB1B
Plate 6	A09	M-004101-02	D-004101-04	BUB1B
Plate 6	A10	M-003966-05	D-003966-08	MAP2K5
Plate 6	A10	M-003966-05	D-003966-10	MAP2K5
Plate 6	A10	M-003966-05	D-003966-11	MAP2K5
Plate 6	A10	M-003966-05	D-003966-24	MAP2K5
Plate 6	A11	M-005009-02	D-005009-01	LAK
Plate 6	A11	M-005009-02	D-005009-03	LAK
Plate 6	A11	M-005009-02	D-005009-04	LAK
Plate 6	A11	M-005009-02	D-005009-05	LAK
Plate 6	B02	M-003241-02	D-003241-05	CDK7
Plate 6	B02	M-003241-02	D-003241-06	CDK7
Plate 6	B02	M-003241-02	D-003241-07	CDK7
Plate 6	B02	M-003241-02	D-003241-08	CDK7
Plate 6	B03	M-005320-02	D-005320-01	LRRK1
Plate 6	B03	M-005320-02	D-005320-03	LRRK1
Plate 6	B03	M-005320-02	D-005320-04	LRRK1
Plate 6	B03	M-005320-02	D-005320-18	LRRK1
Plate 6	B04	M-004624-00	D-004624-01	FLJ25006
Plate 6	B04	M-004624-00	D-004624-02	FLJ25006
Plate 6	B04	M-004624-00	D-004624-03	FLJ25006
Plate 6	B04	M-004624-00	D-004624-04	FLJ25006
Plate 6	B05	M-003512-06	D-003512-15	MAPK14
Plate 6	B05	M-003512-06	D-003512-16	MAPK14
Plate 6	B05	M-003512-06	D-003512-19	MAPK14
Plate 6	B05	M-003512-06	D-003512-32	MAPK14
Plate 6	B06	M-003788-02	D-003788-01	TBK1
Plate 6	B06	M-003788-02	D-003788-02	TBK1
Plate 6	B06	M-003788-02	D-003788-06	TBK1
Plate 6	B06	M-003788-02	D-003788-07	TBK1
Plate 6	B07	M-004878-04	D-004878-10	ERN2
Plate 6	B07	M-004878-04	D-004878-12	ERN2
Plate 6	B07	M-004878-04	D-004878-13	ERN2
Plate 6	B07	M-004878-04	D-004878-26	ERN2
Plate 6	B08	M-004656-02	D-004656-02	PRKCI
Plate 6	B08	M-004656-02	D-004656-03	PRKCI
Plate 6	B08	M-004656-02	D-004656-05	PRKCI
Plate 6	B08	M-004656-02	D-004656-06	PRKCI
Plate 6	B09	M-003723-02	D-003723-03	IKBKE
Plate 6	B09	M-003723-02	D-003723-04	IKBKE
Plate 6	B09	M-003723-02	D-003723-06	IKBKE
Plate 6	B09	M-003723-02	D-003723-07	IKBKE
Plate 6	B10	M-004681-02	D-004681-01	CSNK1A1L
Plate 6	B10	M-004681-02	D-004681-02	CSNK1A1L
Plate 6	B10	M-004681-02	D-004681-04	CSNK1A1L
Plate 6	B10	M-004681-02	D-004681-18	CSNK1A1L
Plate 6	B11	M-004780-02	D-004780-04	PIP5K1A
Plate 6	B11	M-004780-02	D-004780-05	PIP5K1A
Plate 6	B11	M-004780-02	D-004780-06	PIP5K1A
Plate 6	B11	M-004780-02	D-004780-07	PIP5K1A

Plate 6	C02	M-005377-01	D-005377-01	STK17A
Plate 6	C02	M-005377-01	D-005377-02	STK17A
Plate 6	C02	M-005377-01	D-005377-03	STK17A
Plate 6	C02	M-005377-01	D-005377-04	STK17A
Plate 6	C03	M-005386-02	D-005386-03	TEX14
Plate 6	C03	M-005386-02	D-005386-04	TEX14
Plate 6	C03	M-005386-02	D-005386-05	TEX14
Plate 6	C03	M-005386-02	D-005386-06	TEX14
Plate 6	C04	M-003516-02	D-003516-07	MAPKAPK2
Plate 6	C04	M-003516-02	D-003516-08	MAPKAPK2
Plate 6	C04	M-003516-02	D-003516-09	MAPKAPK2
Plate 6	C04	M-003516-02	D-003516-10	MAPKAPK2
Plate 6	C05	M-003152-02	D-003152-06	LTK
Plate 6	C05	M-003152-02	D-003152-07	LTK
Plate 6	C05	M-003152-02	D-003152-08	LTK
Plate 6	C05	M-003152-02	D-003152-21	LTK
Plate 6	C06	M-005311-01	D-005311-01	CASK
Plate 6	C06	M-005311-01	D-005311-02	CASK
Plate 6	C06	M-005311-01	D-005311-05	CASK
Plate 6	C06	M-005311-01	D-005311-06	CASK
Plate 6	C07	M-004806-01	D-004806-01	DYRK1B
Plate 6	C07	M-004806-01	D-004806-02	DYRK1B
Plate 6	C07	M-004806-01	D-004806-04	DYRK1B
Plate 6	C07	M-004806-01	D-004806-05	DYRK1B
Plate 6	C08	M-027174-01	D-027174-01	SBK1
Plate 6	C08	M-027174-01	D-027174-02	SBK1
Plate 6	C08	M-027174-01	D-027174-03	SBK1
Plate 6	C08	M-027174-01	D-027174-04	SBK1
Plate 6	C09	M-004313-02	D-004313-01	PCTK1
Plate 6	C09	M-004313-02	D-004313-02	PCTK1
Plate 6	C09	M-004313-02	D-004313-03	PCTK1
Plate 6	C09	M-004313-02	D-004313-04	PCTK1
Plate 6	C10	M-003789-03	D-003789-06	MAP3K4
Plate 6	C10	M-003789-03	D-003789-07	MAP3K4
Plate 6	C10	M-003789-03	D-003789-09	MAP3K4
Plate 6	C10	M-003789-03	D-003789-10	MAP3K4
Plate 6	C11	M-003313-03	D-003313-05	STK38L
Plate 6	C11	M-003313-03	D-003313-06	STK38L
Plate 6	C11	M-003313-03	D-003313-08	STK38L
Plate 6	C11	M-003313-03	D-003313-09	STK38L
Plate 6	D02	M-005348-00	D-005348-01	MGC4796
Plate 6	D02	M-005348-00	D-005348-02	MGC4796
Plate 6	D02	M-005348-00	D-005348-03	MGC4796
Plate 6	D02	M-005348-00	D-005348-04	MGC4796
Plate 6	D03	M-012321-00	D-012321-01	PKIA
Plate 6	D03	M-012321-00	D-012321-02	PKIA
Plate 6	D03	M-012321-00	D-012321-03	PKIA
Plate 6	D03	M-012321-00	D-012321-04	PKIA
Plate 6	D04	M-006786-00	D-006786-01	RBKS
Plate 6	D04	M-006786-00	D-006786-02	RBKS
Plate 6	D04	M-006786-00	D-006786-03	RBKS
Plate 6	D04	M-006786-00	D-006786-04	RBKS
Plate 6	D05	M-019682-01	D-019682-01	PHKA1
Plate 6	D05	M-019682-01	D-019682-02	PHKA1
Plate 6	D05	M-019682-01	D-019682-03	PHKA1
Plate 6	D05	M-019682-01	D-019682-04	PHKA1
Plate 6	D06	M-004951-02	D-004951-01	ERN1
Plate 6	D06	M-004951-02	D-004951-02	ERN1
Plate 6	D06	M-004951-02	D-004951-03	ERN1
Plate 6	D06	M-004951-02	D-004951-18	ERN1
Plate 6	D07	M-003113-01	D-003113-05	STYK1
Plate 6	D07	M-003113-01	D-003113-06	STYK1
Plate 6	D07	M-003113-01	D-003113-07	STYK1
Plate 6	D07	M-003113-01	D-003113-08	STYK1
Plate 6	D08	M-004931-00	D-004931-01	ARK5
Plate 6	D08	M-004931-00	D-004931-02	ARK5
Plate 6	D08	M-004931-00	D-004931-03	ARK5
Plate 6	D08	M-004931-00	D-004931-04	ARK5
Plate 6	D09	M-004058-02	D-004058-01	PIP5K1B
Plate 6	D09	M-004058-02	D-004058-02	PIP5K1B
Plate 6	D09	M-004058-02	D-004058-03	PIP5K1B
Plate 6	D09	M-004058-02	D-004058-04	PIP5K1B
Plate 6	D10	M-006719-03	D-006719-02	DGUOK
Plate 6	D10	M-006719-03	D-006719-03	DGUOK
Plate 6	D10	M-006719-03	D-006719-04	DGUOK
Plate 6	D10	M-006719-03	D-006719-05	DGUOK
Plate 6	D11	M-006758-00	D-006758-01	PANK3
Plate 6	D11	M-006758-00	D-006758-02	PANK3
Plate 6	D11	M-006758-00	D-006758-03	PANK3
Plate 6	D11	M-006758-00	D-006758-04	PANK3

Plate 6	E02	M-004839-01	D-004839-05	SRPK2
Plate 6	E02	M-004839-01	D-004839-06	SRPK2
Plate 6	E02	M-004839-01	D-004839-07	SRPK2
Plate 6	E02	M-004839-01	D-004839-08	SRPK2
Plate 6	E03	M-004801-02	D-004801-05	CLK2
Plate 6	E03	M-004801-02	D-004801-06	CLK2
Plate 6	E03	M-004801-02	D-004801-07	CLK2
Plate 6	E03	M-004801-02	D-004801-08	CLK2
Plate 6	E04	M-003930-02	D-003930-01	TGFBR2
Plate 6	E04	M-003930-02	D-003930-02	TGFBR2
Plate 6	E04	M-003930-02	D-003930-03	TGFBR2
Plate 6	E04	M-003930-02	D-003930-05	TGFBR2
Plate 6	E05	M-005379-01	D-005379-01	STK22B
Plate 6	E05	M-005379-01	D-005379-02	STK22B
Plate 6	E05	M-005379-01	D-005379-03	STK22B
Plate 6	E05	M-005379-01	D-005379-05	STK22B
Plate 6	E06	M-005005-02	D-005005-03	GAK
Plate 6	E06	M-005005-02	D-005005-04	GAK
Plate 6	E06	M-005005-02	D-005005-05	GAK
Plate 6	E06	M-005005-02	D-005005-18	GAK
Plate 6	E07	M-004663-02	D-004663-02	RPS6KA2
Plate 6	E07	M-004663-02	D-004663-04	RPS6KA2
Plate 6	E07	M-004663-02	D-004663-05	RPS6KA2
Plate 6	E07	M-004663-02	D-004663-18	RPS6KA2
Plate 6	E08	M-003594-02	D-003594-06	MAPK6
Plate 6	E08	M-003594-02	D-003594-07	MAPK6
Plate 6	E08	M-003594-02	D-003594-08	MAPK6
Plate 6	E08	M-003594-02	D-003594-09	MAPK6
Plate 6	E09	M-004628-01	D-004628-01	GRK7
Plate 6	E09	M-004628-01	D-004628-02	GRK7
Plate 6	E09	M-004628-01	D-004628-04	GRK7
Plate 6	E09	M-004628-01	D-004628-17	GRK7
Plate 6	E10	M-004325-02	D-004325-05	ADRBK1
Plate 6	E10	M-004325-02	D-004325-06	ADRBK1
Plate 6	E10	M-004325-02	D-004325-07	ADRBK1
Plate 6	E10	M-004325-02	D-004325-08	ADRBK1
Plate 6	E11	M-003235-05	D-003235-10	CDK10
Plate 6	E11	M-003235-05	D-003235-11	CDK10
Plate 6	E11	M-003235-05	D-003235-12	CDK10
Plate 6	E11	M-003235-05	D-003235-13	CDK10
Plate 6	F02	M-003471-00	D-003471-01	CDKN1A
Plate 6	F02	M-003471-00	D-003471-02	CDKN1A
Plate 6	F02	M-003471-00	D-003471-03	CDKN1A
Plate 6	F02	M-003471-00	D-003471-04	CDKN1A
Plate 6	F03	M-003797-03	D-003797-04	PANK2
Plate 6	F03	M-003797-03	D-003797-05	PANK2
Plate 6	F03	M-003797-03	D-003797-06	PANK2
Plate 6	F03	M-003797-03	D-003797-07	PANK2
Plate 6	F04	M-003117-03	D-003117-05	EPHA3
Plate 6	F04	M-003117-03	D-003117-06	EPHA3
Plate 6	F04	M-003117-03	D-003117-08	EPHA3
Plate 6	F04	M-003117-03	D-003117-09	EPHA3
Plate 6	F05	M-006785-01	D-006785-01	PYCS
Plate 6	F05	M-006785-01	D-006785-02	PYCS
Plate 6	F05	M-006785-01	D-006785-03	PYCS
Plate 6	F05	M-006785-01	D-006785-04	PYCS
Plate 6	F06	M-006737-02	D-006737-02	IHPK1
Plate 6	F06	M-006737-02	D-006737-04	IHPK1
Plate 6	F06	M-006737-02	D-006737-19	IHPK1
Plate 6	F06	M-006737-02	D-006737-20	IHPK1
Plate 6	F07	M-004937-02	D-004937-02	BRD4
Plate 6	F07	M-004937-02	D-004937-03	BRD4
Plate 6	F07	M-004937-02	D-004937-04	BRD4
Plate 6	F07	M-004937-02	D-004937-05	BRD4
Plate 6	F08	M-003177-03	D-003177-18	TEC
Plate 6	F08	M-003177-03	D-003177-19	TEC
Plate 6	F08	M-003177-03	D-003177-20	TEC
Plate 6	F08	M-003177-03	D-003177-21	TEC
Plate 6	F09	M-006691-00	D-006691-01	FRDA
Plate 6	F09	M-006691-00	D-006691-02	FRDA
Plate 6	F09	M-006691-00	D-006691-03	FRDA
Plate 6	F09	M-006691-00	D-006691-04	FRDA
Plate 6	F10	M-004877-02	D-004877-01	PRPS2
Plate 6	F10	M-004877-02	D-004877-03	PRPS2
Plate 6	F10	M-004877-02	D-004877-04	PRPS2
Plate 6	F10	M-004877-02	D-004877-05	PRPS2
Plate 6	F11	M-004897-02	D-004897-02	AK5
Plate 6	F11	M-004897-02	D-004897-06	AK5
Plate 6	F11	M-004897-02	D-004897-07	AK5
Plate 6	F11	M-004897-02	D-004897-08	AK5

Plate 6	G02	M-004633-01	D-004633-01	MAST2
Plate 6	G02	M-004633-01	D-004633-02	MAST2
Plate 6	G02	M-004633-01	D-004633-03	MAST2
Plate 6	G02	M-004633-01	D-004633-04	MAST2
Plate 6	G03	M-008988-01	D-008988-01	CDK5R1
Plate 6	G03	M-008988-01	D-008988-02	CDK5R1
Plate 6	G03	M-008988-01	D-008988-03	CDK5R1
Plate 6	G03	M-008988-01	D-008988-17	CDK5R1
Plate 6	G04	M-005050-02	D-005050-01	WEE1
Plate 6	G04	M-005050-02	D-005050-02	WEE1
Plate 6	G04	M-005050-02	D-005050-03	WEE1
Plate 6	G04	M-005050-02	D-005050-22	WEE1
Plate 6	G05	M-003240-02	D-003240-05	CDK6
Plate 6	G05	M-003240-02	D-003240-06	CDK6
Plate 6	G05	M-003240-02	D-003240-08	CDK6
Plate 6	G05	M-003240-02	D-003240-09	CDK6
Plate 6	G06	M-003247-03	D-003247-01	CDKN2D
Plate 6	G06	M-003247-03	D-003247-05	CDKN2D
Plate 6	G06	M-003247-03	D-003247-10	CDKN2D
Plate 6	G06	M-003247-03	D-003247-23	CDKN2D
Plate 6	G07	M-003525-01	D-003525-05	PRKCQ
Plate 6	G07	M-003525-01	D-003525-06	PRKCQ
Plate 6	G07	M-003525-01	D-003525-07	PRKCQ
Plate 6	G07	M-003525-01	D-003525-08	PRKCQ
Plate 6	G08	M-009693-01	D-009693-02	PRKAG2
Plate 6	G08	M-009693-01	D-009693-03	PRKAG2
Plate 6	G08	M-009693-01	D-009693-17	PRKAG2
Plate 6	G08	M-009693-01	D-009693-18	PRKAG2
Plate 6	G09	M-003301-02	D-003301-05	MAP3K3
Plate 6	G09	M-003301-02	D-003301-07	MAP3K3
Plate 6	G09	M-003301-02	D-003301-08	MAP3K3
Plate 6	G09	M-003301-02	D-003301-09	MAP3K3
Plate 6	G10	M-013064-01	D-013064-01	FGFRL1
Plate 6	G10	M-013064-01	D-013064-02	FGFRL1
Plate 6	G10	M-013064-01	D-013064-03	FGFRL1
Plate 6	G10	M-013064-01	D-013064-17	FGFRL1
Plate 6	G11	M-006821-01	D-006821-01	NME1
Plate 6	G11	M-006821-01	D-006821-03	NME1
Plate 6	G11	M-006821-01	D-006821-04	NME1
Plate 6	G11	M-006821-01	D-006821-05	NME1
Plate 6	H02	M-003180-03	D-003180-06	TNK1
Plate 6	H02	M-003180-03	D-003180-08	TNK1
Plate 6	H02	M-003180-03	D-003180-09	TNK1
Plate 6	H02	M-003180-03	D-003180-22	TNK1
Plate 6	H03	M-005381-03	D-005381-01	STK29
Plate 6	H03	M-005381-03	D-005381-05	STK29
Plate 6	H03	M-005381-03	D-005381-08	STK29
Plate 6	H03	M-005381-03	D-005381-09	STK29
Plate 6	H04	M-003161-02	D-003161-08	NTRK3
Plate 6	H04	M-003161-02	D-003161-21	NTRK3
Plate 6	H04	M-003161-02	D-003161-22	NTRK3
Plate 6	H04	M-003161-02	D-003161-23	NTRK3
Plate 6	H05	M-003149-02	D-003149-05	LMTK2
Plate 6	H05	M-003149-02	D-003149-06	LMTK2
Plate 6	H05	M-003149-02	D-003149-07	LMTK2
Plate 6	H05	M-003149-02	D-003149-21	LMTK2
Plate 6	H06	M-006720-01	D-006720-03	DTYMK
Plate 6	H06	M-006720-01	D-006720-04	DTYMK
Plate 6	H06	M-006720-01	D-006720-17	DTYMK
Plate 6	H06	M-006720-01	D-006720-18	DTYMK
Plate 6	H07	M-005025-02	D-005025-01	PIK3R4
Plate 6	H07	M-005025-02	D-005025-04	PIK3R4
Plate 6	H07	M-005025-02	D-005025-05	PIK3R4
Plate 6	H07	M-005025-02	D-005025-18	PIK3R4
Plate 6	H08	M-010819-01	D-010819-01	GCK
Plate 6	H08	M-010819-01	D-010819-02	GCK
Plate 6	H08	M-010819-01	D-010819-04	GCK
Plate 6	H08	M-010819-01	D-010819-05	GCK
Plate 6	H09	M-003122-03	D-003122-07	EPHB2
Plate 6	H09	M-003122-03	D-003122-08	EPHB2
Plate 6	H09	M-003122-03	D-003122-25	EPHB2
Plate 6	H09	M-003122-03	D-003122-26	EPHB2
Plate 6	H10	M-004162-02	D-004162-01	SGKL
Plate 6	H10	M-004162-02	D-004162-03	SGKL
Plate 6	H10	M-004162-02	D-004162-04	SGKL
Plate 6	H10	M-004162-02	D-004162-05	SGKL
Plate 6	H11	M-009462-02	D-009462-01	DLG3
Plate 6	H11	M-009462-02	D-009462-02	DLG3
Plate 6	H11	M-009462-02	D-009462-05	DLG3
Plate 6	H11	M-009462-02	D-009462-18	DLG3

Plate 7	A02	M-003170-02	D-003170-05	RET
Plate 7	A02	M-003170-02	D-003170-06	RET
Plate 7	A02	M-003170-02	D-003170-08	RET
Plate 7	A02	M-003170-02	D-003170-21	RET
Plate 7	A03	M-003967-01	D-003967-01	MAP2K6
Plate 7	A03	M-003967-01	D-003967-03	MAP2K6
Plate 7	A03	M-003967-01	D-003967-04	MAP2K6
Plate 7	A03	M-003967-01	D-003967-17	MAP2K6
Plate 7	A04	M-005371-02	D-005371-01	RPS6KC1
Plate 7	A04	M-005371-02	D-005371-02	RPS6KC1
Plate 7	A04	M-005371-02	D-005371-05	RPS6KC1
Plate 7	A04	M-005371-02	D-005371-18	RPS6KC1
Plate 7	A05	M-006756-02	D-006756-03	NME7
Plate 7	A05	M-006756-02	D-006756-05	NME7
Plate 7	A05	M-006756-02	D-006756-06	NME7
Plate 7	A05	M-006756-02	D-006756-07	NME7
Plate 7	A06	M-003576-01	D-003576-01	MAP3K10
Plate 7	A06	M-003576-01	D-003576-02	MAP3K10
Plate 7	A06	M-003576-01	D-003576-03	MAP3K10
Plate 7	A06	M-003576-01	D-003576-05	MAP3K10
Plate 7	A07	M-004062-01	D-004062-01	UCK1
Plate 7	A07	M-004062-01	D-004062-03	UCK1
Plate 7	A07	M-004062-01	D-004062-05	UCK1
Plate 7	A07	M-004062-01	D-004062-07	UCK1
Plate 7	A08	M-003132-04	D-003132-05	FGFR2
Plate 7	A08	M-003132-04	D-003132-06	FGFR2
Plate 7	A08	M-003132-04	D-003132-07	FGFR2
Plate 7	A08	M-003132-04	D-003132-08	FGFR2
Plate 7	A09	M-003127-03	D-003127-08	ERBB3
Plate 7	A09	M-003127-03	D-003127-22	ERBB3
Plate 7	A09	M-003127-03	D-003127-23	ERBB3
Plate 7	A09	M-003127-03	D-003127-24	ERBB3
Plate 7	A10	M-004867-02	D-004867-01	NEK3
Plate 7	A10	M-004867-02	D-004867-02	NEK3
Plate 7	A10	M-004867-02	D-004867-03	NEK3
Plate 7	A10	M-004867-02	D-004867-05	NEK3
Plate 7	A11	M-012101-00	D-012101-01	COL4A3BP
Plate 7	A11	M-012101-00	D-012101-02	COL4A3BP
Plate 7	A11	M-012101-00	D-012101-03	COL4A3BP
Plate 7	A11	M-012101-00	D-012101-04	COL4A3BP
Plate 7	B02	M-004688-01	D-004688-01	CDC2L5
Plate 7	B02	M-004688-01	D-004688-02	CDC2L5
Plate 7	B02	M-004688-01	D-004688-03	CDC2L5
Plate 7	B02	M-004688-01	D-004688-04	CDC2L5
Plate 7	B03	M-003103-02	D-003103-05	ALK
Plate 7	B03	M-003103-02	D-003103-06	ALK
Plate 7	B03	M-003103-02	D-003103-07	ALK
Plate 7	B03	M-003103-02	D-003103-09	ALK
Plate 7	B04	M-007687-01	D-007687-01	SPEG
Plate 7	B04	M-007687-01	D-007687-02	SPEG
Plate 7	B04	M-007687-01	D-007687-03	SPEG
Plate 7	B04	M-007687-01	D-007687-05	SPEG
Plate 7	B05	M-003108-02	D-003108-05	TP53RK
Plate 7	B05	M-003108-02	D-003108-07	TP53RK
Plate 7	B05	M-003108-02	D-003108-21	TP53RK
Plate 7	B05	M-003108-02	D-003108-22	TP53RK
Plate 7	B06	M-011649-01	D-011649-02	EFNA5
Plate 7	B06	M-011649-01	D-011649-03	EFNA5
Plate 7	B06	M-011649-01	D-011649-17	EFNA5
Plate 7	B06	M-011649-01	D-011649-18	EFNA5
Plate 7	B07	M-003591-02	D-003591-01	MAPK13
Plate 7	B07	M-003591-02	D-003591-03	MAPK13
Plate 7	B07	M-003591-02	D-003591-04	MAPK13
Plate 7	B07	M-003591-02	D-003591-06	MAPK13
Plate 7	B08	M-005391-01	D-005391-01	TRIB2
Plate 7	B08	M-005391-01	D-005391-02	TRIB2
Plate 7	B08	M-005391-01	D-005391-03	TRIB2
Plate 7	B08	M-005391-01	D-005391-05	TRIB2
Plate 7	B09	M-006716-00	D-006716-01	DGKH
Plate 7	B09	M-006716-00	D-006716-02	DGKH
Plate 7	B09	M-006716-00	D-006716-03	DGKH
Plate 7	B09	M-006716-00	D-006716-04	DGKH
Plate 7	B10	M-003139-01	D-003139-05	FRK
Plate 7	B10	M-003139-01	D-003139-06	FRK
Plate 7	B10	M-003139-01	D-003139-07	FRK
Plate 7	B10	M-003139-01	D-003139-08	FRK
Plate 7	B11	M-003019-02	D-003019-05	PIK3CB
Plate 7	B11	M-003019-02	D-003019-06	PIK3CB
Plate 7	B11	M-003019-02	D-003019-07	PIK3CB
Plate 7	B11	M-003019-02	D-003019-09	PIK3CB

Plate 7	C02	M-006233-02	D-006233-05	KCNH2
Plate 7	C02	M-006233-02	D-006233-18	KCNH2
Plate 7	C02	M-006233-02	D-006233-19	KCNH2
Plate 7	C02	M-006233-02	D-006233-20	KCNH2
Plate 7	C03	M-004323-01	D-004323-01	CDKL1
Plate 7	C03	M-004323-01	D-004323-02	CDKL1
Plate 7	C03	M-004323-01	D-004323-03	CDKL1
Plate 7	C03	M-004323-01	D-004323-05	CDKL1
Plate 7	C04	M-003160-02	D-003160-05	NTRK2
Plate 7	C04	M-003160-02	D-003160-06	NTRK2
Plate 7	C04	M-003160-02	D-003160-07	NTRK2
Plate 7	C04	M-003160-02	D-003160-08	NTRK2
Plate 7	C05	M-005301-03	D-005301-02	AATK
Plate 7	C05	M-005301-03	D-005301-03	AATK
Plate 7	C05	M-005301-03	D-005301-04	AATK
Plate 7	C05	M-005301-03	D-005301-05	AATK
Plate 7	C06	M-004654-01	D-004654-01	PRKCG
Plate 7	C06	M-004654-01	D-004654-03	PRKCG
Plate 7	C06	M-004654-01	D-004654-04	PRKCG
Plate 7	C06	M-004654-01	D-004654-05	PRKCG
Plate 7	C07	M-004674-01	D-004674-02	STK38
Plate 7	C07	M-004674-01	D-004674-03	STK38
Plate 7	C07	M-004674-01	D-004674-04	STK38
Plate 7	C07	M-004674-01	D-004674-17	STK38
Plate 7	C08	M-006782-01	D-006782-01	PMVK
Plate 7	C08	M-006782-01	D-006782-02	PMVK
Plate 7	C08	M-006782-01	D-006782-04	PMVK
Plate 7	C08	M-006782-01	D-006782-17	PMVK
Plate 7	C09	M-003115-03	D-003115-01	EPHA1
Plate 7	C09	M-003115-03	D-003115-02	EPHA1
Plate 7	C09	M-003115-03	D-003115-04	EPHA1
Plate 7	C09	M-003115-03	D-003115-09	EPHA1
Plate 7	C10	M-003601-02	D-003601-01	RAF1
Plate 7	C10	M-003601-02	D-003601-02	RAF1
Plate 7	C10	M-003601-02	D-003601-03	RAF1
Plate 7	C10	M-003601-02	D-003601-04	RAF1
Plate 7	C11	M-010618-00	D-010618-01	PRKCSH
Plate 7	C11	M-010618-00	D-010618-02	PRKCSH
Plate 7	C11	M-010618-00	D-010618-03	PRKCSH
Plate 7	C11	M-010618-00	D-010618-04	PRKCSH
Plate 7	D02	M-003524-01	D-003524-03	PRKCD
Plate 7	D02	M-003524-01	D-003524-04	PRKCD
Plate 7	D02	M-003524-01	D-003524-05	PRKCD
Plate 7	D02	M-003524-01	D-003524-06	PRKCD
Plate 7	D03	M-003202-05	D-003202-05	ATR
Plate 7	D03	M-003202-05	D-003202-17	ATR
Plate 7	D03	M-003202-05	D-003202-31	ATR
Plate 7	D03	M-003202-05	D-003202-32	ATR
Plate 7	D04	M-004942-00	D-004942-01	CAMK2A
Plate 7	D04	M-004942-00	D-004942-02	CAMK2A
Plate 7	D04	M-004942-00	D-004942-03	CAMK2A
Plate 7	D04	M-004942-00	D-004942-04	CAMK2A
Plate 7	D05	M-003148-01	D-003148-05	KDR
Plate 7	D05	M-003148-01	D-003148-06	KDR
Plate 7	D05	M-003148-01	D-003148-07	KDR
Plate 7	D05	M-003148-01	D-003148-08	KDR
Plate 7	D06	M-005041-01	D-005041-01	TAF1
Plate 7	D06	M-005041-01	D-005041-04	TAF1
Plate 7	D06	M-005041-01	D-005041-05	TAF1
Plate 7	D06	M-005041-01	D-005041-06	TAF1
Plate 7	D07	M-004689-00	D-004689-01	CDK11
Plate 7	D07	M-004689-00	D-004689-02	CDK11
Plate 7	D07	M-004689-00	D-004689-03	CDK11
Plate 7	D07	M-004689-00	D-004689-04	CDK11
Plate 7	D08	M-005374-01	D-005374-01	SNARK
Plate 7	D08	M-005374-01	D-005374-05	SNARK
Plate 7	D08	M-005374-01	D-005374-06	SNARK
Plate 7	D08	M-005374-01	D-005374-07	SNARK
Plate 7	D09	M-005373-01	D-005373-01	SCYL1
Plate 7	D09	M-005373-01	D-005373-02	SCYL1
Plate 7	D09	M-005373-01	D-005373-03	SCYL1
Plate 7	D09	M-005373-01	D-005373-04	SCYL1
Plate 7	D10	M-007672-00	D-007672-01	PRKAB2
Plate 7	D10	M-007672-00	D-007672-02	PRKAB2
Plate 7	D10	M-007672-00	D-007672-03	PRKAB2
Plate 7	D10	M-007672-00	D-007672-04	PRKAB2
Plate 7	D11	M-005348-00	D-005348-01	MGC4796
Plate 7	D11	M-005348-00	D-005348-02	MGC4796
Plate 7	D11	M-005348-00	D-005348-03	MGC4796
Plate 7	D11	M-005348-00	D-005348-04	MGC4796

Plate 7	E02	M-004618-00	D-004618-01	STK32B
Plate 7	E02	M-004618-00	D-004618-02	STK32B
Plate 7	E02	M-004618-00	D-004618-03	STK32B
Plate 7	E02	M-004618-00	D-004618-04	STK32B
Plate 7	E03	M-004770-02	D-004770-01	MAP3K7IP1
Plate 7	E03	M-004770-02	D-004770-02	MAP3K7IP1
Plate 7	E03	M-004770-02	D-004770-03	MAP3K7IP1
Plate 7	E03	M-004770-02	D-004770-18	MAP3K7IP1
Plate 7	E04	M-003527-00	D-003527-01	PRKR
Plate 7	E04	M-003527-00	D-003527-02	PRKR
Plate 7	E04	M-003527-00	D-003527-03	PRKR
Plate 7	E04	M-003527-00	D-003527-04	PRKR
Plate 7	E05	M-003534-01	D-003534-01	RIPK3
Plate 7	E05	M-003534-01	D-003534-02	RIPK3
Plate 7	E05	M-003534-01	D-003534-03	RIPK3
Plate 7	E05	M-003534-01	D-003534-04	RIPK3
Plate 7	E06	M-005319-03	D-005319-02	ULK4
Plate 7	E06	M-005319-03	D-005319-03	ULK4
Plate 7	E06	M-005319-03	D-005319-04	ULK4
Plate 7	E06	M-005319-03	D-005319-05	ULK4
Plate 7	E07	M-004831-00	D-004831-01	SPHK2
Plate 7	E07	M-004831-00	D-004831-02	SPHK2
Plate 7	E07	M-004831-00	D-004831-03	SPHK2
Plate 7	E07	M-004831-00	D-004831-04	SPHK2
Plate 7	E08	M-005043-01	D-005043-01	TESK1
Plate 7	E08	M-005043-01	D-005043-02	TESK1
Plate 7	E08	M-005043-01	D-005043-03	TESK1
Plate 7	E08	M-005043-01	D-005043-04	TESK1
Plate 7	E09	M-007679-00	D-007679-01	CSNK2B
Plate 7	E09	M-007679-00	D-007679-02	CSNK2B
Plate 7	E09	M-007679-00	D-007679-03	CSNK2B
Plate 7	E09	M-007679-00	D-007679-04	CSNK2B
Plate 7	E10	M-003128-03	D-003128-06	ERBB4
Plate 7	E10	M-003128-03	D-003128-07	ERBB4
Plate 7	E10	M-003128-03	D-003128-09	ERBB4
Plate 7	E10	M-003128-03	D-003128-22	ERBB4
Plate 7	E11	M-006764-01	D-006764-01	PFKFB4
Plate 7	E11	M-006764-01	D-006764-02	PFKFB4
Plate 7	E11	M-006764-01	D-006764-04	PFKFB4
Plate 7	E11	M-006764-01	D-006764-17	PFKFB4
Plate 7	F02	M-005026-02	D-005026-01	PKMYT1
Plate 7	F02	M-005026-02	D-005026-04	PKMYT1
Plate 7	F02	M-005026-02	D-005026-05	PKMYT1
Plate 7	F02	M-005026-02	D-005026-06	PKMYT1
Plate 7	F03	M-005357-00	D-005357-01	PACE-1
Plate 7	F03	M-005357-00	D-005357-02	PACE-1
Plate 7	F03	M-005357-00	D-005357-03	PACE-1
Plate 7	F03	M-005357-00	D-005357-04	PACE-1
Plate 7	F04	M-003503-03	D-003503-01	IKBKB
Plate 7	F04	M-003503-03	D-003503-02	IKBKB
Plate 7	F04	M-003503-03	D-003503-03	IKBKB
Plate 7	F04	M-003503-03	D-003503-04	IKBKB
Plate 7	F05	M-003579-01	D-003579-01	MAP3K13
Plate 7	F05	M-003579-01	D-003579-02	MAP3K13
Plate 7	F05	M-003579-01	D-003579-04	MAP3K13
Plate 7	F05	M-003579-01	D-003579-05	MAP3K13
Plate 7	F06	M-004946-01	D-004946-01	CAMK1D
Plate 7	F06	M-004946-01	D-004946-02	CAMK1D
Plate 7	F06	M-004946-01	D-004946-03	CAMK1D
Plate 7	F06	M-004946-01	D-004946-04	CAMK1D
Plate 7	F07	M-004762-00	D-004762-01	IRAK3
Plate 7	F07	M-004762-00	D-004762-02	IRAK3
Plate 7	F07	M-004762-00	D-004762-03	IRAK3
Plate 7	F07	M-004762-00	D-004762-04	IRAK3
Plate 7	F08	M-003859-02	D-003859-01	MOS
Plate 7	F08	M-003859-02	D-003859-03	MOS
Plate 7	F08	M-003859-02	D-003859-04	MOS
Plate 7	F08	M-003859-02	D-003859-05	MOS
Plate 7	F09	M-006779-03	D-006779-02	PIP5K2B
Plate 7	F09	M-006779-03	D-006779-04	PIP5K2B
Plate 7	F09	M-006779-03	D-006779-05	PIP5K2B
Plate 7	F09	M-006779-03	D-006779-06	PIP5K2B
Plate 7	F10	M-004157-01	D-004157-01	STK4
Plate 7	F10	M-004157-01	D-004157-02	STK4
Plate 7	F10	M-004157-01	D-004157-03	STK4
Plate 7	F10	M-004157-01	D-004157-05	STK4
Plate 7	F11	M-011922-01	D-011922-01	BAIAP1
Plate 7	F11	M-011922-01	D-011922-02	BAIAP1
Plate 7	F11	M-011922-01	D-011922-03	BAIAP1
Plate 7	F11	M-011922-01	D-011922-04	BAIAP1

Plate 7	G02	M-003850-02	D-003850-01	SLK
Plate 7	G02	M-003850-02	D-003850-02	SLK
Plate 7	G02	M-003850-02	D-003850-05	SLK
Plate 7	G02	M-003850-02	D-003850-06	SLK
Plate 7	G03	M-003244-03	D-003244-05	CDKN1C
Plate 7	G03	M-003244-03	D-003244-08	CDKN1C
Plate 7	G03	M-003244-03	D-003244-09	CDKN1C
Plate 7	G03	M-003244-03	D-003244-10	CDKN1C
Plate 7	G04	M-004782-00	D-004782-01	PIP5K1C
Plate 7	G04	M-004782-00	D-004782-02	PIP5K1C
Plate 7	G04	M-004782-00	D-004782-03	PIP5K1C
Plate 7	G04	M-004782-00	D-004782-04	PIP5K1C
Plate 7	G05	M-006822-00	D-006822-01	PFKL
Plate 7	G05	M-006822-00	D-006822-02	PFKL
Plate 7	G05	M-006822-00	D-006822-03	PFKL
Plate 7	G05	M-006822-00	D-006822-04	PFKL
Plate 7	G06	M-006796-01	D-006796-01	PCK1
Plate 7	G06	M-006796-01	D-006796-02	PCK1
Plate 7	G06	M-006796-01	D-006796-03	PCK1
Plate 7	G06	M-006796-01	D-006796-17	PCK1
Plate 7	G07	M-003243-03	D-003243-05	CDK9
Plate 7	G07	M-003243-03	D-003243-06	CDK9
Plate 7	G07	M-003243-03	D-003243-07	CDK9
Plate 7	G07	M-003243-03	D-003243-08	CDK9
Plate 7	G08	M-003134-02	D-003134-05	FGFR4
Plate 7	G08	M-003134-02	D-003134-09	FGFR4
Plate 7	G08	M-003134-02	D-003134-10	FGFR4
Plate 7	G08	M-003134-02	D-003134-11	FGFR4
Plate 7	G09	M-012023-02	D-012023-01	CRKL
Plate 7	G09	M-012023-02	D-012023-02	CRKL
Plate 7	G09	M-012023-02	D-012023-05	CRKL
Plate 7	G09	M-012023-02	D-012023-18	CRKL
Plate 7	G10	M-004665-02	D-004665-01	RPS6KA5
Plate 7	G10	M-004665-02	D-004665-04	RPS6KA5
Plate 7	G10	M-004665-02	D-004665-06	RPS6KA5
Plate 7	G10	M-004665-02	D-004665-19	RPS6KA5
Plate 7	G11	M-004615-00	D-004615-01	STK32C
Plate 7	G11	M-004615-00	D-004615-02	STK32C
Plate 7	G11	M-004615-00	D-004615-03	STK32C
Plate 7	G11	M-004615-00	D-004615-04	STK32C
Plate 7	H02	M-004197-02	D-004197-05	PRKD2
Plate 7	H02	M-004197-02	D-004197-06	PRKD2
Plate 7	H02	M-004197-02	D-004197-08	PRKD2
Plate 7	H02	M-004197-02	D-004197-21	PRKD2
Plate 7	H03	M-004912-01	D-004912-01	CAMKK1
Plate 7	H03	M-004912-01	D-004912-02	CAMKK1
Plate 7	H03	M-004912-01	D-004912-04	CAMKK1
Plate 7	H03	M-004912-01	D-004912-17	CAMKK1
Plate 7	H04	M-005343-02	D-005343-02	LYK5
Plate 7	H04	M-005343-02	D-005343-03	LYK5
Plate 7	H04	M-005343-02	D-005343-05	LYK5
Plate 7	H04	M-005343-02	D-005343-06	LYK5
Plate 7	H05	M-020053-01	D-020053-01	COMMD3
Plate 7	H05	M-020053-01	D-020053-02	COMMD3
Plate 7	H05	M-020053-01	D-020053-03	COMMD3
Plate 7	H05	M-020053-01	D-020053-04	COMMD3
Plate 7	H06	M-006788-03	D-006788-01	TK2
Plate 7	H06	M-006788-03	D-006788-02	TK2
Plate 7	H06	M-006788-03	D-006788-04	TK2
Plate 7	H06	M-006788-03	D-006788-08	TK2
Plate 7	H07	M-003475-03	D-003475-01	CSNK2A1
Plate 7	H07	M-003475-03	D-003475-02	CSNK2A1
Plate 7	H07	M-003475-03	D-003475-23	CSNK2A1
Plate 7	H07	M-003475-03	D-003475-24	CSNK2A1
Plate 7	H08	M-005376-00	D-005376-01	SRMS
Plate 7	H08	M-005376-00	D-005376-02	SRMS
Plate 7	H08	M-005376-00	D-005376-03	SRMS
Plate 7	H08	M-005376-00	D-005376-04	SRMS
Plate 7	H09	M-003587-01	D-003587-05	MAP4K2
Plate 7	H09	M-003587-01	D-003587-06	MAP4K2
Plate 7	H09	M-003587-01	D-003587-07	MAP4K2
Plate 7	H09	M-003587-01	D-003587-08	MAP4K2
Plate 7	H10	M-004619-02	D-004619-05	KIAA1811
Plate 7	H10	M-004619-02	D-004619-06	KIAA1811
Plate 7	H10	M-004619-02	D-004619-07	KIAA1811
Plate 7	H10	M-004619-02	D-004619-21	KIAA1811
Plate 7	H11	M-005019-00	D-005019-01	PDK1
Plate 7	H11	M-005019-00	D-005019-02	PDK1
Plate 7	H11	M-005019-00	D-005019-03	PDK1
Plate 7	H11	M-005019-00	D-005019-04	PDK1

Plate 8	A02	M-004029-01	D-004029-01	MELK
Plate 8	A02	M-004029-01	D-004029-02	MELK
Plate 8	A02	M-004029-01	D-004029-04	MELK
Plate 8	A02	M-004029-01	D-004029-05	MELK
Plate 8	A03	M-004655-01	D-004655-02	PRKCH
Plate 8	A03	M-004655-01	D-004655-03	PRKCH
Plate 8	A03	M-004655-01	D-004655-04	PRKCH
Plate 8	A03	M-004655-01	D-004655-05	PRKCH
Plate 8	A04	M-003614-00	D-003614-01	PAK3
Plate 8	A04	M-003614-00	D-003614-02	PAK3
Plate 8	A04	M-003614-00	D-003614-03	PAK3
Plate 8	A04	M-003614-00	D-003614-04	PAK3
Plate 8	A05	M-006761-01	D-006761-01	PFKFB1
Plate 8	A05	M-006761-01	D-006761-03	PFKFB1
Plate 8	A05	M-006761-01	D-006761-04	PFKFB1
Plate 8	A05	M-006761-01	D-006761-17	PFKFB1
Plate 8	A06	M-005332-00	D-005332-01	INSRR
Plate 8	A06	M-005332-00	D-005332-02	INSRR
Plate 8	A06	M-005332-00	D-005332-03	INSRR
Plate 8	A06	M-005332-00	D-005332-04	INSRR
Plate 8	A07	M-011252-02	D-011252-01	DLG2
Plate 8	A07	M-011252-02	D-011252-04	DLG2
Plate 8	A07	M-011252-02	D-011252-05	DLG2
Plate 8	A07	M-011252-02	D-011252-06	DLG2
Plate 8	A08	M-005058-05	D-005058-09	PIP5K3
Plate 8	A08	M-005058-05	D-005058-10	PIP5K3
Plate 8	A08	M-005058-05	D-005058-11	PIP5K3
Plate 8	A08	M-005058-05	D-005058-12	PIP5K3
Plate 8	A09	M-004933-04	D-004933-03	BMPR1A
Plate 8	A09	M-004933-04	D-004933-07	BMPR1A
Plate 8	A09	M-004933-04	D-004933-08	BMPR1A
Plate 8	A09	M-004933-04	D-004933-24	BMPR1A
Plate 8	A10	M-006804-00	D-006804-01	PRPS1L1
Plate 8	A10	M-006804-00	D-006804-02	PRPS1L1
Plate 8	A10	M-006804-00	D-006804-03	PRPS1L1
Plate 8	A10	M-006804-00	D-006804-04	PRPS1L1
Plate 8	A11	M-010601-01	D-010601-01	IGF2R
Plate 8	A11	M-010601-01	D-010601-02	IGF2R
Plate 8	A11	M-010601-01	D-010601-03	IGF2R
Plate 8	A11	M-010601-01	D-010601-04	IGF2R
Plate 8	B02	M-010545-02	D-010545-01	TGFBR3
Plate 8	B02	M-010545-02	D-010545-03	TGFBR3
Plate 8	B02	M-010545-02	D-010545-04	TGFBR3
Plate 8	B02	M-010545-02	D-010545-18	TGFBR3
Plate 8	B03	M-004059-00	D-004059-01	UMP-CMPK
Plate 8	B03	M-004059-00	D-004059-02	UMP-CMPK
Plate 8	B03	M-004059-00	D-004059-03	UMP-CMPK
Plate 8	B03	M-004059-00	D-004059-04	UMP-CMPK
Plate 8	B04	M-006704-01	D-006704-01	CHKA
Plate 8	B04	M-006704-01	D-006704-03	CHKA
Plate 8	B04	M-006704-01	D-006704-04	CHKA
Plate 8	B04	M-006704-01	D-006704-17	CHKA
Plate 8	B05	M-005031-02	D-005031-01	WNK4
Plate 8	B05	M-005031-02	D-005031-03	WNK4
Plate 8	B05	M-005031-02	D-005031-04	WNK4
Plate 8	B05	M-005031-02	D-005031-05	WNK4
Plate 8	B06	M-003025-04	D-003025-06	RPS6KA1
Plate 8	B06	M-003025-04	D-003025-07	RPS6KA1
Plate 8	B06	M-003025-04	D-003025-08	RPS6KA1
Plate 8	B06	M-003025-04	D-003025-12	RPS6KA1
Plate 8	B07	M-006739-01	D-006739-01	IHPK3
Plate 8	B07	M-006739-01	D-006739-02	IHPK3
Plate 8	B07	M-006739-01	D-006739-03	IHPK3
Plate 8	B07	M-006739-01	D-006739-17	IHPK3
Plate 8	B08	M-003106-04	D-003106-19	BMX
Plate 8	B08	M-003106-04	D-003106-20	BMX
Plate 8	B08	M-003106-04	D-003106-21	BMX
Plate 8	B08	M-003106-04	D-003106-22	BMX
Plate 8	B09	M-004803-00	D-004803-01	CLK4
Plate 8	B09	M-004803-00	D-004803-02	CLK4
Plate 8	B09	M-004803-00	D-004803-03	CLK4
Plate 8	B09	M-004803-00	D-004803-04	CLK4
Plate 8	B10	M-003597-03	D-003597-05	PAK2
Plate 8	B10	M-003597-03	D-003597-22	PAK2
Plate 8	B10	M-003597-03	D-003597-23	PAK2
Plate 8	B10	M-003597-03	D-003597-24	PAK2
Plate 8	B11	M-032942-00	D-032942-09	LOC390226
Plate 8	B11	M-032942-00	D-032942-10	LOC390226
Plate 8	B11	M-032942-00	D-032942-11	LOC390226
Plate 8	B11	M-032942-00	D-032942-12	LOC390226

Plate 8	C02	M-003957-04	D-003957-09	CSNK1A1
Plate 8	C02	M-003957-04	D-003957-10	CSNK1A1
Plate 8	C02	M-003957-04	D-003957-11	CSNK1A1
Plate 8	C02	M-003957-04	D-003957-12	CSNK1A1
Plate 8	C03	M-005102-02	D-005102-03	NME2
Plate 8	C03	M-005102-02	D-005102-04	NME2
Plate 8	C03	M-005102-02	D-005102-05	NME2
Plate 8	C03	M-005102-02	D-005102-06	NME2
Plate 8	C04	M-004813-01	D-004813-05	MAK
Plate 8	C04	M-004813-01	D-004813-06	MAK
Plate 8	C04	M-004813-01	D-004813-07	MAK
Plate 8	C04	M-004813-01	D-004813-08	MAK
Plate 8	C05	M-006775-02	D-006775-05	PIK3CD
Plate 8	C05	M-006775-02	D-006775-06	PIK3CD
Plate 8	C05	M-006775-02	D-006775-07	PIK3CD
Plate 8	C05	M-006775-02	D-006775-21	PIK3CD
Plate 8	C06	M-003969-00	D-003969-01	MAP3K6
Plate 8	C06	M-003969-00	D-003969-02	MAP3K6
Plate 8	C06	M-003969-00	D-003969-03	MAP3K6
Plate 8	C06	M-003969-00	D-003969-04	MAP3K6
Plate 8	C07	M-004938-02	D-004938-02	BRDT
Plate 8	C07	M-004938-02	D-004938-03	BRDT
Plate 8	C07	M-004938-02	D-004938-04	BRDT
Plate 8	C07	M-004938-02	D-004938-18	BRDT
Plate 8	C08	M-005314-02	D-005314-13	EIF2AK4
Plate 8	C08	M-005314-02	D-005314-14	EIF2AK4
Plate 8	C08	M-005314-02	D-005314-15	EIF2AK4
Plate 8	C08	M-005314-02	D-005314-16	EIF2AK4
Plate 8	C09	M-006755-01	D-006755-05	NME6
Plate 8	C09	M-006755-01	D-006755-06	NME6
Plate 8	C09	M-006755-01	D-006755-07	NME6
Plate 8	C09	M-006755-01	D-006755-08	NME6
Plate 8	C10	M-004805-01	D-004805-01	DYRK1A
Plate 8	C10	M-004805-01	D-004805-02	DYRK1A
Plate 8	C10	M-004805-01	D-004805-04	DYRK1A
Plate 8	C10	M-004805-01	D-004805-17	DYRK1A
Plate 8	C11	M-004944-01	D-004944-01	CAMK4
Plate 8	C11	M-004944-01	D-004944-02	CAMK4
Plate 8	C11	M-004944-01	D-004944-04	CAMK4
Plate 8	C11	M-004944-01	D-004944-05	CAMK4
Plate 8	D02	M-004844-02	D-004844-01	JIK
Plate 8	D02	M-004844-02	D-004844-02	JIK
Plate 8	D02	M-004844-02	D-004844-04	JIK
Plate 8	D02	M-004844-02	D-004844-05	JIK
Plate 8	D03	M-006780-01	D-006780-01	PKLR
Plate 8	D03	M-006780-01	D-006780-02	PKLR
Plate 8	D03	M-006780-01	D-006780-03	PKLR
Plate 8	D03	M-006780-01	D-006780-04	PKLR
Plate 8	D04	M-003973-02	D-003973-09	PAK7
Plate 8	D04	M-003973-02	D-003973-10	PAK7
Plate 8	D04	M-003973-02	D-003973-11	PAK7
Plate 8	D04	M-003973-02	D-003973-12	PAK7
Plate 8	D05	M-004683-02	D-004683-02	VRK1
Plate 8	D05	M-004683-02	D-004683-03	VRK1
Plate 8	D05	M-004683-02	D-004683-04	VRK1
Plate 8	D05	M-004683-02	D-004683-05	VRK1
Plate 8	D06	M-005313-03	D-005313-01	EPHA6
Plate 8	D06	M-005313-03	D-005313-03	EPHA6
Plate 8	D06	M-005313-03	D-005313-04	EPHA6
Plate 8	D06	M-005313-03	D-005313-05	EPHA6
Plate 8	D07	M-005328-01	D-005328-01	GUCY2C
Plate 8	D07	M-005328-01	D-005328-02	GUCY2C
Plate 8	D07	M-005328-01	D-005328-03	GUCY2C
Plate 8	D07	M-005328-01	D-005328-04	GUCY2C
Plate 8	D08	M-027176-02	D-027176-01	PNCK
Plate 8	D08	M-027176-02	D-027176-03	PNCK
Plate 8	D08	M-027176-02	D-027176-04	PNCK
Plate 8	D08	M-027176-02	D-027176-20	PNCK
Plate 8	D09	M-005397-02	D-005397-01	VRK3
Plate 8	D09	M-005397-02	D-005397-03	VRK3
Plate 8	D09	M-005397-02	D-005397-05	VRK3
Plate 8	D09	M-005397-02	D-005397-18	VRK3
Plate 8	D10	M-003162-04	D-003162-08	PDGFRA
Plate 8	D10	M-003162-04	D-003162-09	PDGFRA
Plate 8	D10	M-003162-04	D-003162-10	PDGFRA
Plate 8	D10	M-003162-04	D-003162-23	PDGFRA
Plate 8	D11	M-003111-04	D-003111-08	DDR1
Plate 8	D11	M-003111-04	D-003111-09	DDR1
Plate 8	D11	M-003111-04	D-003111-10	DDR1
Plate 8	D11	M-003111-04	D-003111-24	DDR1

Plate 8	E02	M-003169-01	D-003169-05	PTK9L
Plate 8	E02	M-003169-01	D-003169-06	PTK9L
Plate 8	E02	M-003169-01	D-003169-07	PTK9L
Plate 8	E02	M-003169-01	D-003169-08	PTK9L
Plate 8	E03	M-006771-01	D-006771-01	PIK3C2A
Plate 8	E03	M-006771-01	D-006771-02	PIK3C2A
Plate 8	E03	M-006771-01	D-006771-03	PIK3C2A
Plate 8	E03	M-006771-01	D-006771-04	PIK3C2A
Plate 8	E04	M-004634-01	D-004634-01	STK32A
Plate 8	E04	M-004634-01	D-004634-02	STK32A
Plate 8	E04	M-004634-01	D-004634-03	STK32A
Plate 8	E04	M-004634-01	D-004634-04	STK32A
Plate 8	E05	M-010924-00	D-010924-01	GTF2H1
Plate 8	E05	M-010924-00	D-010924-02	GTF2H1
Plate 8	E05	M-010924-00	D-010924-03	GTF2H1
Plate 8	E05	M-010924-00	D-010924-04	GTF2H1
Plate 8	E06	M-005390-00	D-005390-01	TOPK
Plate 8	E06	M-005390-00	D-005390-02	TOPK
Plate 8	E06	M-005390-00	D-005390-03	TOPK
Plate 8	E06	M-005390-00	D-005390-04	TOPK
Plate 8	E07	M-005068-03	D-005068-02	ZAK
Plate 8	E07	M-005068-03	D-005068-03	ZAK
Plate 8	E07	M-005068-03	D-005068-09	ZAK
Plate 8	E07	M-005068-03	D-005068-10	ZAK
Plate 8	E08	M-019425-02	D-019425-01	PDK4
Plate 8	E08	M-019425-02	D-019425-02	PDK4
Plate 8	E08	M-019425-02	D-019425-03	PDK4
Plate 8	E08	M-019425-02	D-019425-04	PDK4
Plate 8	E09	M-003473-02	D-003473-03	CHUK
Plate 8	E09	M-003473-02	D-003473-04	CHUK
Plate 8	E09	M-003473-02	D-003473-05	CHUK
Plate 8	E09	M-003473-02	D-003473-06	CHUK
Plate 8	E10	M-006789-01	D-006789-01	TPK1
Plate 8	E10	M-006789-01	D-006789-02	TPK1
Plate 8	E10	M-006789-01	D-006789-04	TPK1
Plate 8	E10	M-006789-01	D-006789-17	TPK1
Plate 8	E11	M-005310-00	D-005310-01	C14ORF20
Plate 8	E11	M-005310-00	D-005310-02	C14ORF20
Plate 8	E11	M-005310-00	D-005310-03	C14ORF20
Plate 8	E11	M-005310-00	D-005310-04	C14ORF20
Plate 8	F02	M-032287-02	D-032287-02	PIM3
Plate 8	F02	M-032287-02	D-032287-03	PIM3
Plate 8	F02	M-032287-02	D-032287-20	PIM3
Plate 8	F02	M-032287-02	D-032287-21	PIM3
Plate 8	F03	M-005338-03	D-005338-01	LMTK3
Plate 8	F03	M-005338-03	D-005338-05	LMTK3
Plate 8	F03	M-005338-03	D-005338-06	LMTK3
Plate 8	F03	M-005338-03	D-005338-07	LMTK3
Plate 8	F04	M-003256-06	D-003256-05	CHEK2
Plate 8	F04	M-003256-06	D-003256-13	CHEK2
Plate 8	F04	M-003256-06	D-003256-14	CHEK2
Plate 8	F04	M-003256-06	D-003256-15	CHEK2
Plate 8	F05	M-003145-02	D-003145-05	JAK1
Plate 8	F05	M-003145-02	D-003145-06	JAK1
Plate 8	F05	M-003145-02	D-003145-07	JAK1
Plate 8	F05	M-003145-02	D-003145-08	JAK1
Plate 8	F06	M-004883-03	D-004883-02	EIF2AK3
Plate 8	F06	M-004883-03	D-004883-05	EIF2AK3
Plate 8	F06	M-004883-03	D-004883-06	EIF2AK3
Plate 8	F06	M-004883-03	D-004883-07	EIF2AK3
Plate 8	F07	M-005250-00	D-005250-01	PIK3C3
Plate 8	F07	M-005250-00	D-005250-02	PIK3C3
Plate 8	F07	M-005250-00	D-005250-03	PIK3C3
Plate 8	F07	M-005250-00	D-005250-04	PIK3C3
Plate 8	F08	M-004610-02	D-004610-02	ROCK2
Plate 8	F08	M-004610-02	D-004610-03	ROCK2
Plate 8	F08	M-004610-02	D-004610-05	ROCK2
Plate 8	F08	M-004610-02	D-004610-18	ROCK2
Plate 8	F09	M-006772-01	D-006772-01	PIK3C2B
Plate 8	F09	M-006772-01	D-006772-03	PIK3C2B
Plate 8	F09	M-006772-01	D-006772-04	PIK3C2B
Plate 8	F09	M-006772-01	D-006772-05	PIK3C2B
Plate 8	F10	M-003027-05	D-003027-09	SGK
Plate 8	F10	M-003027-05	D-003027-10	SGK
Plate 8	F10	M-003027-05	D-003027-11	SGK
Plate 8	F10	M-003027-05	D-003027-12	SGK
Plate 8	F11	M-004802-01	D-004802-02	CLK3
Plate 8	F11	M-004802-01	D-004802-03	CLK3
Plate 8	F11	M-004802-01	D-004802-04	CLK3
Plate 8	F11	M-004802-01	D-004802-05	CLK3

Plate 8	G02	M-005367-01	D-005367-01	PXK
Plate 8	G02	M-005367-01	D-005367-02	PXK
Plate 8	G02	M-005367-01	D-005367-03	PXK
Plate 8	G02	M-005367-01	D-005367-04	PXK
Plate 8	G03	M-004214-01	D-004214-01	HUNK
Plate 8	G03	M-004214-01	D-004214-03	HUNK
Plate 8	G03	M-004214-01	D-004214-04	HUNK
Plate 8	G03	M-004214-01	D-004214-05	HUNK
Plate 8	G04	M-003586-01	D-003586-01	MAP4K1
Plate 8	G04	M-003586-01	D-003586-03	MAP4K1
Plate 8	G04	M-003586-01	D-003586-05	MAP4K1
Plate 8	G04	M-003586-01	D-003586-06	MAP4K1
Plate 8	G05	M-004835-01	D-004835-01	PCTK2
Plate 8	G05	M-004835-01	D-004835-04	PCTK2
Plate 8	G05	M-004835-01	D-004835-05	PCTK2
Plate 8	G05	M-004835-01	D-004835-06	PCTK2
Plate 8	G06	M-003014-02	D-003014-05	INSR
Plate 8	G06	M-003014-02	D-003014-06	INSR
Plate 8	G06	M-003014-02	D-003014-07	INSR
Plate 8	G06	M-003014-02	D-003014-08	INSR
Plate 8	G07	M-004808-03	D-004808-01	HIPK4
Plate 8	G07	M-004808-03	D-004808-04	HIPK4
Plate 8	G07	M-004808-03	D-004808-05	HIPK4
Plate 8	G07	M-004808-03	D-004808-21	HIPK4
Plate 8	G08	M-004778-03	D-004778-05	SIK2
Plate 8	G08	M-004778-03	D-004778-09	SIK2
Plate 8	G08	M-004778-03	D-004778-10	SIK2
Plate 8	G08	M-004778-03	D-004778-23	SIK2
Plate 8	G09	M-003156-02	D-003156-09	MET
Plate 8	G09	M-003156-02	D-003156-10	MET
Plate 8	G09	M-003156-02	D-003156-11	MET
Plate 8	G09	M-003156-02	D-003156-12	MET
Plate 8	G10	M-003140-04	D-003140-09	FYN
Plate 8	G10	M-003140-04	D-003140-10	FYN
Plate 8	G10	M-003140-04	D-003140-23	FYN
Plate 8	G10	M-003140-04	D-003140-24	FYN
Plate 8	G11	M-004949-01	D-004949-01	DKFZP434C1
Plate 8	G11	M-004949-01	D-004949-02	DKFZP434C1
Plate 8	G11	M-004949-01	D-004949-03	DKFZP434C1
Plate 8	G11	M-004949-01	D-004949-04	DKFZP434C1
Plate 8	H02	M-004672-02	D-004672-01	SAST
Plate 8	H02	M-004672-02	D-004672-03	SAST
Plate 8	H02	M-004672-02	D-004672-05	SAST
Plate 8	H02	M-004672-02	D-004672-18	SAST
Plate 8	H03	M-004090-03	D-004090-02	NEK2
Plate 8	H03	M-004090-03	D-004090-03	NEK2
Plate 8	H03	M-004090-03	D-004090-04	NEK2
Plate 8	H03	M-004090-03	D-004090-06	NEK2
Plate 8	H04	M-005015-00	D-005015-01	MAPKAPK5
Plate 8	H04	M-005015-00	D-005015-02	MAPKAPK5
Plate 8	H04	M-005015-00	D-005015-03	MAPKAPK5
Plate 8	H04	M-005015-00	D-005015-04	MAPKAPK5
Plate 8	H05	M-024786-03	D-024786-05	NRK
Plate 8	H05	M-024786-03	D-024786-06	NRK
Plate 8	H05	M-024786-03	D-024786-07	NRK
Plate 8	H05	M-024786-03	D-024786-24	NRK
Plate 8	H06	M-006762-02	D-006762-01	PFKFB2
Plate 8	H06	M-006762-02	D-006762-02	PFKFB2
Plate 8	H06	M-006762-02	D-006762-03	PFKFB2
Plate 8	H06	M-006762-02	D-006762-18	PFKFB2
Plate 8	H07	M-005345-02	D-005345-01	MARK4
Plate 8	H07	M-005345-02	D-005345-02	MARK4
Plate 8	H07	M-005345-02	D-005345-05	MARK4
Plate 8	H07	M-005345-02	D-005345-06	MARK4
Plate 8	H08	M-003121-02	D-003121-05	EPHB1
Plate 8	H08	M-003121-02	D-003121-06	EPHB1
Plate 8	H08	M-003121-02	D-003121-07	EPHB1
Plate 8	H08	M-003121-02	D-003121-08	EPHB1
Plate 8	H09	M-009453-02	D-009453-01	MAGI-3
Plate 8	H09	M-009453-02	D-009453-04	MAGI-3
Plate 8	H09	M-009453-02	D-009453-05	MAGI-3
Plate 8	H09	M-009453-02	D-009453-06	MAGI-3
Plate 8	H10	M-005034-01	D-005034-01	SSTK
Plate 8	H10	M-005034-01	D-005034-02	SSTK
Plate 8	H10	M-005034-01	D-005034-03	SSTK
Plate 8	H10	M-005034-01	D-005034-04	SSTK
Plate 8	H11	M-003767-02	D-003767-01	IKBKG
Plate 8	H11	M-003767-02	D-003767-02	IKBKG
Plate 8	H11	M-003767-02	D-003767-03	IKBKG
Plate 8	H11	M-003767-02	D-003767-04	IKBKG

Plate 9	A02	M-019063-01	D-019063-01	N4BP2
Plate 9	A02	M-019063-01	D-019063-02	N4BP2
Plate 9	A02	M-019063-01	D-019063-03	N4BP2
Plate 9	A02	M-019063-01	D-019063-17	N4BP2
Plate 9	A03	M-004864-01	D-004864-01	NEK1
Plate 9	A03	M-004864-01	D-004864-02	NEK1
Plate 9	A03	M-004864-01	D-004864-03	NEK1
Plate 9	A03	M-004864-01	D-004864-04	NEK1
Plate 9	A04	M-006793-01	D-006793-01	XYLB
Plate 9	A04	M-006793-01	D-006793-02	XYLB
Plate 9	A04	M-006793-01	D-006793-03	XYLB
Plate 9	A04	M-006793-01	D-006793-17	XYLB
Plate 9	A05	M-003753-03	D-003753-04	RP6-213H19.1
Plate 9	A05	M-003753-03	D-003753-05	RP6-213H19.1
Plate 9	A05	M-003753-03	D-003753-06	RP6-213H19.1
Plate 9	A05	M-003753-03	D-003753-07	RP6-213H19.1
Plate 9	A06	M-005033-01	D-005033-01	SMG1
Plate 9	A06	M-005033-01	D-005033-02	SMG1
Plate 9	A06	M-005033-01	D-005033-03	SMG1
Plate 9	A06	M-005033-01	D-005033-04	SMG1
Plate 9	A07	M-006738-00	D-006738-01	IHPK2
Plate 9	A07	M-006738-00	D-006738-02	IHPK2
Plate 9	A07	M-006738-00	D-006738-03	IHPK2
Plate 9	A07	M-006738-00	D-006738-04	IHPK2
Plate 9	A08	M-004499-01	D-004499-01	ILK
Plate 9	A08	M-004499-01	D-004499-02	ILK
Plate 9	A08	M-004499-01	D-004499-03	ILK
Plate 9	A08	M-004499-01	D-004499-04	ILK
Plate 9	A09	M-005366-00	D-005366-01	PSKH2
Plate 9	A09	M-005366-00	D-005366-02	PSKH2
Plate 9	A09	M-005366-00	D-005366-03	PSKH2
Plate 9	A09	M-005366-00	D-005366-04	PSKH2
Plate 9	A10	M-005356-02	D-005356-02	NRBP
Plate 9	A10	M-005356-02	D-005356-04	NRBP
Plate 9	A10	M-005356-02	D-005356-05	NRBP
Plate 9	A10	M-005356-02	D-005356-18	NRBP
Plate 9	A11	M-005049-00	D-005049-01	ULK1
Plate 9	A11	M-005049-00	D-005049-02	ULK1
Plate 9	A11	M-005049-00	D-005049-03	ULK1
Plate 9	A11	M-005049-00	D-005049-04	ULK1
Plate 9	B02	M-003523-03	D-003523-08	PRKCA
Plate 9	B02	M-003523-03	D-003523-09	PRKCA
Plate 9	B02	M-003523-03	D-003523-10	PRKCA
Plate 9	B02	M-003523-03	D-003523-11	PRKCA
Plate 9	B03	M-004797-01	D-004797-01	CDKL2
Plate 9	B03	M-004797-01	D-004797-02	CDKL2
Plate 9	B03	M-004797-01	D-004797-03	CDKL2
Plate 9	B03	M-004797-01	D-004797-04	CDKL2
Plate 9	B04	M-003130-01	D-003130-05	FES
Plate 9	B04	M-003130-01	D-003130-06	FES
Plate 9	B04	M-003130-01	D-003130-07	FES
Plate 9	B04	M-003130-01	D-003130-08	FES
Plate 9	B05	M-007675-00	D-007675-01	PRKAB1
Plate 9	B05	M-007675-00	D-007675-02	PRKAB1
Plate 9	B05	M-007675-00	D-007675-03	PRKAB1
Plate 9	B05	M-007675-00	D-007675-04	PRKAB1
Plate 9	B06	M-005330-03	D-005330-01	HAK
Plate 9	B06	M-005330-03	D-005330-03	HAK
Plate 9	B06	M-005330-03	D-005330-05	HAK
Plate 9	B06	M-005330-03	D-005330-06	HAK
Plate 9	B07	M-003236-04	D-003236-06	CDK2
Plate 9	B07	M-003236-04	D-003236-08	CDK2
Plate 9	B07	M-003236-04	D-003236-09	CDK2
Plate 9	B07	M-003236-04	D-003236-10	CDK2
Plate 9	B08	M-003573-03	D-003573-01	MAP2K2
Plate 9	B08	M-003573-03	D-003573-02	MAP2K2
Plate 9	B08	M-003573-03	D-003573-04	MAP2K2
Plate 9	B08	M-003573-03	D-003573-07	MAP2K2
Plate 9	B09	M-004324-00	D-004324-01	MAPK10
Plate 9	B09	M-004324-00	D-004324-02	MAPK10
Plate 9	B09	M-004324-00	D-004324-03	MAPK10
Plate 9	B09	M-004324-00	D-004324-04	MAPK10
Plate 9	B10	M-016674-00	D-016674-01	CALM2
Plate 9	B10	M-016674-00	D-016674-02	CALM2
Plate 9	B10	M-016674-00	D-016674-03	CALM2
Plate 9	B10	M-016674-00	D-016674-04	CALM2
Plate 9	B11	M-006745-03	D-006745-03	KHK
Plate 9	B11	M-006745-03	D-006745-05	KHK
Plate 9	B11	M-006745-03	D-006745-06	KHK

Plate 9	A02	M-019063-01	D-019063-01	N4BP2
Plate 9	C02	M-006734-02	D-006734-01	GUK1
Plate 9	C02	M-006734-02	D-006734-02	GUK1
Plate 9	C02	M-006734-02	D-006734-03	GUK1
Plate 9	C02	M-006734-02	D-006734-05	GUK1
Plate 9	C03	M-006707-00	D-006707-01	CKM
Plate 9	C03	M-006707-00	D-006707-02	CKM
Plate 9	C03	M-006707-00	D-006707-03	CKM
Plate 9	C03	M-006707-00	D-006707-04	CKM
Plate 9	C04	M-003588-02	D-003588-01	MAP4K3
Plate 9	C04	M-003588-02	D-003588-04	MAP4K3
Plate 9	C04	M-003588-02	D-003588-05	MAP4K3
Plate 9	C04	M-003588-02	D-003588-18	MAP4K3
Plate 9	C05	M-005030-01	D-005030-01	PRKDC
Plate 9	C05	M-005030-01	D-005030-03	PRKDC
Plate 9	C05	M-005030-01	D-005030-04	PRKDC
Plate 9	C05	M-005030-01	D-005030-05	PRKDC
Plate 9	C06	M-004074-04	D-004074-01	PRPF4B
Plate 9	C06	M-004074-04	D-004074-06	PRPF4B
Plate 9	C06	M-004074-04	D-004074-08	PRPF4B
Plate 9	C06	M-004074-04	D-004074-09	PRPF4B
Plate 9	C07	M-005040-02	D-005040-01	RIOK3
Plate 9	C07	M-005040-02	D-005040-04	RIOK3
Plate 9	C07	M-005040-02	D-005040-05	RIOK3
Plate 9	C07	M-005040-02	D-005040-06	RIOK3
Plate 9	C08	M-005337-01	D-005337-01	KIAA1765
Plate 9	C08	M-005337-01	D-005337-02	KIAA1765
Plate 9	C08	M-005337-01	D-005337-03	KIAA1765
Plate 9	C08	M-005337-01	D-005337-04	KIAA1765
Plate 9	C09	M-010904-01	D-010904-01	EXOSC10
Plate 9	C09	M-010904-01	D-010904-02	EXOSC10
Plate 9	C09	M-010904-01	D-010904-03	EXOSC10
Plate 9	C09	M-010904-01	D-010904-04	EXOSC10
Plate 9	C10	M-006767-01	D-006767-01	PGK1
Plate 9	C10	M-006767-01	D-006767-02	PGK1
Plate 9	C10	M-006767-01	D-006767-04	PGK1
Plate 9	C10	M-006767-01	D-006767-05	PGK1
Plate 9	C11	M-006701-00	D-006701-01	AK3L1
Plate 9	C11	M-006701-00	D-006701-02	AK3L1
Plate 9	C11	M-006701-00	D-006701-03	AK3L1
Plate 9	C11	M-006701-00	D-006701-04	AK3L1
Plate 9	D02	M-003257-02	D-003257-05	PLK3
Plate 9	D02	M-003257-02	D-003257-07	PLK3
Plate 9	D02	M-003257-02	D-003257-08	PLK3
Plate 9	D02	M-003257-02	D-003257-09	PLK3
Plate 9	D03	M-011261-00	D-011261-01	EFNB3
Plate 9	D03	M-011261-00	D-011261-02	EFNB3
Plate 9	D03	M-011261-00	D-011261-03	EFNB3
Plate 9	D03	M-011261-00	D-011261-04	EFNB3
Plate 9	D04	M-003123-02	D-003123-09	EPHB3
Plate 9	D04	M-003123-02	D-003123-10	EPHB3
Plate 9	D04	M-003123-02	D-003123-11	EPHB3
Plate 9	D04	M-003123-02	D-003123-12	EPHB3
Plate 9	D05	M-003758-04	D-003758-06	PRKCB1
Plate 9	D05	M-003758-04	D-003758-09	PRKCB1
Plate 9	D05	M-003758-04	D-003758-10	PRKCB1
Plate 9	D05	M-003758-04	D-003758-12	PRKCB1
Plate 9	D06	M-006713-03	D-006713-02	DGKD
Plate 9	D06	M-006713-03	D-006713-04	DGKD
Plate 9	D06	M-006713-03	D-006713-06	DGKD
Plate 9	D06	M-006713-03	D-006713-09	DGKD
Plate 9	D07	M-003124-02	D-003124-05	EPHB4
Plate 9	D07	M-003124-02	D-003124-06	EPHB4
Plate 9	D07	M-003124-02	D-003124-07	EPHB4
Plate 9	D07	M-003124-02	D-003124-08	EPHB4
Plate 9	D08	M-005017-02	D-005017-01	MGC45428
Plate 9	D08	M-005017-02	D-005017-02	MGC45428
Plate 9	D08	M-005017-02	D-005017-04	MGC45428
Plate 9	D08	M-005017-02	D-005017-05	MGC45428
Plate 9	D09	M-006705-00	D-006705-01	CHKB
Plate 9	D09	M-006705-00	D-006705-02	CHKB
Plate 9	D09	M-006705-00	D-006705-03	CHKB
Plate 9	D09	M-006705-00	D-006705-04	CHKB
Plate 9	D10	M-007673-00	D-007673-01	PRKAR2B
Plate 9	D10	M-007673-00	D-007673-02	PRKAR2B
Plate 9	D10	M-007673-00	D-007673-03	PRKAR2B
Plate 9	D10	M-007673-00	D-007673-04	PRKAR2B
Plate 9	D11	M-006797-01	D-006797-01	PCK2
Plate 9	D11	M-006797-01	D-006797-02	PCK2
Plate 9	D11	M-006797-01	D-006797-03	PCK2
Plate 9	D11	M-006797-01	D-006797-05	PCK2

Plate 9	E02	M-005307-01	D-005307-01	AMHR2
Plate 9	E02	M-005307-01	D-005307-03	AMHR2
Plate 9	E02	M-005307-01	D-005307-04	AMHR2
Plate 9	E02	M-005307-01	D-005307-05	AMHR2
Plate 9	E03	M-007893-01	D-007893-01	DUSP21
Plate 9	E03	M-007893-01	D-007893-03	DUSP21
Plate 9	E03	M-007893-01	D-007893-04	DUSP21
Plate 9	E03	M-007893-01	D-007893-05	DUSP21
Plate 9	E04	M-003245-03	D-003245-06	CDKN2B
Plate 9	E04	M-003245-03	D-003245-08	CDKN2B
Plate 9	E04	M-003245-03	D-003245-09	CDKN2B
Plate 9	E04	M-003245-03	D-003245-22	CDKN2B
Plate 9	E05	M-009415-01	D-009415-01	DLG1
Plate 9	E05	M-009415-01	D-009415-02	DLG1
Plate 9	E05	M-009415-01	D-009415-03	DLG1
Plate 9	E05	M-009415-01	D-009415-04	DLG1
Plate 9	E06	M-005347-01	D-005347-01	C9ORF96
Plate 9	E06	M-005347-01	D-005347-02	C9ORF96
Plate 9	E06	M-005347-01	D-005347-03	C9ORF96
Plate 9	E06	M-005347-01	D-005347-04	C9ORF96
Plate 9	E07	M-003571-01	D-003571-01	MAP2K1
Plate 9	E07	M-003571-01	D-003571-02	MAP2K1
Plate 9	E07	M-003571-01	D-003571-04	MAP2K1
Plate 9	E07	M-003571-01	D-003571-05	MAP2K1
Plate 9	E08	M-006725-00	D-006725-01	GALK2
Plate 9	E08	M-006725-00	D-006725-02	GALK2
Plate 9	E08	M-006725-00	D-006725-03	GALK2
Plate 9	E08	M-006725-00	D-006725-04	GALK2
Plate 9	E09	M-003159-02	D-003159-05	NTRK1
Plate 9	E09	M-003159-02	D-003159-06	NTRK1
Plate 9	E09	M-003159-02	D-003159-07	NTRK1
Plate 9	E09	M-003159-02	D-003159-08	NTRK1
Plate 9	E10	M-006494-00	D-006494-01	NME4
Plate 9	E10	M-006494-00	D-006494-02	NME4
Plate 9	E10	M-006494-00	D-006494-03	NME4
Plate 9	E10	M-006494-00	D-006494-04	NME4
Plate 9	E11	M-003460-03	D-003460-01	BRAF
Plate 9	E11	M-003460-03	D-003460-05	BRAF
Plate 9	E11	M-003460-03	D-003460-06	BRAF
Plate 9	E11	M-003460-03	D-003460-07	BRAF
Plate 9	F02	M-005018-01	D-005018-05	PASK
Plate 9	F02	M-005018-01	D-005018-06	PASK
Plate 9	F02	M-005018-01	D-005018-07	PASK
Plate 9	F02	M-005018-01	D-005018-08	PASK
Plate 9	F03	M-003267-02	D-003267-06	HUS1
Plate 9	F03	M-003267-02	D-003267-07	HUS1
Plate 9	F03	M-003267-02	D-003267-08	HUS1
Plate 9	F03	M-003267-02	D-003267-21	HUS1
Plate 9	F04	M-004174-00	D-004174-01	TLK1
Plate 9	F04	M-004174-00	D-004174-02	TLK1
Plate 9	F04	M-004174-00	D-004174-03	TLK1
Plate 9	F04	M-004174-00	D-004174-04	TLK1
Plate 9	F05	M-006765-01	D-006765-01	PFKM
Plate 9	F05	M-006765-01	D-006765-03	PFKM
Plate 9	F05	M-006765-01	D-006765-04	PFKM
Plate 9	F05	M-006765-01	D-006765-05	PFKM
Plate 9	F06	M-005361-02	D-005361-02	PRKAA2
Plate 9	F06	M-005361-02	D-005361-03	PRKAA2
Plate 9	F06	M-005361-02	D-005361-04	PRKAA2
Plate 9	F06	M-005361-02	D-005361-05	PRKAA2
Plate 9	F07	M-006743-02	D-006743-05	ITPKB
Plate 9	F07	M-006743-02	D-006743-06	ITPKB
Plate 9	F07	M-006743-02	D-006743-07	ITPKB
Plate 9	F07	M-006743-02	D-006743-09	ITPKB
Plate 9	F08	M-010612-02	D-010612-01	MPP3
Plate 9	F08	M-010612-02	D-010612-02	MPP3
Plate 9	F08	M-010612-02	D-010612-03	MPP3
Plate 9	F08	M-010612-02	D-010612-05	MPP3
Plate 9	F09	M-003237-01	D-003237-05	CDK3
Plate 9	F09	M-003237-01	D-003237-06	CDK3
Plate 9	F09	M-003237-01	D-003237-07	CDK3
Plate 9	F09	M-003237-01	D-003237-08	CDK3
Plate 9	F10	M-003017-02	D-003017-05	PDPK1
Plate 9	F10	M-003017-02	D-003017-06	PDPK1
Plate 9	F10	M-003017-02	D-003017-07	PDPK1
Plate 9	F10	M-003017-02	D-003017-26	PDPK1
Plate 9	F11	M-016512-00	D-016512-01	C10ORF89
Plate 9	F11	M-016512-00	D-016512-02	C10ORF89
Plate 9	F11	M-016512-00	D-016512-03	C10ORF89
Plate 9	F11	M-016512-00	D-016512-04	C10ORF89

Plate 9	G02	M-003118-02	D-003118-05	EPHA4
Plate 9	G02	M-003118-02	D-003118-07	EPHA4
Plate 9	G02	M-003118-02	D-003118-21	EPHA4
Plate 9	G02	M-003118-02	D-003118-22	EPHA4
Plate 9	G03	M-004884-01	D-004884-05	DCAMKL1
Plate 9	G03	M-004884-01	D-004884-06	DCAMKL1
Plate 9	G03	M-004884-01	D-004884-07	DCAMKL1
Plate 9	G03	M-004884-01	D-004884-08	DCAMKL1
Plate 9	G04	M-015091-01	D-015091-03	GK2
Plate 9	G04	M-015091-01	D-015091-05	GK2
Plate 9	G04	M-015091-01	D-015091-06	GK2
Plate 9	G04	M-015091-01	D-015091-07	GK2
Plate 9	G05	M-015098-01	D-015098-01	KUB3
Plate 9	G05	M-015098-01	D-015098-02	KUB3
Plate 9	G05	M-015098-01	D-015098-03	KUB3
Plate 9	G05	M-015098-01	D-015098-04	KUB3
Plate 9	G06	M-005393-03	D-005393-01	TRPM7
Plate 9	G06	M-005393-03	D-005393-03	TRPM7
Plate 9	G06	M-005393-03	D-005393-04	TRPM7
Plate 9	G06	M-005393-03	D-005393-08	TRPM7
Plate 9	G07	M-005351-05	D-005351-05	MYLK
Plate 9	G07	M-005351-05	D-005351-06	MYLK
Plate 9	G07	M-005351-05	D-005351-07	MYLK
Plate 9	G07	M-005351-05	D-005351-17	MYLK
Plate 9	G08	M-004515-02	D-004515-01	GUCY2F
Plate 9	G08	M-004515-02	D-004515-02	GUCY2F
Plate 9	G08	M-004515-02	D-004515-04	GUCY2F
Plate 9	G08	M-004515-02	D-004515-05	GUCY2F
Plate 9	G09	M-003010-03	D-003010-05	GSK3B
Plate 9	G09	M-003010-03	D-003010-06	GSK3B
Plate 9	G09	M-003010-03	D-003010-08	GSK3B
Plate 9	G09	M-003010-03	D-003010-09	GSK3B
Plate 9	G10	M-003157-04	D-003157-10	MST1R
Plate 9	G10	M-003157-04	D-003157-11	MST1R
Plate 9	G10	M-003157-04	D-003157-12	MST1R
Plate 9	G10	M-003157-04	D-003157-13	MST1R
Plate 9	G11	M-006812-00	D-006812-01	AK2
Plate 9	G11	M-006812-00	D-006812-02	AK2
Plate 9	G11	M-006812-00	D-006812-03	AK2
Plate 9	G11	M-006812-00	D-006812-04	AK2
Plate 9	H02	M-003795-02	D-003795-07	NEK7
Plate 9	H02	M-003795-02	D-003795-08	NEK7
Plate 9	H02	M-003795-02	D-003795-09	NEK7
Plate 9	H02	M-003795-02	D-003795-10	NEK7
Plate 9	H03	M-005362-01	D-005362-01	PRKWNK1
Plate 9	H03	M-005362-01	D-005362-02	PRKWNK1
Plate 9	H03	M-005362-01	D-005362-03	PRKWNK1
Plate 9	H03	M-005362-01	D-005362-04	PRKWNK1
Plate 9	H04	M-013077-01	D-013077-02	TSKS
Plate 9	H04	M-013077-01	D-013077-04	TSKS
Plate 9	H04	M-013077-01	D-013077-05	TSKS
Plate 9	H04	M-013077-01	D-013077-06	TSKS
Plate 9	H05	M-005378-02	D-005378-01	STK19
Plate 9	H05	M-005378-02	D-005378-03	STK19
Plate 9	H05	M-005378-02	D-005378-04	STK19
Plate 9	H05	M-005378-02	D-005378-18	STK19
Plate 9	H06	M-003590-03	D-003590-23	MAPK12
Plate 9	H06	M-003590-03	D-003590-24	MAPK12
Plate 9	H06	M-003590-03	D-003590-25	MAPK12
Plate 9	H06	M-003590-03	D-003590-26	MAPK12
Plate 9	H07	M-007728-01	D-007728-03	GALK1
Plate 9	H07	M-007728-01	D-007728-04	GALK1
Plate 9	H07	M-007728-01	D-007728-05	GALK1
Plate 9	H07	M-007728-01	D-007728-06	GALK1
Plate 9	H08	M-006740-02	D-006740-01	IPMK
Plate 9	H08	M-006740-02	D-006740-02	IPMK
Plate 9	H08	M-006740-02	D-006740-04	IPMK
Plate 9	H08	M-006740-02	D-006740-05	IPMK
Plate 9	H09	M-006759-00	D-006759-01	PANK4
Plate 9	H09	M-006759-00	D-006759-02	PANK4
Plate 9	H09	M-006759-00	D-006759-03	PANK4
Plate 9	H09	M-006759-00	D-006759-04	PANK4
Plate 9	H10	M-004651-02	D-004651-01	PRKACG
Plate 9	H10	M-004651-02	D-004651-02	PRKACG
Plate 9	H10	M-004651-02	D-004651-04	PRKACG
Plate 9	H10	M-004651-02	D-004651-06	PRKACG
Plate 9	H11	M-003136-03	D-003136-05	FLT1
Plate 9	H11	M-003136-03	D-003136-06	FLT1
Plate 9	H11	M-003136-03	D-003136-07	FLT1
Plate 9	H11	M-003136-03	D-003136-09	FLT1

Table S2 DNA repair siRNA Set V1.0. Gene symbol and siRNA sequence

Symbol	Plate	row	column	Sense
	C_DNA_01	A	1	
AHCY	C_DNA_01	A	2	CCUGGUCUGUGGACUUAUAtt
ATR	C_DNA_01	A	3	GGCACUAAUUGUUCUUCAAtt
C18orf37	C_DNA_01	A	4	GAAUAGUCCGGAACAGCAAtt
CCT4	C_DNA_01	A	5	GCUCAUAUUGACCAAUUUAtt
CHEK1	C_DNA_01	A	6	ACCUCAUCAUAACAACAAUtt
COL1A2	C_DNA_01	A	7	CGGUGUUGUUGGUCCCACAtt
DNMT1	C_DNA_01	A	8	CAAUGAGACUGACAUCAAAtt
DCLRE1A	C_DNA_01	A	9	GCAUGAUUCACAAGAACAAtt
DUT	C_DNA_01	A	10	CCUUCUCUUCACUAGUCUAtt
EHMT1	C_DNA_01	A	11	CGAAGAAUGGGAACCUAUAtt
	C_DNA_01	A	12	
	C_DNA_01	B	1	
AHCY	C_DNA_01	B	2	GCCGUCAUACUGUUCCAAAtt
ATR	C_DNA_01	B	3	GCUAAUCUUCUAACAUUAAtt
C18orf37	C_DNA_01	B	4	GCAUGGAAGCCAUGAGUGAtt
CCT4	C_DNA_01	B	5	GAGUUGGCCCUACGAUUAAtt
CHEK1	C_DNA_01	B	6	CGCACAGGUCUUUCCUUAUtt
COL1A2	C_DNA_01	B	7	CGGUUACCCUGGCAAUAUUtt
DNMT1	C_DNA_01	B	8	GGAAGUGAAUGGACGUCUAtt
DCLRE1A	C_DNA_01	B	9	GCUUCAUAACAAUGUUACAtt
DUT	C_DNA_01	B	10	GCCUUGGAUGACACCGAAAtt
EHMT1	C_DNA_01	B	11	ACGGAUACAUCUUAAAUAAtt
	C_DNA_01	B	12	
	C_DNA_01	C	1	
ADPRT	C_DNA_01	C	2	GAGAAAUCUCUUACCUCAAtt
ARMET	C_DNA_01	C	3	GCCAGAUAUGUGAGCUUAAtt
CANX	C_DNA_01	C	4	ACUAGUCUGUGUAACUUUAtt
CCT5	C_DNA_01	C	5	CUGUAGAUGCUAUAAUAAAtt
CKS2	C_DNA_01	C	6	GUAAGAUGUUUAAGAUAAAtt
CRIP2	C_DNA_01	C	7	CGGUUUGAGGAUUGCAGAAtt
DDB1	C_DNA_01	C	8	ACUAGAUCGCGAUAAUAAAtt
DCLRE1C	C_DNA_01	C	9	GGUUCAUGUGAAUAAGCUAtt
E2F5	C_DNA_01	C	10	CGAUUCCAUUAAUAAUAGAtt
ERCC3	C_DNA_01	C	11	GGGAAUAUGUGGCAAUCAAtt
	C_DNA_01	C	12	
	C_DNA_01	D	1	
ADPRT	C_DNA_01	D	2	GGUGAUCGGUAGCAACAAAtt
ARMET	C_DNA_01	D	3	GAAGAAGCUCCGAGUUAAAtt
CANX	C_DNA_01	D	4	UGCAUAAUGUUAAGCUUUAtt
CCT5	C_DNA_01	D	5	GCGUCCUUGUUGACAUAAAtt
CKS2	C_DNA_01	D	6	GUUUGUAUGUUGCAUUUAAtt
CRIP2	C_DNA_01	D	7	GCCUUGUGCUGUCAAUAAAtt
DDB1	C_DNA_01	D	8	GCAGAAUCGACUCAAUAAAtt
DCLRE1C	C_DNA_01	D	9	GUACGGAGCCAAAGUAUAAtt
E2F5	C_DNA_01	D	10	ACUUUAAUUUAGAUGAUAAtt
ERCC3	C_DNA_01	D	11	GGUUCACCUCCGAUGCCAAtt
	C_DNA_01	D	12	
	C_DNA_01	E	1	
ADPRTL2	C_DNA_01	E	2	GCAGGGCGAGAGCAUUAAAtt
BLM	C_DNA_01	E	3	GAAUCUCAAUGUACAUAGAtt
CARM1	C_DNA_01	E	4	GGAUAGAAAUCCCAUUCAAtt
CDK7	C_DNA_01	E	5	GGAUGGCUCUGGACGUGAAtt
CETN2	C_DNA_01	E	6	GAAUUACCCUAAUUCUCAAtt
COPB2	C_DNA_01	E	7	GAUUCUUCAGAGUAUGCAAtt
DMC1	C_DNA_01	E	8	CCUGAUUUAUGAUAACUAUtt
DCLRE1B	C_DNA_01	E	9	AGAUCUCUAUAGCAAAGAAtt
DVL3	C_DNA_01	E	10	CAAGUAUGUUCCUCCUGAAtt
	C_DNA_01	E	11	GCAGCACGACUUCUUCAAGtt
	C_DNA_01	E	12	
	C_DNA_01	F	1	
ADPRTL2	C_DNA_01	F	2	GUACUAUCUGAUUCAGCUAtt
BLM	C_DNA_01	F	3	GACCAUCUGUGACUAUAAAtt
CARM1	C_DNA_01	F	4	CAACAACCUGAUUCCUUUAtt
CDK7	C_DNA_01	F	5	GGACAUAGAUCAGAAGCUAtt
CETN2	C_DNA_01	F	6	GAACGACUUUAGACAAGCAtt
COPB2	C_DNA_01	F	7	GGUUUCAAGGGUAGUGAAAtt
DMC1	C_DNA_01	F	8	CCACAUGUUACUAAAGAAAtt
DCLRE1B	C_DNA_01	F	9	CCUACAGGUAUCUAAGCAAtt
DVL3	C_DNA_01	F	10	CCUGGUUACUUCAUCACAAtt
	C_DNA_01	F	11	GCAGCACGACUUCUUCAAGtt
	C_DNA_01	F	12	
	C_DNA_01	G	1	
APEX2	C_DNA_01	G	2	GCUGCAGCACAACAAUCAAtt
BRCA2	C_DNA_01	G	3	GGACACAAUUACAACUAAAtt
CCNH	C_DNA_01	G	4	GAAGCAUAUCAAACGUUUAtt
CKN1	C_DNA_01	G	5	GGUCUAUUCCUGACAGCUAtt
CDKN3	C_DNA_01	G	6	GGGACAAAUUAGCUGCACAtt
DDB2	C_DNA_01	G	7	GGAUUCUUACCGGAUAUUAtt
DDX48	C_DNA_01	G	8	GCAUCUUGGUGAAACGUGAtt
DEPC-1	C_DNA_01	G	9	GAGAGGAUAUAACUUAUCAtt
DOT1L	C_DNA_01	G	10	GGCCUUCGUCGAAGCAGAAtt
	C_DNA_01	G	11	UUCUCCGAACGUGUCACGUtt
	C_DNA_01	G	12	
	C_DNA_01	H	1	
APEX2	C_DNA_01	H	2	GGCUAUCGUUGAGGGUUAUtt
BRCA2	C_DNA_01	H	3	GGAGGAAUAUCGUAGGUAAtt
CCNH	C_DNA_01	H	4	GAGCUUGCACUUAACGUAAtt
CKN1	C_DNA_01	H	5	GAGUCAACACGGAGAGUUUtt
CDKN3	C_DNA_01	H	6	CAAUCAAGAUCUGUAUCAAtt
DDB2	C_DNA_01	H	7	GGAUCAAGCAGUUAUUUGAtt
DDX48	C_DNA_01	H	8	AGAGCAGAUUUACGAUGUAtt
DEPC-1	C_DNA_01	H	9	CGCUAUCAUCUUUAGGCAAtt
DOT1L	C_DNA_01	H	10	GCUGCCGGUCUACGAUAAAtt
	C_DNA_01	H	11	UUCUCCGAACGUGUCACGUtt
	C_DNA_01	H	12	

	C_DNA_02	A	1	
ERCC2	C_DNA_02	A	2	GAAAGUUGCUCAACUUCUAtt
FANCA	C_DNA_02	A	3	GCGUUGAGAUAUCAAAGAUtt
FANCE	C_DNA_02	A	4	CGCCGAGGAGAGCUUGUAAtt
FLJ10858	C_DNA_02	A	5	GGAUUCAUUUCGGAAUGAAtt
GTF2H3	C_DNA_02	A	6	GAGUAAUGGCAUUAAUCAAtt
HDAC1	C_DNA_02	A	7	CCCGGAGGAAAGUCUGUUAtt
HDAC11	C_DNA_02	A	8	AGGUGGAGAGGAACAUCAAtt
ILF2	C_DNA_02	A	9	GGCCCUUUGUACCACAUAUtt
KIAA0101	C_DNA_02	A	10	GGUUGAUAAUGCCUCUACAtt
MAD2L2	C_DNA_02	A	11	GGAAGAGCGCGCUCAUAAAtt
	C_DNA_02	A	12	
	C_DNA_02	B	1	
ERCC2	C_DNA_02	B	2	CGCUCACCCUCCUUGCUAAtt
FANCA	C_DNA_02	B	3	GCAUAUUCAGGAGGCCUUAtt
FANCE	C_DNA_02	B	4	GCCUGAGGAUAAAGGCUGAtt
FLJ10858	C_DNA_02	B	5	UGGAUAUUCUAACAGUGAAtt
GTF2H3	C_DNA_02	B	6	GCAGAUUCUUUGUUGGGAAtt
HDAC1	C_DNA_02	B	7	CGUUCUUAACUUUGAACCAtt
HDAC11	C_DNA_02	B	8	CAGACAGGAGGAACCAUAAtt
ILF2	C_DNA_02	B	9	CCAUAGAAGUGUCAUUCCAtt
KIAA0101	C_DNA_02	B	10	CCUGGUAUUCUAGAAUGUAtt
MAD2L2	C_DNA_02	B	11	CGUGGGCAUCUUCCAGAAAtt
	C_DNA_02	B	12	
	C_DNA_02	C	1	
ERCC4	C_DNA_02	C	2	GCACCUCGAUGUUUAUAAAtt
FANCC	C_DNA_02	C	3	CGAGGACCACCCGAUUUAAtt
FANCF	C_DNA_02	C	4	GCCUUUGGAUACUAAAUUAtt
FLJ35220	C_DNA_02	C	5	GGGUGAGAGUUGAAAUGAAtt
H2AFZ	C_DNA_02	C	6	CAGGACUCUAAAUACUCUAtt
HDAC4	C_DNA_02	C	7	GGCAUGACUUUAUAUUGUAtt
HDAC10	C_DNA_02	C	8	GGUGAACAGUGGUAUAGCAtt
IFNGR2	C_DNA_02	C	9	GCUUCCCAAUGGAUUUCAAtt
LIG1	C_DNA_02	C	10	GGACGUUUGAGAAGAUCGAtt
MCM3	C_DNA_02	C	11	CGAUUUGACUUGCUCUUCAtt
	C_DNA_02	C	12	
	C_DNA_02	D	1	
ERCC4	C_DNA_02	D	2	CGCCGUGUAACAAAUGAAAtt
FANCC	C_DNA_02	D	3	CAUUGUUAGUGUAACUCAAtt
FANCF	C_DNA_02	D	4	CCAGCAUUAGAGCUUUAUAtt
FLJ35220	C_DNA_02	D	5	GAGAGAGAUUGGUGUUAAUtt
H2AFZ	C_DNA_02	D	6	GGUCAUAUCCCAAACUAAAtt
HDAC4	C_DNA_02	D	7	GGUUUAUUCUGAUUGAGAAtt
HDAC10	C_DNA_02	D	8	CCCUUGCGCCGUUAGUAAAtt
IFNGR2	C_DNA_02	D	9	GGGCAUUUAAGCAACAUAUtt
LIG1	C_DNA_02	D	10	CGUCAUUUCUUUCAAUAAAtt
MCM3	C_DNA_02	D	11	GCAGGUAUGACCAGUAUAAtt
	C_DNA_02	D	12	
	C_DNA_02	E	1	
ERCC5	C_DNA_02	E	2	CGGACUCUUUCAGCCAUUAtt
FAP	C_DNA_02	E	3	CACUGAUCAAGAAAUUAAAtt
FANCD2	C_DNA_02	E	4	GGGAGAGAGUCAGAAUCAAtt
G22P1	C_DNA_02	E	5	GGGUUAGCGUUAGCCUUAAtt
GTF2H1	C_DNA_02	E	6	GGCACAGGGUAGACCUUAAtt
HDAC6	C_DNA_02	E	7	CCGUCAACGUGGCAUGGAAtt
HSPE1	C_DNA_02	E	8	GGGUGGAGAGAUUCAACCAtt
HSU24186	C_DNA_02	E	9	GGUGAUGGAUAAAUUGACAtt
KPNA2	C_DNA_02	E	10	GGGCUGGUUUGAUUCCGAAtt
	C_DNA_02	E	11	GCAGCACGACUUCUUCAAGtt
	C_DNA_02	E	12	
	C_DNA_02	F	1	
ERCC5	C_DNA_02	F	2	GAAGAUGCUAAACGUAUUAtt
FAP	C_DNA_02	F	3	GCCUGUUGGGAGUAAAUUAtt
FANCD2	C_DNA_02	F	4	GGAGGAGAUUGAUGGUCUAtt
G22P1	C_DNA_02	F	5	CCUAGUGAGCAGUAGCCAAtt
GTF2H1	C_DNA_02	F	6	CAGAGCUGAUGCUAUUGUAtt
HDAC6	C_DNA_02	F	7	CUUCGAAGCGAAAUAUUAAtt
HSPE1	C_DNA_02	F	8	GGGAGUAAUGGCAGGACAAtt
HSU24186	C_DNA_02	F	9	CGGUCAAUGCACACAUGAUtt
KPNA2	C_DNA_02	F	10	GAAUUGGCAUGGUGGUGAAtt
	C_DNA_02	F	11	GCAGCACGACUUCUUCAAGtt
	C_DNA_02	F	12	
	C_DNA_02	G	1	
ERCC6	C_DNA_02	G	2	GGGCAUUUCUGAUUAUUAAtt
FANCG	C_DNA_02	G	3	GCGGGAACUAACUCUUCAAtt
FEN1	C_DNA_02	G	4	AGUCCAUUGUUACAUGAAAtt
GTF2H2	C_DNA_02	G	5	GACUGACGUGUACUUUAAAtt
HDAC2	C_DNA_02	G	6	GGUCAAUAAGACCAGAUAAtt
ZDHHC17	C_DNA_02	G	7	GGAUGAGUACGAUACCGAAtt
HUS1	C_DNA_02	G	8	CAAUCACCUUGUUAUUGAAtt
KDELR2	C_DNA_02	G	9	UGAUCUACCUGAAAUUUAAtt
LDHA	C_DNA_02	G	10	GUCCAAUAUGGCAACUCUAtt
	C_DNA_02	G	11	UUCUCCGAACGUGUCACGUtt
	C_DNA_02	G	12	
	C_DNA_02	H	1	
ERCC6	C_DNA_02	H	2	GGAUGGUACCACUACAAUAtt
FANCG	C_DNA_02	H	3	CAGGUAAUCGAGACACUUAtt
FEN1	C_DNA_02	H	4	AGAGCUACUUUGGCCGUAAtt
GTF2H2	C_DNA_02	H	5	AGAUUUAAAGCCUAAUAGAtt
HDAC2	C_DNA_02	H	6	GGGUUGUUUCAAUCUAACAtt
ZDHHC17	C_DNA_02	H	7	GUACCUGUUUGAUACGAAAtt
HUS1	C_DNA_02	H	8	CGCACAUCGACACACUGUAtt
KDELR2	C_DNA_02	H	9	GAAACUUAAUGCUGUAUUAtt
LDHA	C_DNA_02	H	10	GCUGAUUUAUAAUCUUCUAtt
	C_DNA_02	H	11	UUCUCCGAACGUGUCACGUtt
	C_DNA_02	H	12	

	C_DNA_03	A	1			C_DNA_04	A	1	
MBD4	C_DNA_03	A	2	GCUUCUCAUCGCUACUAUAtt	POLM	C_DNA_04	A	2	GGAAGGACUGCGAACCUUAtt
MGC90512	C_DNA_03	A	3	GCGGUUUACCCGUGUUUAAtt	PRKDC	C_DNA_04	A	3	CGUGUAUUACAGAAGGAAAtt
MLL	C_DNA_03	A	4	CGAUCAAAUGCCCGCCUAAtt	RAD23A	C_DNA_04	A	4	GGUGCUAAAGGAGAAGAUAtt
MSH6	C_DNA_03	A	5	CGCCAUUGUUCGAGAUUUAtt	REV3L	C_DNA_04	A	5	GGAUGUAGUCAAACUGCAAtt
MTHFD2	C_DNA_03	A	6	CGCGGCAGUUCGAAAUGAAtt	REV1L	C_DNA_04	A	6	GAGAUAUGUCAGUAUUGAAtt
NONO	C_DNA_03	A	7	GUGUUUGAUUUGUCUCAUAtt	SET7	C_DNA_04	A	7	GGGAGUUUACACUUACGAAtt
OK/SW-cl.56	C_DNA_03	A	8	GUUAAUACUUCCUCUUAAAtt	SMUG1	C_DNA_04	A	8	CGAAGUCAUUCUUGGCCAAtt
PMS1	C_DNA_03	A	9	GCGAAUGGUUUCAAGAUAAtt	SUV39H1	C_DNA_04	A	9	GGGUCCGUAUUGAAUGCAAtt
POLG	C_DNA_03	A	10	GAUGCGGGUCACACCUAAAtt	TARS	C_DNA_04	A	10	CCGUUAUUGCUAAAGUAAAtt
PNKP	C_DNA_03	A	11	CGUGAACAGGGACACGCUAtt	TP53BP1	C_DNA_04	A	11	GGACAGUCUUUCCACGAAUtt
	C_DNA_03	A	12			C_DNA_04	A	12	
	C_DNA_03	B	1			C_DNA_04	B	1	
MBD4	C_DNA_03	B	2	GCCGAAUGACCUCCGCAAAtt	POLM	C_DNA_04	B	2	CAGAAUGCCCAGAAGAGAAtt
MGC90512	C_DNA_03	B	3	CGGACGUGUUGCAGUGAUAtt	PRKDC	C_DNA_04	B	3	CCCUGUUGACAGUACUUUAtt
MLL	C_DNA_03	B	4	GGCAAUAGUUCUAAGCAAAtt	RAD23A	C_DNA_04	B	4	GGCCUAUUUCGCGUGUGAAtt
MSH6	C_DNA_03	B	5	GAAGUUGUAGAGCUUCUAAtt	REV3L	C_DNA_04	B	5	GAGUAUGGAUCAUAUACAAtt
MTHFD2	C_DNA_03	B	6	GGAUUAUUCCUUGCUAUUAtt	REV1L	C_DNA_04	B	6	GCGCAUCUGUGCCAAAGAAtt
NONO	C_DNA_03	B	7	AAGUGGACCGCAACAUCAAtt	SET7	C_DNA_04	B	7	CCUGGACGAUGACGGAUUAtt
OK/SW-cl.56	C_DNA_03	B	8	CCAGAAACGUCUUCUUAAUtt	SMUG1	C_DNA_04	B	8	GCAUGGGACAUGAAAUUAAtt
PMS1	C_DNA_03	B	9	GGAACGAUACAAUAGUCAAtt	SUV39H1	C_DNA_04	B	9	GGUGUACAACGUCUUCAUAtt
POLG	C_DNA_03	B	10	CGAGCAAAUCUUCGGGCAAtt	TARS	C_DNA_04	B	10	GGAACAGCGUUUCCGUAAAtt
PNKP	C_DNA_03	B	11	CGUGUGAGACAGCCCUGAAtt	TP53BP1	C_DNA_04	B	11	GUUUGACCAGAGCAAUAAAtt
	C_DNA_03	B	12			C_DNA_04	B	12	
	C_DNA_03	C	1			C_DNA_04	C	1	
MBD3	C_DNA_03	C	2	CGGUGACCAAGAUUACCAAtt	POLK	C_DNA_04	C	2	GGAUGGGACUUAAUGAUAAtt
MNAT1	C_DNA_03	C	3	GGUGUAAGACCACCAAAUAtt	RAD23B	C_DNA_04	C	3	GGUGUCUAAUUACUGUUUAtt
MRPL3	C_DNA_03	C	4	GCCGAAACAGACAGUUAAAtt	RAD18	C_DNA_04	C	4	GGUUGUUGCCCGAGGUUAAtt
MSH2	C_DNA_03	C	5	CAUGGGCUAUCAACUUAAUtt	RPA1	C_DNA_04	C	5	GGAAUUAUGUCGUAAGUCAtt
MUTYH	C_DNA_03	C	6	GGAGGAAUUUCACACCGCAtt	SDHC	C_DNA_04	C	6	GGUAGACCAUAAUAGUGGAtt
NEIL1	C_DNA_03	C	7	ACUGUUCGUUGGUGCUUAAtt	SMARCA4	C_DNA_04	C	7	CGUGGACUUCAAGAAGAUAtt
PAFAH1B3	C_DNA_03	C	8	CACCUACCUCCUAAGUGAAtt	SND1	C_DNA_04	C	8	CCACCGUGUUGCAGAUAUAtt
PMS2	C_DNA_03	C	9	GGAUGUAAAUUUCGAGUUUtt	SUV39H2	C_DNA_04	C	9	GCGUUAAGCUGAUAAUGUAtt
POLE	C_DNA_03	C	10	GCCUCUCCAUUGACCUGAAtt	TMEM30A	C_DNA_04	C	10	CGAUUUAAAGGUACAACAAtt
POLL	C_DNA_03	C	11	CCGGCUCUGCACACUUCAAtt	TPX2	C_DNA_04	C	11	GGAUGAUAUUAACCUGUUAtt
	C_DNA_03	C	12			C_DNA_04	C	12	
	C_DNA_03	D	1			C_DNA_04	D	1	
MBD3	C_DNA_03	D	2	CGGAGAUGGAGCACGUCUAtt	POLK	C_DNA_04	D	2	GGGUGACGACGGGUAGAAAtt
MNAT1	C_DNA_03	D	3	GGAGGUUGAGAUCAGGAAAtt	RAD23B	C_DNA_04	D	3	GGGAUGACUUGGGCUCAUAtt
MRPL3	C_DNA_03	D	4	CAUUAAAUAUAUGAGUUAAtt	RAD18	C_DNA_04	D	4	CGAGGUUAAUGUAGUUGUUtt
MSH2	C_DNA_03	D	5	CAGGCAUGCUUGUGUUGAAtt	RPA1	C_DNA_04	D	5	GUGUGACGAUCCCAUGUUAtt
MUTYH	C_DNA_03	D	6	AGCUGACAUAUCAAGUAUAtt	SDHC	C_DNA_04	D	6	CAGUGUUAUUGAAAGAAGAtt
NEIL1	C_DNA_03	D	7	GAUGUUUGUUUAUGAGUUAtt	SMARCA4	C_DNA_04	D	7	GCGCUACAACCAGAUGAAAtt
PAFAH1B3	C_DNA_03	D	8	GCCUUCCCACAACAUUAAAtt	SND1	C_DNA_04	D	8	GGCUGAACCUGUGGCGCUAtt
PMS2	C_DNA_03	D	9	GACUCGUGAAUGAGGUCUAtt	SUV39H2	C_DNA_04	D	9	CGGAGGAUAUGGAAUAUUAtt
POLE	C_DNA_03	D	10	GCAUCAUCCUCUGUACAAAtt	TMEM30A	C_DNA_04	D	10	CGAGAUGAUAGUCAACUAAtt
POLL	C_DNA_03	D	11	AGAGGAGAAUGGUCAGCAAtt	TPX2	C_DNA_04	D	11	GGCUAAUAAUGAGAUGUAAtt
	C_DNA_03	D	12			C_DNA_04	D	12	
	C_DNA_03	E	1			C_DNA_04	E	1	
MECP2	C_DNA_03	E	2	GGAGCGGAUUGCAAAGCAAtt	POLN	C_DNA_04	E	2	GCGCAUUCUUACACAUUUAtt
MPG	C_DNA_03	E	3	ACCGAGGCAUGUUCAUGAAtt	RAD54L	C_DNA_04	E	3	GGAGGAUCUAAGGAUGAAAtt
MLH3	C_DNA_03	E	4	GAAUAUAAGUUAUGGGCUAtt	RBM4	C_DNA_04	E	4	CAGGAACCGUGGACCUUAAtt
MSH3	C_DNA_03	E	5	GCAAGGAGUUAUGGAUUAAtt	RPA2	C_DNA_04	E	5	CCAGGAGAGUACUUACAUAtt
NBS1	C_DNA_03	E	6	GGAUAUGCUCCAAAGGCAAtt	RRM2B	C_DNA_04	E	6	CCAGGAGGUUAUCAUGGUAtt
NEIL2	C_DNA_03	E	7	GCGUUUGGGUGAACGAUUUtt	SNRPF	C_DNA_04	E	7	GGUGUAAUAAUGUCCUUUAtt
PAICS	C_DNA_03	E	8	CAAGGACUUCUAACAAUAAtt	SSBP1	C_DNA_04	E	8	GGGUUAGAUCGUCAGGAAAtt
POLB	C_DNA_03	E	9	CGAGUUCAUCCAUCAAUUUtt	TDG	C_DNA_04	E	9	GGUAUUGCUUUGGUAUAUAtt
POLH	C_DNA_03	E	10	GGUUGUGAGCAUUCGUGUAtt	TOP2A	C_DNA_04	E	10	GAAUAACCAUAGAAAUGAAtt
	C_DNA_03	E	11	GCAGCACGACUUCUUCAAGtt		C_DNA_04	E	11	GCAGCACGACUUCUUCAAGtt
	C_DNA_03	E	12			C_DNA_04	E	12	
	C_DNA_03	F	1			C_DNA_04	F	1	
MECP2	C_DNA_03	F	2	GAGAUGUCUCUUAUAUCUAtt	POLN	C_DNA_04	F	2	GGAGGCACAUCAACAAUUUtt
MPG	C_DNA_03	F	3	GGGUGUUUGUGCCUCAUAAtt	RAD54L	C_DNA_04	F	3	GCAUUUAUUCGAAGCAUUUtt
MLH3	C_DNA_03	F	4	GAAGGUUGCUAUAUAGUAUtt	RBM4	C_DNA_04	F	4	CGAGCAAUAUAAUGAGCAAtt
MSH3	C_DNA_03	F	5	GCUAGAAUUACAAUACAUAtt	RPA2	C_DNA_04	F	5	CAGUGGAUUCGAAAGCUAUtt
NBS1	C_DNA_03	F	6	GGAAGACUGCCCUACUAUAtt	RRM2B	C_DNA_04	F	6	GCAGUUCAGUGGUACAUAAtt
NEIL2	C_DNA_03	F	7	CCAGGUCCAUGGAAAGAAAtt	SNRPF	C_DNA_04	F	7	GGCAGAGAGUAGCCUGCAAtt
PAICS	C_DNA_03	F	8	CGACUAACAGGGACUAUAAtt	SSBP1	C_DNA_04	F	8	CCUAAAGAUUAGACUGUAAtt
POLB	C_DNA_03	F	9	AGAUAUUGUACUAAAUGAAtt	TDG	C_DNA_04	F	9	GACGUAUUCUAGUACAGAAtt
POLH	C_DNA_03	F	10	CCAUUUAGGUGCUGAGUUAtt	TOP2A	C_DNA_04	F	10	CGUAGGCUGUUUAAAGAAAtt
	C_DNA_03	F	11	GCAGCACGACUUCUUCAAGtt		C_DNA_04	F	11	GCAGCACGACUUCUUCAAGtt
	C_DNA_03	F	12			C_DNA_04	F	12	
	C_DNA_03	G	1			C_DNA_04	G	1	
MLH1	C_DNA_03	G	2	GGCUCAUGUUACUAUUACAtt	PRDX4	C_DNA_04	G	2	GCAAAGCGAAGAUUUCCAAtt
MMP9	C_DNA_03	G	3	CCUUUGAGGGCGACCUCAAtt	RAD9A	C_DNA_04	G	3	GGCUCACCUUCCUAAGGAAtt
MMS19L	C_DNA_03	G	4	GGCUGUACAAAGAACAUAAtt	RECQL4	C_DNA_04	G	4	GGGAGUACCGCACUCUGAAtt
MSH4	C_DNA_03	G	5	GCAGUGAGGUCUAACAUAAtt	RPA3	C_DNA_04	G	5	GGGAGUAAAUCGACCCUCAtt
NCBP2	C_DNA_03	G	6	CGUUAAACUGAGUGUAGAAtt	SET8	C_DNA_04	G	6	GCAGUCUGAAGAAAGGAAAtt
NTHL1	C_DNA_03	G	7	GGAGGAGCAAGGUGAAAUAtt	SOX4	C_DNA_04	G	7	GGACAGACGAAGAGUUUAAtt
PLK1	C_DNA_03	G	8	GGAUCAAGAAGAAUGAAUAtt	SSR1	C_DNA_04	G	8	GAGUGCAGAUACAACUAUAtt
POLD1	C_DNA_03	G	9	GAGAGAGCAUGUUUGGGUAtt	TDP1	C_DNA_04	G	9	GGAGUUAAGCCAAAGUAUAtt
POLI	C_DNA_03	G	10	CGGGAACAUCAGGCUUUAAtt	TRA1	C_DNA_04	G	10	GCCUCAGUUUGAACAUUGAtt
	C_DNA_03	G	11	UUCUCCGAACGUGUCACGUtt		C_DNA_04	G	11	UUCUCCGAACGUGUCACGUtt
	C_DNA_03	G	12			C_DNA_04	G	12	
	C_DNA_03	H	1			C_DNA_04	H	1	
MLH1	C_DNA_03	H	2	GAUACAAAGUGUUGUAUCAtt	PRDX4	C_DNA_04	H	2	AGCUGUGAUCGAUGGAGAAtt
MMP9	C_DNA_03	H	3	GGCUUGCCCUGGUGCAGUAtt	RAD9A	C_DNA_04	H	3	GCGCUGACUUGGAAUUCUAtt
MMS19L	C_DNA_03	H	4	GCGUUUGAAGAAAGAUCUAtt	RECQL4	C_DNA_04	H	4	UCGAUUCCAUUAUCAUUUAtt
MSH4	C_DNA_03	H	5	GCUCAUAUUAAUUGAUGAAtt	RPA3	C_DNA_04	H	5	GCUGAUUGGUGCCGAGAAAtt
NCBP2	C_DNA_03	H	6	GCCUCUGAAAGUUAUUAAAtt	SET8	C_DNA_04	H	6	GAAUAGAUGAAUUGAUUGAtt
NTHL1	C_DNA_03	H	7	CGCUGGGCAAGCUCAUCUAtt	SOX4	C_DNA_04	H	7	CGGUCAAACUGAAAUGGAUtt
PLK1	C_DNA_03	H	8	CCAUAUGAAUUGUACAGAAtt	SSR1	C_DNA_04	H	8	AGAUUUGAACGGCAAUGUAtt
POLD1	C_DNA_03	H	9	GGACCAGGGAGAAUUAAUAtt	TDP1	C_DNA_04	H	9	AGAACUGUAUGGAAGUAAAtt
POLI	C_DNA_03	H	10	GGUUUAUUAAGCUCUUCUAtt	TRA1	C_DNA_04	H	10	GGCUAAUAUCACUGACUGAtt
	C_DNA_03	H	11	UUCUCCGAACGUGUCACGUtt		C_DNA_04	H	11	UUCUCCGAACGUGUCACGUtt
	C_DNA_03	H	12			C_DNA_04	H	12	

	C_DNA_05	A	1				C_DNA_06	A	1		
TSTA3	C_DNA_05	A	2	AGUCGGAUGGGCAGUUUAAtt	OGG1		C_DNA_06	A	2	GGACCUACACCUCAGGAAAtt	
XPA	C_DNA_05	A	3	GAUGAUAAACACAAGCUUAtt	RAD1		C_DNA_06	A	3	GUAUAUGAUUAGAAAUGAAtt	
XRCC3	C_DNA_05	A	4	GAAUUAUUGCUGCAAUUAAtt	RAD51L1		C_DNA_06	A	4	CGGCAUGGGUAGCAAGAAAtt	
PMS2L4	C_DNA_05	A	5	GUGUCUCUUUAUUAGUCGAtt	SMARCA3		C_DNA_06	A	5	CAAUGUGAAUGGAAAUCAAtt	
RPL27	C_DNA_05	A	6	CAAGGUACUCUGUGGAUAUtt	XRCC4		C_DNA_06	A	6	GCUGAUGUAUACACGUUUAtt	
RPL35	C_DNA_05	A	7	GUGUUCUCACAGUUAUUAAtt	TRAF4		C_DNA_06	A	7	GCAGGAGUUCCUCAGUGAAtt	
RPL13	C_DNA_05	A	8	GGUUAGUGACUGAUGUAAAtt	RAD50		C_DNA_06	A	8	GAAAGUGUAUAAUAAGAAAtt	
CDC2	C_DNA_05	A	9	GGGAAAUUUCUCUAUUAAAtt	POLQ		C_DNA_06	A	9	GGGCCUCUUUAGAUAUAAAtt	
IARS	C_DNA_05	A	10	CAGUAAUCUUCACACUUAAtt	BRCA1		C_DNA_06	A	10	GGAAAUGGCUGAACUAGAAtt	
MSH5	C_DNA_05	A	11	GAAAGAUAUUGUUUCUUUAtt	MRPS12		C_DNA_06	A	11	GGACCACUAUUAAGCCAUAtt	
	C_DNA_05	A	12				C_DNA_06	A	12		
	C_DNA_05	B	1				C_DNA_06	B	1		
TSTA3	C_DNA_05	B	2	CGCGGAGGCAGUUCAUAUAtt	OGG1		C_DNA_06	B	2	GGUUCUGCCUUCUGGACAAtt	
XPA	C_DNA_05	B	3	GAAUUGCGGCGAGCAGUAAtt	RAD1		C_DNA_06	B	3	GCACCAAUGUUAUUAAUAAtt	
XRCC3	C_DNA_05	B	4	GACACUUAAGGGAAAUUAAtt	RAD51L1		C_DNA_06	B	4	GAGAGAAGACAGAUUCUUAtt	
PMS2L4	C_DNA_05	B	5	CACAAGCAAGCAUGAUCAAtt	SMARCA3		C_DNA_06	B	5	GGGAGUAGUUAAUAAUAAUtt	
RPL27	C_DNA_05	B	6	CGCCAAGAGAUCAAAGAUAtt	XRCC4		C_DNA_06	B	6	CAUUUAUCAUAUUCAUUCAtt	
RPL35	C_DNA_05	B	7	CAGCAAUGGCCAAGAUCAAtt	TRAF4		C_DNA_06	B	7	GGAGCUGGAAGUACAAGUAtt	
RPL13	C_DNA_05	B	8	AGCCCUGGAUAAUGCUUUAtt	RAD50		C_DNA_06	B	8	GGAACAGAUUCAACAUCUAtt	
CDC2	C_DNA_05	B	9	GGUUAUAUCUCAUCUUUGAtt	POLQ		C_DNA_06	B	9	CCAGAAUGUUUAUAUGAAAtt	
IARS	C_DNA_05	B	10	GGAUAAAGUCCUUAUUCAAtt	BRCA1		C_DNA_06	B	10	CAUACAGCUUCAUAAAUAAtt	
MSH5	C_DNA_05	B	11	CCUUCAUGAUCGACCUCAAtt	MRPS12		C_DNA_06	B	11	CCAUCAGGACCACUAUUAAtt	
	C_DNA_05	B	12				C_DNA_06	B	12		
	C_DNA_05	C	1				C_DNA_06	C	1		
UBE2B	C_DNA_05	C	2	CAGUAUUAGCAAUGAAUUAtt	PCNA		C_DNA_06	C	2	GGAUUUAGAUGUUGAACAAtt	
WRN	C_DNA_05	C	3	GAUUGUAUACGUAACUCCAtt	RAD17		C_DNA_06	C	3	CAGUGGAGAUAAUAAUCAAtt	
XRCC1	C_DNA_05	C	4	GAUACGUCACAGCCUUCAAtt	RAD51L3		C_DNA_06	C	4	GGGUGGAAAUAAGCUUAUAtt	
H2AFX	C_DNA_05	C	5	CGACUAGAACCUUAGGCAUtt	TGIF		C_DNA_06	C	5	CAAGAACUAUAAACUUAAAtt	
PSME2	C_DNA_05	C	6	GCGAAAGCCCGGGCGACUAtt	OGT		C_DNA_06	C	6	GGUAAGUAUAAGUAUUCAAtt	
GTF2H4	C_DNA_05	C	7	AUAAAGUUAUGAUAGCUAAtt	DNMT2		C_DNA_06	C	7	GGUUGAGAAUAUCUACAAAtt	
ACLY	C_DNA_05	C	8	GAGUGAAGUCGAUAAACAAtt	G3BP		C_DNA_06	C	8	GGAGGAGUCUGAAGAAGAAtt	
ERCC1	C_DNA_05	C	9	CCGUGAAGUCAGUCAACAAtt	DNMT3B		C_DNA_06	C	9	GAGUUUACCUUAUGUUUAAtt	
LIG3	C_DNA_05	C	10	GGAAGAUAAUGAGAAGGAAtt	RAD54B		C_DNA_06	C	10	CCAAGAAAUUAUAAAUAAAtt	
NUDT1	C_DNA_05	C	11	GGGUUUCAUCUGGAAUUAAtt	NUP205		C_DNA_06	C	11	GCGUCAGUUUAAAUUUCAAtt	
	C_DNA_05	C	12				C_DNA_06	C	12		
	C_DNA_05	D	1				C_DNA_06	D	1		
UBE2B	C_DNA_05	D	2	CUCUCAUUAGAAAGGCUAAtt	PCNA		C_DNA_06	D	2	GGAUCUUAGGCAUUCUUAAtt	
WRN	C_DNA_05	D	3	GGAGAUGCUUAAGCAUUUAtt	RAD17		C_DNA_06	D	3	GUGGUUUCUAAUAAAUAAAtt	
XRCC1	C_DNA_05	D	4	GAUGGAUCUACAGUUGCAAtt	RAD51L3		C_DNA_06	D	4	GGAAGAGGUAGCUCAGAAAtt	
H2AFX	C_DNA_05	D	5	CCUCCUAGGAGGACAUUUAtt	TGIF		C_DNA_06	D	5	CAUACUGUCUAAUUAAUAAtt	
PSME2	C_DNA_05	D	6	CCGGGAGACCAGAGAUCUAtt	OGT		C_DNA_06	D	6	GAUUAAUGUUCUUCAUAAAtt	
GTF2H4	C_DNA_05	D	7	CCCACCCAGUGAUGCUCAAtt	DNMT2		C_DNA_06	D	7	CAAAGCUGUUAAUACUUAAtt	
ACLY	C_DNA_05	D	8	GCCAGAACUUGGUAGUCAAtt	G3BP		C_DNA_06	D	8	GAAAGAAAUCCACAGGAAAtt	
ERCC1	C_DNA_05	D	9	CGUGAAGUCAGUCAACAAAtt	DNMT3B		C_DNA_06	D	9	GGACUACUUUGCAUGUGAAtt	
LIG3	C_DNA_05	D	10	GGGAAGAGCUGGAAGAUAAtt	RAD54B		C_DNA_06	D	10	GGAUCAAAUUAAGAAUAUAtt	
NUDT1	C_DNA_05	D	11	CCUGCUUCAGAAGAAGAAAtt	NUP205		C_DNA_06	D	11	GACAGGAAUUAUAAGUAAAtt	
	C_DNA_05	D	12				C_DNA_06	D	12		
	C_DNA_05	E	1				C_DNA_06	E	1		
UBE2N	C_DNA_05	E	2	GAUUUGUGUUAAGAUAGUAtt	PPP2R5C		C_DNA_06	E	2	GGAAAUAUUGGGAAGUAUAtt	
XPC	C_DNA_05	E	3	GGCUGGUAUUGUCUCUACAtt	RAD51		C_DNA_06	E	3	CUUCUAAAUUAAUGGUAAAtt	
XAB2	C_DNA_05	E	4	GCGUGUACAAGUCACUGAAtt	RAD52		C_DNA_06	E	4	GGAAGGAAAUAAUCAUCUAtt	
MGMT	C_DNA_05	E	5	CCAGACAGGUGUUAUGGAAtt	UBE2A		C_DNA_06	E	5	GCGUGUUUCUGCAAUAGUAtt	
SNRPE	C_DNA_05	E	6	CCCUCGUGUUACUACAAGAtt	EXO1		C_DNA_06	E	6	GGAUGUACUUUACCUUCUAtt	
ATM	C_DNA_05	E	7	CUUAUUCAUUAGUAAUUUAtt	EZH2		C_DNA_06	E	7	GGAUGGUACUUUCAUUGAAtt	
HRMT1L2	C_DNA_05	E	8	CCAUCGACCUGGACUUCAAtt	PRDX2		C_DNA_06	E	8	GGUUCGGGCCGGGCAUAAAtt	
HNRPA2B1	C_DNA_05	E	9	GGAUUGGAUUAUUUAAUAAtt	CHEK2		C_DNA_06	E	9	GGAUGGAUUUGCCAAUCUUtt	
LIG4	C_DNA_05	E	10	GGAAUUAUUGAGCACUUAAtt	SPO11		C_DNA_06	E	10	GAGUGUACUUACCUAACAAtt	
	C_DNA_05	E	11	GCAGCACGACUUCUUCAAGtt			C_DNA_06	E	11	GCAGCACGACUUCUUCAAGtt	
	C_DNA_05	E	12				C_DNA_06	E	12		
	C_DNA_05	F	1				C_DNA_06	F	1		
UBE2N	C_DNA_05	F	2	GCCAGUCAUAAAUACAUAAtt	PPP2R5C		C_DNA_06	F	2	CGAGCUGCUUUAAGUGAAAtt	
XPC	C_DNA_05	F	3	GCAAAUGGCUUCUAUCGAAtt	RAD51		C_DNA_06	F	3	GGGAAUUAGUGAAGCCAAAtt	
XAB2	C_DNA_05	F	4	CGUACAACACGCAGGUCAAtt	RAD52		C_DNA_06	F	4	GGAGUGACUCAAGAAUUAAtt	
MGMT	C_DNA_05	F	5	GGCUCUUCACCAUCCCGUUtt	UBE2A		C_DNA_06	F	5	CACCCUCUAUGAAAUCAAAtt	
SNRPE	C_DNA_05	F	6	AUUUACAUUGCUUCUUAAAtt	EXO1		C_DNA_06	F	6	GAUGUAGCACGUAAUUCAAtt	
ATM	C_DNA_05	F	7	CCUGUUUGUUAGUUUAUUAtt	EZH2		C_DNA_06	F	7	CCAUGUUUACAACUAUCAAtt	
HRMT1L2	C_DNA_05	F	8	GGCAGUACAAAGACUACAAtt	PRDX2		C_DNA_06	F	8	GCGCCUUCAAAGAGGUGAAtt	
HNRPA2B1	C_DNA_05	F	9	GGAUUAUUUAAUAACAUUAtt	CHEK2		C_DNA_06	F	9	CCGUGGUUUGAACACGAAAtt	
LIG4	C_DNA_05	F	10	AGAUGUUUACAGAAAGGAAtt	SPO11		C_DNA_06	F	10	CAUAUAUUAUCUACAUCAAtt	
	C_DNA_05	F	11	GCAGCACGACUUCUUCAAGtt			C_DNA_06	F	11	GCAGCACGACUUCUUCAAGtt	
	C_DNA_05	F	12				C_DNA_06	F	12		
	C_DNA_05	G	1				C_DNA_06	G	1		
UBE2V2	C_DNA_05	G	2	AGGAGUCCUAGGUAUUAUAtt	PSMA1		C_DNA_06	G	2	GGAGUGUAAUUUAAAUGAAtt	
XRCC2	C_DNA_05	G	3	GCAACGACACAAACUAUAAtt	RAD51C		C_DNA_06	G	3	GCAAAUUAUCAGAAGAGAAtt	
XRCC5	C_DNA_05	G	4	GCAUAACUAUGAGUGUUUAtt	RFC4		C_DNA_06	G	4	GAUUCUGUCUUAUCUGUAAtt	
PTMA	C_DNA_05	G	5	GUCCAACAAUAAACAGGAAtt	UNG		C_DNA_06	G	5	CGCGAGGUUUGUUAAUAAAtt	
UBE2S	C_DNA_05	G	6	CCUCCAACUCUGUCUCUAAtt	MBD2		C_DNA_06	G	6	GAUGAUGCCUAGUAAAUUAtt	
NME1	C_DNA_05	G	7	CGAAGAUCUUCUCAAGGAAtt	MRE11A		C_DNA_06	G	7	GGGUUAUUUGAGCAAGUAAtt	
APEX1	C_DNA_05	G	8	AGAUAUACUGUGCCUUCAAtt	PSMC4		C_DNA_06	G	8	GGAUUGGUUUCUUCAAUAAtt	
HSPD1	C_DNA_05	G	9	CCACCAGAUGAGAAGUUAAtt	CBX3		C_DNA_06	G	9	CCUUCAAGUUAAAUUGAAAtt	
MBD1	C_DNA_05	G	10	GGGAACAGAGAAUGUUUAAtt	TREX1		C_DNA_06	G	10	GCAGGAACUGCCCAGAGAAtt	
	C_DNA_05	G	11	UUCUCCGAACGUGUCACGUtt			C_DNA_06	G	11	UUCUCCGAACGUGUCACGUtt	
	C_DNA_05	G	12				C_DNA_06	G	12		
	C_DNA_05	H	1				C_DNA_06	H	1		
UBE2V2	C_DNA_05	H	2	GAAGCUCCUCCGUCAGUUAtt	PSMA1		C_DNA_06	H	2	CAGUUGGUCUGAAAUCAAAtt	
XRCC2	C_DNA_05	H	3	GGGUACUACGCAAGCCUUAtt	RAD51C		C_DNA_06	H	3	GAGAAUGUCUCACAAAUAAtt	
XRCC5	C_DNA_05	H	4	GCGAGUAACCAGCUCAUAAtt	RFC4		C_DNA_06	H	4	GAAGUCUAUUAUCACAGAAtt	
PTMA	C_DNA_05	H	5	GAUGUAUGUGUGAAACAAUtt	UNG		C_DNA_06	H	5	GGGAUUUGUUGCAGAAGAAtt	
UBE2S	C_DNA_05	H	6	CGAUGGCAUCAAGGUCUUUtt	MBD2		C_DNA_06	H	6	GAAAGAUGAUGCCUAGUAAtt	
NME1	C_DNA_05	H	7	AGUUGGCAGGAACAUUAUAtt	MRE11A		C_DNA_06	H	7	CAUCUUUAUUGAACUUGAAtt	
APEX1	C_DNA_05	H	8	GCAUUCUAUUUCUCAUGUAtt	PSMC4		C_DNA_06	H	8	GAAUGUCAAUGUCAAGGUAtt	
HSPD1	C_DNA_05	H	9	GGGUUUGGUGACAAUAGAAtt	CBX3		C_DNA_06	H	9	GGUUACUUUGAACAAAUAAtt	
MBD1	C_DNA_05	H	10	GGAUGAUUCUGCCUCCAAAtt	TREX1		C_DNA_06	H	10	CCUUUCCUUACCACAUCAAtt	
	C_DNA_05	H	11	UUCUCCGAACGUGUCACGUtt			C_DNA_06	H	11	UUCUCCGAACGUGUCACGUtt	
	C_DNA_05	H	12				C_DNA_06	H	12		

	C_DNA_07	A	1	
DNMT3A	C_DNA_07	A	2	GAACAAGCCCAUGAUUGAAtt
TREX2	C_DNA_07	A	3	CAAUGGCUUUGAUUAUGAUtt
	C_DNA_07	A	4	
	C_DNA_07	A	5	
	C_DNA_07	A	6	
	C_DNA_07	A	7	
	C_DNA_07	A	8	
	C_DNA_07	A	9	
	C_DNA_07	A	10	
	C_DNA_07	A	11	
	C_DNA_07	A	12	
	C_DNA_07	B	1	
DNMT3A	C_DNA_07	B	2	CAGUGGUGUGUGUUGAGAAtt
TREX2	C_DNA_07	B	3	CGACGAGUCUGGUGCCCUAtt
	C_DNA_07	B	4	
	C_DNA_07	B	5	
	C_DNA_07	B	6	
	C_DNA_07	B	7	
	C_DNA_07	B	8	
	C_DNA_07	B	9	
	C_DNA_07	B	10	
	C_DNA_07	B	11	
	C_DNA_07	B	12	
	C_DNA_07	C	1	
DNMT3A	C_DNA_07	C	2	CACCGGGAUCUAUGUUUAAtt
	C_DNA_07	C	3	
	C_DNA_07	C	4	
	C_DNA_07	C	5	
	C_DNA_07	C	6	
	C_DNA_07	C	7	
	C_DNA_07	C	8	
	C_DNA_07	C	9	
	C_DNA_07	C	10	
	C_DNA_07	C	11	
	C_DNA_07	C	12	
	C_DNA_07	D	1	
DNMT3A	C_DNA_07	D	2	GAUUAAUUGGCGUAACUUAtt
	C_DNA_07	D	3	
	C_DNA_07	D	4	
	C_DNA_07	D	5	
	C_DNA_07	D	6	
	C_DNA_07	D	7	
	C_DNA_07	D	8	
	C_DNA_07	D	9	
	C_DNA_07	D	10	
	C_DNA_07	D	11	
	C_DNA_07	D	12	
	C_DNA_07	E	1	
TREX2	C_DNA_07	E	2	GAGGUGAAGAUCCAAGAAAtt
	C_DNA_07	E	3	
	C_DNA_07	E	4	
	C_DNA_07	E	5	
	C_DNA_07	E	6	
	C_DNA_07	E	7	
	C_DNA_07	E	8	
	C_DNA_07	E	9	
	C_DNA_07	E	10	
	C_DNA_07	E	11	GCAGCACGACUUCUUCAAGtt
	C_DNA_07	E	12	
	C_DNA_07	F	1	
TREX2	C_DNA_07	F	2	CGAGGGUCUGUAUAUCACAtt
	C_DNA_07	F	3	
	C_DNA_07	F	4	
	C_DNA_07	F	5	
	C_DNA_07	F	6	
	C_DNA_07	F	7	
	C_DNA_07	F	8	
	C_DNA_07	F	9	
	C_DNA_07	F	10	
	C_DNA_07	F	11	GCAGCACGACUUCUUCAAGtt
	C_DNA_07	F	12	
	C_DNA_07	G	1	
TREX2	C_DNA_07	G	2	CAAUGGCUUUGAUUAUGAUtt
	C_DNA_07	G	3	
	C_DNA_07	G	4	
	C_DNA_07	G	5	
	C_DNA_07	G	6	
	C_DNA_07	G	7	
	C_DNA_07	G	8	
	C_DNA_07	G	9	
	C_DNA_07	G	10	
	C_DNA_07	G	11	UUCUCCGAACGUGUCACGUtt
	C_DNA_07	G	12	
	C_DNA_07	H	1	
TREX2	C_DNA_07	H	2	CGACGAGUCUGGUGCCCUAtt
	C_DNA_07	H	3	
	C_DNA_07	H	4	
	C_DNA_07	H	5	
	C_DNA_07	H	6	
	C_DNA_07	H	7	
	C_DNA_07	H	8	
	C_DNA_07	H	9	
	C_DNA_07	H	10	
	C_DNA_07	H	11	UUCUCCGAACGUGUCACGUtt
	C_DNA_07	H	12	

Table S3 DNA repair Flexitube siRNAs. Gene symbol and siRNA catalog

Plate Id	Row	Col	NCBI gene symbol	Product Id
1128-1	B	2	LIG4	SI00036022
1128-1	B	3	LIG4	SI00036043
1128-1	B	4	LIG4	SI03021179
1128-1	B	5	LIG4	SI03048878
1128-1	B	7	ERCC8	SI02664802
1128-1	B	8	ERCC8	SI00001617
1128-1	B	9	ERCC8	SI03025456
1128-1	B	10	ERCC8	SI03051713
1128-1	C	2	RAD51	SI02663682
1128-1	C	3	RAD51	SI00045010
1128-1	C	4	RAD51	SI02629837
1128-1	C	5	RAD51	SI03061338
1128-1	C	7	RAD54B	SI02665229
1128-1	C	8	RAD54B	SI02665236
1128-1	C	9	RAD54B	SI00100142
1128-1	C	10	RAD54B	SI00100149
1128-1	D	2	DCLRE1C	SI00133945
1128-1	D	3	DCLRE1C	SI02645286
1128-1	D	4	DCLRE1C	SI03090556
1128-1	D	5	DCLRE1C	SI03097787
1128-1	D	7	BRCA1	SI02654575
1128-1	D	8	BRCA1	SI02664361
1128-1	D	9	BRCA1	SI02664368
1128-1	D	10	BRCA1	SI00299495
1128-1	E	2	INO80C	SI04338082
1128-1	E	3	INO80C	SI04370205
1128-1	E	4	INO80C	SI04210626
1128-1	E	5	INO80C	SI04278617
1128-1	E	7	KIAA0101	SI02654295
1128-1	E	8	KIAA0101	SI00107800
1128-1	E	9	KIAA0101	SI00107814
1128-1	E	10	KIAA0101	SI03085040
1128-1	F	2	DCLRE1A	SI02663801
1128-1	F	3	DCLRE1A	SI00108591
1128-1	F	4	DCLRE1A	SI00108598
1128-1	F	5	DCLRE1A	SI03101259
1128-1	F	7	CDKN3	SI02665621
1128-1	F	8	CDKN3	SI02665628
1128-1	F	9	CDKN3	SI04434668
1128-1	F	10	CDKN3	SI04948454
1128-1	G	2	LDHA	SI00300622
1128-1	G	3	LDHA	SI02663535
1128-1	G	4	LDHA	SI04949609
1128-1	G	5	LDHA	SI04949616
1128-1	G	7	MPG	SI00037744
1128-1	G	8	MPG	SI03039995
1128-1	G	9	MPG	SI03058377
1128-1	G	10	MPG	SI03083556
1128-2	B	2	DVL3	SI02781387
1128-2	B	3	DVL3	SI00063469
1128-2	B	4	DVL3	SI00063476
1128-2	B	5	DVL3	SI03095463
1128-2	B	7	SOX4	SI00047859
1128-2	B	8	SOX4	SI00047866
1128-2	B	9	SOX4	SI00047873
1128-2	B	10	SOX4	SI00047880
1128-2	C	2	PARP1	SI02662989
1128-2	C	3	PARP1	SI02662996
1128-2	C	4	PARP1	SI04433982
1128-2	C	5	PARP1	SI04433989
1128-2	C	7	RAD23B	SI00301616
1128-2	C	8	RAD23B	SI02663668
1128-2	C	9	RAD23B	SI02663675
1128-2	C	10	RAD23B	SI00044982
1128-2	D	2	ERCC3	SI02663444
1128-2	D	3	ERCC3	SI00002422
1128-2	D	4	ERCC3	SI00002443
1128-2	D	5	ERCC3	SI03080189
1128-2	D	7	MGMT	SI02781058
1128-2	D	8	MGMT	SI00037282
1128-2	D	9	MGMT	SI00037289
1128-2	D	10	MGMT	SI00037296
1128-2	E	2	CCT5	SI02653721
1128-2	E	3	CCT5	SI02664788
1128-2	E	4	CCT5	SI00096894
1128-2	E	5	CCT5	SI00096901
1128-2	E	7	SND1	SI02665005
1128-2	E	8	SND1	SI02665012
1128-2	E	9	SND1	SI00105567
1128-2	E	10	SND1	SI00105581
1128-2	F	2	UBE2V2	SI02665103
1128-2	F	3	UBE2V2	SI00051086
1128-2	F	4	UBE2V2	SI00051107
1128-2	F	5	UBE2V2	SI03031518
1128-2	F	7	XRCC2	SI02665110
1128-2	F	8	XRCC2	SI00077091
1128-2	F	9	XRCC2	SI00077105
1128-2	F	10	XRCC2	SI03090157
1128-2	G	2	MCM3	SI02664872
1128-2	G	3	MCM3	SI02664879
1128-2	G	4	MCM3	SI00037002
1128-2	G	5	MCM3	SI00037009
1128-2	G	7	XRCC6	SI00423122
1128-2	G	8	XRCC6	SI03025946
1128-2	G	9	XRCC6	SI03033884
1128-2	G	10	XRCC6	SI03039855
1128-2	H	2	DCLRE1B	SI02778692
1128-2	H	3	DCLRE1B	SI02778699
1128-2	H	4	DCLRE1B	SI00134750
1128-2	H	5	DCLRE1B	SI00134757